3-30-2011

Isotopic Studies of the Guerrero Composite Terrane, West-Central Mexico: Implications for Provenance of Crustal Rocks and Genesis of Ore Metals

Adriana Potra
Florida International University, apotr001@fiu.edu

DOI: 10.25148/etd.FI11050301

FLORIDA INTERNATIONAL UNIVERSITY

Miami, Florida

ISOTOPIC STUDIES OF THE GUERRERO COMPOSITE TERRANE, WEST-CENTRAL MEXICO: IMPLICATIONS FOR PROVENANCE OF CRUSTAL ROCKS AND GENESIS OF ORE METALS

A dissertation submitted in partial fulfillment of the

requirements for the degree of

DOCTOR OF PHILOSOPHY

in

GEOSCIENCES

by

Adriana Potra

2011

To: Dean Kenneth Furton
College of Arts and Sciences

This dissertation, written by Adriana Potra, and entitled Isotopic Studies of the Guerrero Composite Terrane, West-Central Mexico: Implications for Provenance of Crustal Rocks and Genesis of Ore Metals, having been approved in respect to style and intellectual content, is referred to you for judgment.

We have read this dissertation and recommend that it be approved.

_____
Grenville Draper

_____
Jennifer L. Gebelein

_____
Rosemary Hickey-Vargas

_____
Andrew W. Macfarlane, Major Professor

Date of Defense: March 30, 2011

The dissertation of Adriana Potra is approved.

_____
Dean Kenneth Furton
College of Arts and Sciences

_____
Interim Dean Kevin O'Shea
University Graduate School

Florida International University, 2011

DEDICATION

I dedicate this dissertation to the memory of my beloved mother, Ildikó, to my father, Gheorghe, to my brother, Marius, and his family, Tünde, Hanna, and Andrea. They gave me their full love, support, and encouragement all the way back to the earliest part of my life.

ACKNOWLEDGMENTS

First and foremost I wish to thank my adviser, Dr. Andrew W. Macfarlane, for his guidance and for teaching me the intricacies of the isotope measurements. I also wish to thank the members of my committee, Dr. Grenville Draper, Dr. Rosemary Hickey-Vargas, and Dr. Jennifer L. Gebelein, for their support and understanding.

This research project would not have taken place without the generous support of Serv. Ind. Peñoles and Victor de la Garza who arranged for the field work and collection of the samples I analyzed. The project was also facilitated by Roberto Tellez and Arturo Broca who made the logistical arrangements, and by Sergio Rodriguez who did virtually all of the driving and provided good cheer, local knowledge and geological expertise in equal measure.

Florida International University's Graduate School provided me with the 2008 Doctoral Evidence Acquisition Fellowship and the 2010 Dissertation Year Fellowship which largely made this dissertation research possible. Similarly, support from the College of Arts and Sciences and the Department of Earth and Environment provided teaching assistantships for five years that made my entire PhD career a possibility.

I also wish to thank Dr. V. J.M. Salters and A. Sachi-Kocher for introducing me to the previously mysterious world of Strontium and Neodymium.

I also wish to thank Mike for showing me how to use the advanced feratures of Microsoft Word that made managing the dissertation and its numerous revisions far easier and more efficient.

Last, but not least, I thank all my colleagues and friends, especially Melroy, Julie, Indra, Kevin, Patricio, and Yukari, for their support throughout my years at FIU.

ABSTRACT OF THE DISSERTATION

ISOTOPIC STUDIES OF THE GUERRERO COMPOSITE TERRANE,

WEST-CENTRAL MEXICO: IMPLICATIONS FOR PROVENANCE

OF CRUSTAL ROCKS AND GENESIS OF ORE METALS

by

Adriana Potra

Florida International University, 2011

Miami, Florida

Professor Andrew W. Macfarlane, Major Professor

A variety of world-class mineral deposits occur in Mesozoic and Tertiary rocks of the Guerrero terrane. New Pb isotope analyses of various crustal units and ores from distinct subterranes of the Guerrero terrane are presented to trace metal sources in these deposits and infer source reservoirs. New Sr and Nd isotope results are provided to gain insight into the provenance of the crustal rocks from the Guerrero terrane.

Triassic schist samples from the Arteaga Complex and Triassic-Jurassic phyllite and slate samples from the Tejupilco metamorphic suite contain radiogenic Pb ($^{206}Pb/^{204}Pb$ = 18.701-19.256) relative to bulk earth models. Cretaceous sedimentary rocks of the Zihuatanejo Sequence are more radiogenic ($^{206}Pb/^{204}Pb$ = 18.763-19.437) than samples from the Huetamo Sequence ($^{206}Pb/^{204}Pb$ = 18.630-18.998). Tertiary intrusive rocks from La Verde, Inguaran, La Esmeralda, and El Malacate plot to the right of the average Pb crust evolution curve of Stacey and Kramers ($^{206}Pb/^{204}Pb$ = 18.705-19.033). Ores from the La Verde and La Esmeralda porphyry copper deposits yield isotopic ratios ($^{206}Pb/^{204}Pb$ = 18.678-18.723) that are generally less radiogenic than the host igneous

rocks, but plot within the field defined by the sedimentary rocks from the Huetamo Sequence.

Tertiary intrusive rocks from the Zimapan and La Negra districts in the Sierra Madre terrane plot above and to the right of the Stacey-Kramers reference line ($^{206}Pb/^{204}Pb$ = 18.804-18.972). Lead isotope ratios of ore minerals from the Zimapan and La Negra skarn mines ($^{206}Pb/^{204}Pb$ = 18.775-18.975) resemble those of the associated igneous rocks, implying a magmatic Pb input in the skarn deposits.

New Sr and Nd isotope data on metamorphic rocks ($^{87}Sr/^{86}Sr$ = 0.707757-0.726494 and $^{143}Nd/^{144}Nd$ = 0.512109-0.512653) suggest that the basement of the Guerrero terrane originated from sources that had been derived from an old cratonic area. The narrow ranges and generally low $^{87}Sr/^{86}Sr$ ratios (0.704860-0.705755) and $^{143}Nd/^{144}Nd$ values (0.512765-0.512772) above that of bulk earth for igneous rocks from Inguaran, El Malacate, and La Esmeralda suggest a relatively low degree of crustal contamination. However, the isotopic values for the La Verde site ($^{87}Sr/^{86}Sr$ = 0.708784 and $^{143}Nd/^{144}Nd$ = 0.512640) may indicate the involvement of a more evolved crustal component.

TABLE OF CONTENTS

LIST OF TABLES

TABLE PAGE

LIST OF FIGURES

FIGURE PAGE

1. BACKGROUND

1.1 Introduction

Convergent plate boundaries are the settings of many of the world's largest ore deposits. Although many of these deposits have been well studied, understanding of the sources of ore metals is still incomplete. Of particular interest is the extent to which ore metals represent the addition of new material to the shallow crust from an enriched mantle source at depth, or remobilizations of metals already enriched in the upper crustal rocks. Magmatic-hydrothermal ore deposits, typically associated with subduction-related arc or back-arc magmatism in continental margin settings, represent the most important sources in the western hemisphere of some base and precious metals, including Cu, Pb, Zn, Ag, and Au (Macfarlane, 1999a). It is important to know the provenance of metals in such a setting in order to understand the processes by which they become concentrated into economically viable deposits. Possible metal sources include the mantle, subducted sediments, the lower crust, the upper crust, and slab-derived fluids; in order to evaluate these sources, we need to distinguish as clearly as possible the input from each potential source. Although far from ideal, so far Pb isotopes represent the best available tracer. Lead shares similar complexing and transport chemistry with other ore metals, such as Zn, Cu, and Ag, and different potential metal sources frequently have distinct isotopic signatures, especially in continental arc settings (Macfarlane, 1999a).

Geologically, southwestern Mexico is highly complex, consisting of several adjacent submarine magmatic arc terranes (Figure 1.1) with poorly known basement that appear to have accreted to the North American margin by early Tertiary time (Campa and Coney,

1983). The Guerrero composite terrane of west-central Mexico represents the second largest tectonostratigraphic unit of the Cordilleran collage of North America, after Wrangellia (Centeno-Garcia et al., 1993a). Debate continues over the paleogeographic evolution of this terrane, as well as uncertainty related to the number and precise boundaries of its subterranes. The nature, origin, and evolution of its crustal rocks are also a matter of debate.

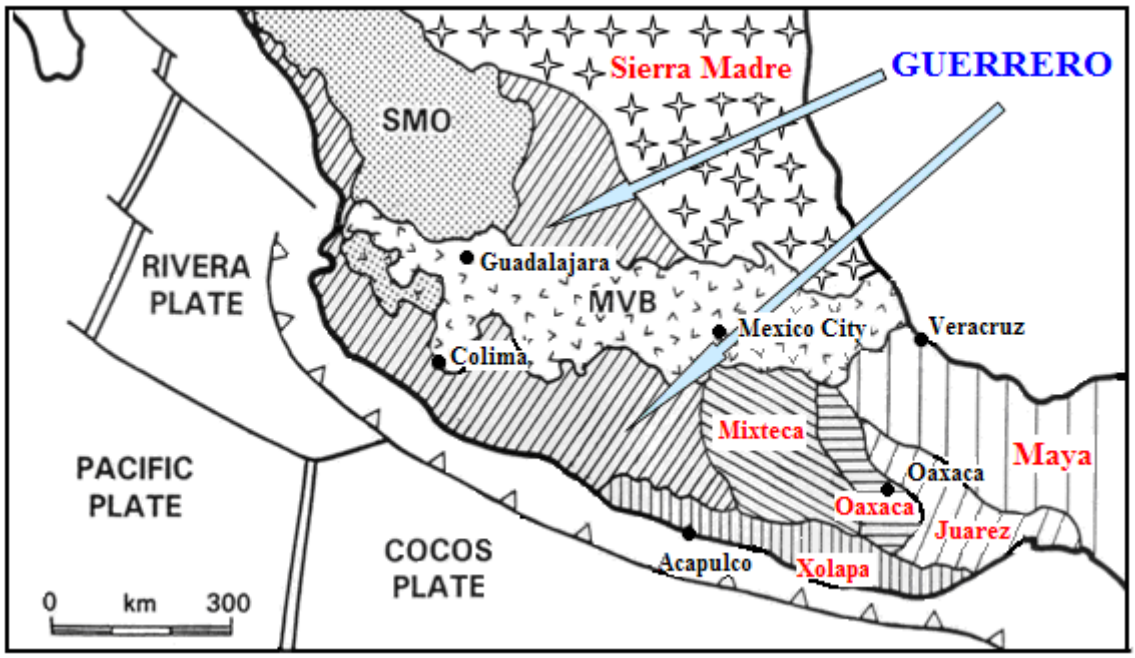

Figure 1.1. Major tectonic features of southwestern Mexico and Pacific Ocean margin. Also shown are the main tectonostratigraphic terranes (Guerrero, Mixteca, Oaxaca, Juarez, Maya, Xolapa, and Sierra Madre) and major volcanic arcs (SMO-Sierra Madre Occidental; MVB-Trans-Mexican Volcanic Belt) (modified after Campa and Coney, 1983).

Some researchers (Centeno-Garcia et al., 1993a; Tardy et al., 1994) argue that they originated in a single intra-oceanic island arc along the Pacific margin, whereas others (Campa and Coney, 1983; Talavera et al., 1993) postulate that they represent remnants of offshore intra-oceanic arcs separated by oceanic basins. Cabral-Cano et al. (2000)

suggested that the Guerrero terrane is a volcanic and sedimentary assemblage deposited on a thinned North American crust that was later deformed by the Laramide orogeny. The suggested timing of the arc-craton collision also varies from Early Cretaceous (Campa et al., 1976; Tardy et al., 1994) to Late Cretaceous (Donnelly and Rogers, 1978; Campa and Coney, 1983; Centeno-Garcia et al., 2008).

The Guerrero composite terrane has produced a large variety of economically important metals (e.g., Ag, Au, Pb, Zn, Cu, and Fe) hosted in Cretaceous and Tertiary ore bodies and generated during three main metallogenetic phases (Miranda-Gasca, 2000). Mineral deposits from the Guerrero terrane can be subdivided into two major groups: the pre-accretion group, formed during the first phase, and the post-accretion group, formed during the second and third metallogenetic phases. The first phase occurred during the Mesozoic and produced volcanogenic massive sulfide (VMS) and sedimentary exhalative (SEDEX) deposits ranging in age from Middle Jurassic (Callovian) to Early Cretaceous (Valanginian; Mortensen et al., 2008). The second phase took place during the Paleocene and was related to the Laramide magmatism in the Sierra Madre Occidental; it produced the Laramide volcanic-plutonic succession of the Lower Volcanic Supergroup (calc-alkaline, granodioritic to granitic batholiths that intrude volcano-sedimentary rocks) and generated porphyry copper deposits between about 53 and 63 Ma (Damon et al., 1983; Miranda-Gasca, 2000; Camprubi et al., 2003). The third phase occurred between around 28 and 36 Ma and was associated with the outpouring of volcanic rocks of the Upper Volcanic Supergroup (silicic ignimbrites, rhyolitic domes, and basaltic to andesitic lavas; Moran-Zenteno et al., 1999) in the Sierra Madre Occidental; it produced porphyry copper

and epithermal deposits of Middle Eocene to Late Oligocene age (Damon et al., 1983; Camprubi and Albinson, 2007).

The VMS and SEDEX deposits represent the earliest phase (Middle Jurassic – Early Cretaceous) and formed as a result of submarine volcanic hydrothermal activity. They are usually associated with juvenile to slightly evolved arc settings, except for a few deposits that occur in a back-arc setting (Mortensen et al., 2008). The VMS and SEDEX are stratabound within volcaniclastic and volcanic rocks, and most of them are of Zn-Pb-Cu Kuroko type (Miranda-Gasca, 2000).

The Cenozoic deposits are generally related to the volcanic activity of the Sierra Madre Occidental province (Staude and Barton, 2001; Camprubi et al., 2003) and include most of Mexico's mineral wealth. Generally, the porphyry copper deposits are between 63 and 33 Ma and have produced important quantities of Cu, W, and Mo (Valencia-Moreno et al., 2007). They formed during the second and third metallogenetic phases. The second phase generated deposits between about 53 and 63 Ma (La Sorpresa and Las Salinas; Damon et al., 1983; Miranda-Gasca, 2000; Camprubi et al., 2003). The third phase produced deposits whose ages range between around 31 and 36 Ma (La Verde, San Isidro, Inguaran, and Tiamaro; Damon et al., 1983; Miranda-Gasca, 2000). The porphyry copper deposits are associated with intrusive rocks of variable composition between granite and diorite, but with a larger abundance of quartz-monzonites (Damon et al., 1983; Miranda-Gasca, 2000; Valencia-Moreno et al., 2007). The epithermal ore deposits, of Middle Eocene to Late Oligocene age, have been the most economically important type of deposit in Mexico, and the Guerrero terrane includes well-known deposits like Guanajuato, Fresnillo, and Zacatecas. They generally occur along the eastern side of the

terrane and are associated with the first bimodal andesitic-rhyolitic volcanic episode of the Upper Volcanic Supergroup of the Sierra Madre Occidental (Camprubi and Albinson, 2007). The Mexican metallogenic provinces of the Sierra Madre Occidental and the Sierra Madre del Sur host base metal-rich (comparable to intermediate sulfidation type) and precious metal-rich (comparable to low sulfidation type) epithermal deposits (Camprubi and Albinson, 2007). The Pacific margin includes many small to moderate sized iron-oxide rich and gold- and copper-bearing skarn and replacement deposits, designated Fe(-Au-Cu) (Miranda-Gasca, 2000).

Considering the diversity of mineral deposits and the complex nature of the composite Guerrero terrane, southwestern Mexico represents an excellent locale to study the effects of terranes and terrane boundaries on the sources of ore metals. I present the results of a comprehensive survey of the Pb, Sr, and Nd isotope compositions of whole rock samples from Mesozoic metamorphic basement rocks, Cretaceous sedimentary rocks, and Tertiary plutons, as well as Pb isotope data of Cenozoic ores from the Guerrero terrane. I also incorporate previously published Pb, Sr, and Nd isotopic data from the literature, chosen from bibliographical compilations by different authors. The objectives of this study are:

● to provide a clearer picture of the potential sources of ore metals in the Guerrero terrane and to determine the role of hydrothermal leaching in the formation of different ore deposits;

● to compare ore Pb isotopes among two adjacent tectonostratigraphic terranes, namely Guerrero and Sierra Madre terranes. For this objective, I analyzed ore samples and the associated igneous rocks collected from the Sierra Madre terrane. The Sierra Madre terrane is considered to rest on a Precambrian basement that was probably accreted to

North America in late Paleozoic due to the collision between North and South America during the opening of Pangea (Stewart, 1988; Yanez et al., 1991);

● to compare ore Pb isotopes of pre-accretion and post-accretion deposits from southern Mexico;

● to gain insight into the nature and provenance of the crustal rocks from the Guerrero composite terrane.

1.2 Isotopic Tracer Studies

1.2.1 Lead

The isotopes ^{238}U, ^{235}U, and ^{232}Th are all radioactive, have different half-lives, and each decay to a different stable isotope of Pb: $^{238}U \rightarrow {}^{206}Pb$, $^{235}U \rightarrow {}^{207}Pb$, and $^{232}Th \rightarrow {}^{208}Pb$ (Faure, 1986). Usually, rocks contain appreciable U and Th; therefore, the measured Pb isotope compositions contain in-situ produced radiogenic Pb. Doe and Zartman (1979) developed a computer program which modeled the Pb isotope evolution of the Earth. They suggested the involvement of three terrestrial reservoirs: upper crust, lower crust, and upper mantle (to 500 km depth). In their computer program, Doe and Zartman modeled orogenies at 400 Ma intervals, based on the evidence that continental accretion started around 4 Ga ago. During the orogenies, portions of pre-existing reservoirs are converted into new upper and lower crust and returned mantle. Initially, all matter resides in the mantle and the first segment of crust is created from it 4 Ga ago. After that, both the mantle and older crust contribute in the generation of new crust during orogenies. Older crust contributions represent erosional processes and crust consumed by overlapping of tectonic provinces and by continental foundering. During an

orogeny Pb, U, and Th are extracted from the three sources, mixed chemically and isotopically, and redistributed into newly formed upper and lower crust and the mantle according to partitioning coefficients. The orogene composition generated by the "plumbotectonics" model was constrained empirically to fit galena ores, and consequent growth curves generated for the other components are presented in Figure 1.2.

The upper crust has a high $^{238}U/^{204}Pb$ ratio. The lower crust consists mostly of pyroxene granulite, or other highly metamorphosed rocks, that have low U contents (0.1 to 1 ppm) and $^{238}U/^{204}Pb$ ratios (0.5 – 5) (Moorbath et al., 1969; Manton and Tatsumoto, 1971). Thorium and Pb contents (1 -10 ppm and 2 – 20 ppm, respectively) are not much lower compared to upper crustal values (Doe and Zartman, 1979). It has been suggested that the preferential depletion of U in the lower crust occurs during major orogenic episodes (Doe and Zartman, 1979). As the crust evolves, the $^{238}U/^{204}Pb$ ratio and the $^{232}Th/^{204}Pb$ ratio (to a lesser extent) are fractionated, so the upper crust produces *in situ* a rather radiogenic Pb in time (Doe, 1970). The most retarded rock Pb for a given geologic age is found within the lower crust of stable Precambrian terranes (Doe and Zartman, 1979). Tholeiitic basalts, which provide the best understanding of the mantle Pb, and mantle-derived ultramafic xenoliths have lower ^{206}Pb and ^{207}Pb compared to most of the continental crust, suggesting that the mantle has been isolated from the continental crust for a long period of geologic time (Doe and Zartman, 1979). The orogenic environment is most obvious in geologically-active island and continental arcs, where tholeiitic basalts, pelagic sediments of the oceanic crust, clastic and chemical detritus of adjacent continental crust, and the lower crustal and mantle material that forms the overlying wedge above subduction zones are all mixed together (Doe and Zartman, 1979).

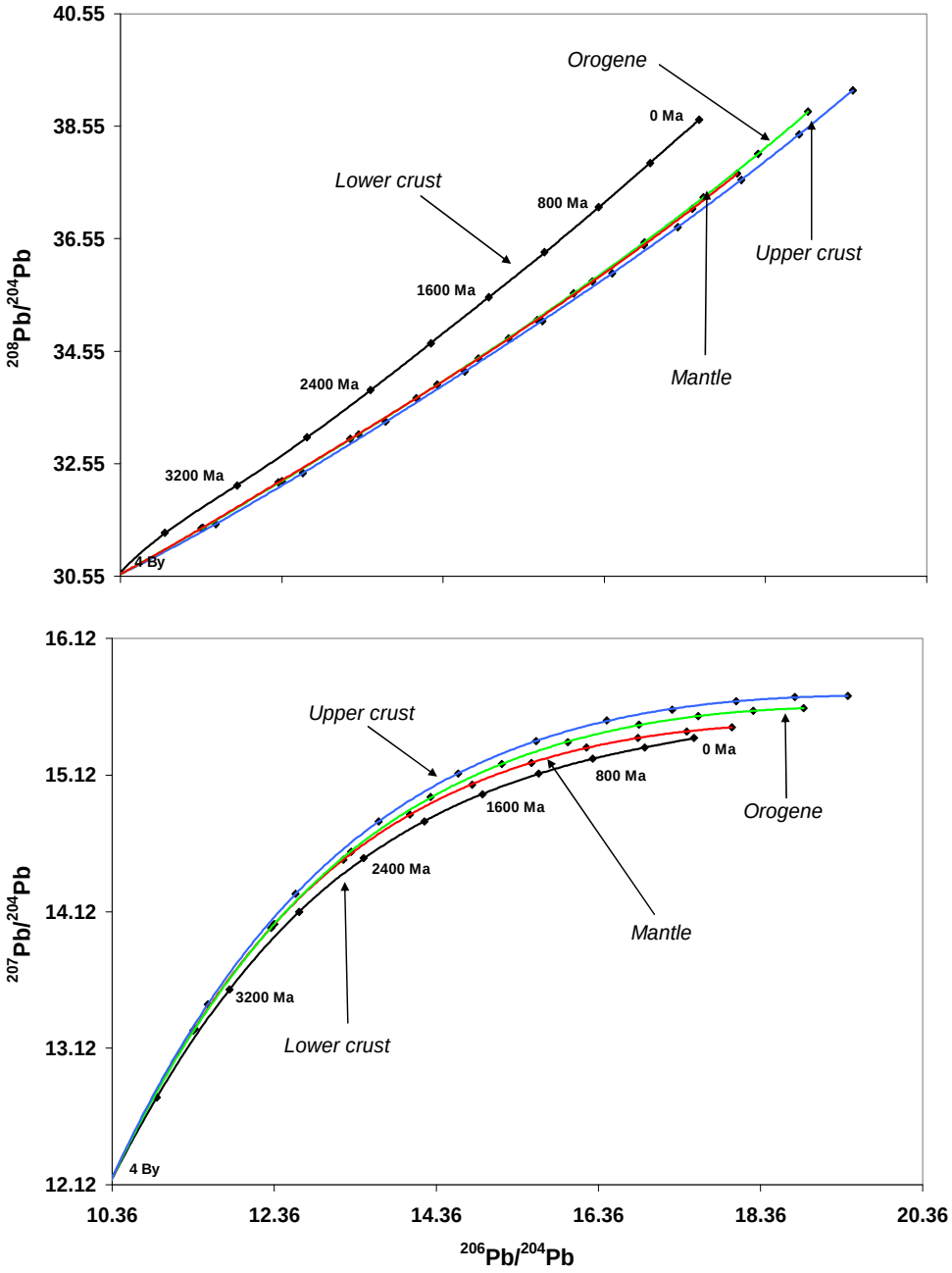

Figure 1.2. Lead isotope evolution curves generated by Doe and Zartman's model (1979) for the mantle, orogene, upper crust contributed to the orogene, and lower crust contributed to the orogene.Marks along the curves indicate progressively older time by 0.4 By increments (modified after Doe and Zartman, 1979). Ending conditions (0 Ma) prevail today at time of final orogeny.

Lead is very useful for identification of metal sources in polymetallic ore deposits. Lead isotope analyses of whole rocks, performed to trace metal sources in ore deposits

and infer source reservoirs in petrogenetic studies, are carried out on the bulk fraction of unaltered rocks (Tilton and Barreiro, 1980; Kamenov et al., 2002; Chiaradia and Fontbote, 2003) or on rock fractions previously leached for short time periods (Sturm et al., 1999; Chiaradia and Fontbote, 2003). Leachates and residua commonly have different compositions from whole rock samples, indicating that fluid leaching may sample different isotopic compositions than bulk assimilation.

Lead isotope compositions of sulfide minerals and rocks associated with an ore deposit can constrain the possible sources of metals in a hydrothermal system, because of the similar geochemical behavior of Pb, Cu, and Zn in hydrothermal fluids (Tosdal et al., 1999) and the occurrence of Pb in the same paragenetic stages as Zn, Cu, Ag, and Cd (Bourcier and Barnes, 1987; Wood et al., 1987). Therefore, Pb reflects the geochemical behavior of ore metals in polymetallic deposits more accurately than radiotracers such as Sr and Nd (Macfarlane, 1989). Lead isotopes are not measurably fractionated by redox reactions in solution or by fluid-mineral interactions; thus, the isotopic composition of Pb in ores is basically similar to that of Pb in its source or sources (Macfarlane, 1989).

It is important to know the provenance of Pb in a hydrothermal ore deposit in order to understand the way Pb, and other associated metals, become concentrated into economically viable deposits. A longstanding problem in understanding ore metal provenance is whether variations in Pb isotope ratios among ore deposits reflect mainly differences in the deep sources of the magmas, or if it is reflected in the shallower crustal sequences where the magmas are emplaced, or a mixture of the two sources (Macfarlane, 1999a; Kamenov, 2000). In the former case, the ore metals are newly added to the upper crust from sources in the mantle wedge or lower crust; in the latter case, the ore metals

are already resident in mostly sedimentary or metamorphic rocks of the upper crust and are remobilized into economic concentrations by magmatic activity (Kamenov, 2000).

Hydrothermal leaching

Crustal lead may be assimilated or hydrothermally leached by a magma. Assimilation can be either from subducted sediments at the magmatic source or from the crust as the magma is passing upward through it (Sillitoe and Hart, 1984; Macfarlane, 1989). Lead may also be hydrothermally leached from host rocks and redeposited in ore minerals (Sillitoe and Hart, 1984; Macfarlane and Petersen, 1990). At elevated temperatures and high acidity, there are reactions between the hydrothermal fluids and the rock matrix through which they pass (Kamenov, 2000). This leads to chemical and isotopic composition of the hydrothermal fluid (and subsequently deposited ore minerals) more or less representative of the metal source (Farmer and DePaolo, 1997).

If hydrothermal leaching of metals from the host rocks plays an important role and the isotope compositions of the host rocks and the associated pluton are different, the isotopic compositions of the ore should be similar to that of the host rocks or reflect mixing between these sources (Macfarlane, 1989; Macfarlane and Petersen, 1990; Kamenov, 2000); in this case, some properties of the upper crustal host rocks, such as their metal content, mineralogy, permeability, and fracturing, will be very important in determining the metal concentration (Macfarlane, 1989).

If hydrothermal leaching of the host rocks is not an important process, the metal budget will be determined by magmatic processes and the Pb isotope compositions of ore and associated pluton at the time of ore formation will be similar (Macfarlane, 1989;

Kamenov, 2000). In this case, assessing the source(s) of metals is more difficult; possible metal sources for continental arc magmas include the subcontinental mantle, the subducted oceanic plate, the continental crust through which the magmas rise, and subducted sediments that may be incorporated into the arc magma at its source (Kamenov et al., 2002).

To determine the source(s) of ore lead it is important to know the Pb isotope compositions of rocks through which the hydrothermal fluid may have flowed (Tosdal et al., 1999). Comparing the Pb isotope ratios of ores from a particular deposit with the associated rocks provides information regarding the possible metal sources and hydrothermal fluid pathways; however, understanding the exact nature and location of these reservoirs is still uncertain (Tosdal et al., 1999; Kamenov et al., 2002). In case of magmatic-related mineral deposits, Pb can be derived from a mixture of magmatic Pb and Pb leached from the host rocks by hydrothermal fluids; the magmatic Pb represents the magmatic common Pb, whereas the leached Pb may be more or less radiogenic compared to the host rock common Pb (Macfarlane and Petersen, 1990). If the system remained closed, the isotopic composition of the magmatic Pb at the time of mineralization can be determined by U-Th correction (Sangster et al., 1998). However, Chiaradia and Fontbote (2003) argued that age-corrected Pb isotope compositions of bulk rocks are not always reliable and easy to perform and suggested that a better way is to determine the Pb isotope compositions of separate leachate and residue fractions. Primary minerals in a rock include silicates and accessory sulfides and oxides formed at the time of rock formation or last recrystallization. Where ore fluids pass through rocks, secondary minerals form and these minerals may consist of exogenous common and radiogenic Pb

introduced after rock formation. The fact that secondary minerals have generally higher solubility than primary minerals enables us to separate Pb introduced into the rock at different times using sequential acid attacks of increasing strength (Chiaradia and Fontbote, 2003). The final signature of the leachate fraction will depend on the relative proportions and isotopic compositions of the exogenous Pb, while the residual fraction will approximate the Pb incorporated by the leach-resistant silicate minerals at the time of their formation or last recrystallization (Chiaradia and Fontbote, 2003).

1.2.2 Strontium and Neodymium

Strontium and Nd isotopes are powerful tracers and are widely used to gain insight into complex problems related to the origin of magma, the formation of igneous rocks, and the evolution of the continental crust from the mantle.

There is a negative correlation between ε_{Nd} and $^{87}Sr/^{86}Sr$ in oceanic and some continental igneous rocks, and it has been suggested (DePaolo and Wasserburg, 1976) that the formation of magma sources in the mantle involved the coupled fractionation of Sm-Nd and Rb-Sr; the continental samples that plot to the right of the main correlation line may have been contaminated by radiogenic Sr from the crust. The MORB (mid-ocean ridge basalt) samples form a relatively tight cluster that defines the upper left-hand corner of the Nd versus Sr isotope diagram (Figure 1.3). The depleted nature (positive ε_{Nd} and negative ε_{Sr} values) of (MORB) source relative to Bulk Earth is complementary to the enriched continental crust. These correlations are consistent with the relative compatibilities of the elements involved: Rb<Sr and Sm>Nd; therefore, mantle regions depleted in incompatible elements have low Rb/Sr that lead to low $^{87}Sr/^{86}Sr$ ratios and

high Sm/Nd that lead to high $^{143}Nd/^{144}Nd$ ratios (Hofmann, 1997). Thus, the upper mantle source regions for MORB have been depleted in materials extracted from the upper mantle and subsequently used to form the continents (Jacobsen and Wasserburg, 1979; O'Nions et al., 1980).

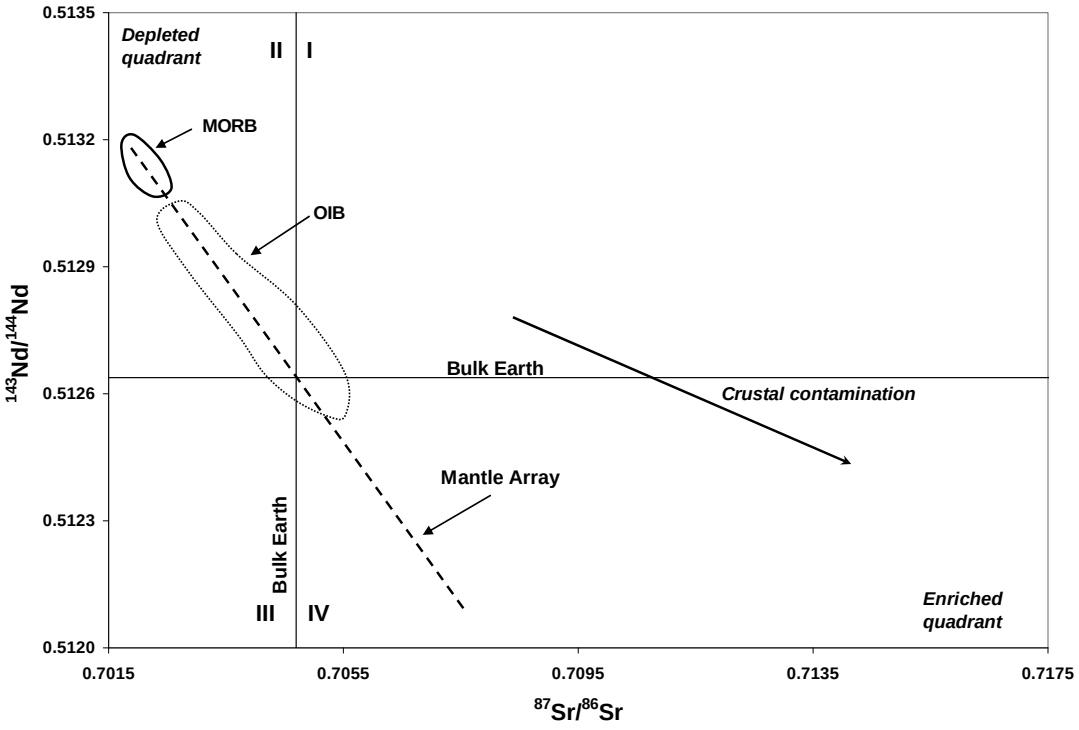

Figure 1.3. Nd versus Sr isotope diagram showing compositional fields for MORB (mid-ocean ridge basalts and OIB (ocean island basalts) and extension of the Mantle Array into the Enriched quadrant relative to Bulk Earth.

The Nd and Sr isotopic values of ocean island basalts (OIB), with higher $^{87}Sr/^{86}Sr$ and lower $^{143}Nd/^{144}Nd$, define a field that plots between the depleted MORB source and the continental crust (Figure 1.3) and imply derivation from a less depleted source compared to that of MORB (DePaolo and Wasserburg, 1979; Hofmann, 1997). The OIB source(s) may be represented by the relatively undepleted lower mantle that is contaminated by

mixing with melts from the depleted MORB source during ascent (DePaolo and Wasserburg, 1979) or they may be the result of back-mixing of various types of continental material into the mantle (Hofmann, 1997). However, the latter sources can not be explained simply by back-mixing because the Pb data do not form a simple trend extending from depleted MORB through OIB to the continental crust (Hofmann, 1997). The presence of two kinds of magma (depleted and undepleted) in the mantle led DePaolo and Wasserburg (1979) to suggest that the array of Nd and Sr isotope ratios of the Mantle Array can be explained by mixing of silicate melts derived from these two sources. However, according to Hawkesworth et al. (1979) and White and Hofmann (1982), the enrichment in radiogenic ^{87}Sr and low $^{143}Nd/^{144}Nd$ of OIBs compared to MORBs may indicate that subducted oceanic or continental crust contributed to their formation.

On their way to the surface, magmas may be contaminated by assimilation of old sialic crustal material, which causes alteration of their isotopic signatures. DePaolo and Wasserburg (1979) suggested that simple two-component mixing on the Sr versus Nd isotope diagram generates hyperbolae whose trajectories depend on the relative Sr/Nd concentration ratio in the two end-members. However, Domenick et al. (1983) implied that the correlation of isotope ratios can also be caused by melting of heterogeneous assemblages of crustal rocks or by mixing of magmas derived from different sources.

2. GEOLOGIC SETTING

2.1.1 General Overview and Isotopic Characteristics of the Crustal Rocks

The accretion of lithospheric fragments to the margin of cratons is a very important process in mountain building (Freydier et al., 2000). In the North American Cordillera, accretion has often involved collision of island arcs with the margin of North America and closure of basins floored by oceanic crust (Freydier et al., 2000). On the basis of petrologic, tectonic, and geochronological differences in the Precambrian and Paleozoic basement, as well as on the petrologic and tectonic nature of Mesozoic terranes bordering the old continental nucleus, it was suggested that southwestern Mexico consists of five tectonostratigraphic terranes: Guerrero, Mixteca, Oaxaca, Juarez, and Xolapa (Figure 1.1; Campa and Coney, 1983). Later, Sedlock et al. (1993) proposed a revision of the tectonostratigraphic terranes division of Campa and Coney (1983) and suggested the following nomenclature: Nahuatl, Mixteco, Zapoteco, Cuicateco, and Chatino terranes. This division is in some respect similar to the previous one, but certain aspects (terrane boundaries, descriptions and interpretations of constituent rocks, terrane-bounding faults) have been changed or clarified.

The Guerrero composite terrane (Figure 2.1) is exposed in the Sierra Madre del Sur, south of the Trans-Mexican volcanic axis (which divides it into two major parts), and makes up most of western Mexico (Campa and Coney, 1983; Mendoza and Suastegui, 2000). North of the volcanic belt, most Guerrero terrane sequences are covered by Tertiary volcanic rocks of the Sierra Madre Occidental and are exposed only along the Pacific coast and in the Guanajuato and Zacatecas areas (Mendoza and Suastegui, 2000).

The Guerrero terrane consists of Late Jurassic (Tithonian)-Late Cretaceous (Cenomanian) volcanic-sedimentary arc sequences, and metamorphic complexes exposed in certain areas (e.g., Arteaga Complex, Placeres Complex, Pinzan Morado Complex, Tejupilco metamorphic suite, and Zacatecas Formation) may represent their basement rocks (Centeno-Garcia et al., 1993a; Mendoza and Suastegui, 2000; Elias-Herrera et al., 2000; Centeno-Garcia and Silva-Romo, 1997).

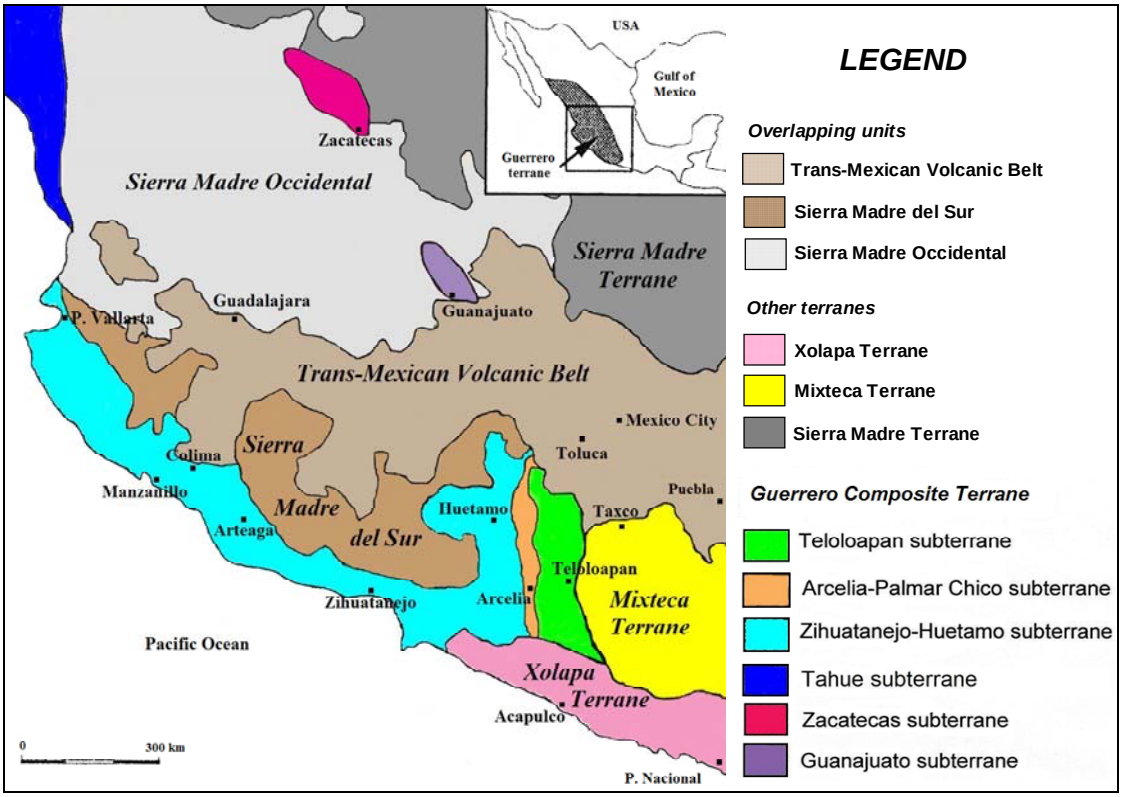

Figure 2.1. Schematic sketch of south-western Mexico showing the main magmatic provinces in Mexico (Sierra Madre Occidental, Sierra Madre del Sur, and the Trans-Mexican Volcanic Belt), the tectonostratigraphic terranes adjacent to the Guerrero terrane (Xolapa, Mixteca, and Sierra Madre terranes), and the distribution of the six subterranes that belong to the Guerrero composite terrane (modified after Mendoza and Suastegui, 2000; Mortensen et al., 2008; Centeno-Garcia et al., 2008).

The eastern portion of the Guerrero terrane was thrust against the Cretaceous calcareous Morelos-Guerrero platform of the Mixteca terrane in Laramide time (Campa

and Coney, 1983). The northeastern border is represented by continental margin strata of the Sierra Madre terrane (Figure 2.1; Mendoza and Suastegui, 2000; Mortensen et al., 2008). Although the Guerrero terrane underlies most of western Mexico, the Mesozoic submarine volcano-sedimentary assemblages outcrop over less than five percent of its surface, represented by erosional windows within the Cenozoic volcanic and sedimentary strata of the Sierra Madre Occidental, Sierra Madre del Sur, and Trans-Mexican volcanic belt (Mortensen et al., 2008).

On the basis of differences in the dominant lithological assemblages, geochemical and isotopic characteristics, and inferred depositional ages, the Guerrero terrane has been subdivided into several subterranes; according to the latest subdivision (Mortensen et al., 2008; Centeno-Garcia et al., 2008), they are represented by the Zihuatanejo-Huetamo, Arcelia-Palmar Chico, and Teloloapan subterranes, situated south of the Trans-Mexican volcanic belt, and the Tahue, Guanajuato and Zacatecas subterranes, located north of the volcanic axis (Figure 2.1).

2.1.1.1 Pre-accretional Characteristics

The eastern ***Teloloapan subterrane*** (Figure 2.1) is a 100 km wide and 300 km long N-S trending belt that is thrust over Albian carbonates and older clastic strata of the Mixteca terrane in a Laramide low-angle thrust fault (Campa and Coney, 1983; Mendoza and Suastegui, 2000; Mortensen et al., 2008). The lithostratigraphic column consists of a more than 3000 m thick succession of lavas (basalts, 85 %; andesites, 10 %; dacites-rhyolites, 5 %) and pillow breccias that are interbedded in the lower levels with Early Cretaceous radiolarian siliceous sediments and, toward the top, with volcanic

conglomerate, debris flow deposits, and reefal limestones containing Aptian fauna (Mendoza and Suastegui, 2000). This column is capped by around 1500 m of Albian to Early Cenomanian sedimentary cover, represented by greywacke, tuffaceous shale, reefal and bioclastic limestone, flysch-like sandstone, and shale (Figure 2.2; Campa and Ramirez, 1979; Centeno-Garcia et al., 1993b; Mendoza and Suastegui, 2000).

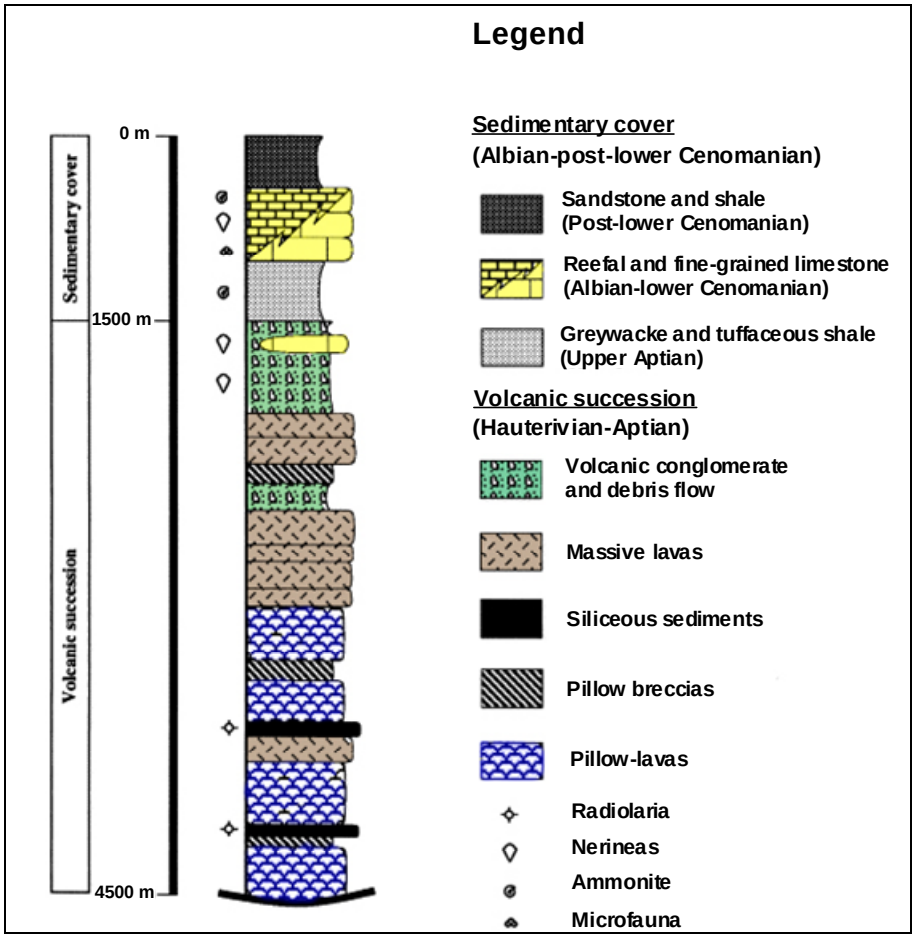

Figure 2.2. Generalized lithostratigraphic column of the Teloloapan subterrane showing paleontologically and radiometrically dated horizons (after Guerrero et al., 1990; Mendoza and Suastegui, 2000).

The lavas are enriched in LFSE (low-field strength elements) and LREE (light rare-earth elements), and show an important negative anomaly in Nb, Zr, and Ti typical of

subduction-related suites (Mendoza and Suastegui, 2000). Previously published (Talavera et al., 1995) Sr and Nd isotope data of Early Cretaceous basalts and andesites of island arc calc-alkaline affinity collected from the eastern Teloloapan subterrane (Figure 2.3) are similar to values noticed in some present-day evolved intra-oceanic island arcs (e.g., the Sunda arc and the Lesser Antilles arc) (Mendoza and Suastegui, 2000, and references therein).

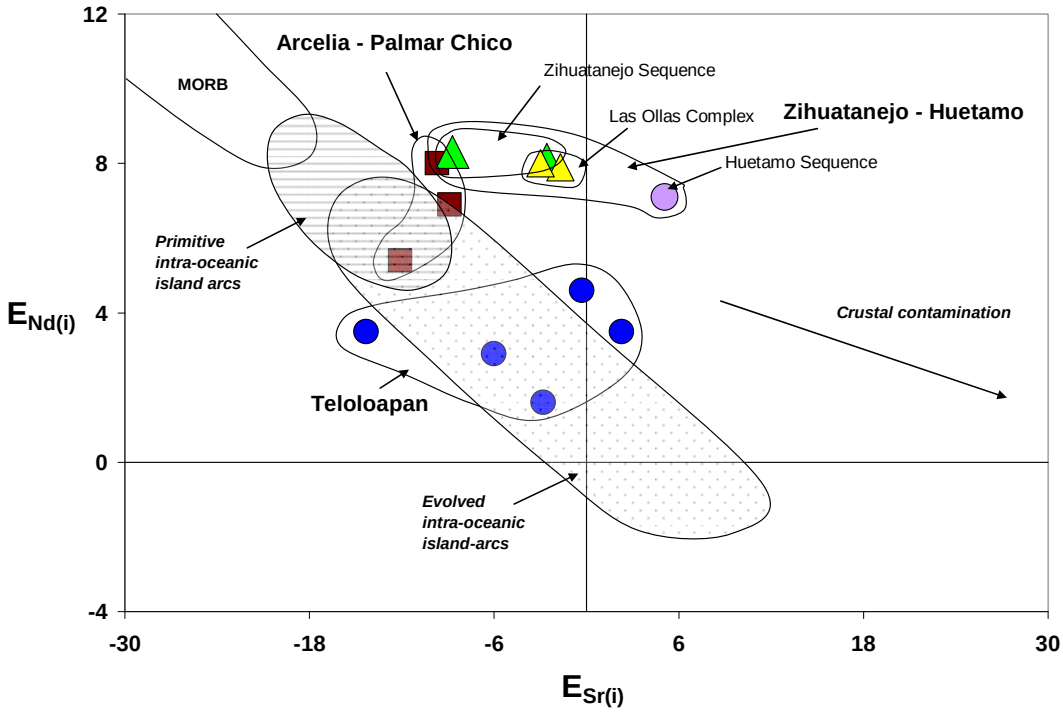

Figure 2.3. Generalized isotopic diagram showing the ε_{Nd} and ε_{Sr} values for J-K arc-related sequences of the Teloloapan, Arcelia-Palmar Chico, and Zihuatanejo-Huetamo subterranes. Typical fields of MORB and primitive and mature island arcs are also shown. Data for the Teloloapan subterrane are from Talavera et al., 1995, for the Arcelia-Palmar Chico subterrane from Tardy et al., 1994, and for the Zihuatanejo-Huetamo subterrane from Freydier et al., 1993. Initial ε_{Nd} and ε_{S} ratios were recalculated at 110 Ma (modified after Mendoza and Suastegui, 2000).

Epsilon Nd values are lower compared to those recorded in entirely intra-oceanic calc-alkaline series (e.g., Aleutian arc), but are typical to high-K calc-alkaline rocks of

evolved island arcs where magma has incorporated subducted sediment (e.g., Indonesian arc) (Mendoza and Suastegui, 2000, and references therein). Epsilon Sr values fall within the mantle array (Mendoza and Suastegui, 2000). It has been suggested (Tardy et al., 1994) that the lower ε_{Nd} values of the Teloloapan calc-alkaline basalts may be due to contamination of the mantle source by subducted Paleozoic sediments or by old source enrichments (OIB source). The lavas contain metamorphic assemblages characteristic of the zeolite through prehnite-pumpellyite to greenschist facies produced by seafloor-type metamorphism (Talavera, 1993). Talavera (1993) and Mendoza and Suastegui (2000) suggested that the Teloloapan subterrane represents an evolved intra-oceanic island arc of Early Cretaceous (Hauterivian) to Late Cretaceous (Cenomanian) age.

The *Tejupilco metamorphic suite*, exposed in the Tejupilco-Taxco region, represents basement for this subterrane (Elias-Herrera et al., 2000). The suite consists of more than 2000 m thick greenschist facies metamorphic rocks and a mylonitic augen gneiss of granitic composition called the Tizapa metagranite (Elias-Herrera et al., 2000). Available Nd (initial ε_{Nd} of -3.5, and depleted mantle Nd model ages of 1.27 Ga) and Sr (initial $^{87}Sr/^{86}Sr$ of 0.7078) isotope data for the Tejupilco metamorphic suite (Figure 2.4) suggest inherited Precambrian zircon in the basement unit, implying that Tejupilco metavolcanics may represent an evolved volcanic arc developed on old crust which assimilated craton-derived sediments (Elias-Herrera et al., 2000). This area is characterized by the presence of the Tizapa VMS deposit (Kuroko-type), with more than five million tons of polymetallic ore (Elias-Herrera et al., 2000), hosted by deformed phyllite and schist of the Teloloapan subterrane (Lewis and Rhys, 2000). Based on U-Pb zircon age of the Tizapa metagranite and Pb/Pb isotopic model ages of the associated Tizapa massive

sulfide deposit, a Late Triassic (Carnian) to Early Jurassic age has been assigned for rocks of the Tejupilco metamorphic suite (Elias-Herrera et al., 2000).

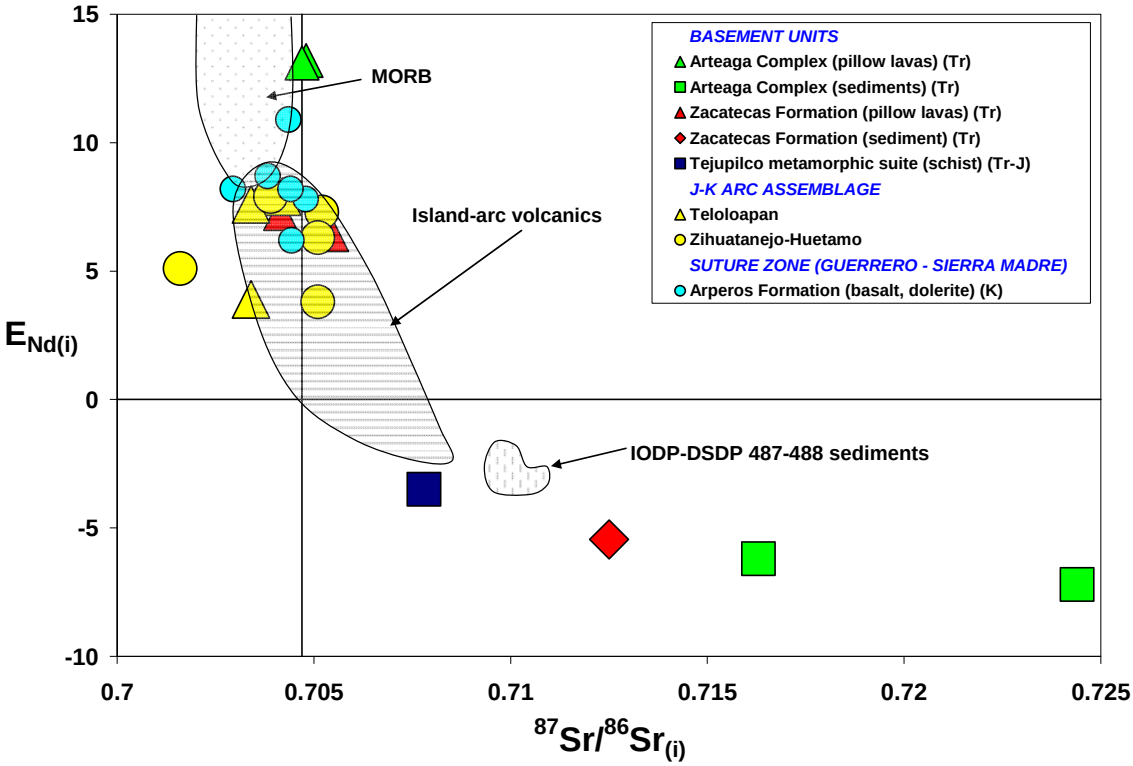

Figure 2.4. Generalized isotopic diagram showing the initial ε_{Nd} values and initial $^{87}Sr/^{86}Sr$ ratios for basement units, J-K arc assemblages, and rocks of the suture zone from the Guerrero terrane. Data for the Arteaga Complex and J-K arc assemblages are from Centeno-Garcia et al. (1993), for the Zacatecas Formation from Centeno-Garcia and Silva-Romo (1997), for the Tejupilco metamorphic suite from Elias-Herrera et al. (2003), for the Arperos Formation from Freydier et al. (1996), and for IODP-DSDP 487-488 sediments from Verma (2000). Initial ε_{Nd} and $^{87}Sr/^{86}Sr$ ratios were recalculated with ages of 225 Ma for the Arteaga Complex, 100 Ma for the J-K arc assemblage, and 110 Ma for the Arperos Formation.

The central ***Arcelia-Palmar Chico subterrane*** (Figure 2.1) is an approximately 40 km wide and 250 km long N-S trending belt that is thrust over the Teloloapan subterrane along a low-angle Laramide fault (Mendoza and Suastegui, 2000). The lithostratigraphic column (Figure 2.5) is around 2000 m thick and consists mostly of pillowed mafic volcanic rocks of arc tholeiite compositions. The volcanic rocks are interlayered with and

covered by pelagic shale and radiolarian-rich siliceous sediments that indicate deposition in a relatively deep water environment; the volcanic rocks are intruded by many sub-parallel and narrow (30 – 60 cm wide) dikes of doleritic basalt and microgabbro (Mendoza and Suastegui, 2000).

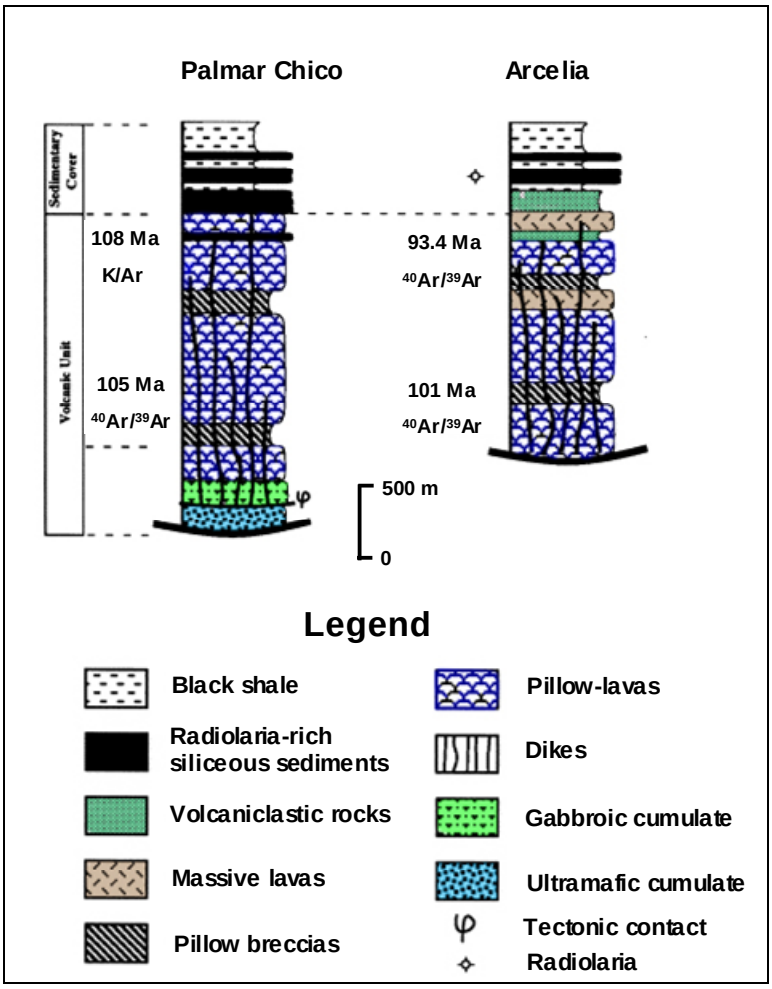

Figure 2.5. Generalized lithostratigraphic columns of the marginal basin and arc assemblages of the Arcelia-Palmar Chico subterrane showing paleontologically and radiometrically dated horizons (after Mendoza and Suastegui, 2000).

On the basis of the radiolarians contained in the chert layers, an Early Cretaceous (Albian) to Late Cretaceous (Cenomanian) age is inferred for the subterrane (Davila and

Guerrero, 1990). Rocks from the Arcelia-Palmar Chico subterrane have been metamorphosed to prehnite-pumpellyite facies by hydrothermal ocean floor metamorphism (Ortiz-Hernandez and Lapierre, 1991; Talavera, 1993).

Available Sr and Nd isotope data (Tardy et al., 1994) on Late Cretaceous basalts of ocean island basalt and island arc tholeiite affinities from the Arcelia-Palmar Chico subterrane (Figure 2.3) imply the least evolved magmatism among all the subterranes that belong to the Guerrero terrane. Palmar Chico shows isotopic characteristics encountered in some present-day immature intra-oceanic island-arc suites (e.g., Aleutian arc or New Britain arc), while Arcelia has isotopic signatures found in many arc-related marginal basins (e.g., Mariana back-arc basin or North and South Fiji basins) (Mendoza and Suastegui, 2000, and references therein). Some authors (Talavera, 1993; Mendoza and Suastegui, 2000) concluded that Palmar Chico (western part) is an immature intra-oceanic island arc associated with a back-arc oceanic basin represented by Arcelia (eastern part); others (Centeno-Garcia et al., 2003) suggested that it is a back-arc basin of the Zihuatanejo-Huetamo subterrane.

The western ***Zihuatanejo-Huetamo subterrane*** (Figure 2.1), along the Pacific coast, is the most extensively exposed Guerrero subterrane, and comprises three different lithological assemblages: the Zihuatanejo volcanic-sedimentary sequence, the Las Ollas Complex, and the Huetamo sedimentary sequence (Ramirez-Espinosa et al., 1991; Talavera et al., 1993; Mendoza and Suastegui, 2000).

The undeformed *Zihuatanejo Sequence* (Early Cretaceous), exposed between Zihuatanejo and Colima, consists of around 1500 m of andesitic to dacitic lava flows that are interbedded in the lower part with volcaniclastic turbidites and in the upper part with

acidic ignimbrites and fall-out deposits (Mendoza and Suastegui, 2000). The volcanic sequence is covered by roughly 500 m of reefal limestones containing Albian fauna and red beds with dinosaur footprints (Figure 2.6; Mendoza and Suastegui, 2000).

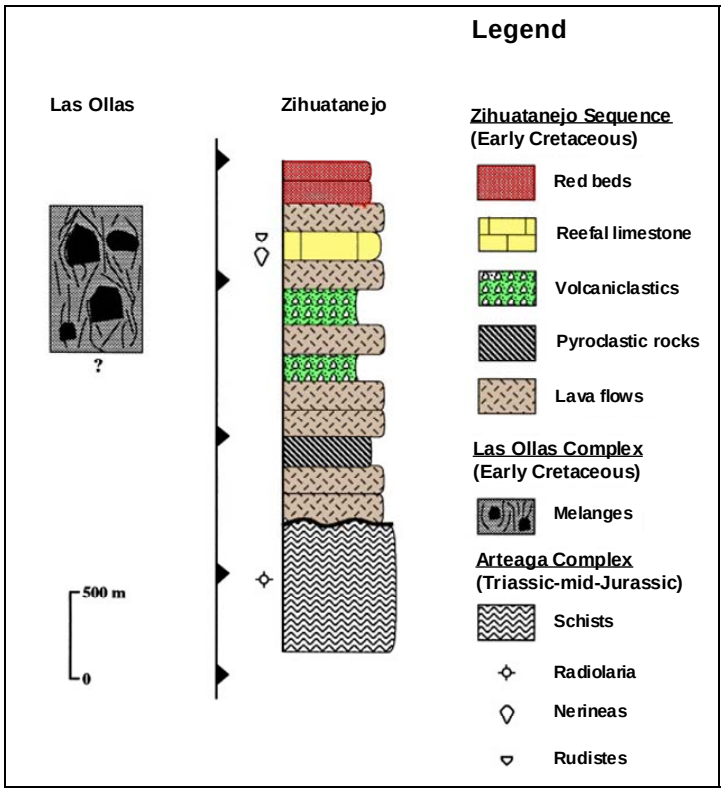

Figure 2.6. Schematic lithostratigraphic columns of the Zihuatanejo volcano-sedimentary Sequence and the Las Ollas Complex showing paleontologically and/or radiometrically dated stratigraphic levels (after Mendoza and Suastegui, 2000).

The volcanic arc products contain secondary assemblages of greenschist to amphibolite facies, the result of thermal metamorphism related to the mid-Tertiary intrusions. The geochemical signatures of the lava flows are similar to those encountered in subduction-related tholeiitic and calc-alkaline magmatic suites: important negative anomalies in Zr and Ti, enrichment in LFSE and depletion in HFSE (high-field strength

elements) relative to N-MORB, and enrichment in LREE relative to HREE (heavy rare-earth elements) (Mendoza and Suastegui, 2000).

Previously published ε_{Nd} values of Early Cretaceous andesites of island arc calc-alkaline affinity from the Zihuatanejo Sequence (Mendoza and Suastegui, 2000) are relatively high, typical of intra-oceanic arc suites, and ε_{Sr} are moderate (Figure 2.3); overall, they define a field typical to arcs that have incorporated crustal material during magma evolution (Mendoza and Suastegui, 2000). However, according to Freydier et al. (1997) the slightly shifted ε_{Sr} values to the right of the mantle array may be due to alteration and they consider a depleted mantle source for the genesis of the Zihuatanejo magmas, without the involvement of crustal material.

The *Las Ollas Complex* (Early Cretaceous), recognized in areas around the town of Zihuatanejo (Figure 2.1), is made up of tectonic slices of tholeiitic arc-derived blocks metamorphosed to blueschist facies enveloped in a matrix of flysch and serpentinite (Mendoza and Suastegui, 2000) (Figure 2.6). It is interpreted to be the subduction complex of the Cretaceous arc (Mendoza and Suastegui, 2000). Blocks within the complex include gabbro, basalt, ultramafic rocks, volcaniclastics, amphibolite, and dolerite (Mendoza and Suastegui, 2000). All samples are enriched in LFSE relative to N-MORB and resemble present-day immature island-arc tholeiitic suites (Pearce, 1983). Previously published (Talavera, 2000) Sr and Nd isotope data of a basalt and a gabbro of island arc tholeiite affinity from the Early Cretaceous Las Ollas Complex are typical of intra-oceanic arc suites and are similar to the isotopic signatures of rocks from the Zihuatanejo Sequence (Figure 2.3), suggesting that the blocks have been derived from a mantle source similar to that of the Zihuatanejo lavas (Mendoza and Suastegui, 2000).

The Copper King VMS deposit (Cu- and Zn-rich) is hosted by this complex (Mortensen et al., 2008).

The undeformed *Huetamo Sequence* (Late Jurassic – Late Cretaceous), exposed in the Huetamo area, consists of a thick succession of around 4500 m of mainly sedimentary rocks (Figure 2.7) deposited in a basin situated in a back-arc position to the east of the Zihuatanejo arc massif (Mendoza and Suastegui, 2000). The base of the sedimentary cover is made up of Tithonian volcaniclastic apron deposits, siliceous sediments, and pillow basalts; the medial part consists of Neocomian volcaniclastic turbidites, and the top of the sequence has Aptian to Cenomanian reefal limestones and red beds (Pantoja, 1959). Conglomerate layers with abundant lava blocks are present throughout the whole sedimentary sequence. The lavas show a temporal variation: basaltic rocks are found in the lower units, clinopyroxene+amphibole-bearing andesites are common in the middle part, and plagioclase-rich andesites and dacites form conglomeratic units in the upper stratigraphic levels (Mendoza and Suastegui, 2000). The volcanic blocks tend to show increasing LREE- and LFSE-enrichment relative to N-MORB from the bottom of the sequence to the top; all samples show negative anomalies in Zr and Ti, indicating provenance from an island-arc source (Mendoza and Suastegui, 2000). Isotopic values of one Cretaceous basalt from the Huetamo Sequence (Mendoza and Suastegui, 2000) show an island arc affinity and plot quite far to the right of the mantle array (Figure 2.3). These patterns are similar to those reported for the New Britain arc of Papua New Guinea or for the Mariana arc (Mendoza and Suastegui, 2000, and references therein). Campa and Ramirez (1979) suggested that the sedimentary rocks of the Huetamo Sequence lie

unconformably on a metamorphosed basement represented by the Pinzan Morado Complex (Figure 2.7).

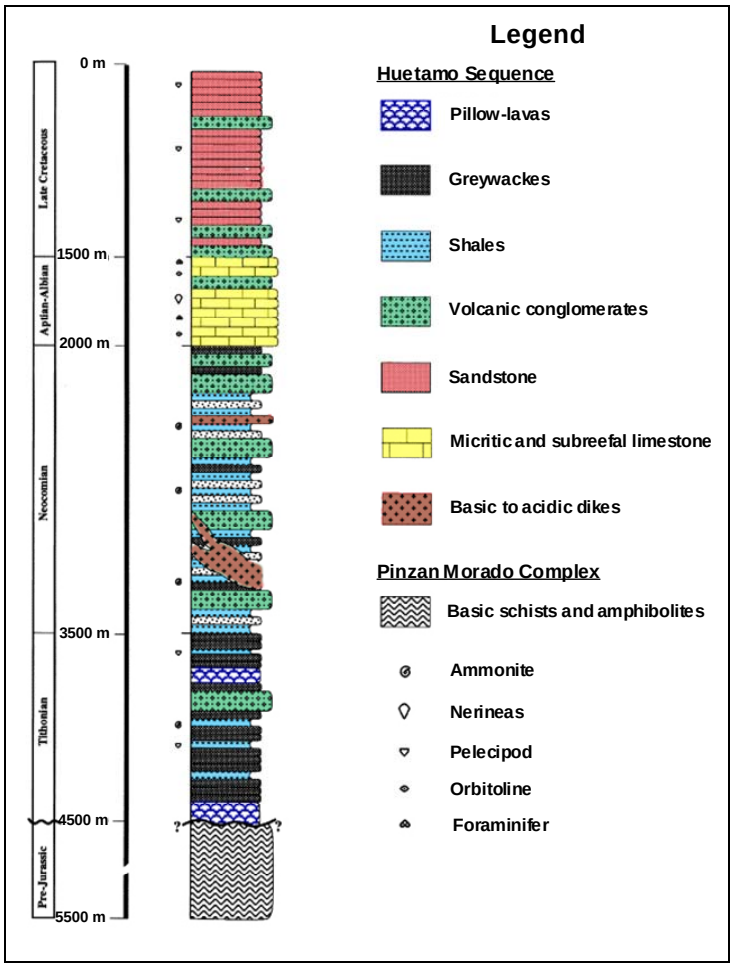

Figure 2.7. Lithostratigraphic column of the Huetamo Sequence (after Pantoja, 1959; Mendoza and Suastegui, 2000).

On the basis of the above-mentioned characteristics, Centeno-Garcia et al. (1993a) and Mendoza and Suastegui (2000) suggested that the Zihuatanejo-Huetamo subterrane represents a complex assemblage of Late Jurassic-Late Cretaceous age made up of an

evolved island-arc (Zihuatanejo Sequence), a basin located in the back-arc position (Huetamo Sequence), and a subduction complex (Las Ollas Complex).

The arc-related sequences of the Zihuatanejo-Huetamo subterrane were deposited on the highly deformed and moderately metamorphosed (greenschist facies) *Arteaga Complex*, exposed around the Arteaga area (Figure 2.1). The Arteaga Complex includes terrigenous siliciclastic sediments (black shale, quartzitic sandstone, and black chert) grouped into the Varales Formation; within this formation there are blocks of basaltic pillow lavas, chert, and limestone interbedded with tuffaceous sandstone that give the complex a "block-in-matrix" appearance (Centeno-Garcia et al., 1993a). According to Centeno-Garcia et al. (1993b), the Pinzan Morado Complex may be correlated with the Arteaga Complex.

Available Sr and Nd isotope data for sandstones from the Varales Formation, part of the Arteaga Complex, show very radiogenic initial $^{87}Sr/^{86}Sr$ (0.7163 and 0.7244) and negative initial ε_{Nd} (-6.2 and -7.2) (Centeno-Garcia et al., 1993a) (Figure 2.4). Depleted mantle Nd model ages for the sedimentary rocks of this formation are 1.3 and 1.4 Ga (DePaolo, 1981), indicating derivation from an evolved continental source (Centeno-Garcia et al., 1993a). Most of the pillow lavas from the Arteaga Complex yield Sr and Nd isotopic values that plot close to the field defined by MORB, suggesting that at least part of the Zihuatanejo-Huetamo subterrane includes oceanic crust (Centeno-Garcia et al., 1993a). Initial ε_{Nd} values (+13) of the basaltic pillow lavas are typical of MORB, whereas initial $^{87}Sr/^{86}Sr$ (0.7047) are more radiogenic than MORB (Figure 2.4), possibly a result of postmagmatic alteration (Centeno-Garcia et al., 1993a). These results are consistent with formation of the Arteaga Complex from MORB which was overlain by sediments

derived from a cratonic area; the cratonic area has similar isotopic characteristics to those recorded in the Acatlan and Oaxaca Complexes (basement rocks of the Mixteca terrane and Oaxaca terrane, respectively) that have published Nd model ages of around 1.4 Ga (Ruiz et al., 1988b; Yanez et al., 1991; Centeno-Garcia et al., 1993a). The Late Permian age of the youngest detrital zircons combined with the presence of Triassic radiolaria found in cherts suggest an approximate Permo-Triassic depositional age for the Arteaga Complex (Campa et al., 1982; Centeno-Garcia et al., 2003). The Pb-rich Arroyo Seco VMS deposit occurs in this area and is entirely hosted within carbonaceous shales and sandstones (Mortensen et al., 2008).

As noted, the arc suites of the Guerrero terrane located south of the Trans-Mexican Volcanic Belt are separated by marginal basins: the Teloloapan calc-alkaline suite is separated from the Palmar Chico tholeiitic suite by the Arcelia back-arc basin, which consists of BABB (back-arc basin basalt) and OIB (ocean island basalt) assemblages; the Palmar Chico suite is separated from the Zihuatanejo calc-alkaline suite by the Huetamo marginal basin (Mendoza and Suastegui, 2000). Although both Teloloapan and Zihuatanejo consist of calk-alkaline lavas, they differ chemically and isotopically; the situation is similar in case of the tholeiitic volcanics of Palmar Chico, Huetamo, and Las Ollas assemblages (Mendoza and Suastgui, 2000).

The ***Guanajuato subterrane*** (Figure 2.1), located at the boundary between the arc-related rocks of the Guerrero terrane and the platform carbonates of the Sierra Madre terrane (Freydier et al., 2000), consists of two components: a package of deep-water sedimentary rocks and associated mafic volcanic rocks known as the *Arperos Formation*, and the *Guanajuato arc*, which was locally thrust eastward over the Arperos Formation

(Mortensen et al., 2008). The Guanajuato arc consists of a juvenile arcassemblage of mafic to felsic volcano-sedimentary rocks (Mortensen et al., 2008) that was metamorphosed to greenschist facies (Ortiz-Hernandez et al., 1992). The Arperos Formation, of Late Jurassic - Early Cretaceous fossil age (Freydier et al., 1996; Ortiz-Hernandez et al., 2003), comprises an assemblage of deep-water sedimentary rocks and mafic igneous rocks (basalts and dolerites) that underlie and are interlayered with the sedimentary strata (Figure 2.8) (Freydier et al., 1996); they underwent prehnite-pumpellyite facies metamorphism (Ortiz-Hernandez et al., 1990).

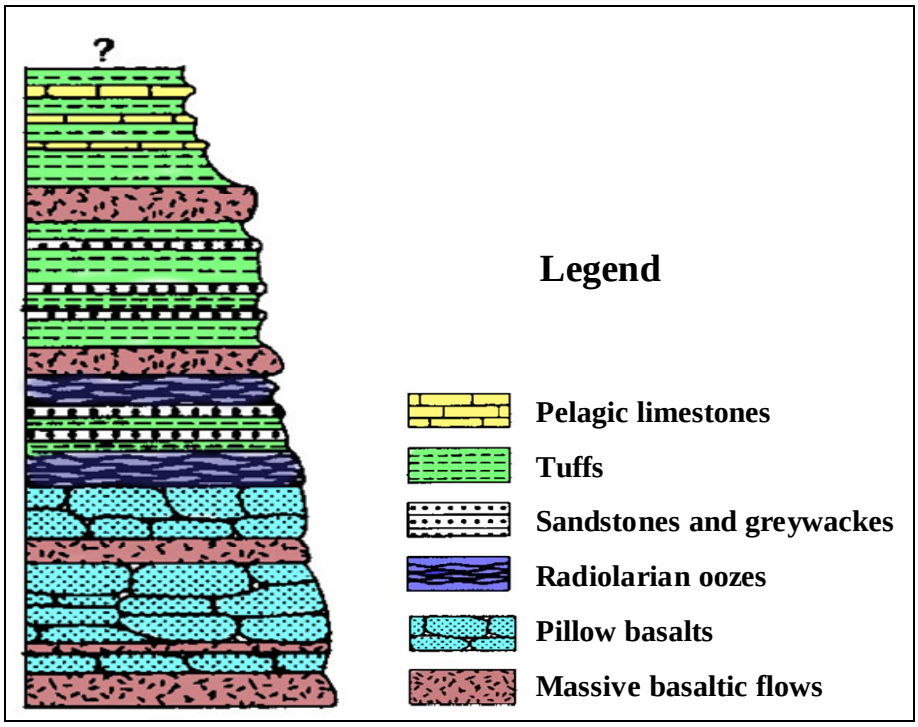

Figure 2.8. Simplified lithostratigraphic column of the sequence from the Arperos Formation, part of the Guanajuato subterrane (after Freydier et al., 1996).

Cretaceous igneous rocks from the Arperos Formation yield positive initial ε_{Nd} values between around +6 and +11 (Figure 2.4) and show geochemical characteristics similar to

oceanic island tholeiites (OIT), with transitional features between OIB and N-MORB (Freydier et al., 1996). An age of 110 Ma has been considered to calculate the initial Nd ratios, in agreement with the Early Cretaceous age of the sediments associated with these igneous rocks (Davila-Alcocer and Martinez-Reyes, 1987). The chemistry of the sedimentary rocks changes according to the location in the stratigraphic column and reflects the sources from which they have been derived: slight enrichment in LREE and ε_{Nd} of around +7 at the base, depletion in LREE and ε_{Nd} of around +9 in the middle part, and enrichment in LREE and ε_{Nd} of around +1.3 in the uppermost part (Freydier et al., 2000). The evolution with time in the chemistry of the Arperos sediments has been interpreted by Freydier et al. (2000) to reflect the approach of the Guerrero juvenile arc to nuclear Mexico: in the incipient stages, the basin was filled with sediments from the ocean floor and/or the arc, and later on with more evolved sources, possibly derived from nuclear Mexico.

The nature of the Arperos basin has been a matter of debate. Some researchers (Tardy et al., 1994; Freydier et al., 1996 and 2000) consider that it represents an oceanic suture zone between the carbonate platforms of the Sierra Madre terrane (part of nuclear Mexico) to the east and the accreted Guerrero terrane to the west; they suggest that the Arperos oceanic basin was subducting under the Pacific plate (west-dipping subduction zone) leading to the Guerrero arc growth. Other investigators (Elias-Herrera and Ortega-Gutierrez, 1998) imply that it is rather a back-arc basin formed in response to east-dipping subduction. It has been suggested (Tardy et al., 1994) that arc activity began with the development of the Early Cretaceous low K-tholeiitic mafic suite of the Guanajuato arc.

Epigenetic base and precious metal deposits (e.g., Guanajuato) have been mined in this subterrane for at least four centuries, but the VMS deposits (e.g., Guanajuato) have only recently been discovered (Mortensen et al., 2008). These latter deposits are hosted within rocks of the Guanajuato arc assemblage (Mortensen et al., 2008).

The ***Zacatecas subterrane*** (Figure 2.1) consists of two major lithological associations: a basement unit called the *Zacatecas Formation* and another assemblage, the *La Borda Formation*, which tectonically overlies this basement, the contact between them being thrust faulted (Figure 2.9) (Centeno-Garcia and Silva-Romo, 1997; Mortensen et al., 2008).

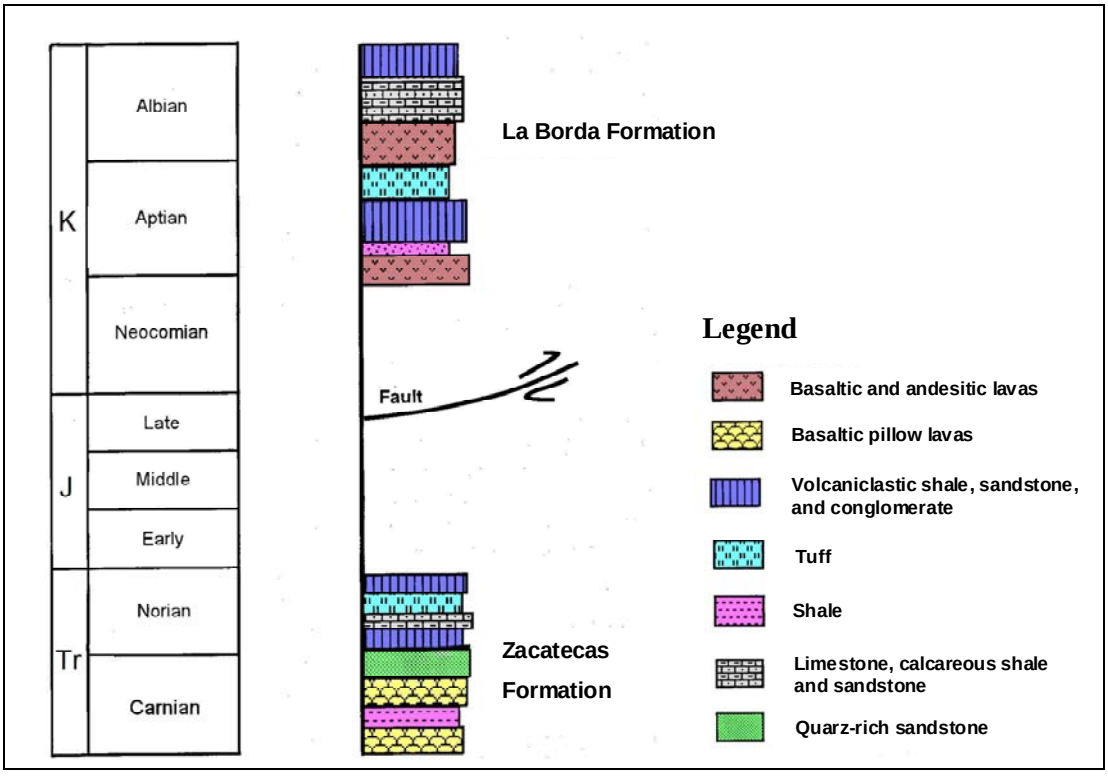

Figure 2.9. Simplified lithostratigraphic column of the sequence from the Zacatecas area (after Centeno-Garcia and Silva-Romo, 1997).

The Zacatecas Formation (Figure 2.9), located at the boundary between the Guerrero and Sierra Madre terranes, is a greenschist metamorphosed clastic-volcaniclastic unit (member A) consisting of alternating shale, quartz-rich sandstone, tuff, limestone, and basaltic pillow lava (Ranson et al., 1982). Tectonically intercalated with member A are thick layers of volcaniclastic rocks and volcanic breccias grouped in member B (Centeno-Garcia and Silva-Romo, 1997). On the basis of the fossil content of ammonoids, a Late Triassic age has been suggested for the Zacatecas Formation (Burckhardt and Scalia, 1906).

Previously published isotopic data on Late Triassic basaltic pillow lavas from the Zacatecas Formation yield initial ε_{Nd} values ranging from +6.4 to +7.2 (Figure 2.4); they plot near the depleted mantle array and are typical of primitive island arc basalts, suggesting little or no crustal contamination (Centeno-Garcia and Silva-Romo, 1997). However, sandstone samples from the Zacatecas Formation show initial ε_{Nd} of -5.5 and Nd model age of 1.3 Ga, indicating derivation from an old continental source (Centeno-Garcia and Silva-Romo, 1997). According to the MORB affinity of the basaltic pillow lavas, Centeno-Garcia and Silva-Romo (1997) suggested that member A of the Zacatecas Formation represents a deformed and partially metamorphosed ocean-floor assemblage.

It is not clear yet whether this formation represents the basement of the northeastern Guerrero terrane; there are petrological similarities with the Arteaga complex which support their correlation (Centeno-Garcia and Silva-Romo, 1997). It has been suggested that the Zacatecas Formation was accreted to the Sierra Madre terrane along with the Cretaceous arc of the Guerrero terrane by Late Cretaceous time (Centeno-Garcia and Silva-Romo, 1997).

The La Borda Formation (Figure 2.9) is made up of andesitic to basaltic lava flows interbedded with volcanic sandstone, tuff, chert, and black shale (Centeno-Garcia and Silva-Romo, 1997). The presence of radiolarians led Yta (1992) to assign a Cretaceous age for the La Borda Formation.

The ***Tahue subterrane*** (Figure 2.1) contains the oldest rocks (Paleozoic) found so far within the Guerrero composite terrane, which are considered to be the basement on which Cretaceous volcanism was built (Centeno-Garcia et al., 2008). It is made up of two Paleozoic assemblages, the *El Fuerte Metamorphic Complex* and the *San Jose de Gracia Formation*; Cretaceous marine arc volcanic rocks that belong to the Guerrero Arc unconformably cover the Paleozoic rocks (Centeno-Garcia et al., 2008, and references therein).

The El Fuerte Metamorphic Complex is a low-greenschist metamorphosed and deformed volcanic-sedimentary unit consisting of Ordovician marine rhyolitic-andesitic lavas and clastic and calcareous rocks that may have originated as an oceanic arc (Mullan, 1978; Centeno-Garcia et al., 2008). It has been suggested that the complex represents either remnants of Gondwanan crust accreted during the formation of Pangea (Poole et al., 2005), or a displaced fragment of the early Paleozoic Antler Arc that collided with the western side of North America during late Paleozoic (Burchfiel et al., 1992; Centeno-Garcia, 2005). Unconformably overlying the basement are strongly deformed Pennsylvanian-Permian deep marine turbidites of the San Jose de Gracia Formation (Carrillo-Martinez, 1971; Centeno-Garcia et al., 2008).

2.1.1.2 Post-accretional Characteristics

The evolution of this part of Mexico during the Tertiary is quite complex: from the early Tertiary and until around 29 Ma the Farallon plate was consumed beneath southern Mexico; between 29 and 12.5 Ma subduction of the Guadalupe plate, formed by fragmentation of the Farallon plate, occurred; since approximately 12.5 Ma the Cocos and Rivera plates have been overridden by the North America plate along the Middle America (Acapulco) Trench (Moran-Zenteno et al., 1999). The subduction of the Farallon plate beneath the North America plate created the NNW trending Sierra Madre Occidental (SMO) province (Moran-Zenteno et al., 1999) (Figure 2.10). The SMO province records three different volcanic episodes: the first one is the Laramide volcano-plutonic succession of the Lower Volcanic Supergroup that is responsible for the occurrence of Mexico's second metallogenetic epoch and the generation of porphyry copper deposits (e.g., La Sorpresa, Las Salinas) (Camprubi et al., 2003). Rocks from the Lower Volcanic Supergroup are of Late Cretaceous to early Tertiary age and consist of calc-alkaline, granodioritic to granitic batholiths that intrude volcano-sedimentary rocks. During the Laramide event (90 – 40 Ma), the convergence rate between North America and the Farallon plate increased considerably (Coney, 1990; Valencia-Moreno et al., 2001).

The Laramide magmatic rocks in Mexico are exposed along a northwest-trending belt; they are widespread in the states of Sonora and Sinaloa and less common toward the south, in the states of Jalisco, Colima, and Guerrero (Valencia-Moreno et al., 2001). In the southern area, the batholith belt extends for about 650 km between Puerto Vallarta and Zihuatanejo, and displays NW-SE decreasing ages from around 100 Ma to 40 Ma

(Schaaf et al., 1995). In the northern part (the northern domain), the Laramide granitoids were emplaced into Proterozoic crystalline rocks and Late Proterozoic through Paleozoic miogeoclinal cover of North American affinity; in the central part (the central domain), the Laramide plutons intruded Paleozoic eugeoclinal rocks covered by Late Triassic clastic rocks; the southern part (the southern domain) of the Laramide belt was emplaced into Mesozoic island-arc-related volcanic and sedimentary rocks of the Guerrero terrane (Valencia-Moreno et al., 2001).

The second and third volcanic episodes in the SMO province formed the Upper Volcanic Supergroup in Early Oligocene and Early Miocene time; rocks from this supergroup consist of silicic ignimbrites, rhyolitic domes, and basaltic to andesitic lavas (Moran-Zenteno et al., 1999). The second episode is responsible for the occurrence of Mexico's third metallogenetic epoch that generated porphyry copper (e.g., La Verde, San Isidro, Inguaran, and Tiamaro) and epithermal (e.g., Guanajuato, Fresnillo, and Zacatecas) ore deposits.

The southernmost outcrops of volcanic rocks belonging to the TMVB delineate the northern limit of the Tertiary magmatic rocks of the Sierra Madre del Sur (SMS), which define two different NW trending belts approximately parallel to the Pacific coast: the coastal plutonic belt (CPB-SMS) and the inland volcanic belt (VB-SMS) (Figure 2.10; Moran-Zenteno et al., 2007; Martinez-Serrano et al., 2008). These belts resulted during subduction episodes along the Pacific margin prior to, and partly contemporary with, the margin truncation due to the displacement of the Chortis block (Moran-Zenteno et al., 2004). The displacement was responsible for the change from SMS magmatism to an E-W trending mafic to intermediate TMVB volcanism during the Miocene, around 16 Ma

ago (Moran-Zenteno et al., 2007). The intrusive and extrusive rocks of this arc extend for around 600 km, from the southern part of Jalisco to the Isthmus of Tehuantepec, with a decreasing age trend from Paleocene in Colima to early Miocene in southeastern Oaxaca (Figure 2.10) (Moran-Zenteno et al., 1999, Martinez-Serrano et al., 2008).

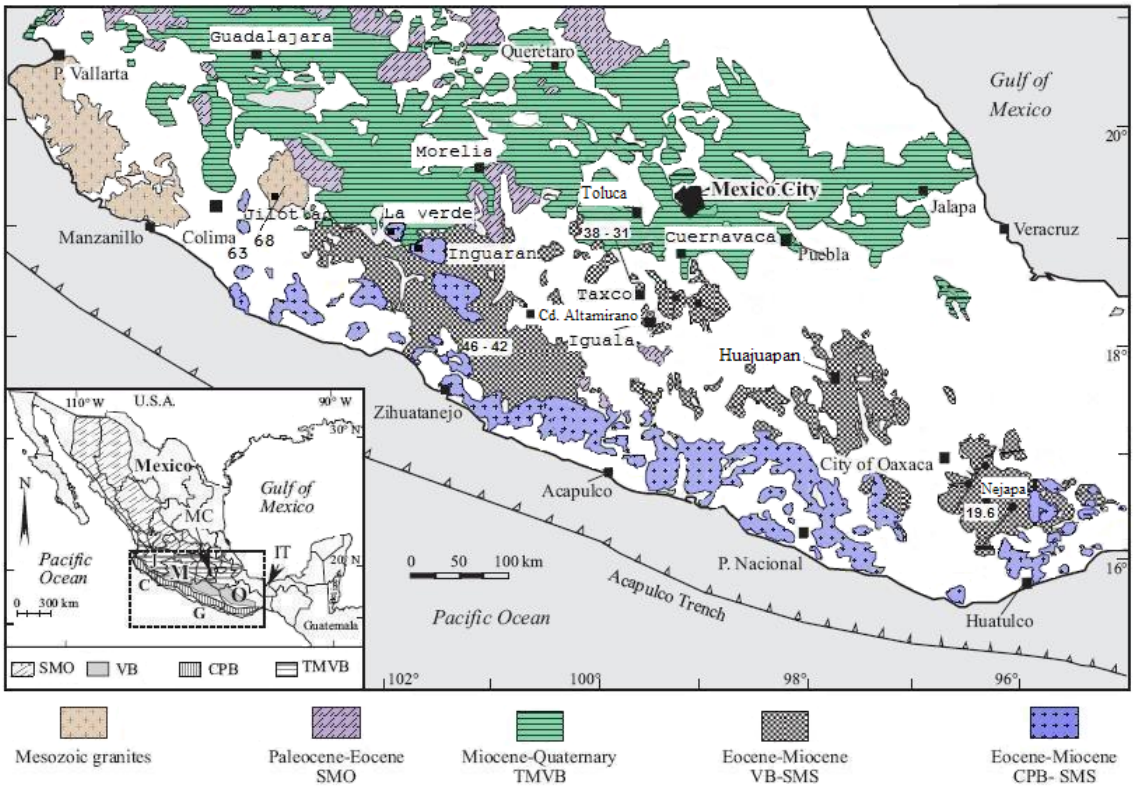

Figure 2.10. Simplified geological sketch of southern Mexico showing the distribution and, in a few cases, the age (in Ma) of the Cenozoic magmatic rocks and the main magmatic provinces in Mexico: SMO – Sierra Madre Occidental; TMVB – Trans-Mexican Volcanic Belt; VB-SMS – Volcanic Belt of the Sierra Madre del Sur; CPB-SMS – Coastal Plutonic Belt of the Sierra Madre del Sur. States displayed in the inset: J – Jalisco; C – Colima; M – Michoacan; G – Guerrero; O – Oaxaca; MC – Mexico City; IT – Isthmus of Tehuantepec (modified after Moran-Zenteno et al., 1999 and Martinez-Serrano et al., 2008).

The CPB-SMS consists of a chain of calc-alkaline, dioritic to granitic batholiths commonly cut by silicic and mafic dikes, and smaller intrusive bodies that outcrop along the southwestern continental margin of Mexico (Moran-Zenteno et al., 1999). In some

areas, for example Manzanillo, gabbroic and dioritic plutons are quite abundant (Schaaf et al., 1990; Moran-Zenteno et al., 2007). The plutons from the CPB-SMS intrude Mesozoic units ranging from volcano-sedimentary arc sequences of the Guerrero terrane to metagraywackes, quartz-amphibolites, quartz-feldspathic gneisses, and marble lenses in the Xolapa terrane (Figure 1.1) (Ortega-Gutierrez, 1981; Schaaf et al., 1995). According to Schaaf et al. (1991), the generation of these granitic batholiths is related to a zone of crustal weakness caused by the strike-slip activity of the truncated continental margin. Crystallization ages of intrusive rocks along the continental margin become younger to the east; they vary from around 80-100 Ma in the Puerto Vallarta area to 60 Ma in the Manzanillo region, 40 Ma in the Zihuatanejo and Acapulco areas, and 29 Ma on the eastern side, in the Huatulco area (Figure 2.10) (Schaaf et al., 1995; Ducea et al., 2004; Moran-Zenteno et al., 2007).

The VB-SMS is represented by a series of volcanic fields consisting of sub-alkalic rhyolites to basaltic andesites found between the CPB-SMS and the TMVB (Moran-Zenteno et al., 1999; Martiny et al., 2000). Generally, they are early Eocene in the Michoacan region and middle Miocene in the southeastern Oaxaca region (Figure 2.10) (Moran-Zenteno et al., 2007). The absence of post middle Miocene magmatic rocks along the Pacific coast suggests a landward jump of the locus of magmatism (Schaaf et al., 1995). The Miocene-Quaternary TMVB reflects the recent arc magmatism related to the current Middle America Trench and the subduction of the Cocos and Rivera plates (Schaaf et al., 1995).

2.1.1.3 Previous Strontium and Neodymium Isotope Studies of Crustal Rocks

As noted in the previous sections, there are numerous isotopic studies related to the origin and evolution of the crustal rocks of the Guerrero composite terrane. Some of them are focused on the basement rocks and others on the arc-related sequences that cover these metamorphic basement units.

The isotopic values ($\varepsilon_{Nd(i)}$ of +13.1 and +13.2, and $^{87}Sr/^{86}Sr_{(i)}$ of 0.7047 and 0.7048) of the pillow lavas of the Arteaga complex, basement of the Zihuatanejo-Huetamo subterrane, plot close to the field defined by the MORB, whereas the sediments of the same complex ($\varepsilon_{Nd(i)}$ of -6.2 and -7.2, and $^{87}Sr/^{86}Sr_{(i)}$ of 0.7163 and 0.7244) suggest that they have been supplied from an evolved continental crust (Centeno-Garcia et al., 1993a). The overall positive ε_{Nd} values and nonradiogenic $^{87}Sr/^{86}Sr$ from available Jurassic-Cretaceous arc-related rocks south of the TMVB are similar to the values of present-day intra-oceanic island arcs, suggesting that the old crust did not influence the magmatism and the sediments from the Arteaga Complex were not involved in the production of the arc assemblage (Centeno-Garcia et al., 1993a). It has been suggested (Centeno-Garcia et al., 1993a) that there were two stages in the evolution of the Guerrero composite terrane: an early pre-Cretaceous stage which involved an oceanic crust that was receiving sediments from an evolved continental source, and a Cretaceous stage that coincided with the development of an intraoceanic island arc on top of the Arteaga Complex.

Available Nd (initial ε_{Nd} of -3.5, and depleted mantle Nd model ages of 1.27 Ga) and Sr (initial $^{87}Sr/^{86}Sr$ of 0.7078) isotope data for the Tejupilco metamorphic suite, basement of the Teloloapan subterrane, suggest inherited Precambrian zircon components in this unit (Elias-Herrera et al., 2003) and preclude the formation of Tejupilco metamorphic

suite magmas from mantle- or oceanic lithosphere-derived melts (Elias-Herrera et al., 2000). The presence of high-grade granulitic xenoliths with Grenvillian Nd isotopic characteristics (depleted mantle Nd model age of 1.5 Ga) in the Oligocene Michoacan-Guanajuato Volcanic Field (Urrutia-Fucugauchi and Uribe-Cifuentes, 1999) indicates the existence of old pre-Mesozoic continental crust beneath the eastern part of the Guerrero terrane (Elias-Herrera et al., 2000). This implies that Tejupilco metavolcanics may represent an evolved volcanic arc developed on old crust with assimilated craton-derived sediments; these sediments may have originated from older Precambrian basement rocks (Elias-Herrera et al., 2000).

Previously published isotopic data on Late Triassic basaltic pillow lavas ($\varepsilon_{Nd(i)}$ of +6.4 and +7.2, and $^{87}Sr/^{86}Sr_{(i)}$ of 0.7054 and 0.7041) from the Zacatecas Formation, basement of the Zacatecas subterrane, plot near the depleted mantle array and are typical of primitive island arc basalts, suggesting little or no crustal contamination (Centeno-Garcia and Silva-Romo, 1997). However, a sandstone sample from the same formation yields initial ε_{Nd} of -5.5 and Nd model age of 1.3 Ga, indicating derivation from an old continental source, most likely represented by the Grenville belt that extends from Chihuahua to Oaxaca (Centeno-Garcia and Silva-Romo, 1997).

Cretaceous igneous rocks from the Arperos basin, part of the Guanajuato subterrane, yield initial ε_{Nd} values between around +6 and +11 and initial $^{87}Sr/^{86}Sr$ between 0.7029 and 0.7047 (Freydier et al., 1996). and show geochemical characteristics similar to oceanic island tholeiites (OIT), with transitional features between OIB and N-MORB. The ε_{Nd} values of the sedimentary rocks change, varying from around +7 at the base, +9 in the middle part, to +1.3 in the uppermost part. This evolution with time in the

chemistry of the Arperos sediments has been interpreted by Freydier et al. (2000) to reflect the approach of the Guerrero juvenile arc to nuclear Mexico: in the incipient stages, the basin was filled with sediments from the ocean floor and/or the arc, and later on with more evolved sources, possibly derived from nuclear Mexico.

The subterranes of the Guerrero composite terrane are considered to represent a Mesozoic multi-arc system that was accreted to the North American plate. Mendoza and Suastegui (2000) performed isotopic work on the Late Mesozoic arc assemblages from three subterranes of the Guerrero terrane: Teloloapan, Arcelia-Palmar-Chico, and Zihuatanejo-Huetamo. According to these authors, the isotopic characteristics of the Teloloapan subterrane sequences ($\varepsilon_{Nd(i)}$ between +1.6 and +4.6 and $\varepsilon_{Sr(i)}$ from -14.3 to +2.3) are similar to those recorded in numerous present-day evolved intra-oceanic island arcs (e.g., Sunda arc and the Lesser Antilles arc). The isotopic signatures of igneous rocks from the Arcelia-Palmar Chico subterrane resemble those of rocks from primitive island arc-marginal basin systems; Palmar Chico yields $\varepsilon_{Nd(i)}$ = +5.4 and $\varepsilon_{Sr(i)}$ = -12.1, typical of immature intra-oceanic island arc (e.g., New Britain arc and the Aleutian arc) and Arcelia is a back-arc basin with isotopic characteristics ($\varepsilon_{Nd(i)}$ = +6.9 and +8, and $\varepsilon_{Sr(i)}$ = -8.9 and -9.7) similar to the Mariana back-arc basin and North and South Fiji basins. The western Zihuatanejo-Huetamo subterrane, an evolved island arc-marginal basin-subduction complex system, has three components: the Zihuatanejo Sequence, the Las Ollas Complex, and the Huetamo Sequence. Rocks from the Zihuatanejo Sequence have isotopic values ($\varepsilon_{Sr(i)}$ = -2.6 and -8.7, and $\varepsilon_{Nd(i)}$ = +8.1 and +8.3) typical of intra-oceanic arc suites. The isotopic signatures of blocks from the Las Ollas Complex ($\varepsilon_{Nd(i)}$ = +7.9

and +8, and $\varepsilon_{Sr(i)}$ = -1.7 and -3), part of a subduction complex, suggest that they were derived from a mantle source similar to that of the Zihuatanejo lavas. A basalt from the Huetamo Sequence has $\varepsilon_{Nd(i)}$ = +7.1, implying an island arc affinity; interesting to note is the very high $\varepsilon_{Sr(i)}$ value (+5.1) that plots to the right of the mantle array. According to the same authors, the Huetamo Sequence represents a back-arc basin that is spatially associated with the Zihuatanejo arc massif.

2.1.2 Mineral Deposits of the Guerrero Terrane

The mineral deposits of the Guerrero terrane can be subdivided into two major groups: the pre-accretion group and the post-accretion group. The pre-accretion group includes Mesozoic VMS and SEDEX deposits formed in intraoceanic island arc and intracontinental marginal basin settings. The post-accretion group refers to mineralization associated with continental-arc magmatism and the subduction of the Farallon/Cocos plate, and consists of Cenozoic porphyry copper, epithermal, and skarn deposits.

2.1.2.1 Mesozoic Volcanogenic Massive Sulfide and Sedimentary Exhalative Deposits

The VMS and SEDEX deposits (Figure 2.11) were generated during the first metallogenetic phase (Middle Jurassic to Early Cretaceous; Mortensen et al., 2008). Generally, VMS deposits are dominated by a Cu-Zn (occasionally with some Pb and Au) metal association and are related to precipitation of metals from hydrothermal solutions flowing through volcanically active submarine environments (Robb, 2005). SEDEX refers to a mainly Zn-Pb (with lesser Cu, but commonly Ba and Ag) deposit type related to hydrothermal fluids venting onto the sea floor, but without a direct connection to volcanic activity (Robb, 2005).

Around 60 deposits of this type have been discovered so far within the Guerrero terrane, most of them hosted within arc or back-arc facies, in stratigraphic sequences that include sedimentary, volcanic, and volcanic-derived sedimentary rocks of local provenance (Mortensen et al., 2008). The VMS deposits are distributed within two major belts. The Coastal belt consists of deposits located in the Zihuatanejo-Huetamo subterrane and includes the Cuale-El Bramador district (28 deposits) and the La Minita, Arroyo Seco, and Copper King deposits (Mortensen et al., 2008; Figure 2.11). The Central belt includes deposits and districts situated in the Teloloapan, Guanajuato, and Zacatecas subterranes: Campo Morado (9 deposits), Tlanilpa-Azulaquez (15 deposits), and Leon-Guanajuato (5 deposits) districts, and Rey de Plata, Tizapa, Francisco Madero, and San Nicolas deposits (Mortensen et al., 2008; Figure 2.11).

The majority of the VMS deposits from the Zihuatanejo and Teloloapan subterranes are Zn-Pb-Cu Kuroko type, reflecting association with arc-related bimodal (felsic and mafic) volcanism (Miranda-Gasca et al., 1993; Robb, 2005); the deposits from the Guanajuato subterrane are Zn-Cu-type and have an oceanic basement (Miranda-Gasca, 2000). The Zn-Pb-Cu Francisco Madero and Pb-type Arroyo Seco deposits can be classified as SEDEX type deposits (Miranda-Gasca, 1995; Mortensen et al., 2008). The Cu-Zn-type Copper King deposit, hosted within the Las Ollas complex, is a Cyprus type, reflecting leaching of a dominantly mafic volcanic source rock (Miranda-Gasca, 2000; Robb, 2005). Pyrite, sphalerite, and chalcopyrite are present in all of the deposits, whereas galena is present in all but Guanajuato (Miranda-Gasca, 2000) (Appendix 1.1). In terms of precious metals, VMS deposits have usually low Ag and Au contents;

exceptions are represented by the Au-rich Campo Morado and Tizapa areas, and the Ag-rich Cuale-El Bramador, Tizapa, and Arroyo Seco regions (Appendix 1.1).

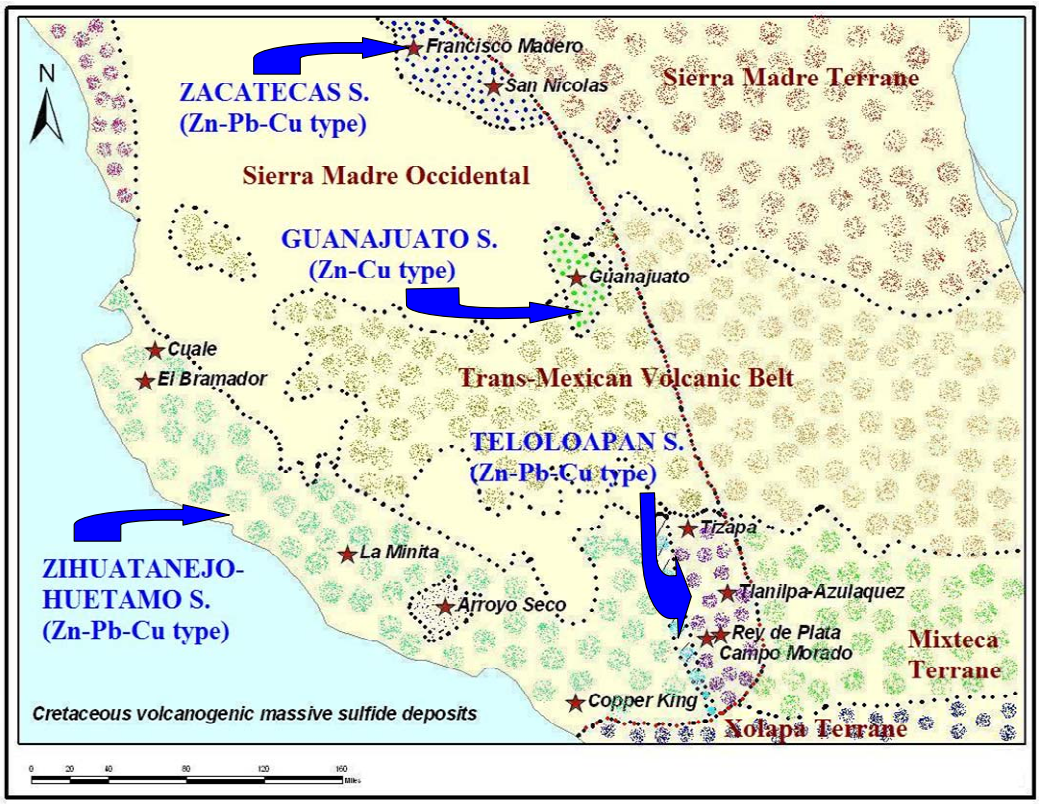

Figure 2.11. Distribution of volcanogenic massive sulfide deposits and districts within distinct subterranes (Zihuatanejo-Huetamo, Teloloapan, Guanajuato, and Zacatecas) of the Guerrero terrane.

2.1.2.2 Cenozoic Porphyry Copper Deposits

By the end of Mesozoic time, Mexico was almost completely emergent and subject to deformation and to the Cenozoic volcanic-plutonic cycle that produced the post-accretion group of ore deposits (Figure 2.12), which includes most of Mexico's mineral wealth (Cumming et al., 1979). Globally, porphyry copper deposits represent the main source of Cu and Mo in the world and are largely related to tectonic regions characterized by abundant calc-alkaline magmatism associated with Andean-type subduction margins

(Valencia-Moreno et al., 2007). In general, the ages of porphyry copper deposits emplaced in rocks of the Guerrero terrane (Figure 2.12) are between around 63 and 33 Ma (Appendix 1.2) (Valencia-Moreno et al., 2007) and were generated in two different metallogenetic episodes (Miranda-Gasca, 2000). The first episode took place during the Paleocene and was related to Laramide magmatism in the Sierra Madre Occidental, generating deposits between about 53 and 63 Ma (La Sorpresa and Las Salinas) (Damon et al., 1983; Miranda-Gasca, 2000). The second episode that produced porphyry-copper deposits occurred between around 28 and 36 Ma and was associated with the outpouring of volcanic rocks of the Sierra Madre Occidental; the age of these deposits is 31 to 36 Ma (La Verde, San Isidro, Inguaran, and Tiamaro) (Damon et al., 1983; Miranda-Gasca, 2000).

The porphyry copper deposits are associated with intrusive rocks of variable composition between granite and diorite, but with a larger abundance of quartz-monzonites (Appendix 1.2) (Damon et al., 1983; Miranda-Gasca, 2000; Valencia-Moreno et al., 2007). The greatest volume of minerals reported for these deposits occurs in La Verde, with 110 Mt of ore, averaging 0.7 % Cu (Appendix 1.2) (Valencia-Moreno et al., 2007). The mineralization occurs as disseminated ore and in stockwork veinlets, but mostly as breccia structures (Appendix 1.2) (Valencia-Moreno et al., 2007). The content of primary sulfides is relatively low (2% - 3%) and is mostly represented by pyrite, chalcopyrite, and some bornite (Valencia-Moreno et al., 2007); La Verde and San Isidro contain trace amounts of galena and sphalerite, whereas scheelite was exploited in the Inguaran breccias (Miranda-Gasca, 2000) (Appendix 1.2). The ore minerals of the

porphyry copper deposits are represented by these primary sulfides, since they have not been enriched by supergene processes (Damon et al., 1983; Miranda-Gasca, 2000).

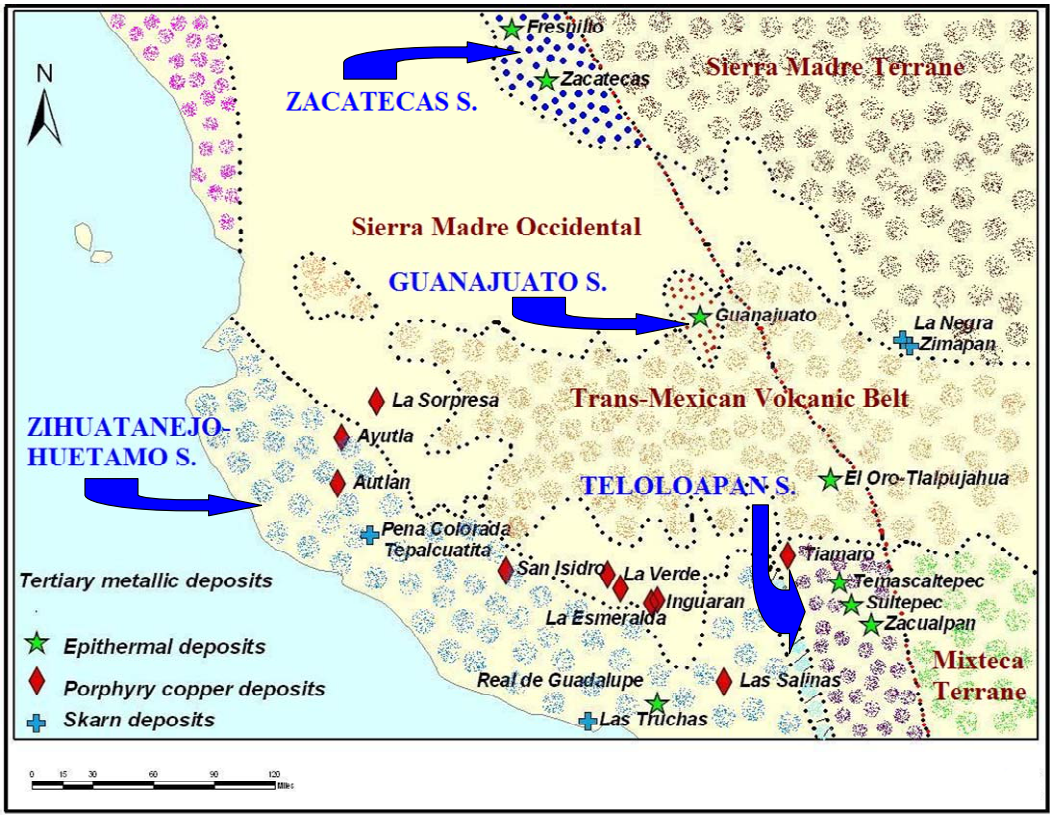

Figure 2.12. Distribution of Tertiary metallic deposits (epithermal, porphyry copper, and skarn) and districts within distinct subterranes (Zihuatanejo-Huetamo, Teloloapan, Guanajuato, and Zacatecas) of the Guerrero terrane. Also shown are the La Negra and Zimapan skarn deposits from the Sierra Madre terrane.

2.1.2.3 Cenozoic Epithermal Ore Deposits

The epithermal ore deposits (Figure 2.12), of Middle Eocene to Late Oligocene age (Appendix 1.3), have been the most economically important type of deposit in Mexico, and the Guerrero terrane includes world-class deposits like Guanajuato, Fresnillo, and Zacatecas. They are associated with the first bimodal andesitic-rhyolitic volcanic episode of the Upper Volcanic Series of the Sierra Madre Occidental (Camprubi and Albinson,

2007). The regional distribution of the deposits indicates a close association in space with regional faults, which act as paths for the emplacement of magmas; magmas represent the main source of heat and fluid that cause hydrothermal activity and subsequent mineral deposition (Camprubi and Albinson, 2007).

The Mexican metallogenic provinces of the Sierra Madre Occidental and the Sierra Madre del Sur host base metal-rich (comparable to intermediate sulfidation type) and precious metal-rich (comparable to low sulfidation type) epithermal deposits. The precious metal-rich deposits contain fluid inclusions with salinities between 0 and ~6 wt% NaCl equiv. and the base metal-rich ones have fluid inclusions with higher salinities, between ~2 and ~20 wt% NaCl equiv. (Camprubi and Albinson, 2007). In most cases, the ores are found in veins (Miranda-Gasca, 2000) (Appendix 1.3). A characteristic sequence of mineral precipitation, as described in the Temascaltepec district, is: (1) base metal sulfides: pyrite (or arsenopyrite in other deposits), sphalerite, galena, and chalcopyrite (may contain late argentite-acanthite); (2) Cu ± Ag sulfosalts (usually Ag-tetrahedrite-tennantite minerals); Ag sulfosalts (proustite-pyrargyrite, pearceite-polybasite, stephanite, miargyrite); and (3) Ag-Pb sulfosalts (Camprubi and Albinson, 2007). A similar precipitation sequence has also been found in case of the Guanajuato, Zacatecas, and Fresnillo deposits. Native Ag, Au, and electrum are common in most of the deposits (Miranda-Gasca, 2000) (Appendix 1.3).

It is well-known that there is a close space-and-time association between intermediate sulfidation type epithermal deposits and metalliferous porphyry and skarn deposits; the difference is represented by the evolutionary path related to the variability of oxidation and sulfidation states in the mineralizing fluids from a proximal thermal source, namely a

porphyry or skarn, toward distal areas (Einaudi et al., 2003; Camprubi and Albinson, 2007).

2.1.2.4 Cenozoic Skarn Deposits

The Pacific margin includes many small to moderate sized iron-oxide rich and gold- and copper-bearing skarn and replacement deposits, designated Fe(-Au-Cu). The Pena Colorada and Las Truchas (Figure 2.12) are Fe skarn deposits hosted by quartz-monzonites and diorites of Tertiary age that intruded K limestones of the Guerrero terrane, and rhyolitic and andesitic tuffs (Miranda-Gasca, 2000). The Las Truchas Fe orebodies developed mainly at the diorite / K limestone contact and consist mostly of magnetite and hematite, with specularite, limonite, and goethite in minor proportions (Mapes, 1991). 67 million tons of ores have been extracted, with an average grade of the entire production of 63.5 % total Fe (Barton et al., 1995).

2.1.2.5 Description of Deposits with Available Ore Samples

The Cenozoic samples analyzed in this study include ores from La Verde, La Esmeralda, El Malacate, and Inguaran porphyry copper deposits, located within the Guerrero terrane, and ores from two skarn deposits situated in the Sierra Madre terrane: Zimapan and La Negra.

Cenozoic Porphyry Copper Deposits in the Guerrero Terrane

Southern Michoacan consists of a cluster of plutons, one of them being represented by the Huacana granodiorite-quartz diorite pluton, which is 70 km long and trends northwest (Coochey and Eckman, 1978). The pluton hosts numerous porphyry copper deposits and in four of them it is intruded by younger porphyries with associated igneous breccias

called La Verde, Inguaran-Manga de Cuimbo, San Isidro, El Malacate, and La Esmeralda (Coochey and Eckman, 1978).

The *La Verde* deposit (Figure 2.12) occurs just south of the Central Volcanic Belt of Mexico, on the Sierra del Marques, an east-west-trending, arc-shaped range of hills around 6 km long consisting mostly of quartz-diorite named the La Verde intrusive complex, intruded by acidic dikes and stocks (Coochey and Eckman, 1978). The deposit has two distinct units known as the East Hill and the West Hill (Figure 2.13), the point of separation being the center of the arc-shaped range (Coochey and Eckman, 1978).

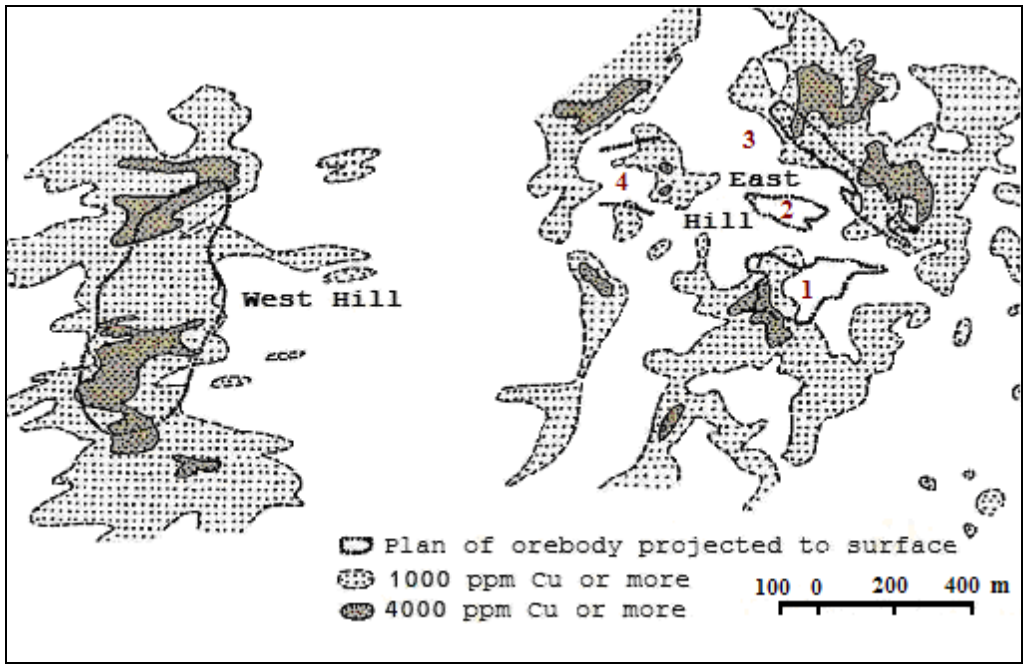

Figure 2.13. Orebodies of the La Verde porphyry copper mine, Sierra de Marques. Numbers represent the location of orebodies (after Coochey and Eckman, 1978).

The East Hill hosts four orebodies (Figure 2.13); one of them is located in a quartz feldspar porphyry stock and the other three in diorite breccia; mineralization is mostly chalcopyrite and bornite, with only minor pyrite content (Coochey and Eckman, 1978).

On the West Hill, around one mile west of the East Hill orebodies, there is only one orebody trending N-NE (Figure 2.13); mineralization is represented by E-W-trending veins consisting of pyrite, pyrrhotite, chalcopyrite, and minor arsenopyrite (Coochey and Eckman, 1978). Morphology of the West Hill is 300x700 m by 200 m depth and of the East Hill 400x600 m by 200 m depth (Barton et al., 1995). Mineralization in both Hills extends up to 1200 feet below the surface (Coochey and Eckman, 1978). Around 110 million tons of ores have been extracted, with an average grade of 0.7 % Cu (Barton et al., 1995).

The *Inguaran Mining District* (Figure 2.12) is located in the south-central part of the Mexican Neovolcanic Axis Metallogenetic Province (Osoria et al., 1991; Figure 2.10). The mineralization is associated with intrusive rocks represented mainly by quartz-monzonite and granodiorite (Valencia-Moreno et al., 2007; Appendix 1); the regional fault systems may have controlled emplacement of brecciated chimneys that represent the most important orebodies (Osoria et al., 1991; Figure 2.14). Eight intrusive quartz-monzonite breccia pipes have been identified in the area (Barton et al., 1995). The principal ore mineral appears to be chalcopyrite (Macfarlane, Field guide / Mexico, Summer '96). Between 1971 and 1982, around 7 million tons of ores were extracted, with an average grade of the entire production of 1.2 % Cu and 0.03 % WO_3 (Osoria et al., 1991).

Cenozoic Skarn Deposits in the Sierra Madre Terrane

The Cenozoic-age samples analyzed in this study include ores from two skarn deposits located in the Sierra Madre terrane--Zimapan and La Negra. In both deposits igneous

rocks associated with the mineralization intruded Cretaceous limestone of the Doctor Formation (Garcia and Querol, 1991; Fraga, 1991).

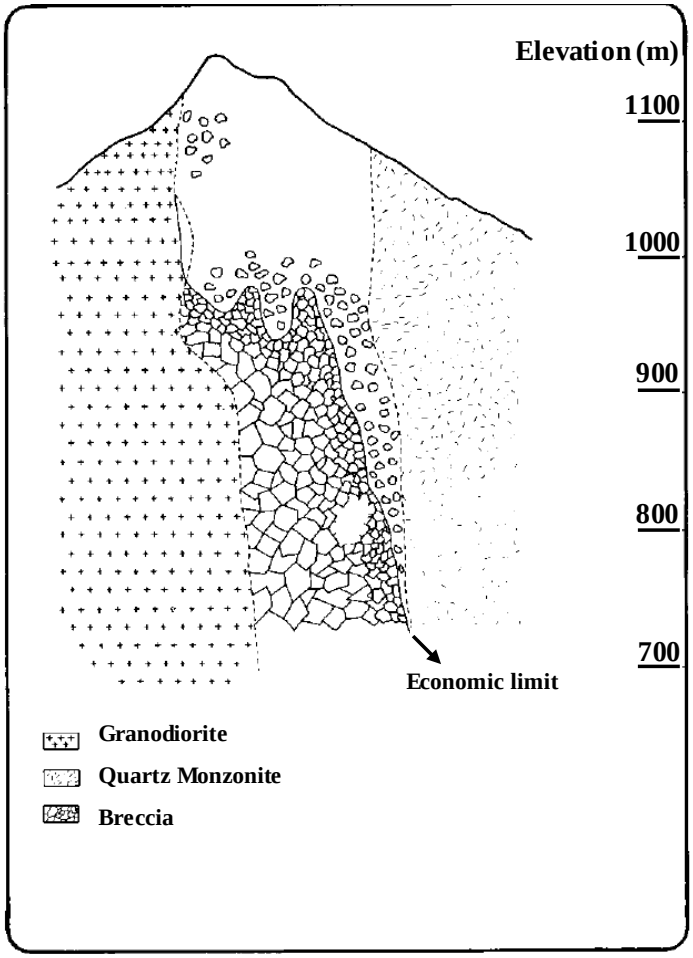

Figure 2.14. Schematic cross section of the San Juan breccia, located in the northeastern part of the Inguaran Mining District (after Osoria et al., 1991).

The *La Negra Mining District* (Figure 2.12) lies in the Sierra Madre Oriental physiographic province. Dikes metamorphosed the Doctor Formation, creating a grossularite-andradite skarn zone and structural channels favorable to subsequent mineralization (Fraga, 1991). Orebody mineralogy is mostly hessite, galena, marmatite,

and chalcopyrite, with pyrite, arsenopyrite, and pyrrhotite as gangue (Fraga, 1991). The ore occurs near the contact of garnet exoskarn with limestone; hornfels, marble, wollastonite, and endoskarns of garnet or pyroxene are all poor ore hosts (Macfarlane, Field guide / Mexico, Summer '96):

Igneous rock	Hedenbergite endoskarn	Wollastonite exoskarn	Garnet exoskarn	Limestone (recrystallized)
			Ore	

The ores display a vertical zonation: in the topographically higher levels there are noncommercial disseminated ores that become manto-type bodies at depth; deeper down, between levels 2000 and 2400, the mantos become the main silver-producing chimney-type orebodies; at even greater depths the Ag-Pb contents decrease and Cu content increases (Fraga, 1991). From 1971 to 1983 the La Negra Mine produced around 2.6 million tons of 157 g/t Ag, 1.04 % Pb, 2.80 % Zn, and 0.20 % Cu) (Fraga, 1991).

The Pb-Zn-Ag ores at the *Zimapan Mining District* (Figure 2.12) are associated with an Early Oligocene quartz-monzonite stock and dike system that intruded K limestones and shales (Gaytan-Rueda, 1975; Macfarlane, Field guide / Mexico, Summer '96). Mineralization appears both as fracture fills and replacement bodies associated with NW-SE trending dikes (Macfarlane, Field guide / Mexico, Summer '96; Garcia and Querol, 1991). Replacement took place along the underside of the thick limestone beds, forming stratabound pipes of mineralization that sometimes coalesce into mantos; mineralized breccias also formed where fluids escaped across bedding (Macfarlane, Field guide / Mexico, Summer '96). The epigenetic mineralization is much younger than the host rocks; fractures in the igneous bodies and the skarn, and the contacts of these bodies with

the host rocks, were the main pathways (Garcia and Querol, 1991). The igneous activity in the district was mostly Early Oligocene magmatism (Gaytan-Rueda, 1975). The ores are interesting because they are clearly associated with the dikes and are largely or entirely hosted in K sediments. The deposits may be classified in general as mesothermal, occasionally epithermal (Garcia and Querol, 1991). Between 1975 and 1984, around 2 million tons of ores were extracted, with an average grade of the entire production of 0.04 g/t Au, 190 g/t Ag, 1.3 % Pb, 3.8 % Zn, and 0.4 % Cu (Barton et al., 1995).

2.1.2.6 Previous Ore Lead Isotope Studies

Cumming et al. (1979) measured the isotopic compositions of Pb in four Mesozoic and thirty Cenozoic mineral deposits in Mexico. They suggested that Mexican ore Pb data could be accounted for by the same process that generated Pb in mature arcs, but with a significant addition of a more radiogenic component. This component could be represented, at least in the northern part of Mexico, by the Precambrian basement. The basement may have contributed sediments to the subducting plate, and thence to the magmatic source region, or may have released Pb to magmas by assimilation or to hydrothermal solutions by hydrothermal leaching that had passed through the basement rocks prior to or during mineralization. They considered hydrothermal leaching unlikely, though, because many deposits formed in Mesozoic and Cenozoic wall rocks, thousands of feet above any possible Precambrian basement. Cumming et al. (1979) favored a model of magmatic assimilation of Pb from the basement by Mesozoic and Cenozoic magmas.

Ruiz and Coney (1985) argued that the Pb isotope signatures of ores from Mexican deposits do not correlate with the geologic setting but are rather related to the tectonostratigraphic terranes which host the deposits. They identified four different compositional clusters corresponding to the Guerrero, Chihuahua, Sierra Madre, and Coahuila tectonostratigraphic terranes of Campa and Coney (1983), and concluded that the crustal source of ore Pb in each terrane is related to the nature of the basement rocks. However, Hosler and Macfarlane (1996) analyzed the Pb isotope ratios of Cu ores from fifteen deposits from southern Mexico and they noticed an overall trend of increasing the radiogenic component of Pb from the West Coast, near the Middle American Trench, to the East Coast. Macfarlane (1999b) suggested that there was no simple correlation between ore Pb isotope ratios and geological terranes. Instead, he attributed the increase in the radiogenic component to assimilation of radiogenic Pb from the crust (Figure 2.15). The nature of this radiogenic component is not yet well understood.

Lopez et al. (1999) analyzed Paleocene Cu ore samples from twenty-one mines situated in the Rio Balsas basin, Guerrero State, near Ciudad Altamirano. They delineated three major trends: the Guerrero eastern high $^{206}Pb/^{204}Pb$ group (18.69 – 18.85), the Guerrero western low $^{206}Pb/^{204}Pb$ group (18.44 – 18.63), and the low $^{207}Pb/^{204}Pb$ group (15.58 – 15.71). The Guerrero eastern high $^{206}Pb/^{204}Pb$ has similar Pb isotope compositions to Cu ore deposits from Michoacan and eastern Jalisco states, while the Guerrero western low $^{206}Pb/^{204}Pb$ resembles the Cu ore deposits from Oaxaca and coastal Jalisco states. They concluded that these two groups can be modeled as mixing of mantle Pb with upper crustal Pb sources, the major difference being a larger input of crustal Pb in the eastern high group.

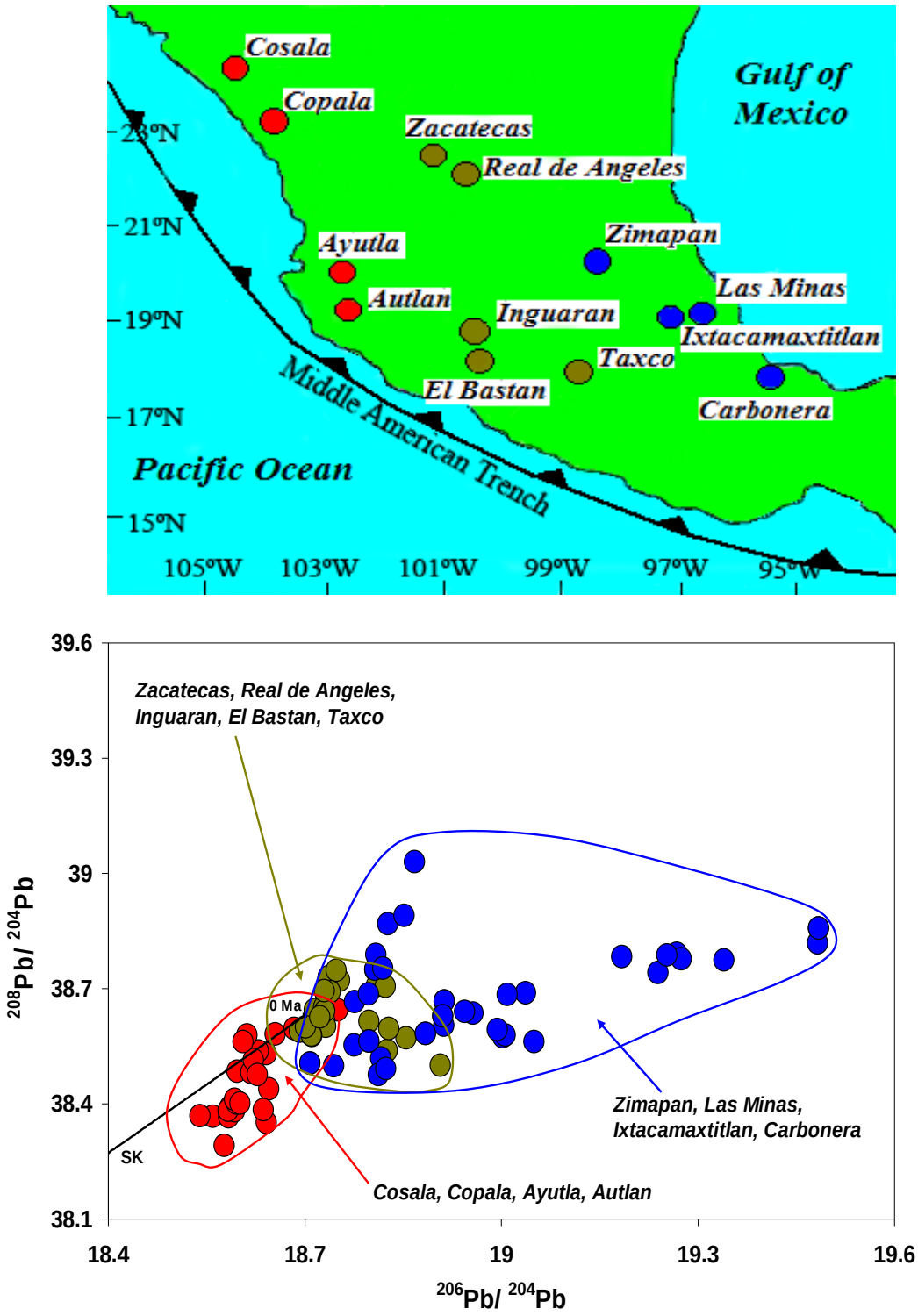

Figure 2.15. Locations of representative Cenozoic mineral deposits from Mexico (top) and their corresponding Pb isotope compositions (bottom). Data from Cumming et al. (1979) and Hosler and Macfarlane (1996). The Pb growth curve of Stacey and Kramers (1975) is shown for reference.

Mortensen et al. (2008) studied the Mesozoic volcanogenic massive sulfide deposits from the Guerrero terrane and compiled Pb isotope data (Cumming et al., 1979; Miranda-Gasca, 1995; Danielson, 2000) from thirty-two deposits. They showed that most of the data were relatively radiogenic, plotting above the average upper crustal growth curve of Doe and Zartman (1979) on the thorogenic diagram. On the basis of Pb isotope data, they suggested that a substantial component of Pb in each deposit may have originated from continent-derived sediments (interlayered with or underlying the host volcanic rocks), from the radiogenic basement, or that the igneous rocks themselves consisted of a significant component of radiogenic crustally derived Pb.

3. SAMPLING AND METHODOLOGY

In the metallogenic models based on the Pb isotope compositions of ore minerals, it is very important to know the isotopic compositions of possible source rocks in a mineral district, and of the fraction of host rocks leached by hydrothermal fluids (Chiaradia et al., 2004). To address this issue, I determined the Pb isotope compositions of sulfide minerals and potential source rocks from various lithologic units of the Guerrero terrane. I also incorporated previously published data from the literature.

Crustal Pb may be hydrothermally leached from host rocks and redeposited in ore minerals. To test whether hydrothermal leaching of metals played an important role in the genesis of the ore deposits from the Guerrero terrane, I analyzed separate leachate and residue fractions of some sedimentary and metamorphic rocks. The two data sets (leachate and residue) from a single sample provide a range of values that represents the isotopic variability of a source rock leached by hydrothermal fluids more accurately than does a single analysis (Chiaradia et al., 2004; Kamenov et al., 2002; Macfarlane and Petersen, 1990).

In order to provide a clearer picture of the origin and evolution of the crustal rocks from the Guerrero terrane, I provide new Sr and Nd isotope data on metamorphic, sedimentary, and igneous whole rocks.

The samples for this study were collected in the summer of 1996 by A.W. Macfarlane, with the assistance of Cia. Minera Peñoles, S.A., from surface outcrops and mine workings. The locations and brief descriptions of the samples from the Guerrero terrane are shown in Figure 3.1 and included in Appendix 2, respectively. Ten Mesozoic

metamorphic rocks (slate, phyllite, and schist) collected from distinct outcrops (around the towns of Arteaga, Arcelia, and Iguala) (Figure 3.1) were analyzed for their isotopic compositions. They belong to the Arteaga Complex and Tejupilco metamorphic suite, which represent basement rocks for the Zihuatanejo-Huetamo subterrane and Teloloapan subterrane, respectively. Thirteen Cretaceous sedimentary rocks (mudstone, siltstone, and sandstone), collected around the towns of Colima, Purificacion, Cd. Altamirano, and Huetamo (Figure 3.1), were used in the present study. They are part of the Zihuatanejo and Huetamo Sequences located in the Zihuatanejo-Huetamo subterrane. The Cenozoic igneous rocks from the Guerrero terrane analyzed for their isotopic compositions are phases of the Huacana granodiorite-quartz diorite pluton and include granite, granodiorite, and diorite from La Verde, and granodiotire from Inguaran, El Malacate, and La Esmeralda (Figure 3.1). Cenozoic quartz-monzonite samples from Zimapan and one diorite from La Negra (Figure 2.12), located in the Sierra Madre terrane, have also been used in this study. Six Cenozoic ore samples (pyrite, galena, and bornite) from porphyry copper deposits located in the Guerrero terrane (La Verde, La Esmeralda, and El Malacate) (Figure 3.1) and fourteen Cenozoic minerals (pyrite, sphalerite, galena, and chalcopyrite) from skarn deposits in the Sierra madre terrane (Zimapan and La Negra) (Figure 2.12) have been analyzed for their Pb isotope compositions.

Most of the processed rock samples (igneous, sedimentary, and metamorphic) lack visible signs of weathering and alteration, in order to minimize the effects of these processes and bias in sampling. Sulfide (pyrite, chalcopyrite, sphalerite, bornite, and galena) and whole rock samples have been analyzed for Pb isotope composition for a few reasons:

● to characterize the ore-Pb isotope signatures of a particular mineralized area;

● to compare-and-contrast the Pb isotope compositions of ore minerals from deposits located in distinct tectonostratigraphic terranes; for this objective, samples from two adjacent terranes, Guerrero and Sierra Madre, have been analyzed;

● to compare the ore Pb isotopes of pre-accretion and post-accretion deposits;

● to identify potential source rocks of Pb and other associated metals by comparing the ore-Pb isotope data to the whole rock Pb isotope data.

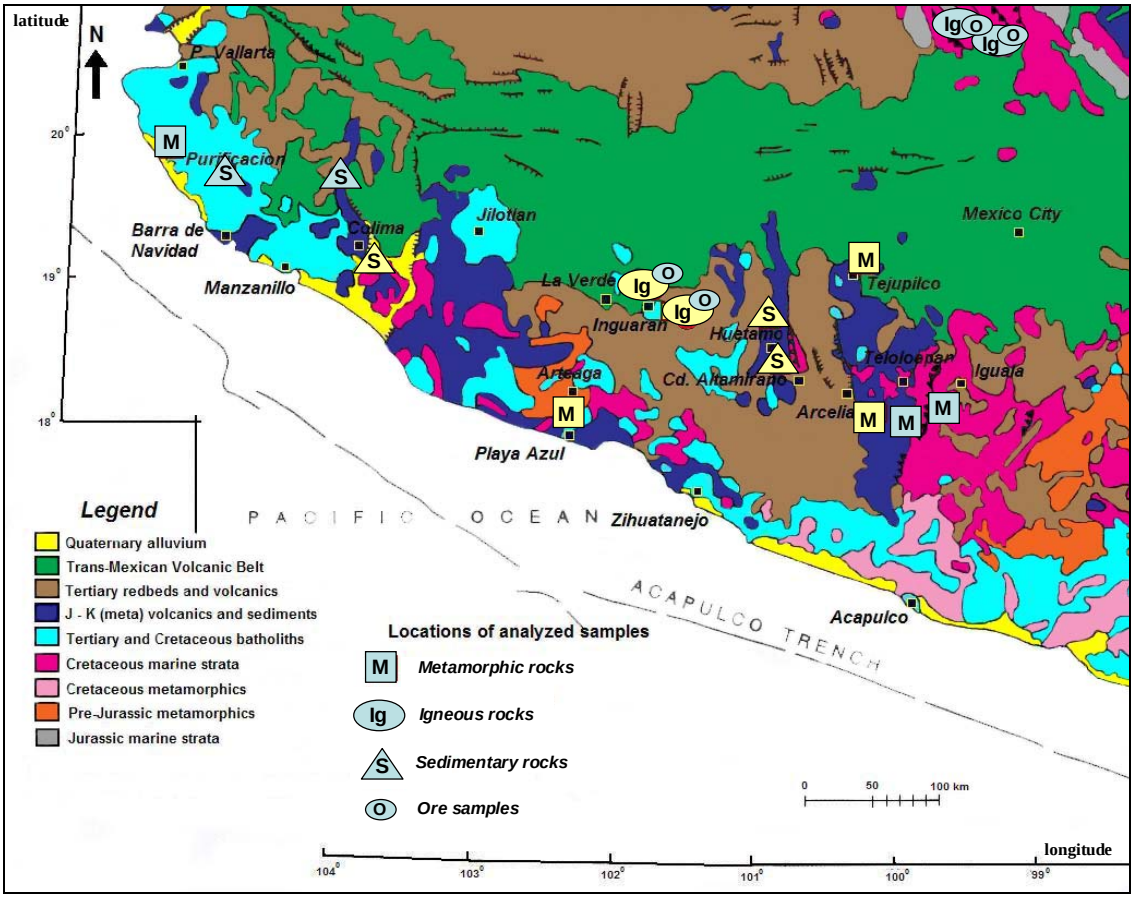

Figure 3.1. Locations of analyzed samples from the Guerrero and Sierra Madre terrane superimposed on the simplified geologic map of southwestern Mexico (geologic map modified after Lang et al., 1996). Locations in yellow represent areas with Pb, Sr, and Nd data; locations in blue indicate areas with Pb isotope data only.

Lead was separated from the whole rock and mineral samples by cation exchange methods. Lead isotope ratio measurements were performed on a VG-354 thermal ionization mass spectrometer in the Radiogenic Isotope clean laboratory of the Earth and Environment Department at Florida International University. The details of sample preparation and other analytical techniques are given in Appendix 3, following the procedures used by Kamenov (2000) and Panneerselvam (2001).

Strontium and Nd isotope analyses were performed at the National High Magnetic Field Laboratory in Tallahassee, under the supervision of Dr. V. J. M. Salters and scientific research specialist A. Sachi-Kocher. Strontium and Nd isotopes were separated following the procedures described by Hart and Brooks (1977) for Sr and Richard et al. (1976) for Nd (see details in Appendix 3). Strontium isotope ratios were measured by thermal ionization mass spectrometry on a Finnigan MAT 262 mass spectrometer, and Nd isotope ratios were determined by inductively coupled plasma mass spectrometry on a Thermo Finnigan NEPTUNE MC-ICP-MS (see details in Appendix 3).

4. RESULTS

4.1 Lead Isotope Compositions of Crustal Rocks

Lead isotope compositions of whole rocks and leachate and residual fractions from various crustal units of the Guerrero terrane were determined (Table 4.1, Table 4.2, and Table 4.4) to make comparisons with ore-lead compositions and to try to identify crustal units that could have supplied ore metals. Lead isotope ratios of ores and igneous rocks from the Sierra Madre terrane are also presented (Table 4.3) to look for systematic differences in ore metal sources among the proposed exotic tectonostratigraphic terranes of southern Mexico.

4.1.1 Compositions of Mesozoic Metamorphic Basement

Ten samples representing metamorphic basement (Figure 3.1) were analyzed for Pb isotope composition. The results are given in Table 4.1 and shown in Figure 4.1. These rocks contain the most radiogenic and isotopically variable Pb measured in this study. A meta-basalt sample collected near Barra de Navidad shows $^{206}Pb/^{204}Pb$ of 18.701, $^{207}Pb/^{204}Pb$ of 15.649, and $^{208}Pb/^{204}Pb$ of 38.711. Five Triassic schist samples from south of the town of Arteaga, part of the Arteaga Complex, yield values ranging between 18.858 and 18.999 for $^{206}Pb/^{204}Pb$, 15.623 and 15.693 for $^{207}Pb/^{204}Pb$, and between 38.906 and 39.216 for $^{208}Pb/^{204}Pb$. A Jurassic black phyllite collected close to Tejupilco, part of the Tejupilco metamorphic suite, has $^{206}Pb/^{204}Pb$ of 18.876, $^{207}Pb/^{204}Pb$ of 15.650, and $^{208}Pb/^{204}Pb$ of 38.694. Two Triassic-Jurassic phyllite (meta-siltstone and meta-sandstone) samples collected close to Arcelia and one Triassic-Jurassic slate sample

collected near Iguala, representing part of the same metamorphic complex that crops out in several areas in the eastern part of the terrane, the Tejupilco metamorphic suite, contain radiogenic lead relative to bulk earth models, with $^{206}Pb/^{204}Pb$ ranging from 19.032 to 19.256, $^{207}Pb/^{204}Pb$ from 15.643 to 15.647, and $^{208}Pb/^{204}Pb$ from 38.780 to 39.098.

Generally, rocks from the Arteaga and Tejupilco complexes define two different trends. Low-grade metamorphic rocks from the Tejupilco metamorphic suite (phyllite and slate) are generally less radiogenic in terms of $^{208}Pb/^{204}Pb$ and $^{207}Pb/^{204}Pb$, but more radiogenic in terms of $^{206}Pb/^{204}Pb$ compared to high-grade rocks from the Arteaga complex (schist and gneiss); they also have highly variable $^{206}Pb/^{204}Pb$ values (Figure 4.1). In conventional isotopic plots, the metamorphic rocks plot far to the right of the average Pb crust evolution curve of Stacey and Kramers (1975) (Figure 4.1). On the thorogenic diagram, the Arteaga samples plot above and to the right of the orogene evolution curve of Zartman and Doe (1981); the Tejupilco rocks define a field between the orogene and upper crust evolution curves, slightly shifted to the right of the orogene growth curve (Figure 4.1). On the uranogenic diagram, rocks from both metamorphic complexes plot below the upper crust evolution curve of Zartman and Doe (1981) and are generally located to the right of the orogene growth curve (Figure 4.1).

4.1.2 Compositions of Cretaceous Sediments

Lead isotope compositions of thirteen Cretaceous sedimentary rocks from the Zihuatanejo-Huetamo subterrane (Figure 3.1) were determined; the results are given in

Table 4.1 and shown in Figure 4.1. Five samples are part of the Zihuatanejo Sequence and eight belong to the Huetamo Sequence.

The Zihuatanejo Sequence consists of a succession of more than 2000 m of arc volcanics and related sedimentary rocks. The base of the sequence is represented by roughly 1500 m of andesitic to dacitic lava flows, which is covered by about 500 m of reefal limestones and red beds (Figure 2.6) (Mendoza and Suastegui, 2000). The section sampled in the study area is represented by siltstone and mudstone samples from the red bed deposits. A siltstone sample collected near Zanzontle, representing part of the Zihuatanejo Sequence, shows Pb isotope ratios of 19.050 for $^{206}Pb/^{204}Pb$, 15.643 for $^{207}Pb/^{204}Pb$, and 38.547 for $^{208}Pb/^{204}Pb$. A mudstone sample from the Purificacion area, part of the same sequence, has $^{206}Pb/^{204}Pb$ of 19.437, $^{207}Pb/^{204}Pb$ of 15.634, and $^{208}Pb/^{204}Pb$ of 38.892. Three siltstone samples collected south of Colima yield values for $^{206}Pb/^{204}Pb$ between 18.763 and 19.053, for $^{207}Pb/^{204}Pb$ between 15.580 and 15.622, and for $^{208}Pb/^{204}Pb$ between 38.510 and 38.849.

The Huetamo Sequence consists of around 4500 m of mainly clastic sedimentary rocks of Late Jurassic – Late Cretaceous age (Figure 2.7) (Mendoza and Suastegui, 2000). Six Cretaceous sedimentary rocks (sandstones, siltstones, and mudstones) of the Huetamo Sequence, collected between Altamirano and Huetamo, have $^{206}Pb/^{204}Pb$ values ranging between 18.630 and 18.998, $^{207}Pb/^{204}Pb$ between 15.563 and 15.641, and $^{208}Pb/^{204}Pb$ between 38.381 and 38.610. Two samples (siltstone and mudstone) collected near Huetamo, representing part of the same sequence, show $^{206}Pb/^{204}Pb$ values of 18.630 and 18.767, $^{207}Pb/^{204}Pb$ ratios of 15.582 and 15.624, and $^{208}Pb/^{204}Pb$ of 38.369 and 38.525.

Rocks from these sequences define two different clusters in conventional isotopic plots (Figure 4.1). On the thorogenic diagram, rocks of the Huetamo Sequence plot between the orogene and upper crust reservoir of Zartman and Doe (1981); samples from the Zihuatanejo Sequence are shifted to more radiogenic values, plotting between the 0 Ma and 400 Ma values of the upper crust reservoir of Zartman and Doe (1981) (Figure 4.1). On the uranogenic diagram, samples from the Huetamo Sequence define a field located along the orogene growth curve of Zartman and Doe (1981) and the Zihuatanejo rocks plot to the right of the same evolution curve (Figure 4.1). In both conventional isotopic plots, the Huetamo samples define a field below and close to the 0 Ma value of the average Pb crust evolution curve of Stacey and Kramers (1975), whereas the Zihuatanejo samples plot far to the right of the same evolution curve (Figure 4.1).

Overall, sedimentary rocks of the Huetamo Sequence are less radiogenic than the metamorphic basement, indicating that they are not simply derived from the basement and that other rocks are involved in their provenance.

4.1.3 Compositions of Tertiary Igneous Rocks

Whole rock Pb isotope results of Cenozoic igneous rocks (granodiorite, granite, diorite, and monzonite) from the Guerrero and Sierra Madre terranes are shown in Table 4.2 and Table 4.3 and represented in Figure 4.2 and Figure 4.3.

The igneous rocks collected from La Verde, Inguaran, and La Esmeralda (Guerrero terrane) are phases of the Huacana granodiorite-quartz diorite pluton (Coochey and Eckman, 1978). The Huacana pluton is part of a cluster of plutons that extends up the

west slope of the Sierra Madre Occidental into the state of Sonora; many of them have associated copper deposits (Coochey and Eckman, 1978).

Six granodiorite, granite, and diorite samples from La Verde have $^{206}Pb/^{204}Pb$ values ranging from 18.705 to 19.033, $^{207}Pb/^{204}Pb$ between 15.565 and 15.654, and $^{208}Pb/^{204}Pb$ between 38.574 and 38.983. A granodiorite collected from Inguaran shows isotopic ratios of 18.839 for $^{206}Pb/^{204}Pb$, 15.621 for $^{207}Pb/^{204}Pb$, and 38.754 for $^{208}Pb/^{204}Pb$. Two granodiorite samples from the small mine called El Malacate (a prospect on a 1-2 m wide vein) and La Esmeralda have $^{206}Pb/^{204}Pb$ ratios of 18.765 and 18.775, $^{207}Pb/^{204}Pb$ values of 15.620 and 15.539, and $^{208}Pb/^{204}Pb$ of 38.663 and 38.473. The Pb isotope range of the Tertiary igneous rocks resembles that of the orogene reservoir in the plumbotectonics model of Zartman and Doe (1981), although a few samples are shifted to the right of the curve, to more radiogenic values (Figure 4.2). In both conventional isotopic diagrams, the samples plot to the right of the average Pb crust evolution curve of Stacey and Kramers (1975).

The igneous rocks collected from Zimapan and La Negra (Sierra Madre terrane) intruded and metamorphosed the K limestones of the Doctor Formation (which represents the host rock for the skarn mineralization) and developed structural channels favorable to subsequent mineralization (Garcia and Querol, 1991; Fraga, 1991).

The Pb isotope ratios of four Tertiary monzonite and diorite samples from Zimapan range between 18.804 and 18.972 for $^{206}Pb/^{204}Pb$, 15.623 and 15.728 for $^{207}Pb/^{204}Pb$, and between 38.671 and 39.057 for $^{208}Pb/^{204}Pb$ (Table 4.3 and Figure 4.3). One diorite sample collected from La Negra mine has Pb isotope values of 18.920 for $^{206}Pb/^{204}Pb$, 15.648 for $^{207}Pb/^{204}Pb$, and 38.841 for $^{208}Pb/^{204}Pb$ (Table 4.3 and Figure 4.3). In both conventional

isotopic diagrams, samples from the Sierra Madre terrane plot above and to the right of the average Pb crust evolution curve of Stacey and Kramers (1975); they are slightly more radiogenic compared to rocks from the Guerrero terrane (Figure 4.3). In terms of $^{208}Pb/^{204}Pb$ vs. $^{206}Pb/^{204}Pb$, the igneous rocks resemble the orogene reservoir of Zartman and Doe's model (1981), with a few samples shifted to more radiogenic values. On the uranogenic diagram they generally plot between the upper crust and orogene growth curves, except for one sample that plots above the upper crust reservoir (Figure 4.3).

4.1.4 Hydrothermal Leaching of Lead

Because of the differential solubility of primary and secondary minerals, Pb introduced in a rock at different times can be separated through sequential acid attacks of increasing strength (Chiaradia and Fontbote, 2003). The residual fraction will characterize Pb incorporated by the leach-resistant silicate minerals at the time of their formation or last recrystallization; the isotopic signature of the leachate fraction will depend on the relative proportions and isotopic compositions of: 1. common and radiogenic Pb associated with easily soluble primary and secondary minerals, and 2. radiogenic Pb removed from lattice defects of silicate minerals (primary and secondary, except zircon) and from rock-grain boundaries (Chiaradia and Fontbote, 2003).

Leaching experiments on four sedimentary and four metamorphic rocks were conducted in this study; the results are presented in Table 4.4 and shown in Figure 4.4.

Lead isotope ratios of the leachate fractions of a meta-basalt (96MR060), a schist (96MR105), and a phyllite (96MR129) are lower than the residual fractions (Figure 4.4 and Table 4.4); the values range between 18.677 and 18.907 for $^{206}Pb/^{204}Pb$, 15.621 and

15.662 for $^{207}Pb/^{204}Pb$, and between 38.630 and 39.060 for $^{208}Pb/^{204}Pb$. Lead isotope compositions of the residues vary between 18.693 and 20.331 for $^{206}Pb/^{204}Pb$, 15.626 and 15.739 for $^{207}Pb/^{204}Pb$, and 38.652 and 39.978 for $^{208}Pb/^{204}Pb$. Overall, the above-mentioned low-grade metamorphic rocks are characterized by residual fractions that are more radiogenic than the leachates (Figure 4.4). According to Chiaradia et al. (2004), this is probably the result of the fact that most common Pb is found in the leachable fraction in low-grade metamorphic rocks, and the presence of refractory zircons. The phyllite sample has significantly radiogenic residue fraction. Residue of a slate sample (96MR133) is less radiogenic in terms of $^{206}Pb/^{204}Pb$ (19.015) and $^{208}Pb/^{204}Pb$ (38.779), but more radiogenic in terms of $^{207}Pb/^{204}Pb$ (15.648), than the bulk rock composition (Figure 4.4 and Table 4.4); there are no available data for the leachate fraction of this sample. The residual fractions of the schist and the phyllite are more radiogenic than the bulk rock compositions, but both leachate and residue analyses of the meta-basalt are less radiogenic than the whole-rock analysis; this is difficult to explain unless the whole-rock powder was not well homogenized (Kamenov et al., 2002).

Lead isotope ratios of the residual fractions of two siltstones (96MR069 and 96MR117), a marl (96MR114), and a mudstone (96MR127) are consistently higher than the bulk rock compositions in terms of $^{208}Pb/^{204}Pb$ (Figure 4.4), with values ranging between 38.399 and 38.907 (Table 4.4). The trend is similar in terms of $^{206}Pb/^{204}Pb$, except for one siltstone samples (96MR069) whose residual fraction is less radiogenic than its bulk rock composition. The $^{207}Pb/^{204}Pb$ ratios of the siltstone (96MR069) and the marl residues are higher than the bulk rock composition; on the contrary, the residues of the other siltstone (96MR117) and the mudstone are less radiogenic than their bulk rock

composition (Figure 4.4). Data on the leachate fractions are only available for the siltstone samples, which show opposite trends.

4.2 Lead Isotope Compositions of Ores

Lead isotope compositions of Cenozoic sulfide ore samples collected from representative deposits in the Guerrero and Sierra Madre terranes (Figure 3.1) were determined. The results are given in Table 4.2 and Table 4.3 and represented in Figure 4.5 and Figure 4.6. Lead isotope compositions of sulfide minerals and rocks associated with an ore deposit can constrain the possible sources of metals in a hydrothermal system. This is because of the similar geochemical behavior of Pb, Cu, and Zn in hydrothermal fluids (Tosdal et al., 1999) and the occurrence of Pb in the same paragenetic stages as Zn, Cu, Ag, and cadmium (Cd) (Bourcier and Barnes, 1987; Wood et al., 1987).

Six ore samples (pyrite, galena, and bornite) from the La Verde porphyry-copper prospect, the La Esmeralda copper-bearing breccia pipe, and El Malacate (~ 31 – 36 Ma), all part of the Guerrero terrane, show isotopic ratios ranging between 18.678 and 18.723 for $^{206}Pb/^{204}Pb$, 15.569 and 15.618 for $^{207}Pb/^{204}Pb$, and 38.423 and 38.602 for $^{208}Pb/^{204}Pb$; with a few exceptions, they plot within the field defined by the sedimentary rocks from the Huetamo Sequence (Figure 4.6). This indicates that a substantial component of the Pb in these deposits might have been incorporated from continent-derived sediments. One pyrite sample from the La Verde porphyry copper prospect showed anomalously high values (19.457, 15.635, and 38.519); however, the cause of this anomaly is not clear. On conventional Pb isotope diagrams, the analyzed samples define a narrow field just below

the average Pb crust evolution curve of Stacey and Kramers (1975) and resemble the orogene reservoir in the plumbotectonics model of Zartman and Doe (1981) (Figure 4.5 and Figure 4.6).

Ten minerals (pyrite, sphalerite, galena, and chalcopyrite) from the Zimapan skarn mine in the Sierra Madre terrane yield Pb isotope compositions varying from 18.775 to 18.975 for $^{206}Pb/^{204}Pb$, 15.593 to 15.844 for $^{207}Pb/^{204}Pb$, and 38.553 to 39.404 for $^{208}Pb/^{204}Pb$ (Figure 4.5). The Pb isotope values are highly variable, reflecting hydrothermal mobilizations of metals from host rocks and incomplete homogenization. The Zimapan ores define a field shifted to more radiogenic values compared to ores from the Guerrero terrane, and they generally plot above the Stacey and Kramers (1975) reference line (Figure 4.5). On the thorogenic diagram most samples resemble the orogene reservoir in the plumbotectonics model of Zartman and Doe (1981) and on the uranogenic plot they scatter between the orogene and upper crust reservoirs (Figure 4.5).

Four samples of pyrite, sphalerite, and galena from the La Negra skarn deposit in the Sierra Madre terrane have similar Pb isotopic signatures to ores from the Zimapan mine, with ratios ranging between 18.828 and 18.973 for $^{206}Pb/^{204}Pb$, 15.623 and 15.839 for $^{207}Pb/^{204}Pb$, and 38.718 and 39.357 for $^{208}Pb/^{204}Pb$ (Figure 4.5). The close resemblance in their isotopic signatures implies similar ore metal sources; this is not surprising, considering that the igneous rocks associated with the mineralization in both skarn deposits intruded and metamorphosed the same K limestone of the Doctor Formation. Overall, the compositional field of minerals from these two deposits defines a steep trend in the uranogenic and thorogenic diagrams that generally plots above and to the right of the average Pb crust evolution curve of Stacey and Kramers (1975) (Figure 4.5).

4.3 Strontium and Neodymium Isotope Compositions of Rocks

Strontium and Nd isotopes are powerful tracers for geochemical processes and have been used to shed light on the evolution of the continental crust from the mantle. Since there are still uncertainties regarding the nature, origin, and evolution of the crustal rocks from the Guerrero composite terrane, I present new Sr and Nd isotope data on Mesozoic metamorphic rocks, Cretaceous sedimentary rocks, and Cenozoic igneous rocks in order to gain a better understanding of the tectonic history of this region. The results are shown in Table 4.5 and represented in Figure 4.7.

Two Triassic schist samples from south of Arteaga, part of the Arteaga Complex, yield $^{87}Sr/^{86}Sr$ values of 0.708378 and 0.726494, and $^{143}Nd/^{144}Nd$ ratios of 0.512542 and 0.512109. They plot in the fourth quadrant of the Nd-Sr correlation diagrams (Figure 1.3; Figure 4.7), suggesting that they were derived from sources that had been enriched in Rb and depleted in Sm and then remained isolated for a relatively long time (Faure, 1986). They show variable isotopic ratios, indicating a larger interaction of the source rocks with the crust. These results are in agreement with previously published data on sedimentary rocks from the Arteaga Complex (Figure 2.4) (Centeno-Garcia et al., 1993a).

Two Jurassic phyllite samples, part of the Tejupilco metamorphic suite, have $^{87}Sr/^{86}Sr$ values of 0.707757 and 0.722946, and $^{143}Nd/^{144}Nd$ ratios of 0.512565 and 0.512653. In case of the latter sample, the shift of the $^{87}Sr/^{86}Sr$ ratios towards higher values reflects enrichment in radiogenic Sr, which correlates with the Pb isotope data (Figure 4.7); there is no negative correlation between the Sr and Nd isotope values, which may indicate that the enrichment in radiogenic Sr is linked to seawater alteration. The isotopic values determined for the former phyllite sample are close to previously published isotopic data

on a schist sample from the Tejupilco metamorphic suite (Figure 2.4) (Elias-Herrera et al., 2003).

Two Cretaceous siltstone samples collected south of Colima, part of the Zihuatanejo Sequence, show isotopic ratios of 0.708848 and 0.709362 for $^{87}Sr/^{86}Sr$, and 0.512728 and 0.512729 for $^{143}Nd/^{144}Nd$ (Figure 4.7). Both samples fall in the first quadrant of the Nd-Sr correlation diagram (Figure 1.3), implying that they originated from sources whose Sm/Nd and Rb/Sr ratios are greater than their respective values in CHUR (chondritic uniform reservoir) and UR (uniform reservoir), which is a very rare scenario considering the geochemical properties of these elements (Faure, 1986). One Cretaceous siltstone sample collected between Altamirano and Huetamo, part of the Huetamo Sequence, has $^{87}Sr/^{86}Sr$ value of 0.705301 and $^{143}Nd/^{144}Nd$ of 0.512786, plotting above the $\varepsilon^0_{CHUR}(Nd)$ and to the right of the $\varepsilon^0_{UR}(Sr)$ (Figure 4.7). One Cretaceous mudstone sample from near Huetamo, part of the same Huetamo Sequence, yields isotopic ratios of 0.707575 for $^{87}Sr/^{86}Sr$ and 0.512541 for $^{143}Nd/^{144}Nd$ (Figure 4.7). In contrast to the siltstone sample, the Nd isotope ratio of the mudstone falls below that of bulk earth, implying that it might have been derived from more evolved crustal rocks.

One Cenozoic granite sample collected from the La Verde quarry has $^{87}Sr/^{86}Sr$ of 0.708784 and $^{143}Nd/^{144}Nd$ of 0.512615. One massive granodiorite from Inguaran has isotopic ratios of 0.704860 for $^{87}Sr/^{86}Sr$ and 0.512747 for $^{143}Nd/^{144}Nd$. Two Cenozoic granodiorite samples from the small mine called El Malacate and from La Esmeralda display values of 0.704909 and 0.705755 for $^{87}Sr/^{86}Sr$, and 0.512740 and 0.512746 for $^{143}Nd/^{144}Nd$. In case of the igneous rocks from Inguaran, El Malacate, and La Esmeralda, the narrow ranges and generally low $^{87}Sr/^{86}Sr$ ratios, and $^{143}Nd/^{144}Nd$ values above that of

bulk earth suggest a relatively low degree of crustal contamination. In contrast, the isotopic values for the La Verde site may indicate more crustal contamination or a more evolved crustal component (Figure 4.7).

Table 4.1. Lead Isotope Compositions of Crustal Rocks from the Guerrero Terrane

Mesozoic crystalline rocks				
Sample	**Rock type**	**$^{206}Pb/^{204}Pb$**	**$^{207}Pb/^{204}Pb$**	**$^{208}Pb/^{204}Pb$**
96MR060	meta-basalt	18.701	15.649	38.711
96MR101	schist	18.858	15.641	38.906
96MR102	schist	18.981	15.623	38.936
96MR103	schist	18.956	15.664	39.076
96MR105	schist	18.999	15.674	39.202
96MR107	schist	18.962	15.693	39.216
96MR111	phyllite	18.876	15.650	38.694
96MR129	phyllite	19.256	15.646	39.098
96MR131	phyllite	19.033	15.647	38.807
96MR133	slate	19.032	15.643	38.780
Cretaceous sedimentary rocks				
Sample	**Rock type**	**$^{206}Pb/^{204}Pb$**	**$^{207}Pb/^{204}Pb$**	**$^{208}Pb/^{204}Pb$**
96MR055	siltstone	19.050	15.643	38.547
96MR057	mudstone	19.437	15.634	38.892
96MR067	siltstone	19.001	15.601	38.795
96MR068	siltstone	18.763	15.580	38.510
96MR069	siltstone	19.053	15.622	38.849
96MR114	marl	18.998	15.627	38.610
96MR116	sandstone	18.649	15.641	38.587
96MR117	siltstone	18.630	15.563	38.381
96MR118	siltstone	18.796	15.632	38.562
96MR119	sandstone	18.696	15.603	38.404
96MR121	sandstone	18.705	15.582	38.482
96MR127	mudstone	18.767	15.624	38.525
96MR128	siltstone	18.630	15.582	38.369

Table 4.2. Lead Isotope Compositions of Tertiary Intrusions and Ores from the Guerrero Terrane

Tertiary igneous rocks				
Sample	**Rock type**	**$^{206}Pb/^{204}Pb$**	**$^{207}Pb/^{204}Pb$**	**$^{208}Pb/^{204}Pb$**
96MR071	granodiorite	18.968	15.595	38.904
96MR076	diorite	18.989	15.565	38.711
96MR078	granodiorite	18.844	15.598	38.772
96MR079	granodiorite	19.033	15.628	38.983
96MR083	granodiorite	18.705	15.613	38.574

96MR088	granite	18.883	15.654	38.874
96MR095	granodiorite	18.839	15.621	38.754
96MR096	granodiorite	18.765	15.620	38.663
96MR099	granodiorite	18.775	15.539	38.473
Ore samples				
Sample	**Mineral**	**$^{206}Pb/^{204}Pb$**	**$^{207}Pb/^{204}Pb$**	**$^{208}Pb/^{204}Pb$**
96MR079	pyrite	18.723	15.585	38.568
96MR082	pyrite	19.457	15.635	38.519
96MR084	bornite	18.678	15.569	38.423
96MR095g	galena	18.699	15.597	38.521
96MR098B	pyrite	18.699	15.607	38.562
96MR098G	pyrite	18.721	15.618	38.602

Table 4.3. Lead Isotope Compositions of Tertiary Intrusions and Ores from the Sierra Madre Terrane

Tertiary igneous rocks				
Sample	**Rock type**	**$^{206}Pb/^{204}Pb$**	**$^{207}Pb/^{204}Pb$**	**$^{208}Pb/^{204}Pb$**
96MR157	monzonite	18.972	15.728	39.057
96MR166	endoskarn	18.838	15.663	38.849
96MR167	monzonite	18.945	15.669	38.936
96MR173	monzonite	18.804	15.623	38.671
96MR177	diorite	18.920	15.648	38.841
Ore samples				
Sample	**Mineral**	**$^{206}Pb/^{204}Pb$**	**$^{207}Pb/^{204}Pb$**	**$^{208}Pb/^{204}Pb$**
96MR152	pyrite	18.776	15.619	38.666
96MR153	pyrite	18.827	15.684	38.868
96MR154	pyrite	18.807	15.649	38.750
96MR159	sphalerite	18.868	15.738	39.030
96MR164	sphalerite	18.975	15.844	39.404
96MR165g	galena	18.808	15.666	38.789
96MR169	chalcopyrite	18.775	15.593	38.553
96MR170g	galena	18.798	15.626	38.685
96MR170	pyrite	18.819	15.648	38.753
96MR171g	galena	18.851	15.694	38.889
96MR182	pyrite	18.973	15.839	39.357
96MR183	sphalerite	18.921	15.765	39.129
96MR183g	galena	18.828	15.623	38.718
96MR184	sphalerite	18.865	15.679	38.853

Table 4.4. Lead Isotope Compositions of Whole Rocks, Leachates (L), and Residues (R) of Metamorphic and Sedimentary Rocks from the Guerrero Terrane

Sample	Rock type	$^{206}Pb/^{204}Pb$	$^{207}Pb/^{204}Pb$	$^{208}Pb/^{204}Pb$
96MR060	metabasalt	18.701	15.649	38.711
96MR060L		18.677	15.621	38.630
96MR060R		18.693	15.626	38.652
96MR069	siltstone	19.053	15.622	38.849
96MR069R		19.043	15.639	38.907
96MR069L		19.128	15.602	38.916
96MR105	schist	18.999	15.674	39.202
96MR105L		18.907	15.661	39.060
96MR105R		19.016	15.705	39.278
96MR114	marl	18.998	15.627	38.610
96MR114R		19.005	15.637	38.660
96MR117	siltstone	18.630	15.563	38.381
96MR117L		18.617	15.601	38.469
96MR117R		18.711	15.562	38.399
96MR127	mudstone	18.767	15.624	38.525
96MR127R		18.776	15.620	38.550
96MR129	phyllite	19.256	15.646	39.098
96MR129L		18.891	15.662	38.960
96MR129R		20.331	15.739	39.978
96MR133	slate	19.032	15.643	38.780
96MR133R		19.015	15.648	38.779

Table 4.5. Strontium and Neodymium Isotope Compositions of Whole Rocks from the Guerrero Terrane

Sample	Rock type	$^{87}Sr/^{86}Sr$	2se	$^{143}Nd/^{144}Nd$	2se
96MR101	schist	0.708378	±7	0.512567	±3
96MR105	schist	0.726494	±7	0.512133	±3
96MR111	phyllite	0.707757	±7	0.512589	±4
96MR129	phyllite	0.722946	±7	0.512677	±3
96MR088	granite	0.708784	±7	0.512640	±3
96MR095	granodiorite	0.704860	±7	0.512772	±4
96MR096	granodiorite	0.704909	±7	0.512765	±4
96MR099	granodiorite	0.705755	±7	0.512771	±3
96MR067	siltstone	0.708848	±7	0.512753	±4
96MR069	siltstone	0.709362	±7	0.512753	±3
96MR117	siltstone	0.705301	±7	0.512810	±3
96MR127	mudstone	0.707575	±10	0.512565	±3

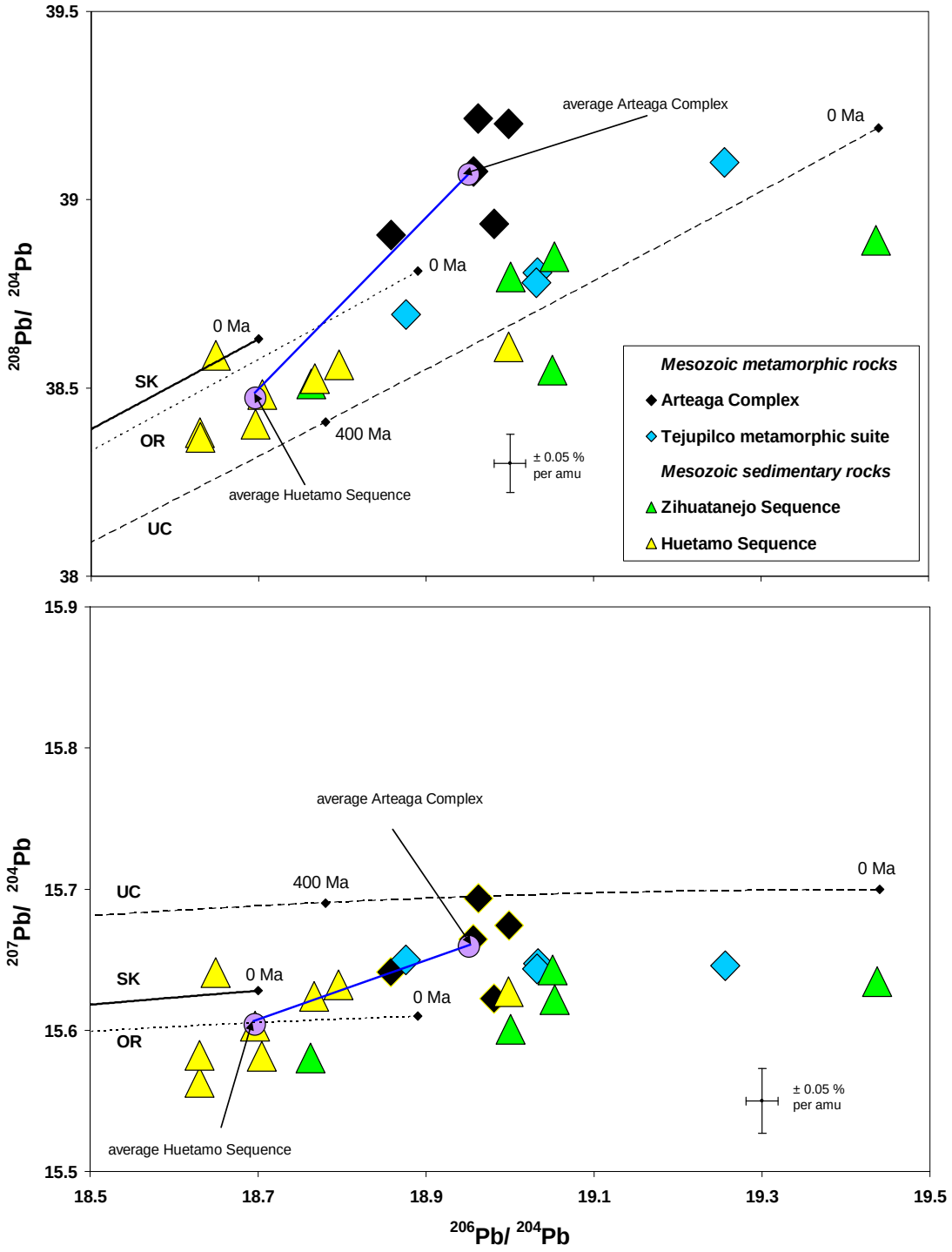

Figure 4.1. Lead isotope compositions of Mesozoic metamorphic and sedimentary rocks from the Guerrero terrane. The average upper crustal (UC) and orogene (OR) growth curves are from Zartman and Doe (1981); the lead growth curve (SK) is from Stacey and Kramers (1975). Also shown are average values for metamorphic rocks from the Arteaga Complex and sedimentary rocks from the Huetamo Sequence.

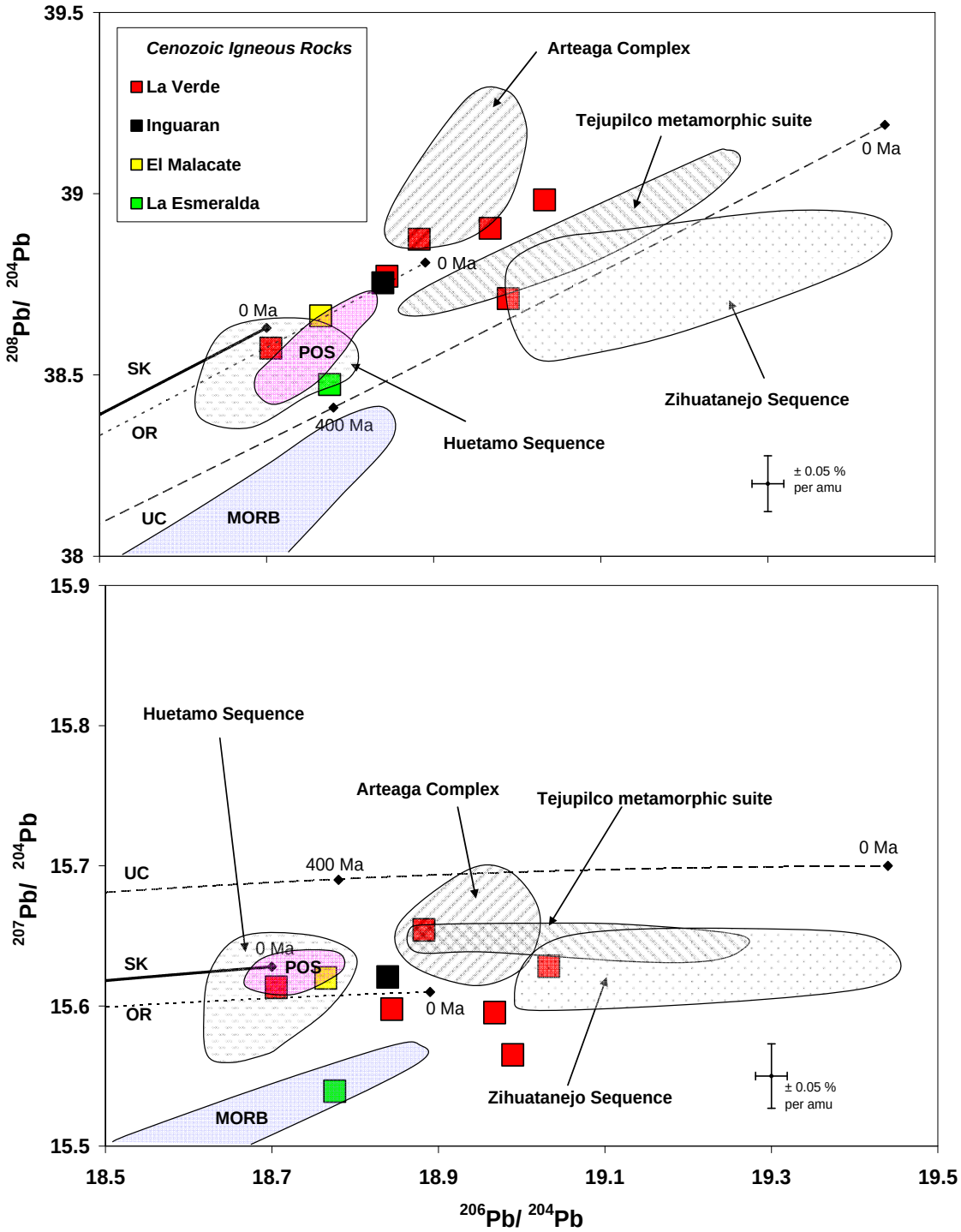

Figure 4.2. Lead isotope compositions of Cenozoic igneous rocks from the Guerrero terrane. For reference, the compositional fields of Mesozoic metamorphic and sedimentary rocks from the Guerrero terrane (this study), Pacific Ocean sediments (POS; Hemming and McLennan, 2001), and MORB-EPR (White et al., 1987) are also shown. The average upper crustal (UC) and orogene (OR) growth curves are from Zartman and Doe (1981); the lead growth curve (SK) is from Stacey and Kramers (1975).

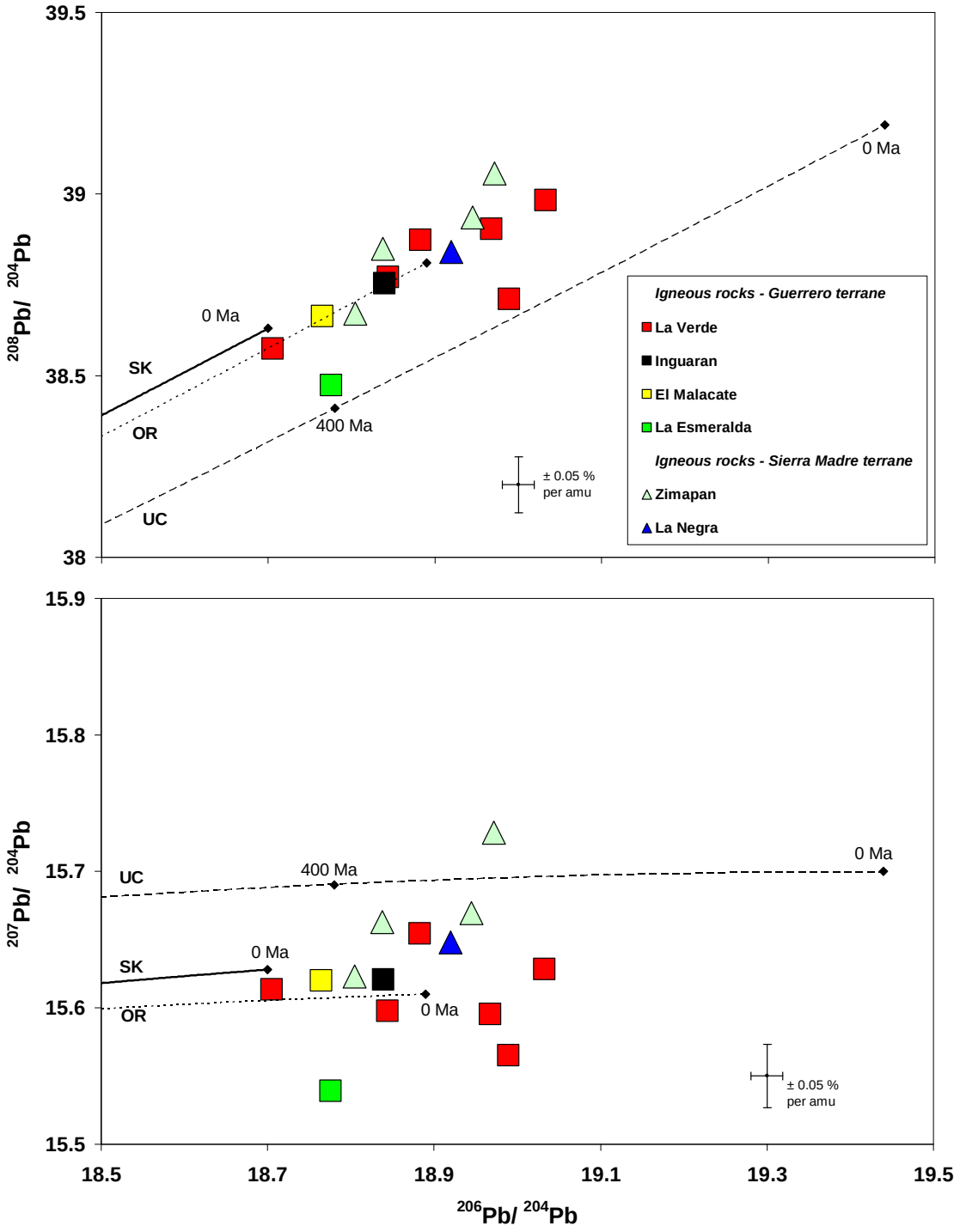

Figure 4.3. Lead isotope compositions of Cenozoic igneous rocks from the Guerrero and Sierra Madre terranes. The average upper crustal (UC) and orogene (OR) growth curves are from Zartman and Doe (1981); the lead growth curve (SK) is from Stacey and Kramers (1975).

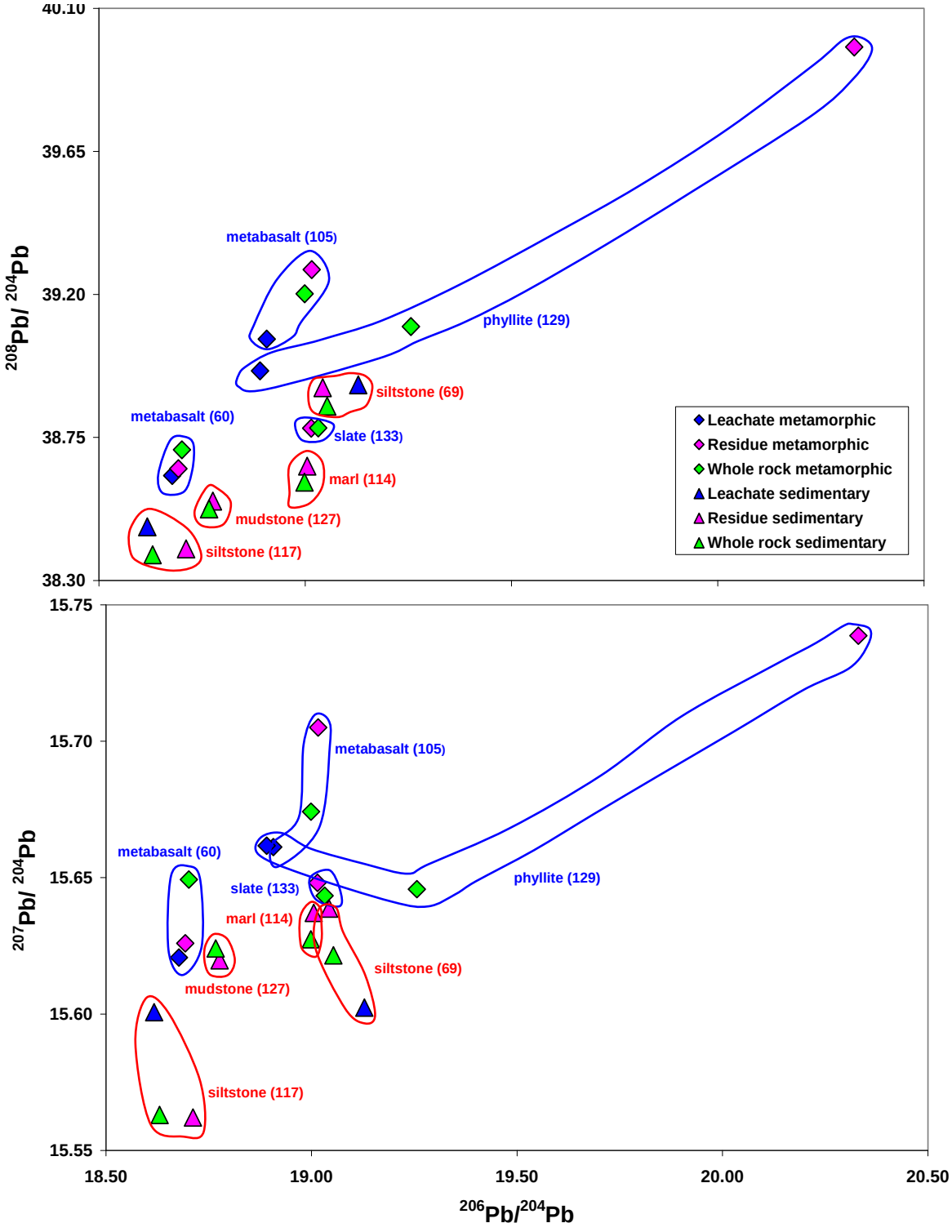

Figure 4.4. Lead isotope compositions of leachates, residues, and whole rocks of basement and sedimentary rocks from the Guerrero terrane.

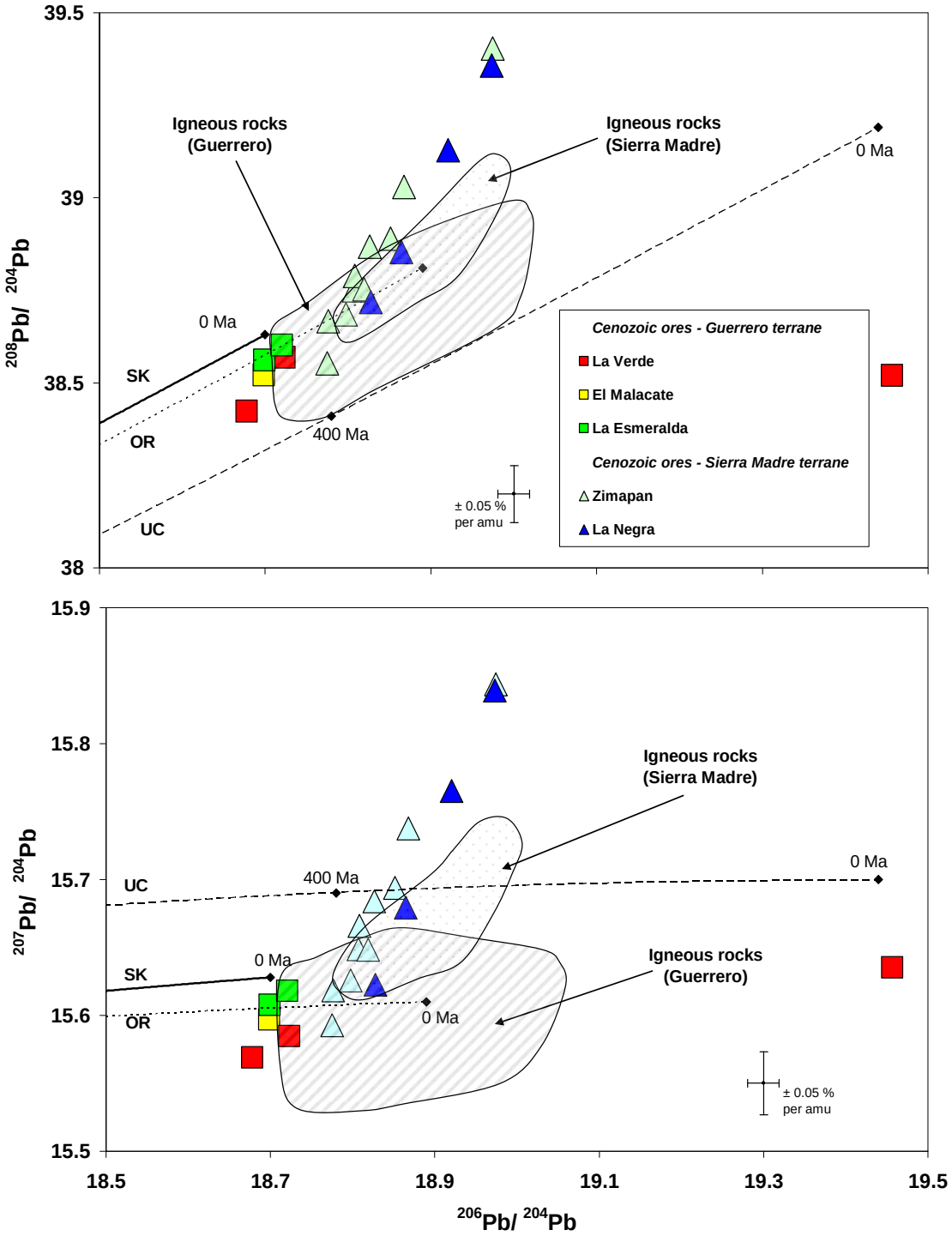

Figure 4.5. Lead isotope compositions of Cenozoic ores from deposits located in the Guerrero and Sierra Madre terranes. For reference, the compositional fields of the associated Cenozoic igneous rocks are also shown. The average upper crustal (UC) and orogene (OR) growth curves are from Zartman and Doe (1981); the lead growth curve (SK) is from Stacey and Kramers (1975).

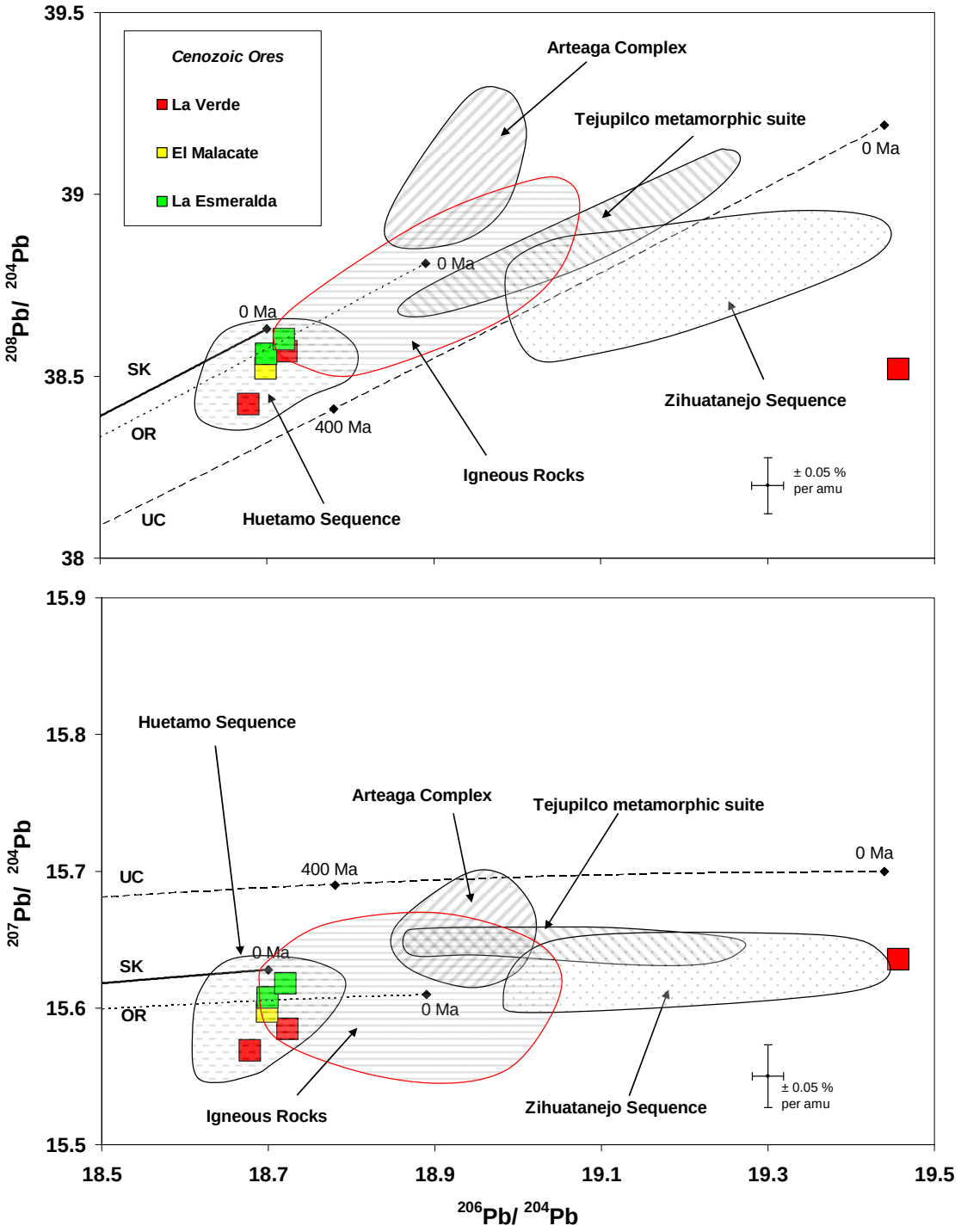

Figure 4.6. Lead isotope compositions of Cenozoic ores from La Verde, El Malacate, and La Esmeralda porphyry copper deposits in the Guerrero terrane. For reference, the compositional fields of Mesozoic metamorphic and sedimentary rocks and Cenozoic igneous rocks from the Guerrero terrane are also shown. The average upper crustal (UC) and orogene (OR) growth curves are from Zartman and Doe (1981); the lead growth curve (SK) is from Stacey and Kramers (1975).

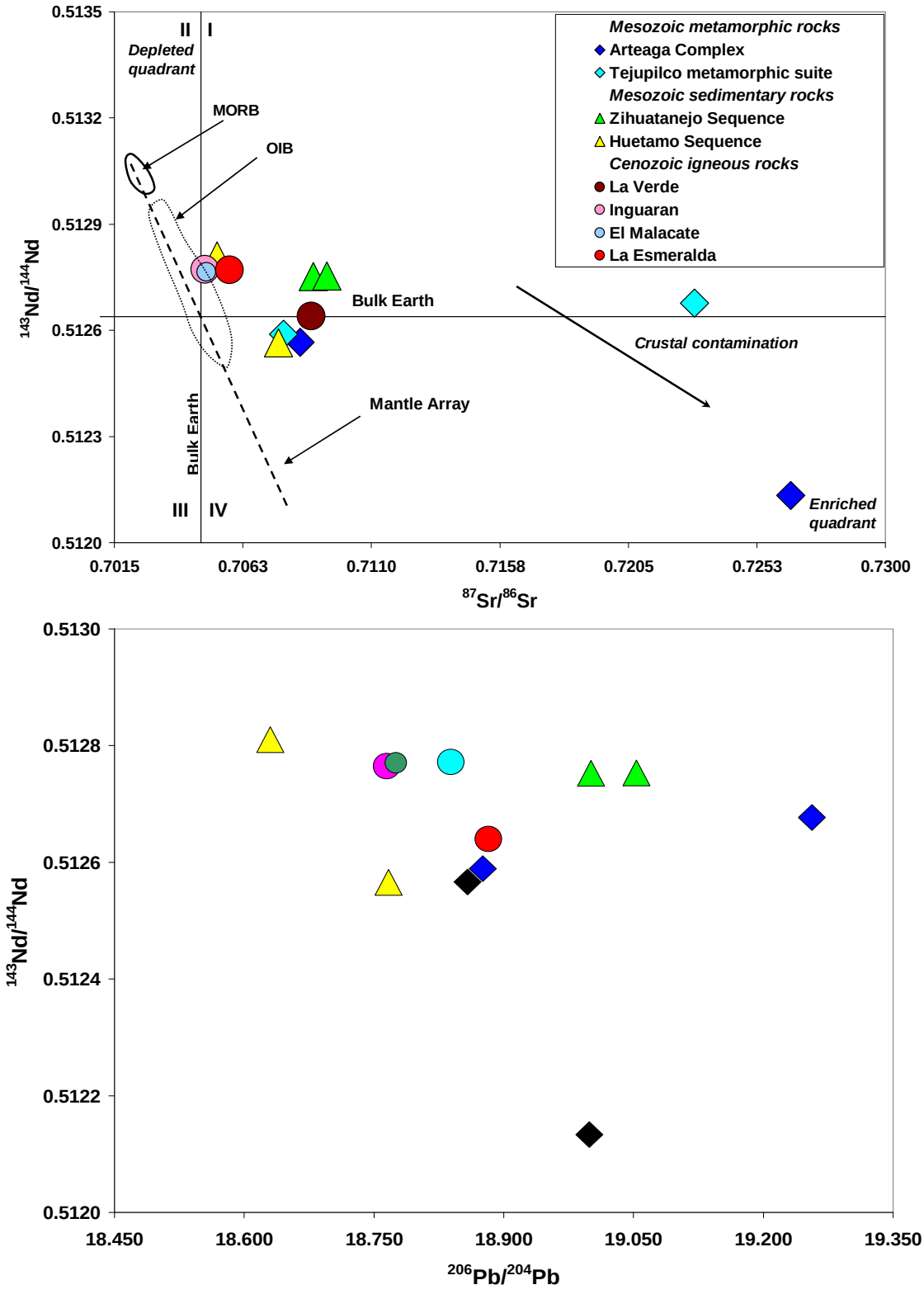

Figure 4.7. Isotope correlation digrams showing the location of the crustal rocks from the Guerrero terrane in $^{143}Nd/^{144}Nd$, $^{87}Sr/^{86}Sr$, and $^{206}Pb/^{204}Pb$ space.

5. GENESIS AND PROVENANCE OF CRUSTAL ROCKS

The genesis and provenance of crustal rocks from the Guerrero composite terrane are discussed in the light of new and previously published Pb, Sr, and Nd isotope data on Mesozoic metamorphic rocks, Cretaceous sedimentary rocks, and Cenozoic igneous rocks. Isotopic data represent a powerful tool for provenance study because of their usefulness as tracers of mixing processes (Dickin, 1995).

5.1 Isotopic Characteristics and Provenance of Mesozoic Metamorphic Rocks

The subvolcanic basement rocks of the Guerrero terrane have been recognized only in a few areas and have received different names at different outcrops: Arteaga Complex (exposed in the area of Arteaga, of Permo-Triassic age), Tejupilco metamorphic suite (exposed in the Tejupilco-Taxco region, northeast of Huetamo, of pre-Upper Jurassic age), Zacatecas Formation (exposed near Zacatecas, of Late Triassic age), and the Pinzan Morado Complex (exposed southwest of Huetamo, which may be correlated with the Arteaga Complex).

5.1.1 Whole Rock Pb Isotopic Compositions

The Pb isotopic characteristics of metamorphic rocks from the Guerrero terrane are described on the basis of new and previously published data of basement rocks from Mexico (the Guerrero, the Mixteca, the Oaxaca, the Juarez, and the Maya terranes), Colombia (Santa Marta and Garzon massifs), United States (Texas), and Peru (Olmos and Maranon complexes) (Figure 5.1).

The rocks analyzed in this study for Pb isotope ratios include Triassic schist samples from the Arteaga Complex, and Jurassic phyllite and slate samples from the Tejupilco

metamorphic suite. Overall, the isotopic compositions of Pb in these Mesozoic basement rocks are substantially more radiogenic than published data on high-grade metamorphic rocks (metagabbro and charnockite) from the Grenvillian-age (Precambrian) Oaxaca terrane (Martiny et al., 2000; Figure 5.2 and Figure 5.3). On conventional Pb isotope diagrams, the samples from the Oaxaca Complex plot in a narrow range below the average Pb crust evolution curve of Stacey and Kramers (1975), close to the 1000 Ma field of the growth curve, whereas samples from both metamorphic suites in the Guerrero terrane plot to the right of the curve, falling in a more scattered area (Figure 5.2). The nonradiogenic Pb isotope compositions of the granulites from the Oaxaca Complex (Figure 5.1 - location 7), the oldest known metamorphic belt in southern Mexico (900 – 1100 Ma, established by K-Ar dating of pegmatitic micas and by U-Pb isotopic studies of zircon from pegmatite and gneiss) (Fries et al., 1962; Ortega-Gutierrez et al., 1977), is related to the loss of U during the Grenville orogeny. The radiogenic Pb in basement rocks of the Guerrero terrane, with a much lower metamorphic grade, reflects a different history from that of the ancient, high-grade metamorphic Oaxaca terrane. Thus, Pb isotope evidence indicates the basement rocks in Guerrero are unrelated to those in Oaxaca.

Present-day Pb isotope compositions of whole rocks from the Grenville-age Oaxaca Complex are similar to those of Grenville-age rocks in the Santa Marta Massif in northernmost Colombia (Figure 5.1 - location 9, and Figure 5.3). Samples from the Guichicovi Complex, exposed at the boundary between the Maya and the Juarez terranes (Figure 5.1 - location 8), have Pb isotopic values that define a field lying along the average Pb crustal growth curve and close to the field defined by samples from the

Garzon Massif, the southernmost Colombian massif (Figure 5.3). These data suggest that these now widely- separated basement blocks shared a common history in the late Proterozoic: the Oaxaca Complex with the Santa Marta Massif, and the Guichicovi Complex with the Garzon Massif (Ruiz et al., 1999). It has been suggested (Yanez et al., 1991; Restrepo-Pace et al., 1997; Ruiz et al., 1999) that they were part of Gondwana during the early Paleozoic, and that the Oaxaca and Guichicovi complexes were transferred from that part of northwestern Gondwana presently occupied by Colombia to the southern end of Laurentia during Paleozoic orogenies related to the opening and closing of the proto-Atlantic Ocean. On the basis of geologic considerations and isotopic data, Ruiz et al. (1988b) suggested that basement rocks underlying most of southern and central Mexico were part of South America and were involved in Laurentia-Gondwana collisions in the Paleozoic.

The Pb isotope ratios of basement rocks from the Arteaga and Tejupilco Complexes resemble those of metamorphic xenoliths (represented by phyllite, schist, and gneiss) from continental crust beneath Nevado de Toluca volcano (Martinez-Serrano et al., 2004; Figure 5.1 - location 4; Figure 5.3); this may indicate a possible connection of the basement in these areas. They are also similar to the Pb isotopic field defined by rocks of the Paleozoic Acatlan Complex, the basement of the Mixteca terrane (Martiny et al., 1997; Figure 5.1 – location 6; Figure 5.3). Isotopic dating of garnets (Sm-Nd) and zircons (U-Pb) from schists and eclogites of the Acatlan Complex yields metamorphic ages of 410 – 380 Ma (Yanez et al., 1991). Whole rock (schist) Pb isotope data of the Paleozoic Acatlan Complex define a field that lies above and to the right of the average Pb crust evolution curve of Stacey and Kramers (Figure 5.3). Unlike the Oaxaca, Santa Marta,

Guichicovi, and Garzon basement areas, which reflect variable depletion of U relative to Pb, these rocks reflect a history of elevated U/Pb relative to bulk earth models.

Grenville-age basement exposures in Texas (Llano uplift) have Pb isotopic compositions (Smith et al., 1997) with lower $^{207}Pb/^{204}Pb$ ratios for a given $^{206}Pb/^{204}Pb$ ratio than the Mexican samples (Figure 5.3), reflecting an older metamorphism and a different history. Unlike the basement exposures of Grenville-age from Mexico, which are located on continental margins deformed during Mesozoic and Tertiary time, the Texas "Grenville" rests on pre-Late Mesozoic rocks of the North American craton (Figure 5.1).

Metamorphic basement rocks from the Olmos and Maranon Complexes, northern Peru (Figure 5.1 - locations 12 and 13), represented mainly by schist, have Pb isotope compositions (Macfarlane and Petersen, 1990) similar to metamorphic basement from the Mexican terranes of Mixteca (Martiny et al., 1997; Martiny et al., 2000) and Guerrero (Figure 5.3). It is possible that these blocks had been related spatially and shared a common history prior to ending up in their current location.

Common Pb isotope compositions of the Mexican basement rocks more closely resemble those of the northern part of South America (Colombia and northern Peru) than exposures from North America: the Oaxaca Complex is similar to the Santa Marta Massif, the Guichicovi complex is similar to the Garzon Massif, and the Acatlan, Arteaga, and Tejupilco Complexes are similar to the Olmos and Maranon Complexes (Figure 5.3). Common occurrences of high $^{206}Pb/^{204}Pb$ are present on the western side of Mexico (with exposures of the Arteaga Complex, Tejupilco metamorphic suite, Nevado de Toluca xenoliths, and the Acatlan Complex) and northern Peru (with exposures of the

Olmos and Maranon complexes), whereas areas of low $^{206}Pb/^{204}Pb$ are located on the southeastern part of Mexico (with exposures of the Oaxaca and Guichicovi complexes) and Colombia (Santa Marta and Garzon massifs).

During Late Cretaceous time, a Mesozoic oceanic island arc (the "proto-Caribbean arc") collided with the continental margins of North America and northern South America (Stephan et al., 1990), generating the proto-Caribbean arc of the Greater Antilles (Cuba, Hispaniola, Puerto Rico, and the nearby islands) in the north (Donnelly and Rogers, 1978); in the south, the remnants of the accreted arc lie along the South American margin, from Colombia, Venezuela, to the West Indies (Tobago) (Tardy et al., 1994; Figure 5.1). On the basis of available geochemical data (presented in detail by Tardy et al., 1994) and paleogeographic reconstructions of the Gulf of Mexico and the Caribbean (Pindell, 1994), it seems that the late Mesozoic Guerrero arc sequences and the proto-Caribbean arc shared a similar magmatic evolution in time and have both been developed in an intra-oceanic environment. However, a major difference is that the Guerrero composite terrane is partly built on continental blocks and oceanic lithosphere, while the proto-Caribbean arc is entirely oceanic (Tardy et al., 1994). Tardy et al. (1994) concluded that the diverse but mainly submarine arc segments of the late Mesozoic intra-Pacific arc rimmed the North and South American cratons in a similar way to the present Tertiary arcs rimming Southeast Asia.

5.1.2 Whole Rock Sr and Nd Isotope Data

The Sr and Nd isotopic characteristics of the metamorphic rocks from the Guerrero terrane are described using new and previously published data of basement rocks from

four Precambrian exposures in eastern and southern Mexico (Los Filtros, Novillo Gneiss, Huiznopala Gneiss, and Oaxaca Complex), from the Arteaga Complex (Guerrero terrane), the Acatlan Complex (Mixteca terrane), the Peru (Olmos and Maranon complexes) (Figure 5.1).

As described in Chapter 1, the Arteaga Complex consists of mainly terrigenous sediments (Varales Formation) and minor basaltic pillow lavas, chert, tuff, and limestone (Centeno-Garcia et al., 1993a). The sedimentary rocks show an evolved isotopic signature, with $^{87}Sr/^{86}Sr$ between 0.7083 and 0.7341, $^{143}Nd/^{144}Nd$ between 0.5121 and 0.5125 (Figure 5.6; this study and Centeno-Garcia et al., 1993a), and depleted mantle Nd model ages for the sedimentary rocks of 1.3 and 1.4 Ga (DePaolo, 1981; Centeno-Garcia et al., 1993a). They show variable ratios, suggesting a larger interaction of the source rocks with the crust. However, initial ε_{Nd} values of +13 and present-day $^{143}Nd/^{144}Nd$ = 0.5133 of the pillow-basalts imply a MORB-like affinity (Figure 5.6), indicating that the basement rocks from the Arteaga Complex represent a mixture of depleted mantle-derived material and a recycled Precambrian crust (Centeno-Garcia et al., 1993a).

The Sr and Nd isotopic values of a Jurassic phyllite from the Tejupilco metamorphic suite do not show the typical negative correlation (Figure 5.6), plotting in quadrant I of the Nd-Sr correlation diagram (Figure 1.3) and indicating that it had been derived from sources enriched in both Rb and Sm, which is a very rare scenario due to the geochemical properties of these elements. However, another Jurassic phyllite sample from the same metamorphic suite has similar Sr and Nd isotopic signatures to a Triassic schist sample from the Arteaga Complex. The Tejupilco metamorphic suite, a submarine metavolcanic-sedimentary sequence of island-arc affinity, has a Precambrian Nd model age of 1.27 Ga

and present-day ε_{Nd} = -5, indicating generation from an old crustal component with or without the involvement of juvenile mantle-derived material (Elias-Herrera et al., 2000). The similar Nd model ages of the Arteaga and Tejupilco metamorphic rocks and the resemblance in their Sr and Nd isotopic ratios suggest that they had been derived from similar sources.

Overall, Sr and Nd isotope data of basement units from the Arteaga Complex, Tejupilco metamorphic suite, and Zacatecas Formation (Figure 2.4 and Figure 5.6) imply derivation from an evolved continental source. The old component in these basement units may have been derived from the Grenville belt that extends from central Chihuahua to Oaxaca (Centeno-Garcia and Silva-Romo, 1997). The cratonic rocks of Sonora, northern Chihuahua, and western United States are not suitable as primary sources for the sediments because they have much older Nd model ages (1.7 – 2.3 Ga) (DePaolo, 1981; Ruiz et al., 1988b; Nelson and Bentz, 1990; Centeno-Garcia and Silva-Romo, 1997).

Neodymium isotope results of the Pepechuca high-grade gneiss xenoliths found in a Tertiary volcanic field (La Goleta), around 50 km SW of Nevado de Toluca, indicate continental affinity (ε_{Nd} = -6.7 and -7.3 and Nd model ages of 1.54 and 1.79 Ga; Elias-Herrera et al., 1996) and are similar to values of Grenvillian rocks in Mexico. The basement rocks (phyllite, schist, and gneiss) under Nevado de Toluca (Figure 5.1 - location 4) have Nd model ages between 1 and 1.8 Ga (Martinez-Serrano et al., 2004). These results suggest the existence of an old (pre-Mesozoic) sialic continental crust under the southern border of the Trans-Mexican Volcanic Belt, which was covered by Mesozoic arc sequences of the Guerrero terrane (Elias-Herrera et al., 1996; Martinez-

Serrano et al., 2004) and may have been involved in the pre-Cretaceous magmatic evolution of the Guerrero composite terrane.

The metasedimentary rocks and Paleozoic granitoids from the Acatlan Complex, basement of the Mixteca terrane, have present-day $^{143}Nd/^{144}Nd$ varying between around 0.5120 and 0.5128 (Yanez et al., 1991; Figure 5.6), with crustal residence ages between around 1.4 and 1.7 Ga, indicating derivation at least partly from a Proterozoic source area (Yanez et al., 1991). The crustal residence ages correlate well with the model age of the Oaxaca Complex, which is considered the most likely source area for the basement rocks of the Acatlan Complex. These and the Pb isotope results presented in the previous section imply that the possible source of the the Acatlan Complex was Colombia, and the complex was transferred to North America during the breakup of Pangea in Mesozoic times (Yanez et al., 1991).

Grenville-age rocks outcrop widely along the entire Appalachian Province (King, 1959) and continue south into Mexico (Ortega-Gutierrez, 1981). Isotopic dating of garnets (Sm-Nd) and hornblende (K-Ar) from four Precambrian exposures in eastern and southern Mexico (Oaxaca Complex, Huiznopala Gneiss, Novillo Gneiss, and Los Filtros metagranites and amphibolites; Figure 5.1 - locations 7, 3, 2, and 1) yield metamorphic cooling ages between 0.9 and 1 Ga (Figure 5.6; Patchett and Ruiz, 1987; Ruiz et al., 1988a; Ruiz et al., 1988b). These imply a cooling history following Grenville metamorphism (1.05 – 1 Ga). Depleted mantle Nd model ages (T_{DM}) for the same exposures vary between 1.37 and 1.6 Ga (Figure 5.6), suggesting that these basement rocks originated from crustal protoliths which had been separated from the mantle roughly 0.5 Ga before the Grenville Orogeny (Patchett and Ruiz, 1987). Patchett and

Ruiz (1987) suggested that the Mexican Precambrian outcrops represent mixtures between recycled Proterozoic crustal material and around 80 % of new material derived from the mantle during 1.1 – 1 Ga, as a result of tectonic and magmatic processes during the Grenville Orogeny. The nature of these Grenville-age rocks in eastern and southern Mexico is similar and indicates that they may be connected beneath the Trans-Mexican Volcanic Belt (Ortega-Gutierrez, 1981).

Gneiss units from the Texas Precambrian outcrops have igneous / metamorphic ages between 1.23 and 1.31 Ga (U-Pb dating of zircon; Walker, 1988) and T_{DM} ages between 1.6 and 1.2 Ga, with the highest frequency at 1.4 Ga (Patchett and Ruiz, 1989). On the basis of the similarity between the Nd isotopic results for granulite-facies terranes in Mexico and Texas metamorphic rocks, Patchett and Ruiz (1989) concluded that, similar to the Mexican Precambrian exposures, the rocks in the Texas area were derived from depleted mantle around 1.3 – 1 Ga ago, with a minor addition (0 – 20 %) of older crustal material.

Northern Peru basement rocks have much lower $^{143}Nd/^{144}Nd$ ratios (Macfarlane, 1999a) than any metamorphic basement rock from Mexico (Figure 5.6). According to Macfarlane (1999a), model ages of the northern Peruvian crust (1.43 – 2.06 Ga) are close to those of basement rocks farther to the east, suggesting that the northern Peru basement may be a reactivated margin of the Brazil shield. The Nd model ages of the Olmos Complex (Figure 5.1 - location 12) are similar to those of the Mexican Grenville-age outcrops (Figure 5.6) and suggest that these basement units had been separated from the mantle roughly 1.4 - 1.8 Ga before present. Model ages of the Maranon Complex (Figure 5.1 - location13) extend to older values, up to 2 Ga.

5.2 Isotopic Characteristics and Provenance of Sedimentary Rocks

The sedimentary rocks sampled in the study area consist of Early Cretaceous siltstones and mudstones from the Zihuatanejo Sequence, and Cretaceous sandstones, siltstones, and mudstones from the Huetamo Sequence. The Zihuatanejo Sequence crops out along the Pacific margin from Zihuatanejo to Purificación, whereas the Huetamo Sequence has been recognized in the Huetamo region, west of the Arcelia-Palmar Chico subterrane (Figure 3.1).

The sedimentary rocks from the Zihuatanejo-Huetamo subterrane define two different clusters on conventional Pb isotope diagrams (Figure 5.2). Samples from the Huetamo Sequence are less radiogenic than the metamorphic basement, indicating they are not simply derived from the basement and that other rocks are involved in their provenance. They plot close to the radiogenic end of the MORB-EPR field (Figure 5.4 and Figure 5.5), suggesting a possible mixing line between the metamorphic basement (probably represented by Tejupilco metamorphic suite rocks to the east) and the MORB component. Overall, the Pb isotopic ratios of the Huetamo sedimentary rocks are close to the published data for the sediments from the IODP-DSDP Leg 66 Sites 487 and 488, Cocos Plate (Verma, 2000; Figure 5.2) and for the Pacific Ocean sediments (Hemming and McLennan, 2001; Figure 5.4 and Figure 5.5). On conventional Pb isotope diagrams, samples from this sequence plot close to the 0 Ma field of the Stacey and Kramers (1975) Pb growth curve and define a narrow field just below this reference line; overall, they are fairly typical of the orogene reservoir of Zartman and Doe (1981) (Figure 5.2).

One Cretaceous mudstone sample from the Huetamo Sequence has Sr and Nd isotopic ratios that plot close to the field defined by the basement rocks of the Arteaga Complex

and Tejupilco metamorphic suite (Figure 5.8), indicating that it may have been derived from the subjacent metamorphic basement. However, the isotopic signatures of a siltstone sample suggest derivation from less evolved sources, and plot close to the igneous samples from Inguaran, El Malacate, and La Esmeralda (Figure 5.8).

Unlike rocks from the Huetamo Sequence, samples from the Zihuatanejo Sequence, located in the western part of the Guerrero terrane, contain more radiogenic Pb and describe a field that plots far to the right of the average Pb crust evolution curve of Stacey and Kramers (Figure 5.4 and Figure 5.5). They plot along the upper crust reservoir of Zartman and Doe on the thorogenic diagram and to the right of the orogene reservoir of Zartman and Doe on the uranogenic diagram. A few samples have similar Pb isotopic compositions to metamorphic rocks from the Tejupilco Complex (Figure 5.5), implying that the metamorphic rocks may have been involved in their provenance.

5.3 Isotopic Characteristics and Provenance of Igneous Rocks

5.3.1 Whole Rock Pb Isotope Data

The compositional fields depicted in Figure 4.2 for igneous rocks include Cenozoic granodiorite, granite, and diorite samples from La Verde, Inguaran, El Malacate, and La Esmeralda in the Guerrero terrane, as well as Cenozoic monzonite and diorite samples from Zimapan and La Negra in the Sierra Madre terrane (Figure 2.12 and Figure 3.1).

5.3.1.1 Guerrero Terrane

Lead in plutonic rocks from the La Verde area is more radiogenic and variable than any other analyzed igneous rocks from the Guerrero terrane, plotting along and to the

right of the orogene reservoir of Zartman and Doe (Figure 4.2). They plot close to the field defined by the metamorphic rocks, indicating the involvement of radiogenic basement rocks in the generation of the Cenozoic magma. The isotopic variability of rocks from La Verde area suggests that these subduction-related magmas were very short lived and did not have sufficient time to become isotopically homogenized, as suggested by Sundblad et al. (1991) for Cenozoic igneous rocks from Nicaragua (formed as a result of the subduction of oceanic crust belonging to the Cocos plate under pre-Mesosoiz sialic crust of the Caribbean plate). The isotopic compositions of Pb in the igneous rocks from La Verde are compatible with derivation from ocean-floor basalts from the Cocos plate that have been enriched with radiogenic Pb from the basement, possibly represented by the Arteaga Complex (Figure 4.2). The Pb isotope composition of a granodiorite sample from Inguaran overlaps the field defined by the La Verde igneous rocks, indicating derivation from similar sources (Figure 4.2).

On the thorogenic diagram, the Pb isotope compositions of igneous rocks from La Esmeralda and El Malacate overlap the isotopic compositions of the sedimentary rocks of the Huetamo Sequence and that of the Pacific Ocean Sediments (Figure 4.2), suggesting metal derivation from one of these sources. The marine pelagic sediments may play an important role in the generation of an enriched mantle wedge (Macfarlane et al., 1990). Lead in subducted sediments may be expelled in fluids as the downgoing slab is metamorphosed and accumulate in the overlying mantle wedge (Barreiro, 1984). However, the trend described by the igneous rocks from La Esmeralda and El Malacate may also be interpreted to reflect variable degrees of mixing between ocean-floor basalts and basement rocks of the Guerrero terrane (Figure 4.2).

Involvement of crustal material is required to explain the Pb isotope characteristics of Cenozoic igneous rocks in the study area, either as subducted pelagic sediments incorporated at the source regions of the magma or by later assimilation of metamorphic basement or sedimentary rocks during the rise of the magma (El Malacate, La Esmeralda, and La Verde).

5.3.1.2 Sierra Madre Terrane

The Pb isotope compositions of igneous rocks from Zimapan and La Negra skarn deposits, located in the Sierra Madre terrane, form a steep linear trend on both the uranogenic and thorogenic plots (Figure 4.3). The data show variability in terms of $^{208}Pb/^{204}Pb$ and $^{207}Pb/^{204}Pb$, which reflects heterogeneity of the source region and suggests that the igneous rocks may be the result of mixing of two reservoirs. The Pb isotope compositions of the Tertiary magmatic rocks from Zimapan and La Negra appear to define a steep mixing trend between a mantle component and a ^{208}Pb- and ^{207}Pb-rich reservoir. Steep mixing trends are common in some subduction-related rocks (e.g., Aleutian, Cascades, Mariana, Lesser Antilles arcs, province II in the Andes) and have been interpreted as being the result of the incorporation of radiogenic Pb from subducted sediments (Kay et al., 1978; Woodhead and Fraser, 1985; White and Dupre, 1986; Macfarlane, 1989; Mukasa et al, 1990). Inasmuch as no data are available on the isotopic composition of Pb in sediments and basement rocks of the Sierra Madre terrane, it is premature to identify them as the source of ore Pb.

5.3.2 Whole Rock Sr and Nd Isotopic Compositions

5.3.2.1 Jurassic-Cretaceous Arc-related and Laramide Magmatic Rocks

Strontium and Nd isotope data for Laramide magmatic rocks of northwestern Mexico, mostly from the states of Sonora and Sinaloa, show a north-south progression in the initial isotope compositions, with higher initial Sr ratios and lower initial Nd ratios for granitoids of the northern and central domains and inversely for granitoids of the southern domain (Valencia-Moreno et al., 2001; Valencia-Moreno et al., 2007; Figure 5.7). In the northern and central parts (with available samples from places located between approximately 30ºN and 28ºN latitude), the Laramide plutons were emplaced through Proterozoic crystalline rocks and Proterozoic-Paleozoic miogeoclinal cover of North American affinity, and through a sequence of Paleozoic eugeoclinal rocks covered by Late Triassic clastic units, respectively; in the southern part (with available samples from locales situated at around 26ºN, in the northernmost part of the Guerrero terrane), they intruded Mesozoic island-arc-related volcanic and sedimentary rocks of the Guerrero terrane (Valencia-Moreno et al., 2001). In the northern and central domains, the similarities in the isotopic compositions between the granitoids and their corresponding basement rocks (Figure 5.7) indicate that the interaction of various basement types with the Laramide magmas was important in defining the final chemical and isotopic composition of the associated granitic plutons (Valencia-Moreno et al., 2001). However, the isotopic ratios of the granitoids from the southern domain, characterized by lower Sr and higher Nd isotope ratios, plot around the field defined by the arc-related rocks of the Guerrero terrane (Figure 5.7). In this case, it seems that the granites were contaminated

by assimilation of materials from the accreted volcanic and volcaniclastic rocks of the Guerrero terrane (Valencia-Moreno et al., 2001). In the northern part of the Guerrero terrane, the basement is represented by the Paleozoic El Fuerte Metamorphic Complex. Lack of isotopic data from this complex does not allow assessment of the involvement of the El Fuerte Metamorphic Complex in the production of the granites from the southern domain.

The Cretacoeus granitoid complexes from Puerto Vallarta, Manzanillo, and Jilotlan, south of the Trans Mexican Volcanic Belt (Figure 2.10), intruded Late Triassic to Early Cretaceous volcano-sedimentary arc units of the Zihuatanejo Sequence, located on the southern part of the Guerrero terrane (Freydier et al., 1997). The Puerto Vallarta intrusives have lower ε_{Nd} values and higher $^{87}Sr/^{86}Sr$ ratios compared to the Manzanillo and Jilotlan complexes (Figure 5.7). These two different trends are surprising, considering that the batholiths intruded rocks of the same Zihuatanejo-Huetamo subterrane. Freydier et al. (1997) argued for the emplacement of the Puerto Vallarta batholith on an oceanic crust thickened by continent-derived sediments or a continental lithosphere as an explanation for the more evolved isotopic signatures. However, new Sr and Nd isotopic data of sedimentary rocks from the Zihuatanejo Sequence have much higher present-day $^{87}Sr/^{86}Sr$ values (Figure 5.8) than the Puerto Vallarta batholith; this excludes the involvement of the sedimentary rocks in the generation of the batholith. On the contrary, the positive ε_{Nd} values and lower $^{87}Sr/^{86}Sr$ ratios in the SE intrusions (Manzanillo and Jilotlan; Figure 5.7) suggest younger basement rocks and less crustal contamination (Schaaf et al., 1990). The isotopic values of the Manzanillo and Jilotlan complexes overlap partly with the field defined by the arc-related rocks of the Guerrero

terrane (Figure 5.7). This similarity may indicate that they had a common source or that the Manzanillo and Jilotlan intrusives were contaminated by assimilation of materials from the accreted arc volcanic and volcaniclastic rocks of the Guerrero terrane. However, Solis-Pichardo et al. (2008) argued for a mantle origin associated with Cordilleran subduction processes for the SE continental arc intrusives to account for their primitive Sr and Nd isotopic ratios (Figure 5.7), which are even more primitive than most of Trans Mexican Volcanic Belt volcanics.

Schaaf et al. (1991) suggested a multicomponent and multistage magma evolution as an explanation for the heterogeneous $\varepsilon_{Nd(i)}$ (between -7 and +3) and less uniform Nd model ages (T_{DM} between 500 and 1400 Ma) of the Puerto Vallarta intrusives. On the basis of the more homogeneous isotopic signature and more uniform Nd model ages (T_{DM} between 250 and 500 Ma), the same authors argued for a single-stage magma generation for the SE granitoids.

The overall positive ε_{Nd} values, $^{143}Nd/^{144}Nd$ above that of bulk earth, and nonradiogenic $^{87}Sr/^{86}Sr$ of Jurassic-Cretaceous arc-related rocks from the Teloloapan, Arcelia-Palmar Chico, and Zihuatanejo-Huetamo subterranes (Mendoza and Suastegui, 2000; Centeno-Garcia et al., 1993a; Figure 2.3; Figure 2.4) are similar to the values of present-day intra-oceanic island arcs (Figure 2.4). They have lower initial $^{87}Sr/^{86}Sr$ and higher initial ε_{Nd} than basement rocks (e.g., the Arteaga Complex or the Tejupilco metamorphic suite); this suggests that the basement rocks did not influence the magmatism and were not involved in the production of the Jurassic-Cretaceous arc assemblage (Figure 2.4; Centeno-Garcia et al., 1993a).

5.3.2.2 Cenozoic Magmatic Rocks from the Coastal Plutonic Belt of the Sierra Madre del Sur

The isotopic characteristics of the intrusive rocks from the Coastal Plutonic Belt of the Sierra Madre del Sur (Figure 2.10) are discussed in the light of new and previously published data on rocks from the Guerrero and the Xolapa terranes (Figure 1.1). The Guerrero and Xolapa terranes accreted to the continental margin of Mexico in Late Cretaceous to early Tertiary time (Herrmann et al., 1994). While Guerrero is part of a relatively young crustal block, the Xolapa terrane has an older basement (Martiny et al., 2000). It has been suggested (Moran-Zenteno et al., 1993) that the amphibolite facies metamorphic rocks of the Xolapa terrane are reworked portions of the Precambrian and Paleozoic basements of the Oaxaca and Mixteca terranes.

The Cenozoic igneous rocks from Inguaran, El Malacate, and La Esmeralda, part of the Guerrero terrane, have homogeneous and generally low $^{87}Sr/^{86}Sr$ ratios, and $^{143}Nd/^{144}Nd$ above that of bulk earth (Figure 5.8); these results suggest a relatively low degree of evolved crustal contamination. They have isotopic ratios that are very similar to that of a Cretaceous siltstone from the Huetamo Sequence; this indicates a common source or contamination of the igneous rocks by assimilation of materials from the Huetamo Sequence. However, a granitic sample from La Verde has higher $^{87}Sr/^{86}Sr$ and lower $^{143}Nd/^{144}Nd$ ratios and plots within the field defined by the metamorphic rocks of the Arteaga Complex and Tejupilco metamorphic suite (Figure 5.8); this indicates the involvement of basement rocks in its generation. Current data suggest that igneous rocks from La Verde may have assimilated a more evolved crustal component that any other magmatic rock from southern Mexico (Figure 5.8).

Oligocene plutonic rocks (La Muralla pluton and Rio Verde batholith) from the Xolapa terrane (Martiny et al., 2000), located along the coast and close to the P. Nacional area (Figure 2.10), yield quite variable isotopic ratios (Figure 5.8); their isotopic signature may suggest greater crustal assimilation during magma ascent or assimilation of crust with a heterogeneous isotopic composition (Martiny et al., 2000).

5.3.2.3 Cenozoic Magmatic Rocks from the Inland Volcanic Field of the Sierra Madre del Sur

The isotopic characteristics of the volcanic rocks from the Inland Volcanic Belt of the Sierra Madre del Sur (Figure 2.10) are discussed in the light of published data on rocks from the Guerrero, the Mixteca, the Oaxaca, and the Xolapa terranes (Figure 1.1).

Strontium and Nd isotopic data of Eocene-Oligocene volcanic rocks from the Mixteca terrane (Martiny et al., 2000, Martinez-Serrano et al., 2008) suggest a relatively low degree of crustal contamination compared to volcanic rocks from the Oaxaca and the Juarez terranes (Martinez-Serrano et al., 2008; Figure 5.8). The oldest component of the Oaxaca terrane is represented by a granulite-facies metamorphic basement of Grenvillian age (900-1100 to 1300 Ma; Ortega-Gutierrez, 1981, Martinez-Serrano et al., 2008), while the Juarez terrane consists of strongly deformed Jurassic and Cretaceous oceanic and arc volcanic rocks (Ortega-Gutierrez, 1981; Martinez-Serrano et al., 2008). The basement of the Cenozoic volcanics in the Mixteca terrane is represented by the Acatlan Complex of Paleozoic age, which consists of metamorphic units ranging from greenschist to eclogite facies (Ortega-Gutierrez, 1993, Martiny et al., 2000). Volcanic rocks from the northeastern part of the Guerrero terrane, collected around 40 km east of Taxco (Moran-

Zenteno et al., 1998, Martinez-Serrano et al., 2008) define two distinct trends (Figure 5.8). Rocks with more primitive isotopic signatures are about 2 Ma younger compared to the ones that are more evolved, indicating the input into the magma chamber of more primitive magmas (Moran-Zenteno et al., 2004).

Overall, it seems that the highest degree of crustal contamination is encountered in case of the volcanic rocks from the Oaxaca and Guerrero terranes, except for the granite sample from the La Verde area (Figure 5.8).

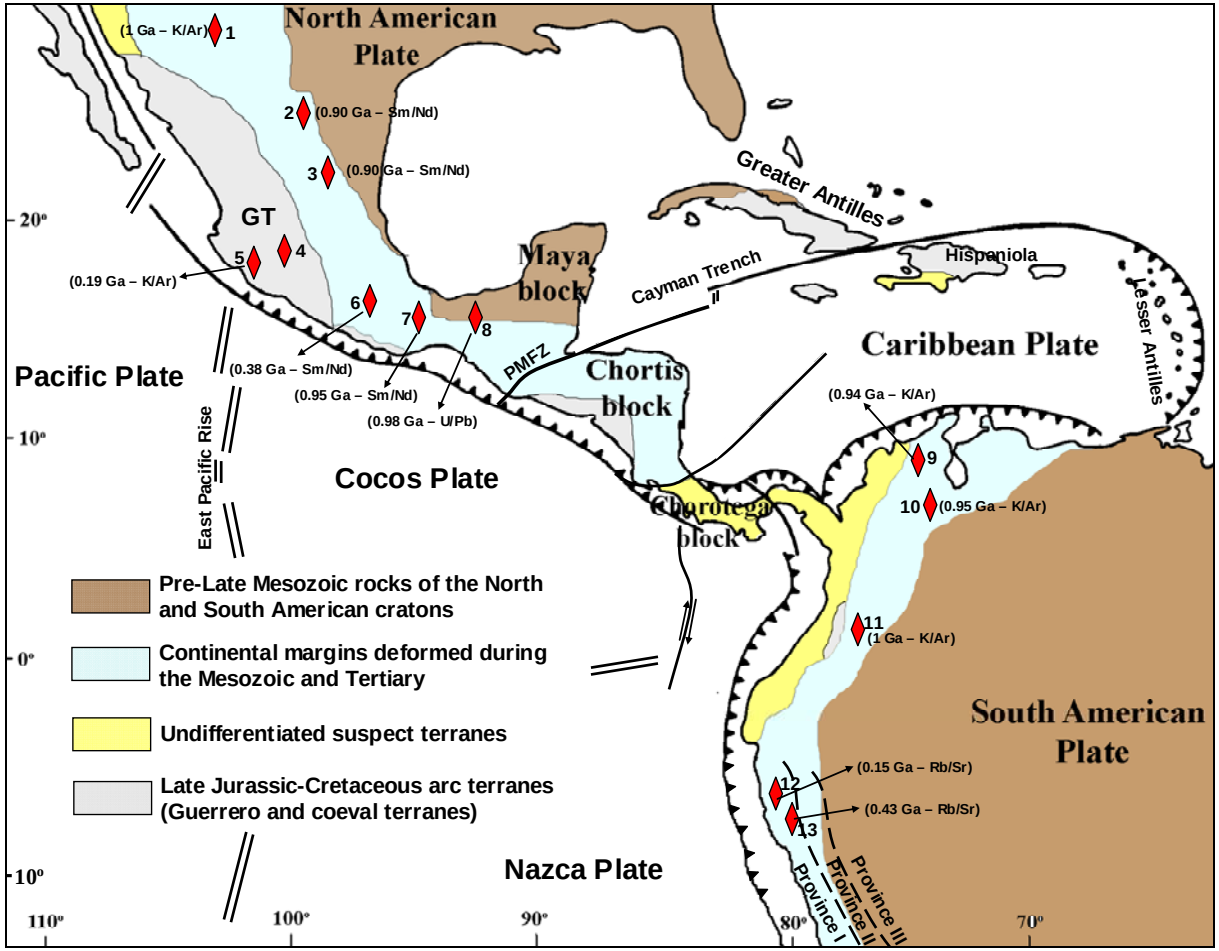

Figure 5.1. Structural schematic map of the North and South American Cordilleras showing the locations of basement exposures discussed in this chapter (1 through 13) and the Pb isotope provinces of Central Andes (I, II, and III; Macfarlane et al., 1990). GT = Guerrero terrane; 1 = Los Filtros; 2 = Novillo Gneiss; 3 = Huiznopala Gneiss; 4 = Nevado de Toluca; 5 = Arteaga Complex; 6 = Acatlan Complex; 7 = Oaxaca Complex; 8 = Guichicovi Complex; 9 = Santa Marta Massif; 10 = Santander Massif; 11 = Garzon Massif; 12 = Olmos Complex; 13 = Maranon Complex (modified after Tardy et al., 1994 and Sundblad et al., 1991). Also shown in parantheses are the isotopic ages for the metamorphic basement.

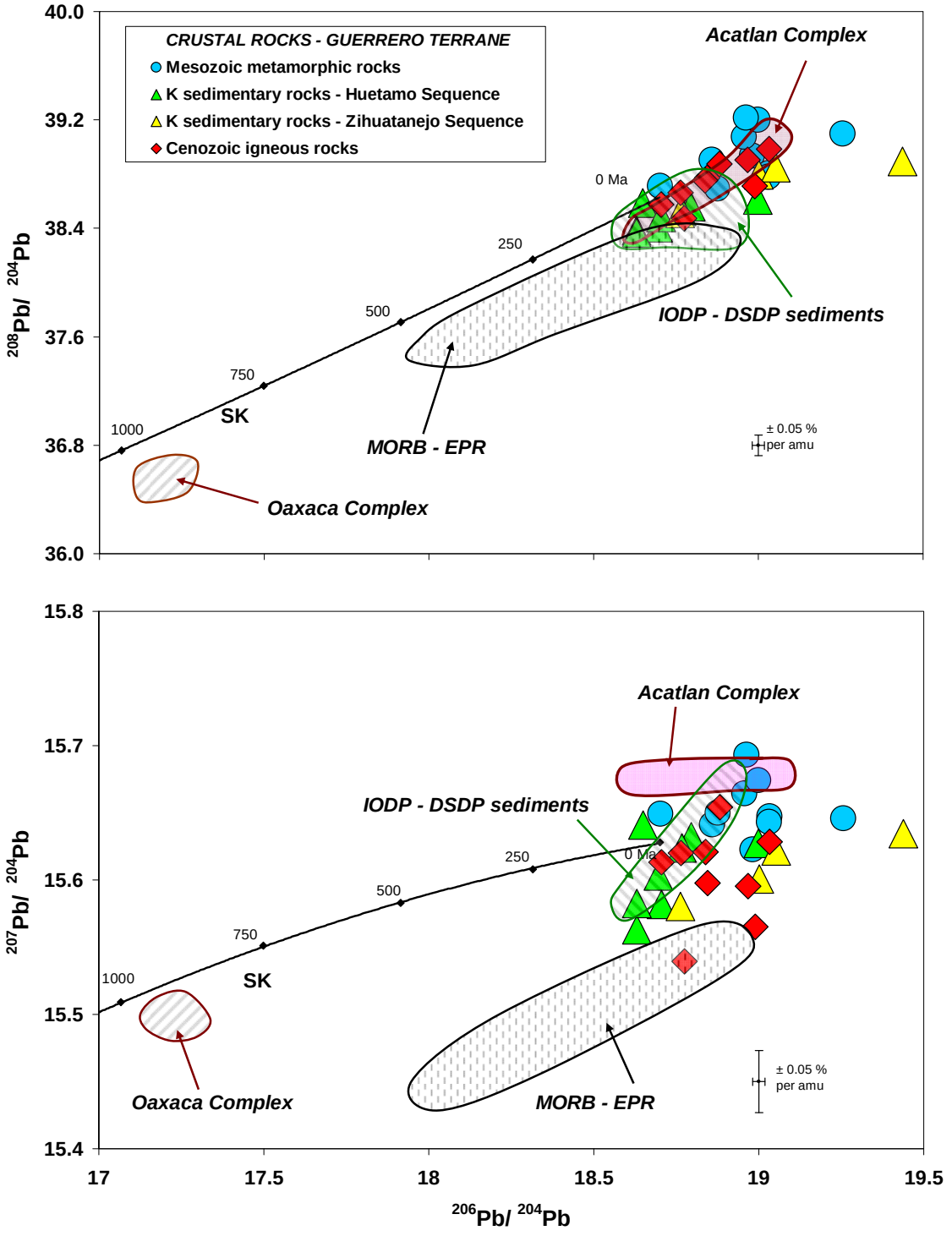

Figure 5.2. Thorogenic and uranogenic diagrams representing lead isotope ratios of rocks from various crustal units of the Guerrero terrane compared with reference data for metamorphic rocks from the Mixteca (Martiny et al., 1997; Martiny et al., 2000) and Oaxaca (Martiny et al., 2000) terranes, MORB-EPR (White et al., 1987), and IODP-DSDP 487-488 sediments (Verma, 2000). Lead growth curve from Stacey and Kramers (1975).

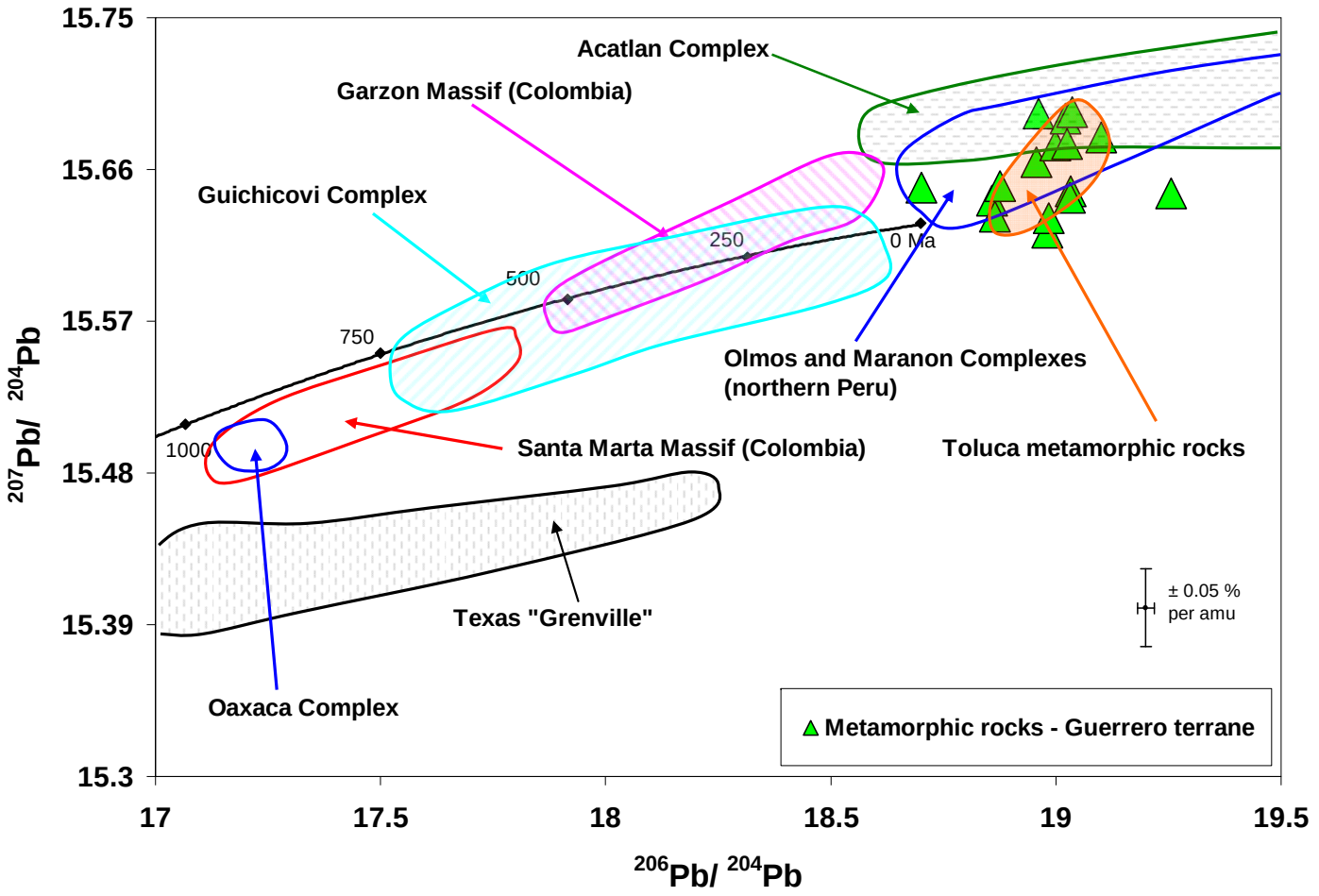

Figure 5.3. Whole rock Pb isotope compositions of metamorphic rocks from the Guerrero terrane compared with reference data for the Mixteca (Martiny et al., 1997; Martiny et al., 2000), and the Oaxaca (Martiny et al., 2000) terranes; the Texas "Grenville" (Smith et al., 1997; Cameron and Ward, 1998); the Santa Marta and Garzon Massifs (Colombia) and the Guichicovi Complex (Ruiz et al., 1999); and the Olmos and Maranon Complexes (northern Peru) (Macfarlane and Petersen, 1990). SK represents the Stacey and Kramers (1975) average crustal Pb isotopic evolution curve.

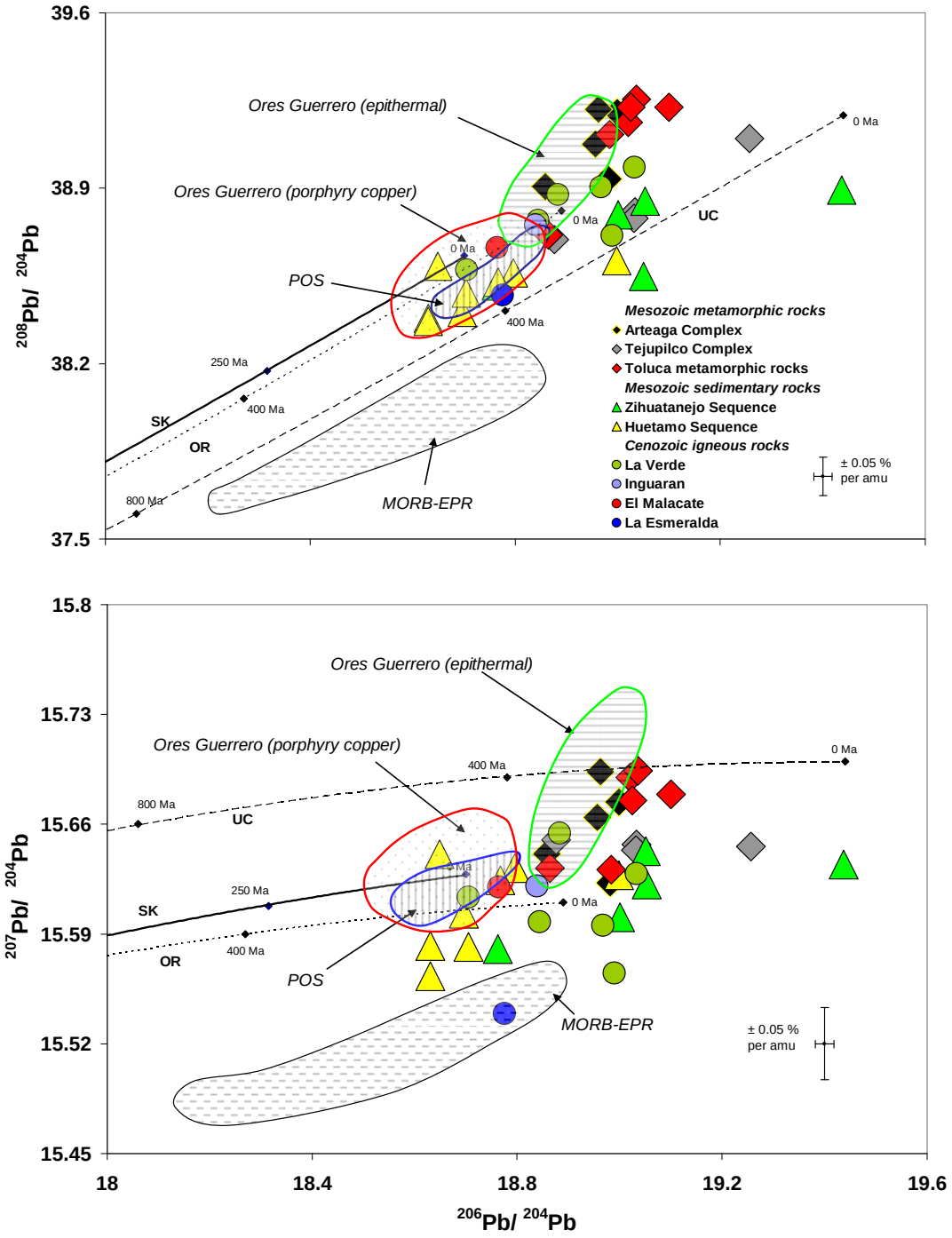

Figure 5.4. Lead isotope compositions of rocks and Tertiary ores from the Guerrero terrane. Data for porphyry copper and epithermal deposits are from Miranda-Gasca (1995), Hosler and Macfarlane (1996), and the present study; for Toluca metamorphic rocks from Martinez-Serrano et al. (2004); for MORB-EPR from White et al. (1987); for Pacific Ocean sediments (POS) from Hemming and McLennan (2001). The average upper crustal (UC) and orogene (OR) growth curves are from Zartman and Doe (1981); the lead growth curve (SK) is from Stacey and Kramers (1975).

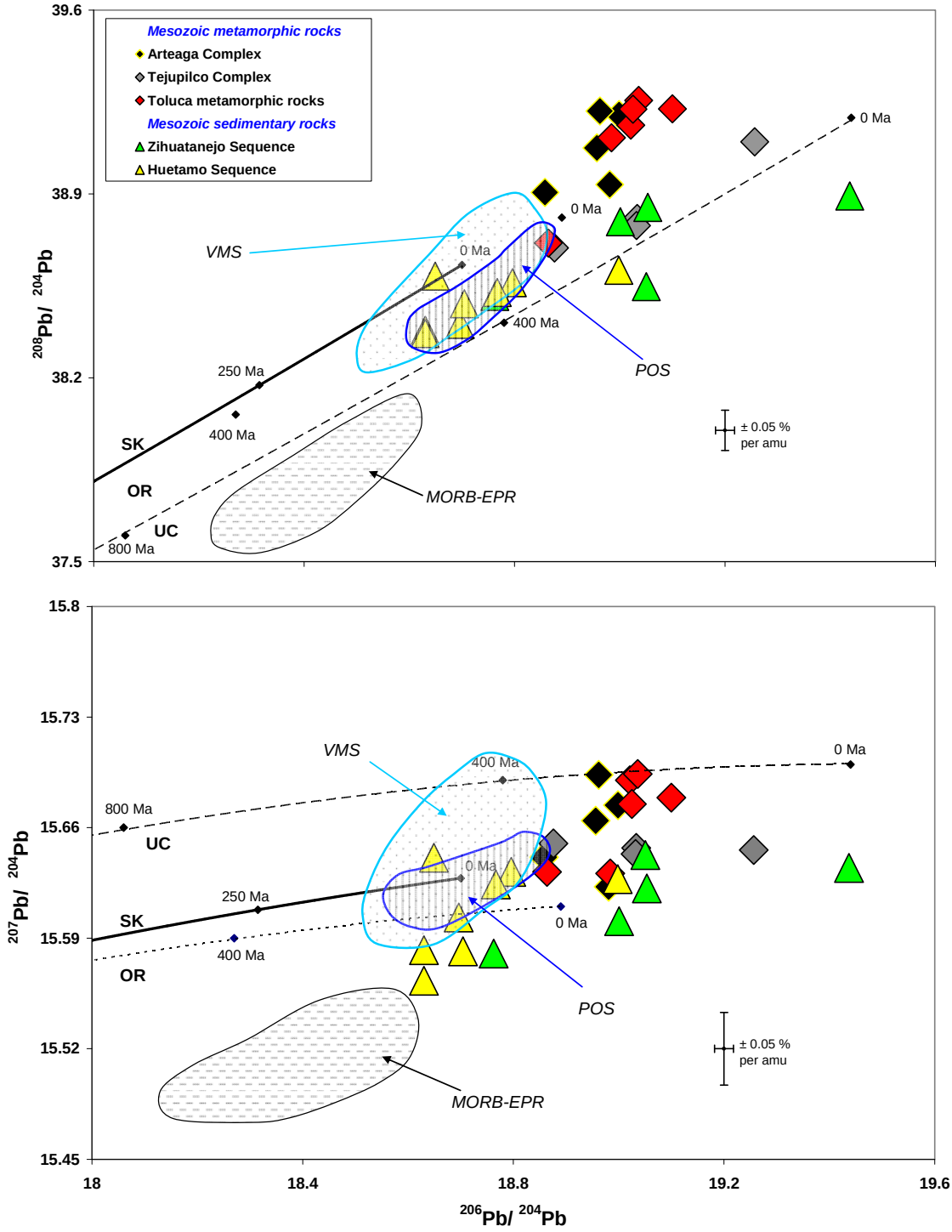

Figure 5.5. Lead isotope compositions of rocks and Cretaceous volcanogenic massive sulfide deposits from the Guerrero terrane. Data field for VMS deposits is from data by Danielson (2000), Cumming et al. (1979), JICA-MMAJ (1991), Miranda-Gasca (1995), and Mortensen et al. (2008); for Toluca metamorphic rocks from Martinez-Serrano et al. (2004); for MORB-EPR from PETDB (2002); for Pacific Ocean sediments (POS) from Hemming and McLennan (2001). References for the evolution curves (UC, OR, and SK) are as in Figure 5.4.

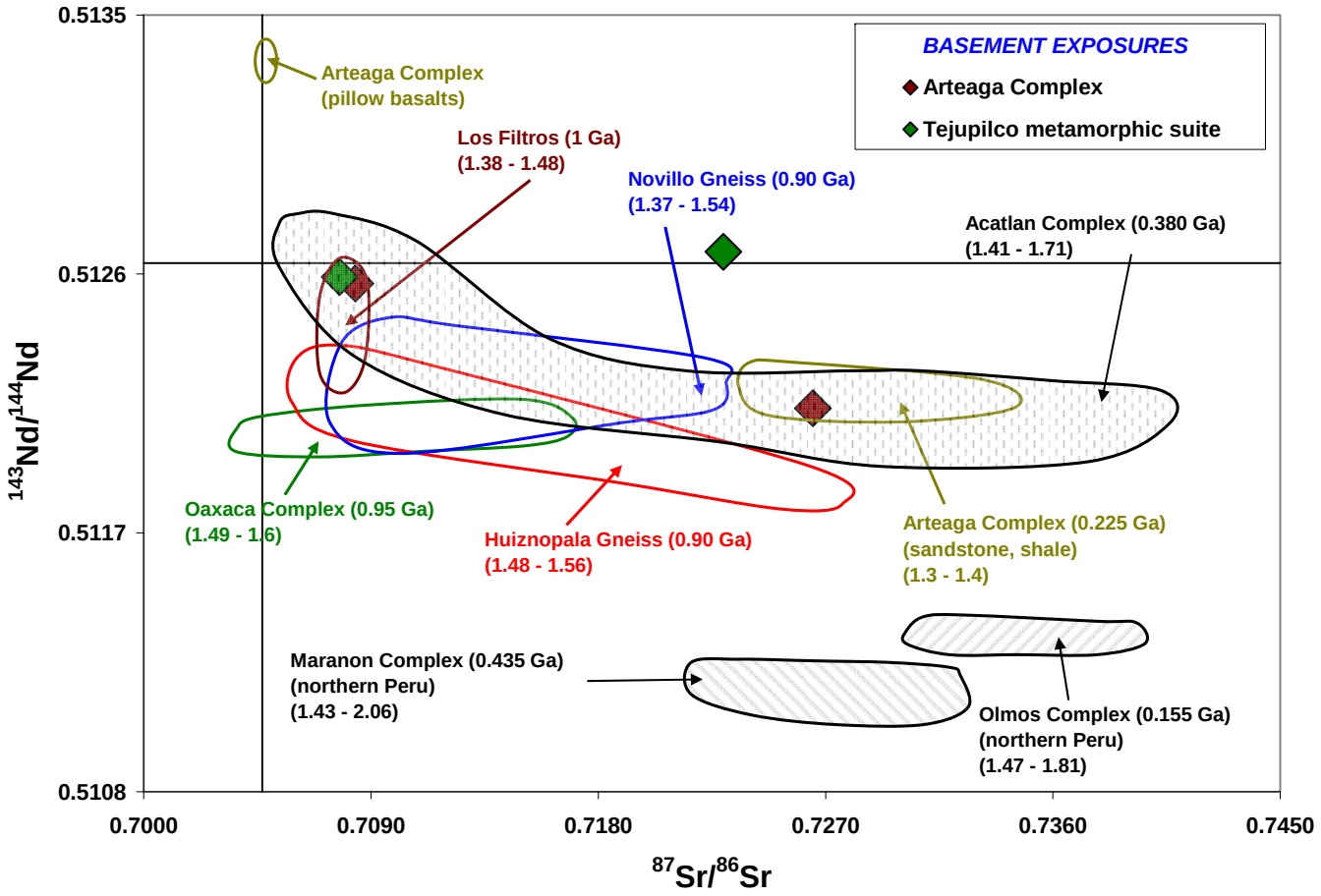

Figure 5.6. Sr-Nd isotopic correlation diagram for basement exposures from the Guerrero terrane compared with reference data for Precambrian exposures in eastern and southern Mexico (Oaxaca Complex, Huiznopala Gneiss, Novillo Gneiss, and Los Filtros) (Patchett and Ruiz, 1987; Ruiz et al., 1988a; Ruiz et al., 1988b); for the Acatlan Complex (Yanez et al., 1991); for the Arteaga Complex (Centeno-Garcia et al., 1993a); and for the Olmos and Maranon Complexes (northern Peru) (Macfarlane, 1999a). Also shown in parentheses are the ages and the crustal residence times of the basement exposures.

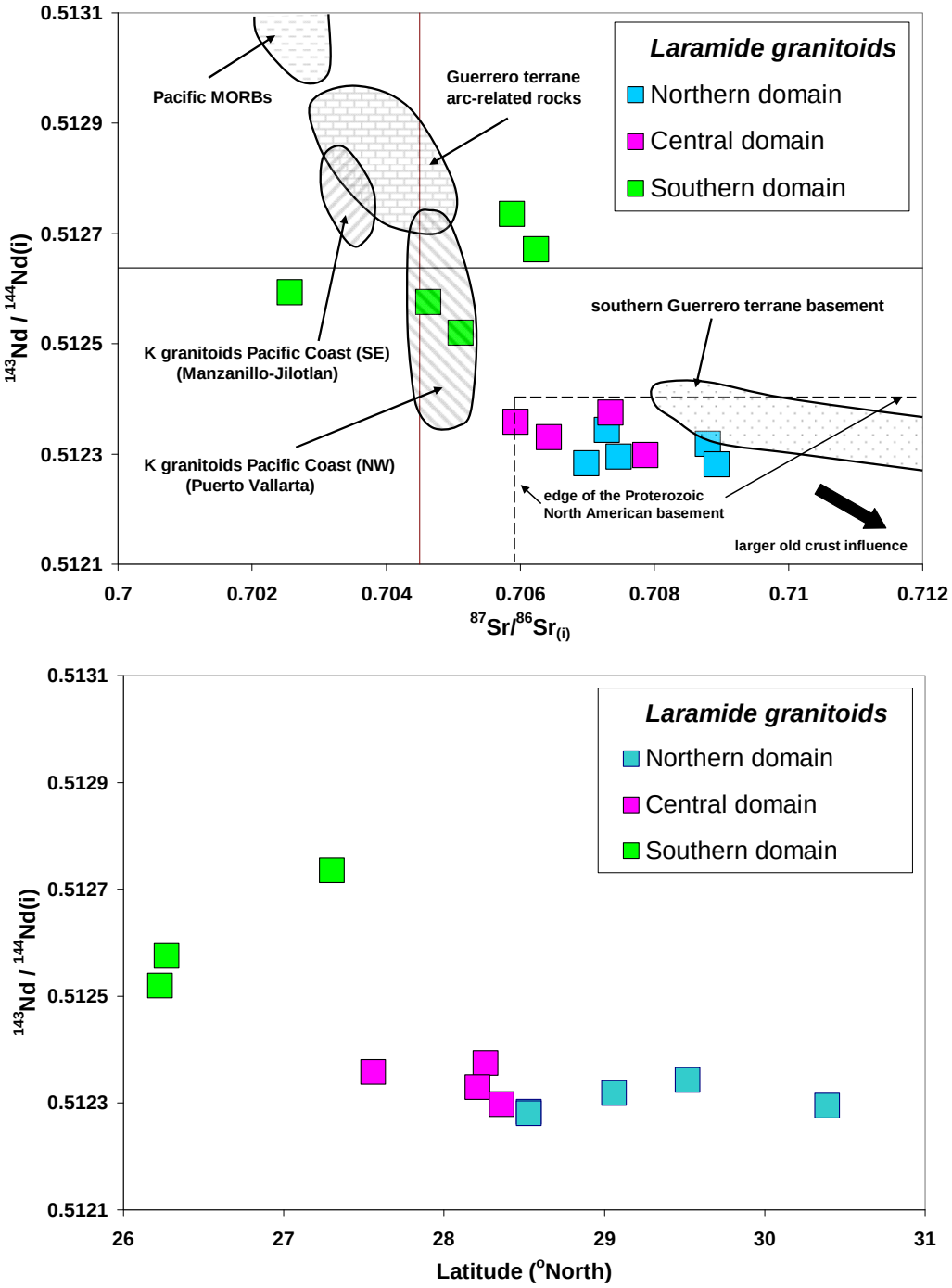

Figure 5.7. Top: Sr-Nd isotopic correlation diagram for Laramide granitic rocks (Valencia-Moreno et al., 2001 and 2003). The compositional fields of the Cretaceous granitoids along the Pacific coast (Schaaf et al., 1990; Schaaf et al., 1991), the Guerrero terrane arc-related rocks (Centeno-Garcia et al., 1993a; Mendoza and Suastegui, 2000), the basement from the southern part of the Guerrero terrane (Centeno-Garcia et al., 1993a; Elias-Herrera et al., 2003), and Pacific MORB are also shown. Bottom: Latitudinal variation of initial $^{143}Nd/^{144}Nd$ in the laramide granitoids (Valencia-Moreno et al., 2001).

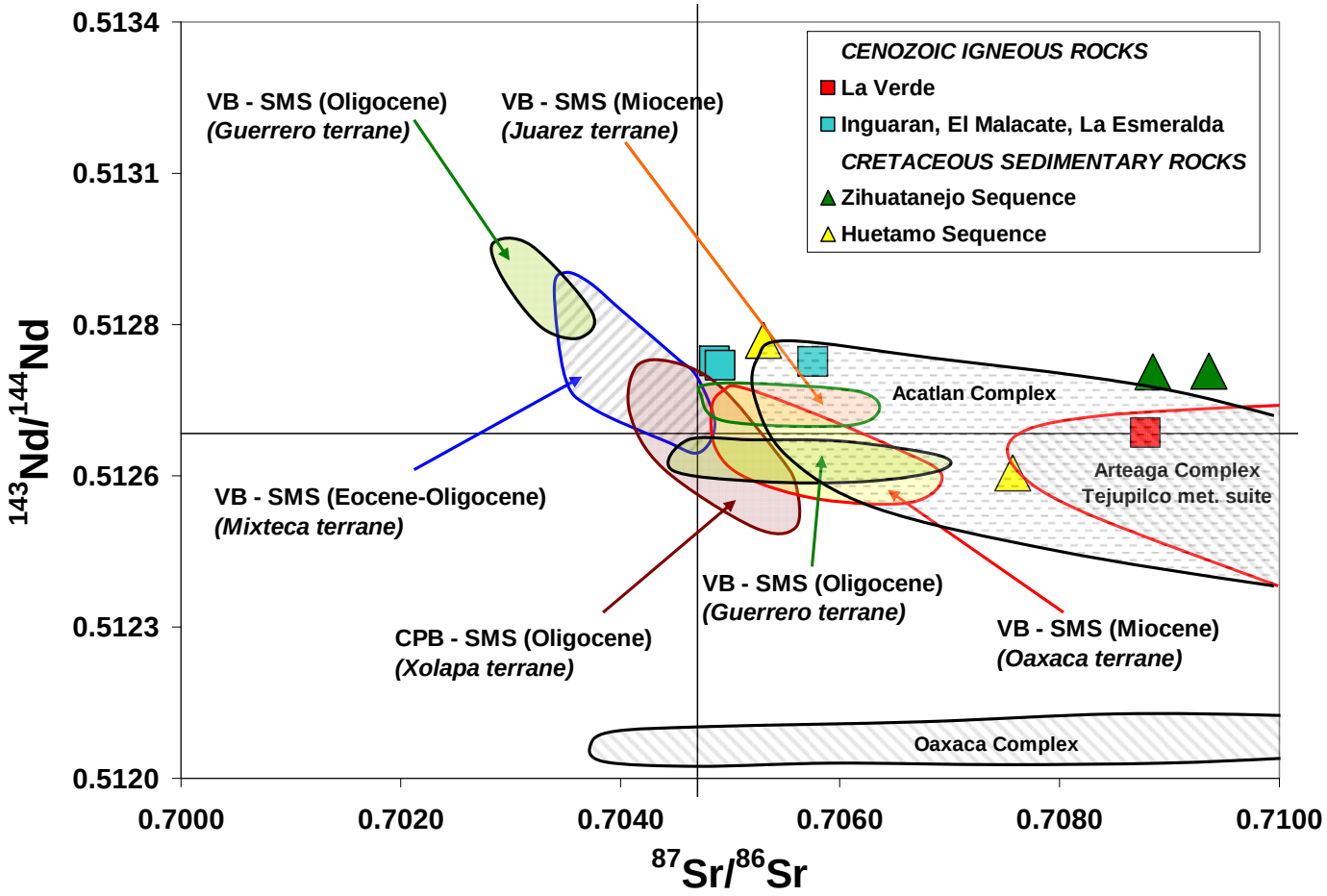

Figure 5.8. Sr-Nd isotopic correlation diagram for Cenozoic igneous rocks and Cretaceous sedimentary rocks from the Guerrero terrane compared with reference data for Oligocene magmatic rocks from the Coastal Plutonic Belt of the Sierra Madre del Sur (Xolapa terrane) (Martiny et al., 2000), and for Eocene through Miocene magmatic rocks from the Inland Volcanic Belt of the Sierra Madre del Sur located in the Guerrero (Moran-Zenteno et al., 1998; Martinez-Serrano et al., 2008), Mixteca (Martiny et al., 2000; Moran-Zenteno et al., 2004), Oaxaca, and Juarez (Martinez-Serrano et al., 2008) terranes. The compositional fields described by the Arteaga Complex, Tejupilco metamorphic suite (this study), Oaxaca Complex (Ruiz et al., 1988a; Ruiz et al., 1988b), and Acatlan Complex (Yanez et al., 1991) are also shown.

6. SOURCES OF LEAD IN DEPOSITS FROM THE GUERRERO TERRANE AND ORE LEAD ISOTOPE TRENDS

The genesis and provenance of lead in Guerrero terrane ores is considered in light of new and published Pb isotope data. Ores are divided into a pre-accretion group and a post-accretion group. The pre-accretion group includes Mesozoic volcanogenic massive sulfide (VMS) and sedimentary exhalative (SEDEX) deposits formed in an intraoceanic island arc and intracontinental marginal basin setting. The post-accretion group refers to mineralization associated with continental-arc magmatism and subduction of the Farallon/Cocos plate, and consists of Cenozoic porphyry copper, epithermal, and skarn deposits. Comparison of the Pb isotope compositions of ore minerals with those of the related igneous rocks, the regional sedimentary rocks, and the underlying regional metamorphic basement yields a picture of the likely provenance of metals in these deposits.

Lead isotope data for ores and the associated igneous rocks from deposits located in the Sierra Madre terrane, east of the main study area, are also presented to examine whether ore metal sources differ among the proposed tectonostratigraphic exotic terranes of Mexico.

Lead isotope analyses of separate leachate and residue fractions of sedimentary and metamorphic rocks are also performed in order to test whether hydrothermal leaching of metals from crustal rocks played an important role in the genesis of the ore deposits from the Guerrero terrane.

6.1 Sources of Ore Lead

6.1.1 Sources of Lead in the Pre-accretion Mesozoic VMS Deposits

6.1.1.1 Zihuatanejo-Huetamo Subterrane

The VMS deposits from the Cuale-El Bramador district, located on the western side of the Zihuatanejo-Huetamo subterrane (Figure 2.11), are around 157.4 ± 4.1 Ma based on U-Pb zircon dating of a hyaloclastic rhyolite from the Cuale volcanic sequence and are the oldest VMS deposits within the Guerero terrane (Bissig et al., 2008; Mortensen et al., 2008). The VMS mineralization of the Cuale district, which consists of 19 deposits (Bissig et al., 2008), is hosted mostly within the upper part of the Cuale volcanic sequence (Bissig et al., 2008; Mortensen et al., 2008). The base of the sequence is represented by rhyolitic flows and associated volcaniclastic units, while the upper part, hosting the main mineralization, consists of rhyolitic flows and tuffs interlayered with volcaniclastic and epiclastic units with lenses of carbonaceous argillite (Mortensen et al., 2008). The volcanic rocks of the Cuale sequence have calc-alkaline to tholeiitic-arc affinity (Bissig et al., 2008; Mortensen et al., 2008). The VMS bodies of the El Bramador district, comprising nine deposits, are located at the contact between felsic volcanic rocks represented by andesitic and rhyolitic tuffs and overlying carbonaceous shales (Miranda-Gasca, 1995; Mortensen et al., 2008).

Samples of galena and mixed sulfides from the Mesozoic VMS Cuale-El Bramador district have Pb isotope ratios that plot around and to the left of the average crustal growth curve (Cumming et al., 1979; Miranda-Gasca, 1995; Mortensen et al., 2008) (Figure 6.1). Newly determined Pb isotope ratios of Cretaceous sedimentary rocks from

the Zihuatanejo Sequence plot far to the right of the average Pb crust evolution curve of Stacey and Kramers; deposits from the western part of the Zihuatanejo-Huetamo subterrane have the tendency toward higher $^{208}Pb/^{204}Pb$ ratios (Figure 6.1). On the other hand, Pb isotope composition of a meta-basalt sample collected south of Puerto Vallarta plots within the field defined by ores from the western side of the Zihuatanejo-Huetamo subterrane (Figure 6.1) and suggests that the basement rocks may have supplied Pb to these VMS deposits. The isotopic composition of the leachate of this meta-basalt sample plots within the field defined by the ore minerals from the Cuale-El Bramador district (Figure 6.2A); hydrothermal mobilization of Pb from the basement rocks could therefore supplied some ore Pb. Inasmuch as no data are available on the isotopic composition of Pb in the host volcanic rocks, it is premature to identify or exclude them as the source of ore Pb.

Three Mesozoic VMS deposits from the central and eastern part of the Zihuatanejo-Huetamo subterrane (e.g., La Minita, Arroyo Seco, and Copper King) (Figure 2.11) have highly variable Pb isotope values (Miranda-Gasca, 1995) that plot outside of the main field defined by VMS ores from the Guerrero terrane (Figure 6.1). This may be the result of the different types of rocks hosting each deposit. The host rock of the Copper King VMS deposit is represented by the Las Ollas subduction complex (Miranda- Gasca, 1995), which consists of both sediment- and serpentinite-matrix mélange, some of which has undergone blueschist facies metamorphism in a subduction zone (Mendoza and Suastegui, 2000). The igneous rocks within the sedimentary package have island-arc tholeiitic affinities with juvenile isotopic signatures, whereas the sedimentary rocks are characterized by more evolved isotopic signatures (Mendoza and Suastegui, 2000;

Centeno-Garcia et al., 2003). Leaching experiments performed on a siltstone sample collected near Cd. Altamirano, part of the Huetamo Sequence, may imply hydrothermal mobilization of Pb from lithologies of this sedimentary sequence, since the isotopic composition of the leachate is very similar to that of one chalcopyrite sample from the Copper King VMS deposit (Figure 6.2A). The Arroyo Seco VMS deposit is hosted entirely within carbonaceous shales and sandstones of the Varales Formation in the Arteaga Complex (Miranda-Gasca, 1995; Mortensen et al., 2008), which have highly radiogenic isotopic values. One galena sample from the Arroyo Seco deposit has high Pb isotope ratios ($^{206}Pb/^{204}Pb$ = 18.7180; $^{207}Pb/^{204}Pb$ = 15.8220; $^{208}Pb/^{204}Pb$ = 39.1410) (Miranda-Gasca, 1995; Figure 6.1 and Figure 6.2A), higher than the sedimentary rocks from the Arteaga Complex in terms of $^{207}Pb/^{204}Pb$; consequently, the sedimentary rocks may not have supplied much Pb to this deposit. However, one analysis from the Arroyo Seco deposit does not allow a good assessment of the sources of ore Pb. The La Minita deposit is stratabound and it is unusually barite rich (48 %; Miranda-Gasca, 1995). Lead isotope data of two galena samples (Miranda-Gasca, 1995) from this deposit yield the least radiogenic values ($^{206}Pb/^{204}Pb$ = 18.4950 and 18.4830; $^{207}Pb/^{204}Pb$ = 15.6170 and 15.5970; $^{208}Pb/^{204}Pb$ = 38.3640 and 38.3020; Miranda-Gasca, 1995) and plot outside of the main field defined by VMS ores from the Guerrero terrane (Figure 6.1).

6.1.1.2 Teloloapan Subterrane

The Teloloapan subterrane hosts the largest concentration of VMS deposits within the Guerrero terrane (Figure 2.11). In most cases, the mineralization is represented by sulfide lenses closely associated with felsic volcanic or volcaniclastic rocks, usually within

carbonaceous clastic sedimentary rocks (Oliver et al., 1999; Mortensen et al., 2008). The Campo Morado district consists of nine individual deposits. The majority of sulfide mineralization occurs at the upper contact of the felsic volcanic sequence of the Campo Morado Formation with the overlying clastic sedimentary rocks (Oliver et al., 1999; Weston, 2002). The Campo Morado Formation is represented mainly by massive rhyolite, rhyolitic breccia, and volcaniclastic and hemipelagic sedimentary rocks (Oliver et al., 1999). The deposits within the Campo Morado district formed between 146.2 and 142.3 Ma (U-Pb zircon dating of four felsic igneous units within and in close proximity to the district; Mortensen et al., 2008). The Tlanilpa-Azulaquez district hosts around 15 VMS deposits of 139.7 ± 2.5 Ma (U-Pb zircon dating of a felsic tuff and a diorite), being the youngest district within the Guerrero terrane (Mortensen et al., 2008). The mineralization is hosted by carbonaceous mudstone and felsic tuff (Rhys et al., 2000). The Rey de Plata deposit, located between the Campo Morado and Tlanilpa-Azulaquez districts, consists of sulfide lenses hosted within a 400 m thick sequence of felsic volcanic and volcaniclastic rocks with interlayered carbonaceous siliciclastic rocks and andesitic volcanic rocks (Mortensen et al., 2008). The VMS ore lenses of the Tizapa deposit, situated on the northern part of the Teloloapan subterrane, are hosted by a sericite schist unit (Mortensen et al., 2008).

The Pb isotope ratios of twelve galena samples from deposits located within the Teloloapan subterrane (Cumming et al., 1979; JICA-MMAJ, 1991; Miranda-Gasca, 1995) have variable $^{207}Pb/^{204}Pb$ and $^{208}Pb/^{204}Pb$ ratios, but they are quite homogeneous in terms of $^{206}Pb/^{204}Pb$ values; overall, they define a linear array on conventional Pb isotope diagrams (Figure 6.1). Leaching experiments conducted on a phyllite sample of the

Tejupilco metamorphic suite, collected near the town of Arcelia, preclude the involvement of the basement rocks in the generation of the VMS deposits in the Teloloapan subterrane, as even the least radiogenic fraction of this rock, which is the leachate, is much more radiogenic than the Pb isotope field defined by the ores from this subterrane (Figure 6.2A).

6.1.1.3 Guanajuato and Zacatecas Subterranes

The Guanajuato district, located within the Guanajuato subterrane, comprises around five VMS deposits (Hall and Gomez-Torres, 2000). Mineralization is hosted by the Guanajuato arc assemblage, which consists of a thin sequence, less than 100 m thick, of intermediate and felsic flows and volcaniclastic rocks (Mortensen et al., 2008). On conventional Pb isotope diagrams, three galena samples (Miranda-Gasca, 1995) from deposits of the Guanajuato district plot around and to the left of the 0 Ma field of the Stacey and Kramers (1975) Pb growth curve (Figure 6.1).

San Nicolas and Francisco Madero are among the most important VMS deposits within the Zacatecas subterrane. The San Nicolas deposit consists of a large keel-shaped mass of sulfides underlain by a sequence of carbonaceous mudstone and minor limestone interlayered with mafic and felsic volcanic and volcaniclastic rocks (Johnson et al., 2000; Danielson, 2000). The hanging wall of the sulfide body consists of carbonaceous mudstones with locally abundant mafic flows and sills (Johnson et al., 2000; Danielson, 2000). The Francisco Madero deposit is hosted by Late Jurassic to Early Cretaceous sedimentary strata of the Zacatecas subterrane and it seems that the bulk of the ore is coarser grained, suggesting a rather skarn or manto-style mineralization (Mortensen et al.,

2008). Lead isotope data of five galena samples from the Francisco Madero deposit (Miranda-Gasca, 1995; Danielson, 2000) are significantly more radiogenic than data of nine pyrite and mixed sulfides from the San Nicolas deposit (Danielson, 2000) (Figure 6.1); ores from the Francisco Madero deposit are the most radiogenic among all the VMS deposits of the Guerrero terrane.

6.1.1.4 Summary

Lead isotope data on ore minerals from the VMS deposits plot along and above the orogene growth curve of Zartman and Doe (1981) on the thorogenic diagram, while on the uranogenic diagram the majority fall between the orogene and upper crust growth curves (Figure 5.5 and Figure 6.1). This led Mortensen at al. (2008) to suggest that the Pb in each deposit was mainly supplied by continent-derived sediments that are interlayered with the host volcanic rocks or from the radiogenic basement. New Pb isotope data on metamorphic rocks from the western Zihuatanejo-Huetamo subterrane (Puerto Vallarta area; Figure 3.1) indicate the involvement of the basement rocks in the generation of the VMS deposits from this area (e.g., Cuale and El Bramador; Figure 2.11). However, on the eastern side of the same subterrane, it seems more likely that the sedimentary rocks from the Huetamo Sequence (Figure 3.1) supplied Pb to the Copper King VMS deposit (Figure 2.11), since the Pb isotope ratios of the leachate fraction of the sedimentary rock and those of the ores are very similar (Figure 6.2A). Whole-rock and leaching experiments performed on a metamorphic sample from Arcelia (Figure 3.1) suggest that rocks from the Tejupilco metamorphic suite in the Teloloapan subterrane were not involved in the generation of the VMS deposits in this subterrane (e.g., Tizapa, Tlanilpa-

Azulaquez, Rey de Plata, and Campo Morado; Figure 2.11). Because of the lack of data on igneous and sedimentary rocks from the Teloloapan subterrane, it is premature to identify a possible source of the ore Pb for the VMS deposits located in this subterrane.

6.1.2 Sources of Lead in the Post-accretion Cenozoic Deposits

6.1.2.1 Guerrero Terrane

6.1.2.1.1 Porphyry Copper Deposits

Lead isotope data of ores from porphyry copper deposits located in the Zihuatanejo-Huetamo subterrane (e.g., Autlan, Inguaran, La Verde, and La Esmeralda; data from Hosler and Macfarlane, 1996, and this study) fall between the orogene and upper crustal growth curves of Zartman and Doe (1981) on the thorogenic diagram (Figure 6.3 and Figure 6.4). Ores from porphyry copper deposits located on the western side (e.g., Ayutla and Autlan) contain less radiogenic Pb than the ores situated on the eastern side (e.g., Inguaran, La Verde, and La Esmeralda) of the Zihuatanejo-Huetamo subterrane (Figure 6.4). On conventional Pb isotope diagrams, samples located on the western side plot close and to the left of the Stacey and Kramers (1975) Pb growth curve; ores located on the eastern side define a field that plots to the right and below the same reference line (Figure 6.4). Overall, the values are fairly typical of the orogene reservoir of Zartman and Doe (1981). The higher Pb isotopic ratios of the ores from the eastern Zihuatanejo-Huetamo subterrane may be due to the crustal thickening toward the east, which increased the amount of assimilation by intrusions rising through the crust.

Pyrite samples from La Verde, El Malacate, and La Esmeralda porphyry copper deposits (eastern side of the Zihuatanejo-Huetamo subterrane) analyzed in this study contain less radiogenic Pb than the host igneous rocks, but overlap the isotopic compositions of the sedimentary rocks of the Huetamo Sequence (Figure 4.6). The similarity of Pb isotope compositions of Pacific Ocean sediments and sedimentary rocks of the Huetamo Sequence (Figure 5.4) makes it difficult to say which was the source of ore Pb. Superimposed on the sedimentary rocks signature are inputs of Pb assimilated from more radiogenic metamorphic rocks of the Arteaga Complex (Figure 6.4). However, the leachate of a meta-basalt sample collected south of Arteaga contains more radiogenic Pb than the ore minerals from deposits located on the eastern side of the Zihuatanejo-Huetamo subterrane (Figure 6.2B), so hydrothermal leaching of rocks from the metamorphic basement could not have supplied a significant proportion of the ore metal.

The situation is different on the western side of the Zihuatanejo-Huetamo subterrane, where the sedimentary rocks of the Zihuatanejo Sequence are much more radiogenic than the ores from porphyry copper deposits (e.g., Ayutla and Autlan) (Figure 6.4). This rules out the involvement of the sedimentary rocks of the Zihuatanejo Sequence in the generation of porphyry copper deposits located on the western side of the Zihuatanejo-Huetamo subterrane. A leaching experiment conducted on a meta-basalt sample collected near Purificacion (Figure 3.1) suggests some hydrothermal mobilization of Pb from lithologies of the metamorphic basement rocks because the Pb isotopic compositions of the leachate plots very close to the field defined by the ores from the western side of the Zihuatanejo-Huetamo subterrane (Figure 6.2B).

Generally, data from individual porphyry copper deposits (e.g., ores from Zihuatanejo-Huetamo subterrane) form clusters (Figure 6.4), indicating that the mineralizing process caused, to some extent, homogenization of Pb from the different metal sources which contributed to these deposits. Some of the variability within deposits is probably due to different amounts of scavenging of Pb from the crustal host rocks.

Genetic models of porphyry deposits derive metals from a degassing magma chamber beneath the porphyry stocks, which channel exsolved magmatohydrothermal fluids into the cupola area (Burnham, 1979; Candela and Holland, 1986; Cline, 1995). There is debate regarding the final stages involved in the evolution of a porphyry system. Gustafson and Hunt (1975) consider that the outward flowing circulation system eventually collapses during the phyllic stage, allowing an influx of meteoric fluids to overprint the magmatic-related potassic alteration. Hedenquist and Shinohara (1997) consider that fluids responsible for the late sericitic alteration in the phyllic stage are also of magmatic origin and in this case any transported metals are of magmatic origin. Norton (1988) argues that nonmagmatic and externally derived fluids contribute all or most of the metals to a porphyry hydrothermal system regardless of the paragenetic stage. Using Pb isotope data, case studies have shown that in case of some porphyry systems (Ann-Mason, Nevada; Toquepala and Cerro Verde, Peru; Bagdad, Arizona) an external metal contribution can be noticed in the potassic core of deposits; however, in case of other deposits (El Salvador and Rio Blanco-Los Bronces, Chile) there is no evidence of external Pb (Tosdal et al., 1999). Overall, it appears that some Pb and maybe other metals are contributed from the country rocks at different times to an evolving porphyry hydrothermal system (Tosdal et al., 1999).

Recent studies have shown that large quantities of Pb are transferred from subducted sediments to the continental arc mantle wedge (Miller et al., 1994; Chauvel et al., 1995). Dasch (1981) showed that Pb in metalliferous sediments is a mixture of Pb from pelagic sources, represented by manganese nodules, and Pb hydrothermally extracted from MORB. Miller et al. (1994) estimated that 40 to 60 percent of the Pb in modern Aleutian lavas is derived from subducted pelagic sediment, and an additional 40 percent is hydrothermally extracted from MORB and subducted as metalliferous sediment. Thus, the Pb isotopic trend described by most porphyry copper ores from the eastern side of the Zihuatanejo-Huetamo subterrane is most simply explained by derivation from a geochemically enriched upper mantle, which acquired its isotopic signature mainly from subducted sediments. However, on the basis of the similarity in the Pb isotopic compositions between the ores and the associated igneous rocks, the involvement of the igneous rocks in the generation of the porphyry copper deposits is not excluded.

6.1.2.1.2 Epithermal Deposits

Available data for epithermal deposits (Fresnillo, Zacatecas, Temascaltepec, Sultepec, and Zacualpan; data from Cumming et al., 1979, and Miranda-Gasca, 1995) show higher Pb isotope ratios than porphyry copper (Figure 5.4 and Figure 6.3) and VMS (Figure 5.5) deposits. This may be partly a result of their shallow depth of formation, mainly from meteoric water-dominated hydrothermal systems (Simmons, 1995). The epithermal deposits are complex hydrologic systems, and depending on the geological environment, can provide multiple fluid pathways from which Pb, and other metals, could be contributed to a hydrothermal system (Sanford, 1992). Locally, the upper part of a

porphyry system can grade to epithermal ore deposits, whose connection with the porphyry copper deposits is mainly supported by geochemical and geological evidence (Camprubi and Albinson, 2007; Valencia-Moreno et al., 2007).

Data from the epithermal ore deposits plot well above the Stacey and Kramers lead growth curve (1975) and the orogene growth curve of Zartman and Doe (1981), whereas those from the porphyry copper and VMS deposits usually cluster around the 0 Ma intercept of the Stacey and Kramers lead growth curve (Figure 5.5 and Figure 6.3). This is consistent with studies that have shown a tendency for Pb isotope ratios to increase outward from a magmatic porphyry core to peripheral deposits (Bouse et al., 1999; Stacey et al., 1968). These patterns might reflect dilution of a magmatic-derived ore fluid of homogeneous Pb isotope composition as it moved outward, cooled, and mixed with meteoric or connate water and scavenged Pb from the country rocks (Tosdal et al., 1999).

The distinct Pb isotope compositions in some base and precious metal deposits (e.g., ores from Zacatecas and Teloloapan subterranes) (Figure 6.3) could reflect local hydrothermal systems driven by the thermal energy of magmatic systems but that are otherwise isolated from a hydrothermal system in a porphyry core; in this case, Pb and other metals would be locally derived and their composition reflect that of the local rocks (Tosdal et al., 1999). Lead isotope data of ores from epithermal deposits located in the Teloloapan and Zacatecas subterranes (Cumming et al., 1979; Miranda-Gasca, 1995) show Pb isotope compositions shifted toward more radiogenic values (Figure 6.3 and Figure 6.4), reflecting mobilization of radiogenic Pb. The distribution of data from these ores on co-variation diagrams reflects variable degrees of mixing between a mantle-derived Pb, such as the MORB-EPR, and a more radiogenic component, possibly

represented by the Toluca metamorphic basement rocks (Figure 5.4 and Figure 6.4). The isotopic composition of leachate of a phyllite sample collected near Arcelia plots within the field defined by the ore minerals from the Teloloapan subterrane (Figure 6.2B), suggesting that hydrothermal leaching of the basement rocks could have provided a significant proportion of the ore metal. The trend is compatible with hydrothermal mobilization of radiogenic compositions of Mesozoic metamorphic rocks by magmas derived from a MORB-type mantle. Nevertheless, the isotopic signature described by the epithermal ores of the Teloloapan subterrane may also be the result of mixing between the Toluca metamorphic rocks and Pacific Ocean sediments (Figure 6.4).

The host rocks for the epithermal deposits commonly have different origins, even at a scale of a district, namely magmatic, sedimentary, or metasedimentay rocks (Appendix 1). Previous S isotopic studies in the sulfides reflect a heterogeneous host rock lithology with its variable isotopic values (Gross, 1975; Pearson et al., 1988; Gilmer et al., 1988; Camprubi et al., 2001). However, even though in epithermal deposits the sources for S may be diverse, the authors concluded that the contribution of magmatic S is essential: it can be contributed either directly through magmatic fluids released to the brittle crust by a cooling and crystallizing magma or by leaching of preexisting magmatic rocks. On the basis of microthermometry, stable and He isotopes, and volatile geochemistry studies in fluid inclusions (Simmons et al., 1988; Norman et al., 1997; Simmons, 1995; Albinson et al., 2001; Camprubi et al., 2006), the analyzed fluids in samples from intermediate sulfidation and low sulfidation epithermal deposits in Mexico are of mixed origins, consisting of both meteoric (shallow and evolved) waters and magmatic fluids (Camprubi and Albinson, 2007).

6.1.2.2 Sierra Madre Terrane

Lead isotopic ratios of ores from two skarn deposits located in the Sierra Madre terrane, La Negra and Zimapan, are generally similar to the igneous rocks (Figure 4.5); the orebodies relate closely to an intrusive granodioritic-dioritic (La Negra) and quartz-monzonitic (Zimapan) stock. The close resemblance in their isotopic signatures implies a magmatic Pb input in these deposits. The heterogeneous isotopic pattern in the La Negra and Zimapan ores suggest a model of hydrothermal mobilizations of metals from host rocks and incomplete homogenization. The variability also reveals a more complex metal derivation and indicates that these replacement orebodies were formed through much larger hydrothermal cells. Because no data are available on the isotopic composition of Pb in supracrustal sediments and basement rocks of the Sierra Madre terrane, it is premature to identify them as the source of ore Pb.

6.1.2.3 Summary

The sedimentary rocks of the Huetamo Sequence, Pacific Ocean sediments, or the host igneous rocks may have supplied Pb to the porphyry copper deposits from the eastern part of the Zihuatanejo-Huetamo subterrane (La Verde, Inguaran, and La Esmeralda). On the western side of the same subterrane, newly determined Pb isotope ratios suggest hydrothermal mobilization of lead from lithologies of the metamorphic basement rocks to the porphyry copper deposits (Ayutla and Autlan).

The epithermal deposits of the Teloloapan subterrane (Temascaltepec, Sultepec, and Zacualpan) may have acquired their isotopic signatures by hydrothermal leaching of the basement rocks represented by the Tejuplico metamorphic suite.

6.1.3 Comparison of Pre-accretion and Post-accretion Deposits

Newly determined Pb isotope values for crustal rocks of the Guerrero terrane indicate that the basement rocks may have supplied Pb to both, the pre-accretion and the post-accretion group of deposits located on the western side of the Zihuatanejo-Huetamo subterrane (e.g., Cuale, El Bramador, Ayutla, Autlan). Some of the Mesozoic and Cenozoic deposits from the central and eastern part of the same subterrane (e.g., Copper King, La verde, La Esmeralda, Inguaran) appear to have acquired their Pb isotopic signature from the sedimentary rocks of the Huetamo Sequence or Pacific Ocean sediments. However, the situation in the Teloloapan subterrane is different, since the sources of ore Pb for the pre-accretion and post-accretion deposits differ. An input of ore Pb from the basement rocks may be possible for the post-accretion deposits; for the pre-accretion group, the isotopic signatures of the metamorphic rocks preclude their involvement in the generation of the VMS deposits.

The Pb isotope field defined by ores from the Mesozoic Francisco Madero VMS deposit overlaps the field defined by the Tertiary epithermal deposits from the Zacatecas subterrane (Figure 6.1 and Figure 6.4), supporting the interpretation that Francisco Madero is an epigenetic deposit of probable Tertiary age (Mortensen et al., 2008).

6.2 Lead Isotope Trends

6.2.1 Ore Lead Isotopes of Post-Accretion Cenozoic Deposits

Metals in the Cenozoic ore deposits were mostly concentrated during major magmatic events related to subduction along the newly assembled continental margin, a very important one being the Laramide orogeny (90 – 40 Ma) (Clark et al., 1982; Damon et

al., 1983; Camprubi and Albinson, 2007; Valencia-Moreno et al., 2007). Geochemical and Sr and Nd isotopic studies (Valencia-Moreno et al., 2001, 2003) indicate contamination of the granitic plutons along the Laramide belt by materials derived from the different crustal blocks (Figure 5.7). The generation of both porphyry copper and epithermal deposits of Mexico are related to the late stages of crystallization of the main granitoids (Damon, 1986; Camprubi et al., 2003); therefore, Valencia-Moreno et al. (2007) suggested that the local intruded basement played an important role in the metallogenesis of these ore deposits. Cumming et al. (1979) proposed that the basement rocks could have affected the ore Pb isotopic composition either by subduction of sediments or by magmatic assimilation or hydrothermal leaching of basement rocks prior to mineralization. Suspect terranes of southern Mexico are considered to have had greatly different origins and their rocks are thought to vary greatly in average age (Campa and Coney, 1983; Macfarlane, 1999b). The Pb isotopic signatures of basement rocks in such geologically distinct terranes are different (e.g., Mixteca, Oaxaca, and Maya terranes; Figure 5.3); consequently, if the intruded basement played an important role in the metallogenesis of these ore deposits, the Pb isotope signatures of ores from different terranes should be distinct from one another.

However, new and previously published data on Cenozoic ores (Cumming et al., 1979; Miranda-Gasca, 1995) show only minor differences in Pb isotope compositions among different subterranes of the Guerrero terrane (e.g., the epithermal deposits from the Zacatecas and Teloloapan subterranes: Fresnillo, Zacatecas, Temascaltepec, Sultepec, and Zacualpan) and ores from the Sierra Madre terrane (e.g., the skarn deposits from La Negra and Zimapan; Figure 6.3). The fields defined by ores from Guerrero subterranes

and the Sierra Madre terrane overlap in both the thorogenic and uranogenic diagrams, with isotopic ratios of ores from the Sierra Madre terrane showing the largest variability. On the thorogenic diagram, most of the data plot far to the right of the Stacey and Kramers Pb growth curve (1975) and along and close to the 0 Ma field of the orogene reservoir of Zartman and Doe (1981) (Figure 6.3). On the uranogenic diagram, the vast majority of the ratios cluster to the right of the average Pb growth curve and between the orogene and upper crust reservoirs (Figure 6.3). The largest difference is between the isotopic signatures of the Guerrero terrane porphyry copper ores from the Zihuatanejo-Huetamo subterrane (Autlan, Inguaran, La Verde, and La Esmeralda; data from this study and Hosler and Macfarlane, 1996) and the Guerrero terrane epithermal ores from the Teloloapan and Zacatecas subterranes (Zacualpan, Sultepec, Temascaltepec, Zacatecas, and Fresnillo; data from Cumming et al., 1979 and Miranda-Gasca, 1995) (Figure 2.12). The Pb isotopic field defined by ores from the Maya block (Cumming et al., 1981) partly overlaps the field defined by ores from the central and eastern part of the Guerrero terrane (Figure 6.5). However, the Pb isotopic characteristics of the basement units are different: the metamorphic rocks from the Guichicovi complex (Ruiz et al., 1999), exposed at the boundary between the Juarez and Maya terranes, are less radiogenic than basement rocks from the Guerrero terrane (Figure 5.3).

Overall, it seems that the porphyry copper deposits from the Guerrero terrane, which are situated relatively close to the Pacific coast, have the least radiogenic Pb isotope compositions of all Cenozoic deposits, while the deposits located further inland, represented by epithermal to mesothermal Pb-Zn-Cu-Ag (Au) and Au-Ag deposits, have

interacted to varying degrees with crustal Pb characterized by elevated $^{207}Pb/^{204}Pb$ and $^{208}Pb/^{204}Pb$ values (Figure 6.6).

According to Barreiero and Clark (1984), Hildreth and Moorbath (1988), and Tosdal et al. (1999), in the Oligocene to present orogenic cycle, trends of increasing $^{207}Pb/^{204}Pb$ ratios that are not accompanied by time-integrated growth of $^{206}Pb/^{204}Pb$ (which are generally noticed in all the Cenozoic deposits from the Guerrero and Sierra Madre terranes; Figure 6.4) are considered to represent crustal thickening and assimilation of crustal material by the melts as they pass through the thickened crust.

These results show that there is no simple correlation between ore Pb isotope ratios and the metamorphic rocks underlying distinct subterranes of the Guerrero composite terrane. Instead, Pb in Cenozoic ores becomes more radiogenic from the West Coast, near the Middle America Trench, to the East Coast (Figure 6.6), as suggested also by Hosler and Macfarlane (1996), who attributed this increase to contribution of radiogenic component from the crust to mantle-derived magmas as the arc advanced onto a progressively thicker continental crust toward the east (Figure 6.6).

6.2.2 Comparison of Pre-accretion and Post-accretion Deposits

Data from individual Mesozoic and Cenozoic deposits or districts form clusters with a few outliers. However, there is a difference between them: with a few exceptions, there is no obvious distinction between the clusters defined by the Mesozoic deposits (Figure 6.1), whereas in case of Cenozoic deposits the clusters reflect variability; ores from the latter deposits plot and define different fields for the porphyry copper, epithermal, and skarn deposits (Figure 6.3). According to Mortensen et al. (2008), this clustering implies

that the mineralizing process has led to a degree of homogenization of Pb from the distinct individual metal sources that contributed to each deposit. The same authors suggest that the scatter within each cluster may reflect variability in the relative proportions of Pb that were contributed from each source.

As noted in the previous section, Pb in Cenozoic ores becomes more radiogenic from the West Coast, near the Middle America Trench, to the East Coast (Figure 2.15), due to assimilation of radiogenic component from the crust (Hosler and Macfarlane, 1996; Cumming et al., 1979)**.** However, this trend is not recognized in case of the Mesozoic VMS deposits, where ores from some deposits located closer to the trench (e.g., Cuale and El Bramador) have more radiogenic Pb than ores from deposits located further inland (e.g., San Nicolas) (Figure 6.7). This is probably because of the amalgamation of the Guerrero composite terrane to the continental margin during Late Cretaceous (Turonian – Maasstrichtian) (Centeno-Garcia et al., 2008). The Tertiary deposits formed after this event in a continental arc setting and the Mesozoic deposits developed prior to it.

Newly determined Pb isotope values for crustal rocks of the Guerrero terrane indicate that the basement rocks may have supplied Pb to both, the pre-accretion and the post-accretion group of deposits located on the western side of the Zihuatanejo-Huetamo subterrane (e.g., Cuale, El Bramador, Ayutla, Autlan). Some of the Mesozoic and Cenozoic deposits from the central and eastern part of the same subterrane (e.g., Copper King, La verde, La Esmeralda, Inguaran) appear to have acquired their Pb isotopic signature from the sedimentary rocks of the Huetamo Sequence or Pacific Ocean sediments. However, the situation in the Teloloapan subterrane is different, since the sources of ore Pb for the pre-accretion and post-accretion deposits differ. An input of ore

Pb from the basement rocks may be possible for the post-accretion deposits; for the pre-accretion group, the isotopic signatures of the metamorphic rocks preclude their involvement in the generation of the VMS deposits.

The Pb isotope field defined by ores from the Mesozoic Francisco Madero VMS deposit overlaps the field defined by the Tertiary epithermal deposits from the Zacatecas subterrane (Figure 6.1 and Figure 6.4), supporting the interpretation that Francisco Madero is an epigenetic deposit of probable Tertiary age (Mortensen et al., 2008).

6.3 Relation of Mexican, Caribbean, and South American Lead Isotopic Compositions and Sources of the Ore Lead

Lead isotope ratios of galena samples from the Cenozoic Pb-Zn deposits of the Maya block (part of the Caribbean Plate; Figure 5.1), hosted by Cretaceous and Paleozoic limestones (Cumming and Kesler, 1976; Cumming et al., 1981), show close similarities in their $^{206}Pb/^{204}Pb$ ratios to the Central and East Mexican galena ores (Cumming et al., 1979; Miranda-Gasca, 1995) (Figure 6.5). However, the Mexican ores have a much wider range of $^{208}Pb/^{204}Pb$ and $^{207}Pb/^{204}Pb$ ratios. These results may imply that the same processes or crustal influence led to the generation of Pb in deposits from the Maya block and deposits from the central and eastern part of Mexico.

Interesting to note is also the similarity in Pb isotope compositions between galena samples from deposits of the Chortis block (Figure 5.1), part of the Caribbean Plate (Cumming et al., 1981), and ores from the western Mexican deposits, part of the North American Plate (Hosler and Macfarlane, 1996; Figure 6.5). The ores from the Chortis block are represented by (1) Ag-Pb-Zn limestone replacement deposits hosted in

Cretaceous limestone and (2) Ag-Au-Pb-Zn veins in Cenozoic volcanic rocks (Cumming et al., 1981). According to Sundblad et al. (1991), the near-coincidence of the average MORB Pb isotope composition with the extrapolated Chortis block trend suggests a model involving mixing of Pb from ocean-floor basalts and highly evolved old continental crust, with increasing contribution of the basement rocks away from the subduction trench. Newly determined Pb isotope ratios of ores from deposits located on the westernmost side of the Guerrero terrane support this hypothesis. Even though there are still many details to be answered regarding the provenance of the Chortis block, it is now generally accepted that it was part of the North American plate prior to its detachment from western Mexico and eastward move in Cenozoic time (Karig et al., 1978; Wadge and Burke, 1983; Burke et al., 1984). The similarity of ore Pb isotopic data from the Chortis block and western Mexican deposits makes this possibility even more plausible.

Cenozoic ores from the Chorotega block, part of the Caribbean plate, have Pb isotopic compositions characterized by low $^{207}Pb/^{204}Pb$ ratios and relatively high $^{206}Pb/^{204}Pb$ values (Figure 6.5), even though some deposits in this area (e.g., Boston mine in Costa Rica) are underlain by crust over 40 km thick (Cumming et al., 1981). Cenozoic ores from the Chortis block are characterized by higher $^{207}Pb/^{204}Pb$ ratios and lower $^{206}Pb/^{204}Pb$ ratios than deposits from the Chorotega block (Figure 6.5), even though in some places (e.g., Monte Cristo deposit in El Salvador, possibly underlain by Paleozoic rocks) the crust is relatively thin (Cumming et al., 1981). It appears that unlike the correlation noticed between the Pb isotope ratios of ores from North America and the

crustal thickness, in Central America the Pb isotope composition may be more closely associated with crustal type, as suggested by Cumming et al. (1981).

There is a close similarity between the Pb isotope compositions of Cenozoic ores from the Sierra Madre terrane (Zimapan and La Negra skarn deposits) and province II from western South America (Figure 6.8). However, ores from the Sierra Madre terrane display a larger variability in their Pb isotope data. The isotopic compositions of Pb in deposits from the Guerrero terrane fall within the field defined by ores from province I of western South America; a few ores from the Sierra Madre terrane have Pb isotopic compositions that also plot within province I (Figure 6.8).

Overall, it appears that there is similarity between the Pb isotopic compositions of ores from:

- western Mexico (Guerrero terrane), Chortis block from northern Central America, and province I of western South America;
- eastern Mexico (Sierra Madre terrane) and province II of western South America;
- Maya block from northern Central America, Chorotega block from southern Central America, Greater Antilles from the Caribbean plate, and province III of western South America (Figure 5.1; Figure 6.5; Figure 6.8).

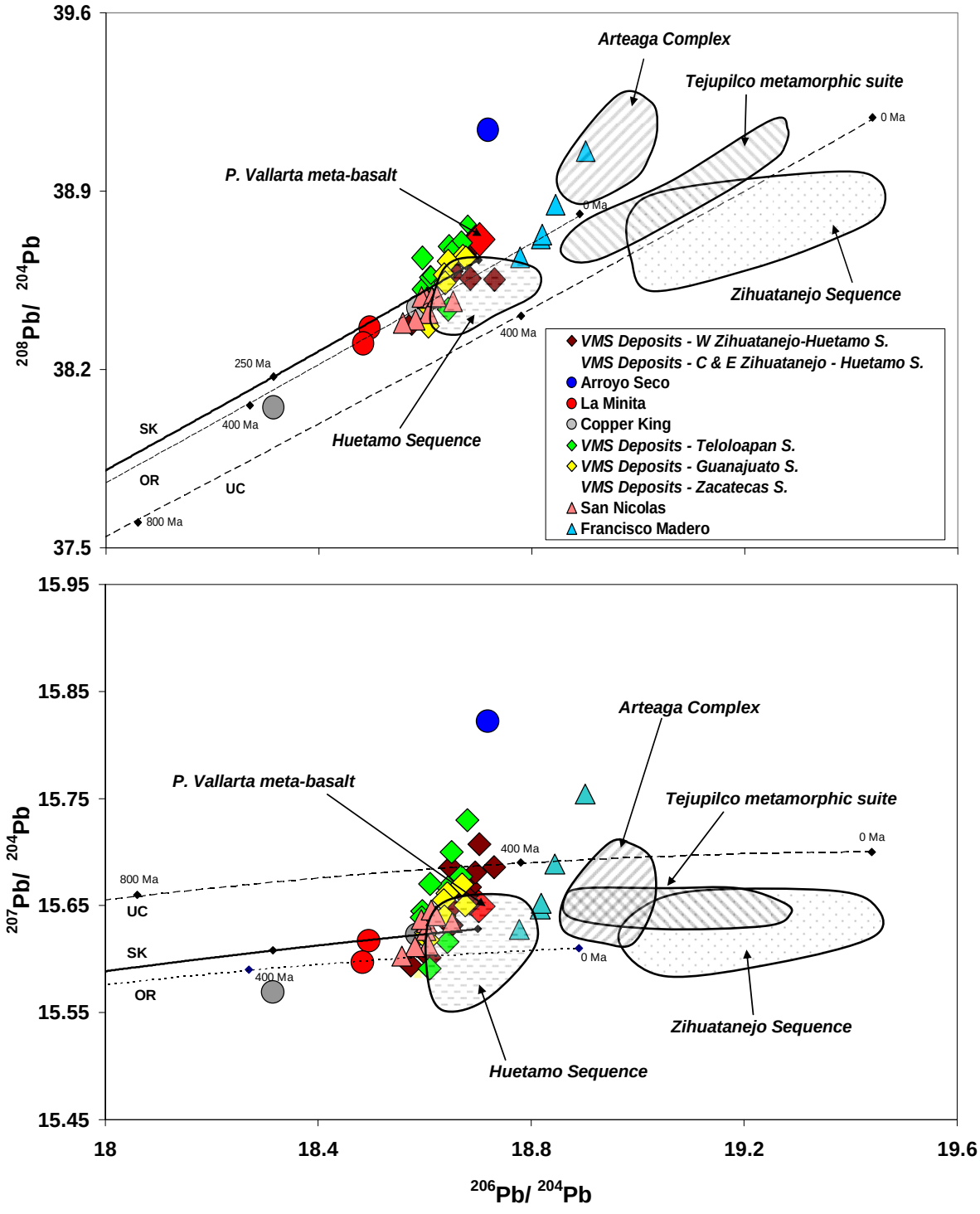

Figure 6.1 Lead isotope compositions of ores from Mesozoic volcanogenic massive sulfide deposits from the Guerrero terrane. The fields represent Pb isotope data of metamorphic and sedimentary rock from the Guerrero terrane. Data for the deposits are from Mortensen et al. (2008) and references therein. References for the evolution curves (UC, OR, and SK) are as in Figure 5.4.

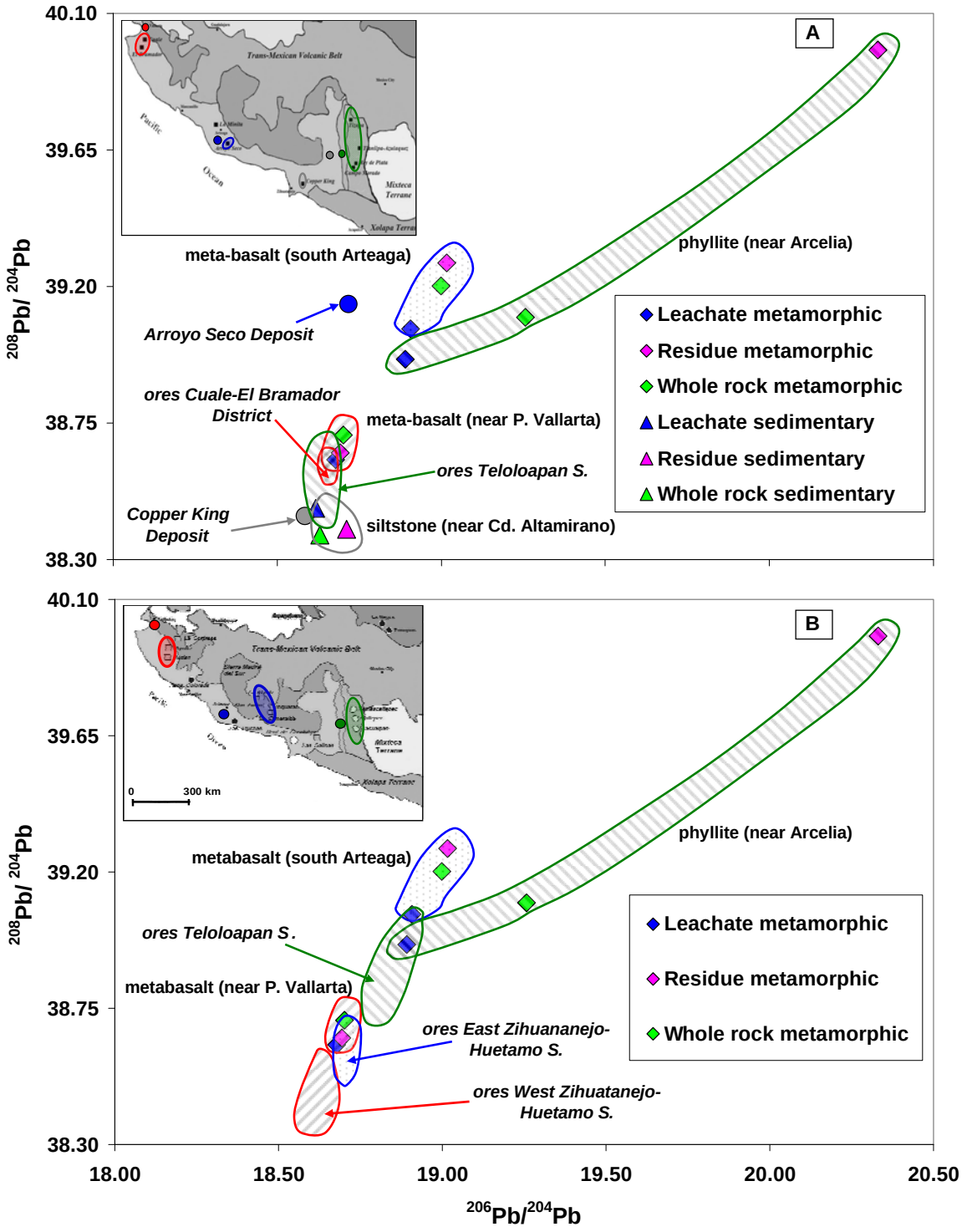

Figure 6.2 Lead isotope compositions of leachate fractions, residue fractions, and whole rocks of Mesozoic metamorphic and sedimentary rocks from the Guerrero terrane. Also shown are Pb isotope compositions and fields defined by ore minerals from Mesozoic (A) and Cenozoic (B) deposits from the Guerrero terrane.

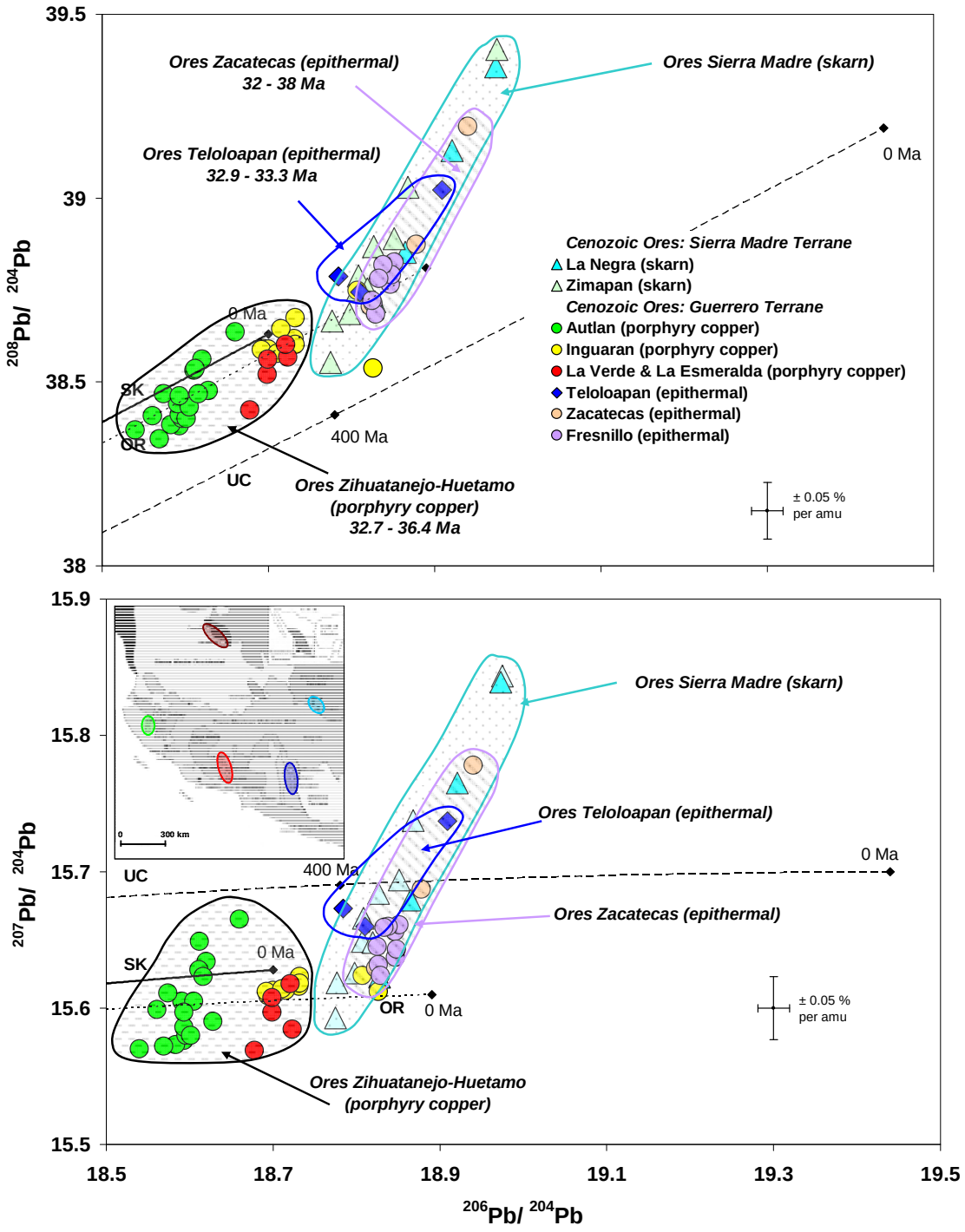

Figure 6.3. Lead isotope compositions of Cenozoic ores from deposits in the Guerrero and Sierra Madre terranes. Also shown are the approximate ages of deposits from the Guerrero terrane. Data are from Cumming et al. (1979), Miranda-Gasca (1995), Hosler and Macfarlane (1996), and the present study. Ores Teloloapan field includes the Temascaltepes, Sultepec, and Zacualpan deposits. References for the evolution curves (UC, OR, and SK) are as in Figure 5.4**.**

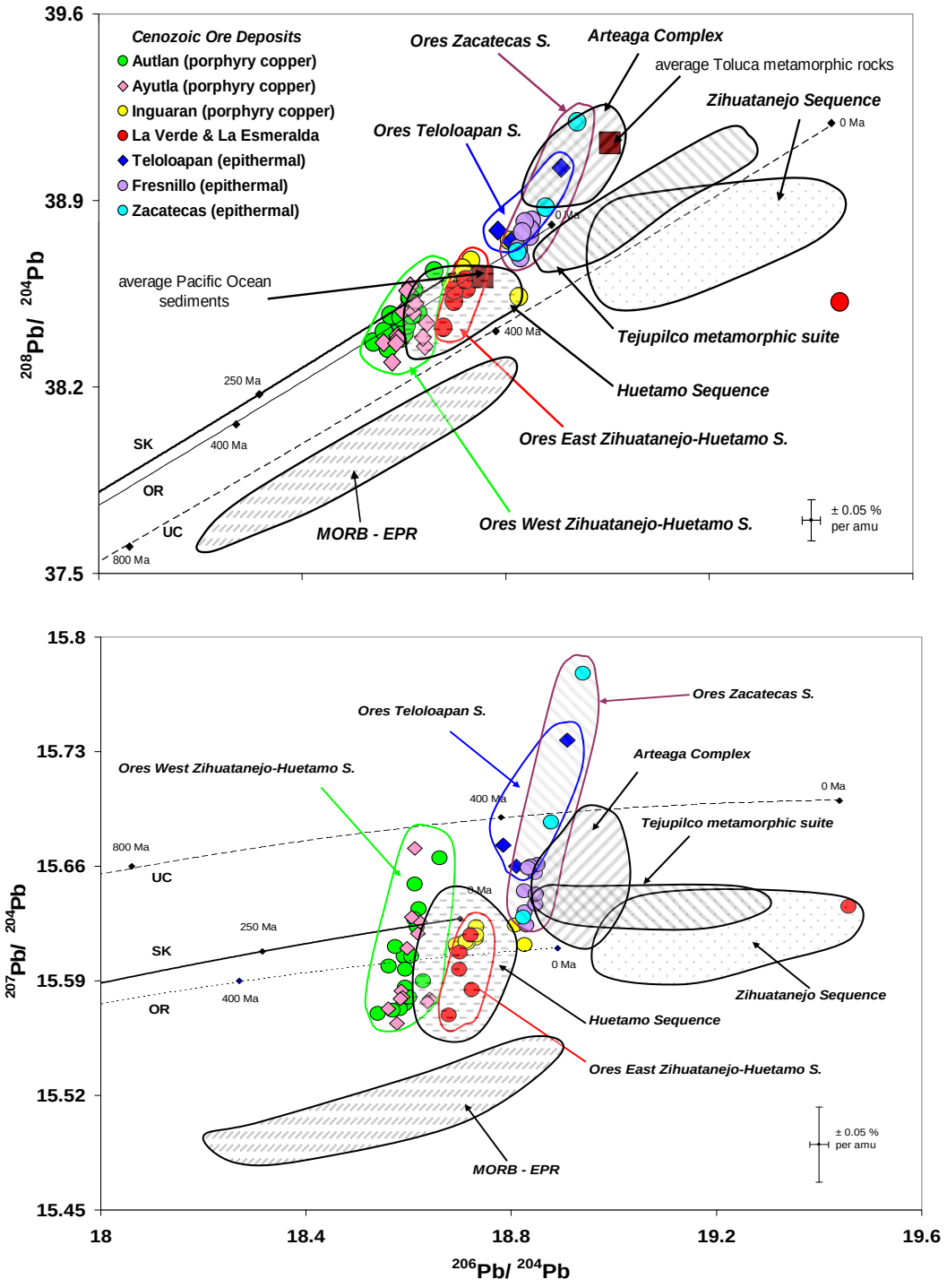

Figure 6.4. Lead isotope compositions of Cenozoic ore deposits from the Guerrero terrane. The fields represent Pb isotope data of metamorphic and sedimentary rocks from the Guerrero terrane and MORB-EPR. Also shown on the thorogenic diagram are the average Pb isotope values for Toluca metamorphic rocks and Pacific Ocean sediments. References for the Cenozoic ores from the Guerrero terrane are as in Figure 5.3. References for the evolution curves (UC, OR, and SK) and Toluca metamorphic rocks are as in Figure 5.4.

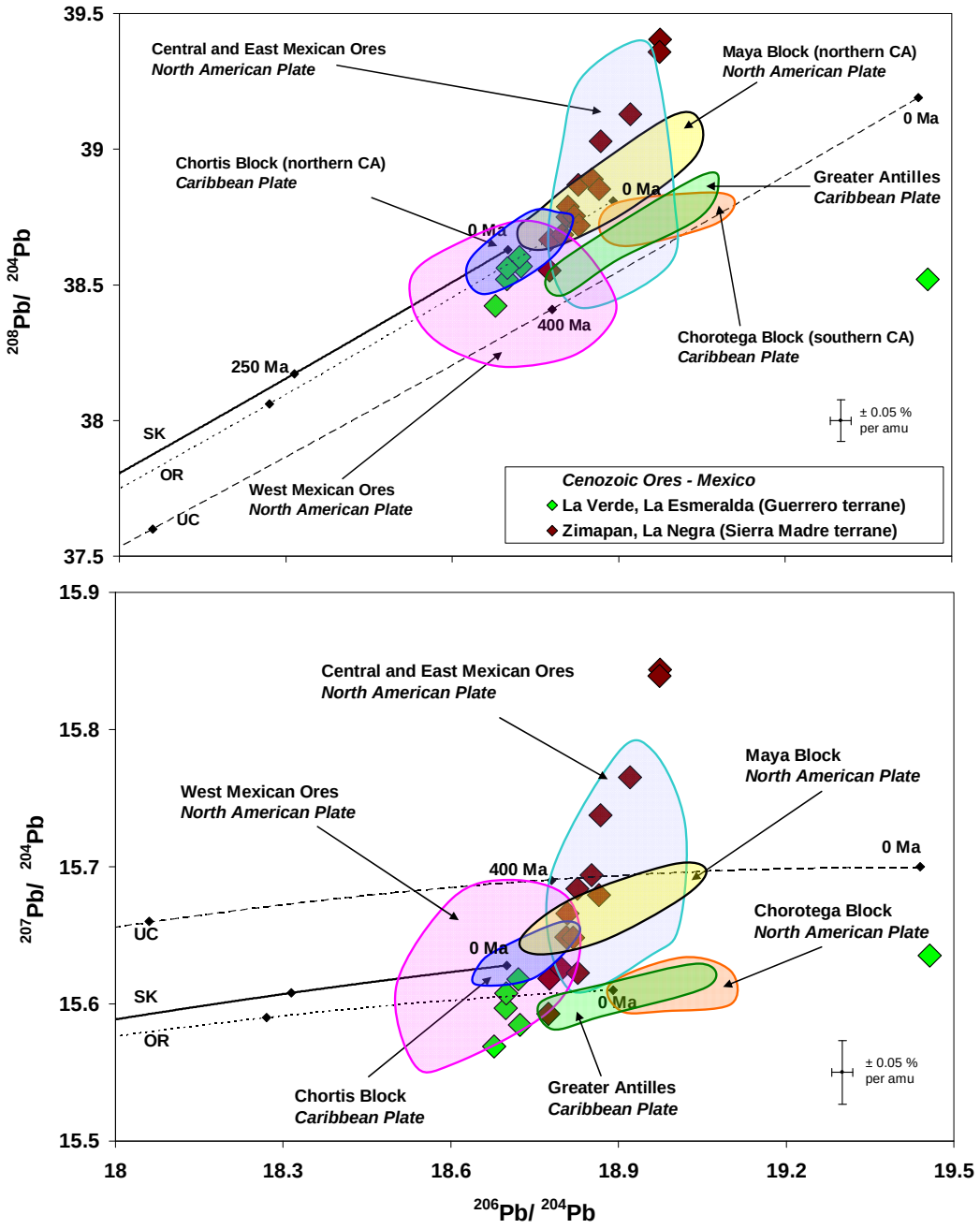

Figure 6.5. Lead isotope compositions of minerals from Cenozoic deposits located in the Guerrero (La Verde and La Esmeralda) and Sierra Madre (Zimapan and La Negra) terranes compared with reference data for ores from the Chorotega Block (Costa Rica and Panama) (Cumming et al., 1981), the Chortis Block (Guatemala, Honduras, Nicaragua, and El Salvador) (Cumming et al., 1981; Sundblad et al., 1991), the Maya Block (Guatemala) (Cumming et al., 1981), the Greater Antilles (Haiti, Puerto Rico, and Jamaica) (Cumming et al., 1981), western Mexico (Cumming et al., 1979; Hosler and Macfarlane, 1996), and eastern Mexico (Cumming et al., 1979; Miranda-Gasca, 1995). References for the evolution curves (UC, OR, and SK) are as in Figure 5.4**.**

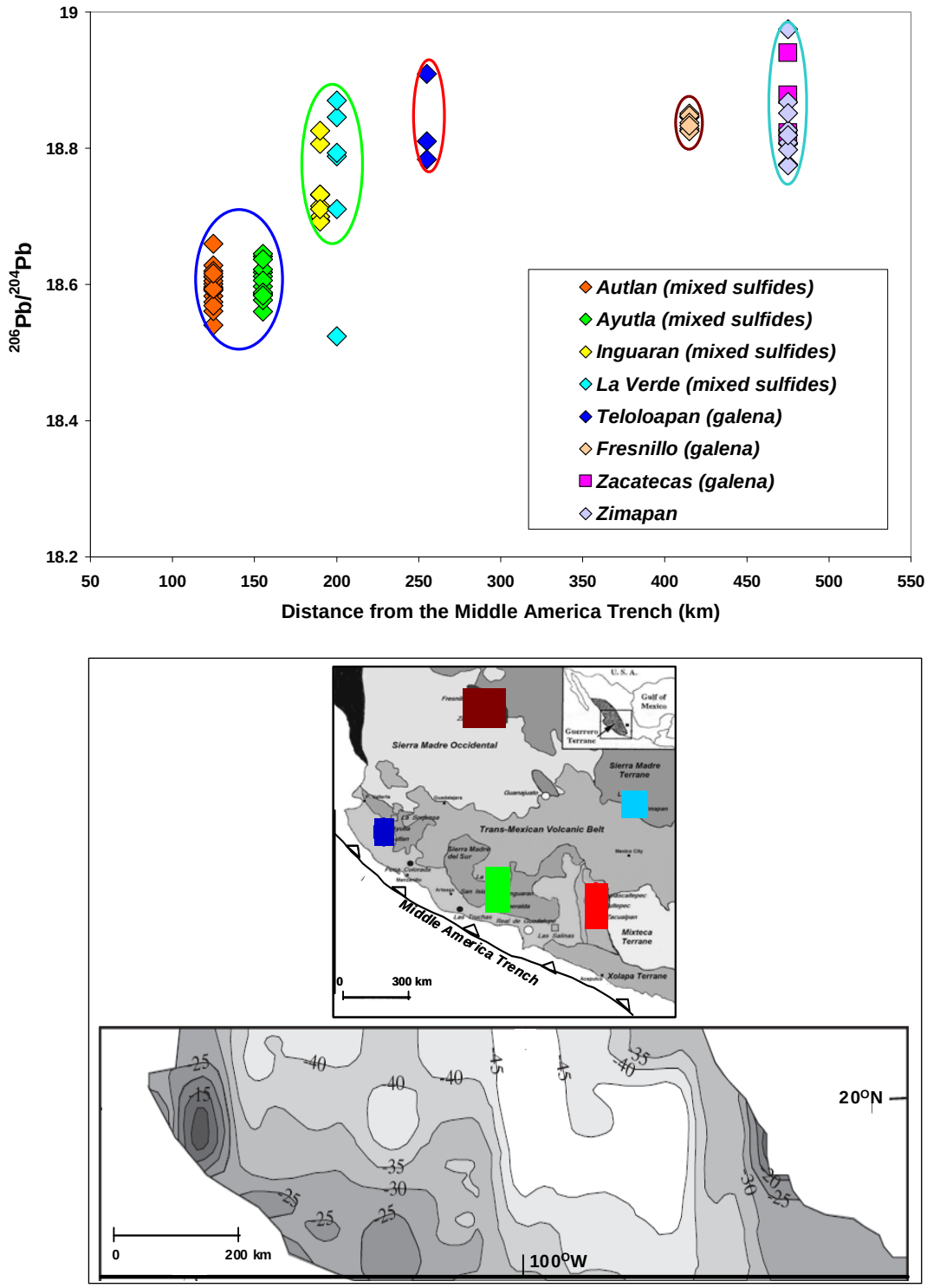

Figure 6.6. Graphs showing the variation of the $^{206}Pb/^{204}Pb$ values of ores from the Cenozoic deposits of the Guerrero terrane with distance increase from the Middle America Trench (top). Locations of deposits (central) and regional crustal thickness (in km) across the Trans-Mexican Volcanic Belt (bottom) are also shown. Data from Cumming et al. (1979), Miranda-Gasca (1995), Hosler and Macfarlane (1996), Danielson (2000), Mortensen et al. (2008), and Gomez-Tuena et al. (2007).

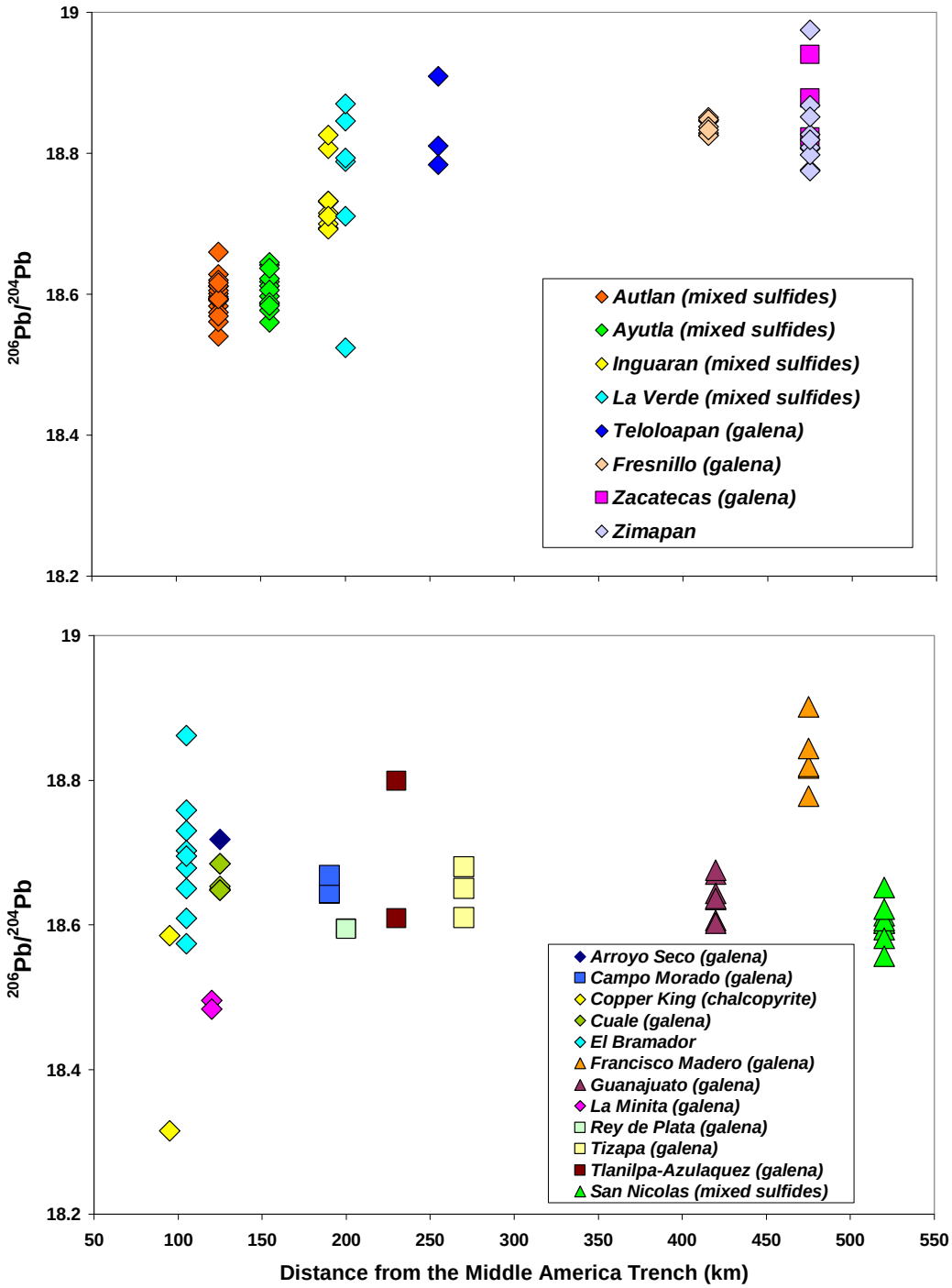

Figure 6.7. Graphs showing the variation of the $^{206}Pb/^{204}Pb$ values of ores from the Cenozoic (top) and Mesozoic (bottom) deposits of the Guerrero terrane with distance increase from the Middle America Trench. Data from Cumming et al. (1979), Miranda-Gasca (1995), Hosler and Macfarlane (1996), Danielson (2000), and Mortensen et al. (2008).

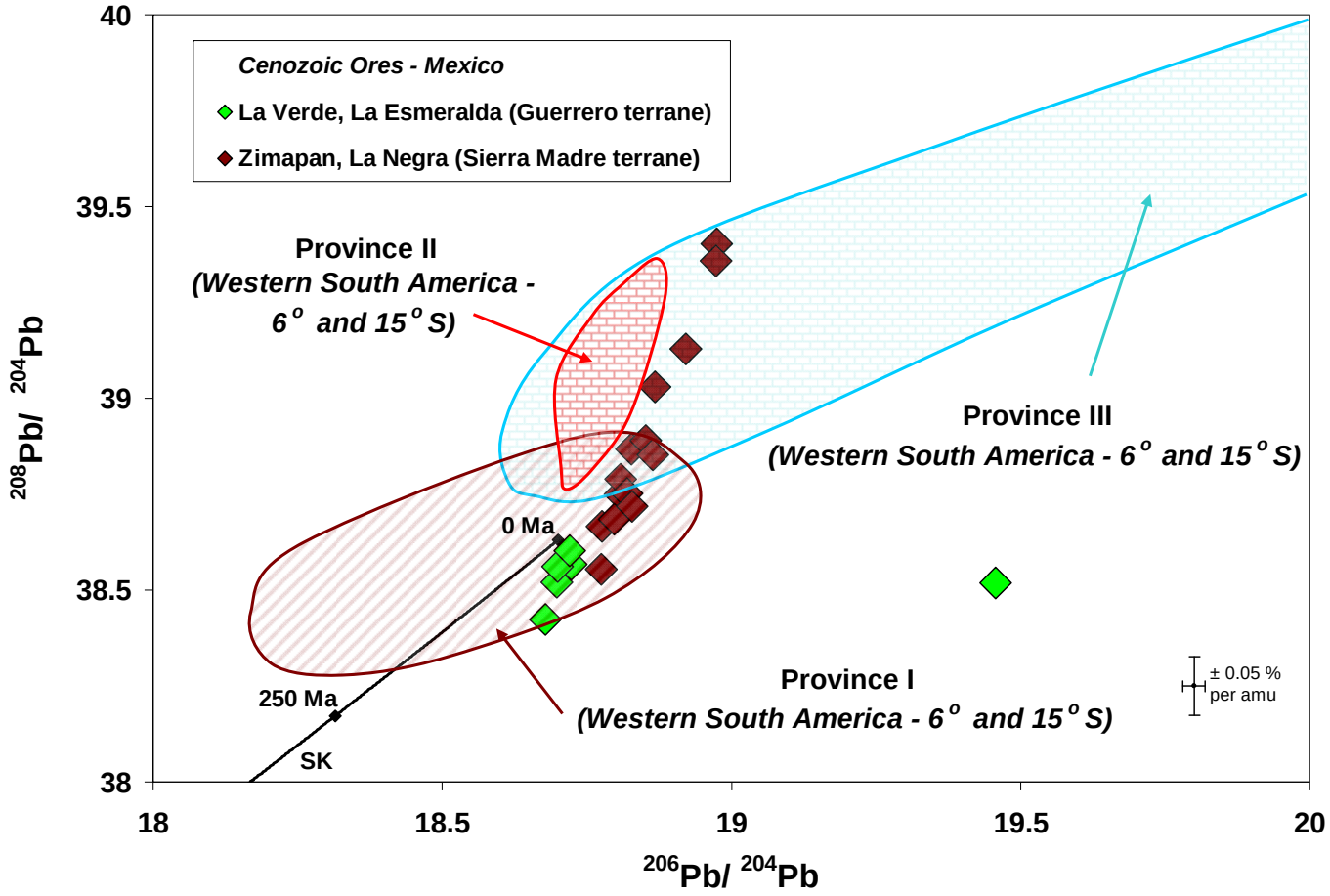

Figure 6.8. Lead isotope compositions of minerals from Cenozoic deposits located in the Guerrero (La Verde and La Esmeralda) and Sierra Madre (Zimapan and La Negra) terranes compared with reference data for ores from province I (subprovinces Ib and Ic), province II, and province III (subprovince IIIb) of Western South America (Tilton et al., 1981; Puig, 1988; Macfarlane, 1989; Mukasa et al., 1990; Macfarlane et al., 1990). For locations of provinces, see Figure 5.1.

7. SUMMARY AND CONCLUSIONS

7.1 Provenance of Crustal Rocks

The isotopic compositions of Pb in the Mesozoic basement rocks of the Guerrero terrane are substantially more radiogenic than published data on high-grade metamorphic rocks (metagabbro and charnockite) from the Grenvillian-age Oaxaca terrane (Figure 5.2). The radiogenic Pb in basement rocks of the Guerrero terrane, with a much lower metamorphic grade, reflects a different history from that of the ancient, high-grade metamorphic Oaxaca terrane. The Pb isotope ratios of metamorphic samples from the Arteaga and Tejupilco Complexes are similar to published data on Paleozoic basement rocks (augen schist) from the Acatlan Complex, implying similar sources (Figure 5.3). On the basis of similar crustal residence ages, it has been suggested that the most likely source for the basement rocks of the Acatlan Complex is represented by rocks of the Oaxaca Complex. Overall, Sr and Nd isotope data of basement units from the Arteaga Complex and Tejupilco metamorphic suite indicate derivation from an evolved continental source (Figure 5.6). Therefore, it is possible that the old component in these basement units may have been derived from the Oaxaca Complex, which was part of northwestern Gondwana during the early Paleozoic and was transferred to the southern end of Laurentia during Paleozoic orogenies related to the opening and closing of the proto-Atlantic Ocean.

Overall, it seems that there was involvement of crustal material at some stage in the evolution of many magmas, but whether this was subducted sedimentary material incorporated at the source regions of the magma during melting or crustal material

assimilated during the rise of the magma is not clear. Assimilation of crustal material during magma ascent is a possibility in the Guerrero terrane, where the igneous rocks were emplaced through the Mesozoic metamorphic basement. The slightly higher radiogenic signature of the igneous rocks from La Verde and Inguaran may be the result of contamination with older crustal components to a larger extent than the igneous rocks from La Esmeralda and El Malacate. Current data indicate that igneous rocks from La Verde may have assimilated a more evolved crustal component that any other magmatic rock from southern Mexico (Figure 5.8).

7.2 Sources of Ore Metals

Newly determined Pb isotope values for crustal rocks of the Guerrero terrane indicate that the basement rocks may have supplied Pb to both, the pre-accretion and the post-accretion group of deposits located on the western side of the Zihuatanejo-Huetamo subterrane (e.g., Cuale, El Bramador, Ayutla, Autlan; Figure 6.1; Figure 6.2; Figure 6.4). Some of the Mesozoic and Cenozoic deposits from the central and eastern part of the same subterrane (e.g., Copper King, La verde, La Esmeralda, Inguaran) appear to have acquired their Pb isotopic signature from the sedimentary rocks of the Huetamo Sequence or Pacific Ocean sediments. However, the situation in the Teloloapan subterrane is different, since the sources of ore Pb for the pre-accretion and post-accretion deposits differ. An input of ore Pb from the basement rocks may be possible for the post-accretion deposits; for the pre-accretion group, the isotopic signatures of the metamorphic rocks preclude their involvement in the generation of the VMS deposits.

7.3 Ore Lead Isotope Trends in Pre-accretion and Post-accretion Deposits

Lead in Cenozoic ores becomes more radiogenic from the West Coast, near the Middle America Trench, to the East Coast, due to assimilation of radiogenic component from the crust (Figure 6.3; Figure 6.6)**.** However, this trend is not recognized in case of the Mesozoic VMS deposits (Figure 6.7). This is probably because of the amalgamation of the Guerrero composite terrane to the continental margin during Late Cretaceous. The Tertiary deposits formed after this event in a continental arc setting and the Mesozoic deposits developed prior to it.

Comparison between the isotopic signatures of ores from the Sierra Madre terrane, Maya terrane, and distinct subterranes of the Guerrero terrane supports the idea that there is no direct correlation between the distinct suspect terranes of Mexico and the isotopic signatures of the associated ores. Rather, these Pb isotope patterns are interpreted to reflect increasing crustal contribution to mantle-derived magmas as the arc advanced eastward onto a progressively thicker continental crust. It appears that unlike the correlation noticed between the Pb isotope ratios of ores from North America and the crustal thickness, in Central America the Pb isotope composition may be more closely associated with crustal type, as suggested by Cumming et al. (1981).

New and published data support the hypothesis that subducted crustal material, possibly seafloor sediment, or sedimentsry rocks of the Huetamo Sequence, supplied Pb to porphyry copper deposits located on the eastern part of the Zihuatanejo-Huetamo subterrane (e.g., La Verde, El Malacate, Inguaran, La Esmeralda). These deposits consist of ores that are characterized by higher Pb isotope ratios compared to ores located on the western side of the Zihuatanejo-Huetamo subterrane (Autlan and Ayutla), regardless of

their similar age. Hydrothermal deposits situated further inland (Teloloapan and Zacatecas subterranes) contain more radiogenic Pb; this pattern is compatible with assimilation of Mesozoic metamorphic rocks of the Guerrero terrane by the rising magma. Overall, it appears that ores from Cenozoic porphyry copper and epithermal deposits show different trends, with the ores from epithermal deposits being more radiogenic. One possible interpretation of increasing Pb isotope values is that epithermal deposits have interacted to varying degrees with crustal Pb characterized by elevated $^{208}Pb/^{204}Pb$ and $^{207}Pb/^{204}Pb$ values.

8. SIGNIFICANCE OF THE STUDY AND FUTURE DIRECTIONS

8.1 Provenance of Crustal Rocks

There are still questions concerning the possible tectonic interactions between North and South America in the Proterozoic and early Paleozoic, and the small continental fragments called suspect terranes are of utmost importance in trying to shed light on this issue. The present study provides information on the possible source areas for some of the crustal units from the Guerrero terrane. However, further detailed analyses involving measurement of parent/daughter concentration ratios (i.e., U/Pb, Th/Pb, Rb/Sr, Sm/Nd) are required to apply corrections to the isotope ratios of possible source rocks for *in-situ* decay. The corrected compositions may resolve ambiguities in interpretations. Also, Nd model ages and initial Sr ratios will be much more useful for provenance studies.

8.2 Sources of Ore Metals and Ore Lead Isotope Trends

The presence of a large variety of mineral deposits formed both, before and after the accretion of the Guerrero composite terrane to nuclear Mexico, makes it an excellent locale to study the sources of ore metals and the ore Pb isotope trends in pre-accretional and post-accretional deposits.

It is important to constrain the origin of metals in an ore deposit in order to clarify issues related to the processes by which they become concentrated into economically important ore deposits. This study shows that ores from the porphyry copper deposits (located mainly in the Zihuatanejo-Huetamo subterrane) have lower Pb isotope ratios than epithermal deposits, which are situated more inland (mostly in the Teloloapan,

Guanajuato, and Zacatecas subterranes). It has been suggested that generally the largest Pb deposits contain the lowest isotope ratios (Doe and Stacey, 1974), so isotopic zonation has been suggested as a tool for regional mineral exploration (Ewing, 1979). However, in case of the ore deposits located in the Guerrero terrane, this proposal is not supported, since there are large deposits (e.g., Zacatecas, Guanajuato) that show high Pb isotope ratios. Here, ore deposits may have formed by local geological processes of volcanism, with only secondary regional relationships (Ewing, 1979).

The results of the current study provide valuable information on the sources of metals and the ore lead isotope trends in the Mesozoic pre-accretion and Cenozoic post-accretion deposits and also raise interesting questions. One of the questions is the thickness of the crust when Pb from the rocks starts to be incorporated into the ores. This can be addressed by developing models that show the relationshop between the precise thickness of the crust and the Pb isotope compositions of the associated ores.

LIST OF REFERENCES

Albinson, T., Norman, D.I., Cole, D., and Chomiak, B.A. (2001) Controls on formation of low-sulfidation epithermal deposits in Mexico: Constraints from fluid inclusion and stable isotope data. *Society of Economic Geologists Special Publication Series*, v. 8, 1-32.

Barreiro, B.A. (1984) Lead isotopes and Andean magmagenesis. *In* Harmon, R.S., and Barreiro, B.A., eds., Andean Magmatism, chemical and isotopic constraints. Cheshire, Shiva, 21-30.

Barreiro, B.A., and Clark, A.H. (1984) Lead isotopic evidence for evolutionary changes in magma-crust interaction, central Andes, southern Peru. *Earth and Planetary Science Letters* v. 69, no. 1, 30-42.

Barton, M.D., Staude, J.M., Zurcher, L., and Megaw, P.K.M. (1995) Porphyry copper and other intrusion-related mineralization in Mexico. *In* Pierce, F.W., and Bolm, J.G., eds., Porphyry copper deposits of the American Cordillera. *Arizona Geological Society Digest*, v. 20, 487-524.

Bissig, T., Mortensen, J.K., Tosdal, R.M., and Hall, B.V. (2008) The rhyolite-hosted volcanogenic massive sulfide district of Cuale, Guerrero Terrane, west-central Mexico: Silver-rich, base metal mineralization emplaced in a shallow marine continental margin setting. *Economic* Geology, v. 103, 141-159.

Bourcier, W.L., and Barnes, H.L. (1987) Ore solution chemistry, VII: Stabilities of chloride and bisulfide complexes of zinc to 350 degrees C. *Economic* Geology, v. 82, 1839-1863.

Bouse, R.M., Ruiz, J., Titley, S.R., Tosdal, R.M., and Wooden, J.L. (1999) Lead isotope compositions of Late Cretaceous and early Tertiary igneous rocks and sulfide minerals in Arizona: Implications for the sources of plutons and metals in porphyry copper deposits. *Economic* Geology, v. 94, 211-244.

Burchfiel, B. C., Cowan, D.S., and Davis, G.A. (1992) Tectonic overview of the Cordilleran Orogen in the Western United States. *In* Burchfiel, B.C. et al., eds., The Cordilleran Orogen, Conterminous United States: Boulder, Colorado, *Geological Society of America, The Geology of North America*, v. G-3, 407-479.

Burckhardt, C., and Scalia, S. (1906) Geologie des environs de Zacatecas, Mexico. *International Geological Congress*, 10th, Excursion Guidebook 16, 26 p.

Burke, K., Cooper, C., Dewey, J.F., Mann, P., and Pindell, J.L. (1984) Caribbean tectonics and relative plate motions. *Geological Society of America Memoir*, v. 162, 31-63.

Burnham, C. W. (1979) Magmas and hydrothermal fluids. *In* H. L. Barnes, H.L.,ed., *Geochemistry of hydrothermal ore deposits*, 2nd ed. New York, John Wiley, 71-136.

Cabral-Cano, E., Draper, G., Lang, H.R., and Harrison, C.G.A. (2000) Constraining the Late Mesozoic and Early Tertiary Tectonic Evolution of Southern Mexico: Structure and Deformation History of the Tierra Caliente Region. *Journal of Geology*, v. 108, 427-446.

Cameron, K. L., and Ward, R.L. (1998) Xenoliths of Grenvillian granulite basement constrain models for the origin of voluminous Tertiary rhyolites, Davis Mountains, west Texas. *Geology*, v. 26, no. 12, 1087-1090.

Campa, M.F., and Ramirez, J. (1979) La Evolucion Geologica y la Metalogenesis del Noroccidente de Guerrero. *Universidad Autonoma de Guerrero, Serie Tecnico-Cientifica*, v. 1, 71 p.

Campa, M.F., and Coney, P.J. (1983) Tectono-stratigraphic terranes and mineral resource distributions in Mexico. *Canadian Journal of Earth Sciences*, v. 20, 1040-1051.

Campa, M.F., Oviedo, R., and Tardy, M. (1976) La cabalgadura laramidica del dominio volcano-sedimentario (Arco de Alisitos – Teloloapan) sobre el miogeosinclinal mexicano en los limites de los estados de Guerrero y Mexico. *Abstracts, III Congreso Latino-Americano de Geologia, Mexico,* 23.

Campa, M.F., Ramirez, J., and Bloome, C. (1982) La secuencia volcanico-sedimentaria metamorfizada del Triasico (Ladiniano-Carnico) de la region de Tumbiscatio, Michoacan. *Sociedad Geologica Mexicana, VI Convencion Geologica Nacional, 6 Resumenes*, 48 p.

Camprubi, A., and Albinson, T. (2007) Epithermal deposits in Mexico - Update of current knowledge, and an empirical reclassification. *In* Alaniz-Alvarez, S.A., and Nieto-Samaniego, A.F., eds., Geology of Mexico: Celebrating the centenary of the Geological Society of Mexico. *Geological Society of America Special Paper* 422, 377-415.

Camprubi, A., Cardellach, E., Canals, A., and Lucchini R. (2001) The La Guitarra Ag-Au low-sulfidation epithermal deposit, Temascaltepec district, Mexico: Fluid inclusion and stable isotope data. *Society of Economic Geologists Special Publication Series*, v. 8, 159-185.

Camprubi, A., Ferrari, L., Cosca, M.A., Cardellach, E., and Canals, A. (2003) Ages of epithermal deposits in Mexico: regional significance and links with the evolution of Tertiary volcanism. *Economic Geology*, v. *98*, 1029-1037.

Camprubi, A., Chomiak, B.A., Villanueva-Estrada, R.E., Canals, A., Norman, D.I., Cardellach, E., and Stute, M. (2006) Fluid sources for the La Guitarra epithermal deposit (Temascaltepec district, Mexico): Volatile and helium isotope analyses in fluid inclusions. *Chemical Geology*, v. 231, no. 3, 252-284.

Candela, P.A., and Holland, H.D. (1986) A mass transfer model for copper and molybdenum in magmatic hydrothermal systems: the origin of porphyry-type ore deposits. *Economic Geology*, v. 81, 1-19.

Carrillo-Martinez, L. (1971) *Geologia de la Hoja San Jose de Gracia, Sinaloa* [senior thesis]. Mexico City, Universidad Nacional Autonoma de Mexico, 154 p.

Centeno-Garcia, E. (2005) Review of Upper Paleozoic and Lower Mesozoic stratigraphy and depositional environments of central and west Mexico: Constraints on terrane analysis and paleogeography. *In* Anderson, T.H. et al., eds., The Mojave-Sonora Megashear Hypothesis: Development, Assessment, and Alternatives. *Geological Society of America Special Paper* 393, 233-258.

Centeno-Garcia, E., and Silva-Romo, G. (1997) Petrogenesis and tectonic evolution of central Mexico during Triassic-Jurassic time. Universidad Nacional Autonoma de Mexico, Instituto de Geologia. *Revista Mexicana de Ciencias Geologicas*, v. 14, 244-260.

Centeno-Garcia, E., Ruiz, J., Coney, P.J., Patchett, J.P., and Ortega-Gutierrez, F. (1993a) Guerrero Terrane of Mexico: Its role in the Southern Cordillera from new geochemical data. *Geology*, v. 21, 419-422.

Centeno-Garcia, E., Garcia, J.L., Guerrero, M., Ramirez, J., Salinas, J.C., and Talavera, O. (1993b) Geology of the southern part of the Guerrero Terrane, Ciudad Altamirano-Teloloapan area. *Proceedings of the First Circum-Pacific and Circum-Atlantic Terrane Conference, Guanajuato, Mexico, Field Trip Guide II*, 22-33.

Centeno-Garcia, E., Olvera-Carranza, K., Corona-Esquivel, R., Camprubi, A., Tritlla, J., and Sanchez-Martinez, S. (2003) Depositional environment and paleogeographic distribution of the Jurassic-Cretaceous arc in the western and northern Guerrero Terrane, Mexico. *Geological Society of America 99th Cordilleran Section Annual Meeting Abstracts with Programs*, v. 35, no. 4, 76.

Centeno-Garcia, E., Gehrels, G., Diaz-Salgado, C., and Talavera-Mendoza, O. (2005) Zircon provenance of Triassic (Paleozoic?) turbidites from central and western

Mexico: Implications for the early evolution of the Guerrero Arc. *Geological Society of America Abstracts with Programs*, v. 37, no. 4, 64.

Centeno-Garcia, E., Guerrero-Suastegui, M., and Talavera-Mendoza, O. (2008) The Guerrero composite terrane of western Mexico: Collision and subsequent rifting in a supra-subduction zone. *In* Draut, A.E., Clift, P.D., and Scholl, D.W., eds., Formation and applications of the sedimentary record in arc collision zones. *Geological Society of America Special Paper* 436, 279-308.

Chauvel, C., Goldstein, S.L., and Hofmann, A.W. (1995) Hydration and dehydration of oceanic crust controls Pb evolution in the mantle: Mafic magmatism through time. *Chemical Geology*, v. 126, 65-75.

Chiaradia, M., and Fontbote, L. (2003) Separate lead isotope analyses of leachate and residue rock fractions: Implications for metal source tracing in ore deposit studies. *Mineralium Deposita*, v. 38, 185-195.

Chiaradia, M., Fontbote, L., and Paladines, A. (2004) Metal sources in mineral deposits and crustal rocks of Ecuador (1 degrees N-4 degrees S): A lead isotope synthesis. *Economic Geology*, v. 99, 1085-1106.

Clark, K.F., Foster, C.T., and Damon, P.E. (1982) Cenozoic mineral deposits and subduction-related magmatic arcs in Mexico. *Geological Society of America Bulletin*, v. 93, 533-544.

Cline, J.S. (1995) Genesis of porphyry copper deposits: The behavior of water, chloride, and copper in crystallizing melts. *Arizona Geological Society Digest*, v. 20, 69-82.

Coney, P.J. (1990) Terranes, tectonics and the Pacific Rim. *Earth Science Series*, v. 13, 49-69.

Coochey, D.V., and Eckman, P. (1978) Geology of the La Verde copper deposits, Michoacan, Mexico. *Arizona Geological Society Digest*, v. 11, 129-137.

Cumming, G.L., and Kesler, S.E. (1976) Source of lead in Central American and Caribbean mineralization. *Earth and Planetary Science Letters*, v. 31, 262-268.

Cumming, G.L., Kesler, S.E., and Krstic, D. (1979) Isotopic composition of lead in Mexican mineral deposits. *Economic Geology*, v. 74, 1395-1407.

Cumming, G.L., Kesler, S.E., and Krstic, D. (1981) Source of lead in Central American and Caribbean mineralization; II. Lead isotope provinces. *Earth and Planetary Science Letters*, v. 56, 199-209.

Damon, P.E. (1986) Batholith-volcano coupling in the metallogeny of porphyry copper deposits. *In* Friedrich, G.H. et al., eds., Geology and metallogeny of copper deposits. Berlin, Springer-Verlag, 216-234.

Damon, P.E., Clark, K.C., and Shafiqullah, M. (1983) Geochronology of the porphyry copper deposits and related mineralization of Mexico. *Canadian Journal of Earth Sciences*, v. 20, 1052-1071.

Danielson, T.J. (2000) *Age, paleotectonic setting, and common Pb isotope signature of the San Nicolas volcanogenic massive sulfide deposit, southeastern Zacatecas State, central Mexico* [M.S. Thesis]. Vancouver, University of British Columbia, 120 p.

Dasch, E.J. (1981) Lead isotopic composition of metalliferous sediments from the Nazca Plate. *Geological Society of America Memoir*, v. 154, 199-209.

Davila-Alcocer, A.V., and Martinez-Rejes, J. (1987) Una edad Cretacica para las rocas basales de la Sierra de Guanajuato. *In* Resumenes del Simposio sobre la Geologia de la Sierra de Guanajuato. *Instituto de Geologia, Universidad Nacional Autonoma de Mexico*, 19-20.

Davila, V.M., and Guerrero, M. (1990) Una edad basada en radiolarios para la secuencia volcanica-sedimentaria de Arcelia: Edo. De Guerrero. *Abstracts, X Convencion Geologica Nacional, Sociedad Geologica Mexicana,* 83.

DePaolo, D.J. (1981) Neodymium isotopes in the Colorado Front Range and crust-mantle evolution in the Proterozoic. *Nature*, v. 291, 193-196.

DePaolo, D.J., and Wasserburg, G.J. (1976) Inferences about magma sources and mantle structure from variations of Nd-143/Nd-144. *Geophysical Research Letters*, v. 3, 743-746.

DePaolo, D.J., and Wasserburg, G.J. (1979) Petrogenetic mixing models and Nd-Sr isotopic patterns. *Geochimica et Cosmochimica Acta*, v. 43, 615-628.

Dickin, A.P. (1995) *Radiogenic isotope geology.* Cambridge University Press, Cambridge, United Kingdom (GBR).

Doe, B.R. (1970) Lead isotopes. New York, Springer-Verlag, 137 p.

Doe, B.R., and Zartman, R.E. (1979) Plumbotectonics I, The Phanerozoic. *In* Barnes, H.L., ed., *Geochemistry of hydrothermal ore deposits*, 2nd ed. New York, Wiley Interscience, 22-70.

Domenick, M.A., Kistler, R.W., Dodge, F.C.W., and Tatsumoto, M. (1983) Nd and Sr isotopic study of crustal and mantle inclusions from the Sierra Nevada and

implications for batholith petrogenesis. *Geological Society of America Bulletin*, v. 94, 713-719.

Donnelly, T.W., and Rogers, J.J.W. (1978) The distribution of igneous rock suites throughout the Caribbean. *Geologie en Mijnbouw. Netherlands Journal of Geosciences*, v. 57, 151-162.

Ducea, M.N., Gehrels, G.E., Shoemaker, S., Ruiz, J., and Valencia, V.A. (2004) Geologic evolution of the Xolapa Complex, southern Mexico: Evidence from U-Pb zircon geochronology. *Geological Society of America Bulletin*, v. 116, 1016-1025.

Einaudi, M.T., Hedenquist, J.W., and Inan, E.E. (2003) Sulfidation state of fluids in active and extinct hydrothermal systems: transitions from porphyry to epithermal environments. *Society of Economic Geologists Special Publication Series*, v. 10, 285-313.

Elias-Herrera, M., and Ortega-Gutierrez, F. (1998) The Early Cretaceous Arperos oceanic basin (western Mexico): Geochemical evidence for an aseismic ridge formed near a spreading center – Comment. *Tectonophysics*, v. 292, 321-326.

Elias-Herrera, M., Ortega-Gutierrez, F., and Cameron, K.L. (1996) Pre-Mesozoic continental crust beneath the southern Guerrero terrane; xenolith evidence. *GEOS*, v. 16, 234.

Elias-Herrera, M., Sanchez-Zavala, J.L., and Macias-Romo, C. (2000) Geologic and geochronologic data from the Guerrero Terrane in the Tejupilco area, southern Mexico: new constraints on its tectonic interpretation. *Journal of South American Earth Sciences*, v. 13, 355-375.

Elias-Herrera, M., Ortega-Gutierrez, F., Sanchez-Zavala, J.L., and Macias-Romo, C. (2003) The real Guerrero Terrane, southern Mexico: new insights from recent studies. *Geological Society of America 99th Cordilleran Section Annual Meeting Abstracts with Programs*, v. 35, no. 4, 66.

Farmer, G.L., and DePaolo, D.J. (1997) Sources of hydrothermal components: Heavy isotopes. *In* H. L. Barnes, H.L.,ed., *Geochemistry of hydrothermal ore deposits*, 2nd ed. New York, John Wiley and Sons, Inc., 31-61.

Faure, G. (1986) *Principles of isotope geology.* New York, John Wiley and Sons, 589 p.

Fraga, P.M. (1991) Geology and mineralization of the La Negra mining unit, Queretaro. *In* Salas, G.P., ed., *Economic geology, Mexico*. Geological Society of America, Boulder, CO., 291-294.

Freydier, C., Martinez, R.J., Lapierre, H., Tardy, M., and Coulon, C. (1996) The Early Cretaceous Arperos oceanic basin (western Mexico): Geochemical evidence for an aseismic ridge formed near a spreading center. *Tectonophysics*, v. 259, 343-367.

Freydier, C., Lapierre, H., Briqueu, L., Tardy, M., Coulon, C., Martinez-Reyes, J. (1997) Volcaniclastic sequences with continental affinities within the Late Jurassic-Early Cretaceous Guerrero intra-oceanic arc terrane (western Mexico). *Journal of Geology*, v. 105, 483-502.

Freydier, C., Martinez, R.J., Lapierre, H., Tardy, M., and Coulon, C. (1998) The Early Cretaceous Arperos oceanic basin (western Mexico): Geochemical evidence for an aseismic ridge formed near a spreading center - Reply. *Tectonophysics*, v. 292, 327-331.

Freydier, C., Lapierre, H., Ruiz, J., Tardy, M., Martinez-R., J., and Coulon, C. (2000) The Early Cretaceous Arperos Basin: an oceanic domain dividing the Guerrero arc from nuclear Mexico evidenced by the geochemistry of the lavas and sediments. *Journal of South American Earth Sciences*, v. 13, 325-336.

Fries, C., Schmitter E., Damon, P.E., and Livingston, D.E. (1962) Rocas Precambricas de edad grenvilliana de la parte central de Oaxaca en el sur de Mexico. *Boletin - Universidad Nacional Autonoma de Mexico, Instituto de Geologia,* 45-53.

Garcia, G., and Querol F.S. (1991) Description of some deposits in the Zimapan District, Hidalgo. *In* Salas, G.P., ed., *Economic geology, Mexico*. Geological Society of America, Boulder, CO., 295-313.

Gaytan-Rueda, J.E. (1975) *Exploration and development at the La Negra Mine, Maconi, Queretaro, Mexico* [M.S. Thesis]. Tucson, Univeristy of Arizona, 98 p.

Gilmer, A.L., Clark, K.F., Conde, C., Hernandez, I., Figueroa, J.I., and Porter, E.W. (1988) Sierra de Santa Maria, Velardena mining district, Durango, Mexico. *Economic Geology*, v. 83, 1802-1829.

Gomez-Tuena, A., Orozco-Esquivel, M.T., and Ferrari, L. (2007) Igneous petrogenesis of the Trans-Mexican Volcanic Belt. *In* Alaniz-Alvarez, S.A., and Nieto-Samaniego, A.F., eds., Geology of Mexico: Celebrating the Centenary of the Geological Society of Mexico. *Geological Society of America Special Paper* 422, 129-181.

Gross, W.H. (1975) New ore discovery and source of silver-gold veins, Guanajuato, Mexico. *Economic Geology*, v. 70, 1175-1189.

Guerrero, M., Ramirez, J., and Talavera, O. (1990) Estudio estratigrafico del arco volcanico Cretacico inferior de Teloloapan, Guerrero. *Abstracts, X Convencion Geologica Nacional, Sociedad Geologica Mexicana*, 67.

Gustafson, L.B., and Hunt, J.P. (1975) The porphyry copper deposit at El Salvador, Chile. *Economic Geology*, v. *70*, 857-912.

Hall, B.V., and Gomez-Torres, P.P. (2000) The El Gordo volcanogenic massive sulfide deposit, Leon-Guanajuato district, central Mexico. *Geological Association of Canada, Mineral Deposits Division Special Publication*, v. 2, 163-166.

Hamelin, B., Manhes, G., Albarede, F., and Allegre, C.J. (1985) Precise lead isotope measurements by the double spike technique: a reconsideration. *Geochimica et Cosmochimica Acta*, v. 49, 173-182.

Hart, S.R., and Brooks, C. (1977) The geochemistry and evolution of early Precambrian mantle. *Contributions to Mineralogy and Petrology*, v. 61, 109-128.

Hawkesworth, C.J., Norry, M.J., Roddick, J.C., and Vollmer, R. (1979) (super 143) Nd/ (super 144) Nd and (super 87) Sr/ (super 86) Sr ratios from the Azores and their significance in LIL-element enriched mantle. *Nature*, v. 280, 28-31.

Hedenquist, J.W., and Shinohara, H. (1997) K-silicate- to sericite-stage transition in porphyry Cu deposits: collapse of magmatic plume, or overprint by meteoric water? *Geological Society of America Abstracts with Programs*, v. 29, no. 6, 359.

Hemming, S.R., and McLennan, S.M. (2001) Pb isotope compositions of modern deep sea turbidites. *Earth and Planetary Science Letters*, v. 184, 489-503.

Herrmann, U.R., Nelson, B.K., and Ratschbacher, L. (1994) The origin of a terrane: U/Pb zircon geochronology and tectonic evolution of the Xolapa Complex (southern Mexico). *Tectonics*, v. 13, 455-474.

Hildreth, W., and Moorbath, S. (1988) Crustal contributions to arc magmatism in the Andes of central Chile. *Contributions to Mineralogy and Petrology*, v. 98, 455-489.

Hofmann, A.W. (1997) Mantle geochemistry: The message from oceanic volcanism. *Nature*, v. *385*, 219-229.

Hosler, D., and Macfarlane, A.W. (1996) Copper sources, metal production, and metals trade in late postclastic Mesoamerica. *Science*, v. 273, 1819-1824.

Jacobsen, S.B., and Wasserburg, G.J. (1979) Nd and Sr isotopic study of the Bay of Islands ophiolite complex and the evolution of the source of midocean ridge basalts. *Journal of Geophysical Research*, v. 84, 7429-7445.

JICA-MMAJ (1991) Informe de la Exploracion Cooperativa de Mineral en la Region de Arcelia, Estados Unidos de Mexico, Fase IV. *Japan International Cooperation Agency – Metal Mining Agency of Japan*, 155 p.

Johnson, B.J., Montante-Martinez, A., Canela-Barboza, M., and Danielson, T.J. (2000) Geology of the San Nicolas deposit, Zacatecas, Mexico. *Geological Association of Canada, Mineral Deposits Division Special Publication*, v. 2, 71-85.

Kamenov, G.D. (2000) *Sources of metals in San Cristobal and Pulacayo mining districts, southwest Bolivia: a lead isotope study* [M.S. Thesis]. Miami, Florida International University, 87 p.

Kamenov, G.D, Macfarlane, A.W., and Riciputi, L.R. (2002) Sources of lead in the San Cristobal, Pulacayo, and Potosi mining districts, Bolivia, and a reevaluation of regional ore lead isotope provinces. *Economic Geology*, v. 97, 573-592.

Karig, D.E., Cardwell, R.K., Moore, G.F., and Moore, D.G. (1978) Late Cenozoic subduction and continental margin truncation along the northern Middle America Trench. *Geological Society of America Bulletin*, v. 89, 265-276.

Kay, R.W., Sun, S.S., and Lee-Hu, C. (1978) Pb and Sr isotopes in volcanic rocks from the Aleutian Islands and Pribilof Islands, Alaska. *Geochimica et Cosmochimica Acta*, v. 42, 263-274.

King, P.B. (1959) The evolution of North America. New Jersey, Princeton University Press, 189 p.

Lang, H.R., Barros, T., Cabral-Cano, E., Draper, G., Jansma, P., and Johnson, C. (1996) Terrane deletion in northern Guerrero, *Geofisica Internacional*, v. 35, 349-359.

Lewis, P.D., and Rhys, D.A. (2000) Geological setting of the Tizapa volcanogenic massive sulfide deposit, Mexico State, Mexico. *Geological Association of Canada, Mineral Deposits Division Special Publication*, v. 2, 87-112.

Lopez, R., Hosler, D., Pantoja, J., Martiny, B., Morales-Contreras, J., Solis-Pichardo, G., and Moran-Zenteno, D. (1999) Coastal and inland Pb isotope groups of Paleocene Cu ores from the Rio Balsas Basin, Guerrero State, Mexico. *EOS Transactions, American Geophysical Union*, v. 80, no. 46, 1082.

Macfarlane, A.W. (1989) *Lead, sulfur and strontium isotopes in the Hualgayoc area, Peru, and lead isotope provinces of the Central Andes* [Ph.D. Dissertation]. Cambridge, Harvard University, 374 p.

Macfarlane, A.W. (1999a) Isotopic studies of Northern Andean crustal evolution and ore metal sources. *Society of Economic Geologists Special Publication Series*, v. 7, 195-217.

Macfarlane, A.W. (1999b) The lead isotope method for tracing the sources of metals in archaeological artefacts: strengths, weaknesses and applications in the Western

Hemisphere. *In* Young, S.M.M. et al., eds., *Metals in Antiquity*, BAR International Series 792. Oxford, Archaeopress, 310-316.

Macfarlane, A.W., and Petersen, U. (1990) Pb isotopes of the Hualgayoc area, northern Peru: Implications for metal provenance and genesis of a Cordilleran polymetallic mining district. *Economic Geology*, v. 85, 1303-1327.

Macfarlane, A.W., Marcet, P., LeHuray, A.P., and Petersen, U. (1990) Lead isotope provinces of the Central Andes inferred from ores and crustal rocks. *Economic Geology*, v. 85, 1857-1880.

Manhes, G., Minster, J.F., and Allegre, C.J. (1978) Comparative uranium-thorium-lead and rubidium-strontium study of the Saint Severin amphoterite: consequences for early solar system chronology. *Earth and Planetary Science Letters*, v. 39, 14-24.

Manton, W.I., and Tatsumoto, M. (1971) Some Pb and Sr isotopic measurements on eclogites from the Roberts Victor Mine, South Africa. *Earth and Planetary Science Letters* 10, no. 2:217-226.

Mapes, E. (1991) La Truchas iron deposits, Michoacan. *In* Salas, G.P., ed., *Economic geology, Mexico*. Geological Society of America, Boulder, CO., 339-342.

Martinez-Serrano, R.G., Schaaf, P., Solis-Pichardo, G., Hernandez-Bernal, M., Hernandez-Trevino, T., Morales-Contreras, J., and Macias, J.L. (2004) Sr, Nd and Pb isotope and geochemical data from the Quaternary Nevado de Toluca Volcano, a source of recent adakitic magmatism, and the Tenango volcanic field, Mexico. *Journal of Volcanology and Geothermal Research*, v. 138, 77-110.

Martinez-Serrano, R.G., Solis-Pichardo, G., Flores-Marquez, L., Macias-Romo, C., and Delgado-Duran, J. (2008) Geochemical and Sr-Nd isotopic characterization of the Miocene volcanic events in the Sierra Madre del Sur, central and southeastern Oaxaca, Mexico. *Revista Mexicana de Ciencias Geologicas*, v. 25, 1-20.

Martiny, B., Martinez-Serrano, R., Ayuso, R.A., Macias-Romo, C., Moran-Zenteno, D.J., Alba-Aldave, L. (1997) Pb isotope geochemistry of Tertiary igneous rocks and continental crustal complexes, southern Mexico. *EOS Transactions, American Geophysical Union*, v. 78, no. 6, 844.

Martiny, B., Martinez-Serrano, R.G., Moran-Zenteno, D.J., Macias-Romo, C., and Ayuso, R.A. (2000) Stratigraphy, geochemistry and tectonic significance of the Oligocene magmatic rocks of western Oaxaca, southern Mexico. *Tectonophysics*, v. 318, 71-98.

Mendoza, O.T., and Suastegui, M.G. (2000) Geochemistry and isotopic composition of the Guerrero Terrane (western Mexico): implications for the tectono-magmatic

evolution of southwestern North America during the late Mesozoic. *Journal of South American Earth Sciences*, v. 13, 297-324.

Miller, D.M., Goldstein, S.L., and Langmuir, C.H. (1994) Cerium/lead and lead isotope ratios in arc magmas and the enrichment of lead in the continents. *Nature*, v. 368, 514-520.

Miranda-Gasca, M.A. (1995) *The volcanogenic massive sulfide and sedimentary exhalative deposits of the Guerrero Terrane, Mexico* [Ph.D. Dissertation]. Tucson, The University of Arizona, 294 p.

Miranda-Gasca, M.A. (2000) The metallic ore-deposits of the Guerrero Terrane, western Mexico: an overview. *Journal of South American Earth Sciences*, v. 13, 403-413.

Miranda-Gasca, M.A., Ruiz, J., Titley, S.R., and Coney, P.J. (1993) Tectonic evolution of the Guerrero terrane from lead isotope data and base metal composition of ore deposits. *In* Ortega-Gutierrez, F., Centeno-Garcia, E., Moran-Zenteno, D.J., and Gomez-Caballero, D.J., eds., *Proceedings of the First Circum-Pacific and Circum-Atlantic Terrane Conference, Guanajuato, Mexico*, 86-89.

Moorbath, S., Welke, H., and Gale, N.H. (1969) The significance of lead isotope studies in ancient, high-grade metamorphic basement complexes, as exemplified by the Lewisian rocks of northwest Scotland. *Earth and Planetary Science Letters*, v. 6, 245-256.

Moran-Zenteno, D.J., Tolson, G., Solis-Pichardo, G., and Victoria-Morales, A. (1993) Tectonic relationships of the Xolapa magmatic arc with surrounding terranes of southwestern Mexico. *EOS Transactions, American Geophysical Union*, v. 74, no. 43, 575.

Moran-Zenteno, D.J., Alba-Aldave, L.A., Martinez-Serrano, R.G., Reyes-Salas, M.A., Corona-Esquivel, R., and Angeles-Garcia, S. (1998) Stratigraphy, geochemistry and tectonic significance of the Tertiary volcanic sequences of the Taxco-Quetzalapa region, southern Mexico. *Revista Mexicana de Ciencias Geologicas*, v. 15, 167-180.

Moran-Zenteno, D.J., Tolson, G., Martinez-Serrano, R.G., Martiny, B., Schaaf, P., Silva-Romo, G., Macias-Romo, C., Alba-Aldave, L., Hernandez-Bernal, M.S., Solis-Pichardo, G. (1999) Tertiary arc-magmatism of the Sierra Madre del Sur, Mexico, and its transition to the volcanic activity of the Trans-Mexican volcanic belt. *Journal of South American Earth Sciences*, v. 12, 513-535.

Moran-Zenteno, D.J., Alba-Aldave, L.A., Sole, J., and Iriondo, A. (2004) A major resurgent caldera in southern Mexico: the source of the late Eocene Tilzapotla Ignimbrite. *Journal of Volcanology and Geothermal Research*, v. 136, 97-119.

Moran-Zenteno, D.J., Cerca, M., and Keppie, J.D. (2007) The Cenozoic tectonic and magmatic evolution of southwestern Mexico: Advances and problems of interpretation. *In* Alaniz-Alvarez, S.A., and Nieto-Samaniego, A.F., eds., Geology of Mexico: Celebrating the centenary of the Geological Society of Mexico. *Geological Society of America Special Paper* 422, 71-91.

Mortensen, J.K., Hall, B.V., Bissig, T., Friedman, R.M., Danielson, T., Oliver, J., Rhys, D.A., Ross, K.V., and Gabites, J.E. (2008) Age and paleotectonic setting of volcanogenic massive sulfide deposits in the Guerrero Terrane of central Mexico: Constraints from U-Pb age and Pb isotope studies. *Economic Geology*, v. 103, 117-140.

Mukasa, S.B., Vidal, C.E., and Injoque-Espinoza, J. (1990) Pb isotope bearing on the metallogenesis of sulfide ore deposits in central and southern Peru. *Economic Geology*, v. 85, 1438-1446.

Mullan, H.S. (1978) Evolution of part of the Nevadan Orogen in northwestern Mexico. *Geological Society of America Bulletin*, v. 89, 1175-1188.

Nelson, B.K., and Bentz, K.L. (1990) Isotopic and trace element evidence for the provenance of metagraywackes from the Franciscan Complex, CA. *EOS Transactions, American Geophysical Union*, v. 71, no. 43, 1689.

Norman, D.I., Chomiak, B., Albinson, T., and Moore, J. (1997) Volatiles in epithermal systems: The big picture. *Geological Society of America Abstracts with Programs*, v. 29, no. 6, 206.

Norton, D.L. (1988) Metasomatism and permeability. *American Journal of Science*, v. 288, 604-618.

Oliver, J., Payne, J., Rebagliati, M., and Cluff, R. (1999) Precious-metal-bearing volcanigenic massive sulfide deposits, Campo Morado, Guerrero, Mexico. *In* Jambor, J.J., ed., VMS and carbonate-hosted polymetallic deposits of Central Mexico. *British Columbia and Yukon Chamber of Mines, Cordilleran Roundup Special Volume*, 63-76.

O'Nions, R.K., Hamilton, P.J., and Evensen, N.M. (1980) The chemical evolution of the Earth's mantle. *Scientific American*, v. 242, 120-121.

Ortega-Gutierrez, F. (1981) Metamorphic belts of southern Mexico and their tectonic significance. *Geofisica Internacional*, v. 20, 177-202.

Ortega-Gutierrez, F. (1993) Tectonostratigraphic analysis and significance of the Paleozoic Acatlan Complex of southern Mexico. *In* Ortega-Gutierrez, F., Centeno-Garcia, E., Moran-Zenteno, D.J., and Caballero, G., eds., Terrane geology of

southern Mexico. *Universidad Nacional Autonoma de Mexico, Instituto de Geologia, First circum-Pacific and circum-Atlantic terrane conference, Guanajuato, Mexico, Guidebook of field trip B*, 54-60.

Ortega-Gutierrez, F., Anderson, T.H., and Silver, L.T. (1977) Lithologies and geochronology of the Precambrian craton of southern Mexico. *Geological Society of America Abstracts with Programs*, v. 9, 1121-1122.

Ortiz-Hernandez, L.E., and Lapierre, H. (1991) Field, petrological and geochemical evidences for the intraoceanic environment of the Upper Jurassic-Early Cretaceous Palmar Chico-Arcelia Arc sequence, southern Mexico. *Meeting on the Geological Evolution of Mexico and the First Mexican Congress on Mineralogy – Memoirs*, 144-146.

Ortiz-Hernandez, L.E., Acevedo-Sandoval, O.A., and Flores-Castro, K. (2003) Early Cretaceous intraplate seamounts from Guanajuato, central Mexico: geochemical and mineralogical data. *Revista Mexicana de Ciencias Geologicas*, v. 20, 27-40.

Ortiz-Hernandez, L.E., Chiodi, M., Lapierre, H., Monod, O., and Calvet, P. (1992) The intraoceanic allochthonous arc (Lower Cretaceous) of Guanajuato - petrographic, geochemical, structural and isotopic characteristics of the veinlike deposit and associated basaltic lavas, geodynamic implications. *Revista Mexicana de Ciencias Geologicas*, v. 9, 126-145.

Osoria, A.H., Leija, N.V, and Esquivel, R. (1991) Economic geology of the Inguaran mining district, Michoacan. *In* Salas, G.P., ed., *Economic geology, Mexico*. Geological Society of America, Boulder, CO., 365-368.

Panneerselvam, K. (2001) *Sources of metals and sulfur in the mineral deposits of central Idaho, USA* [Ph.D. Dissertation]. Miami, Florida International University, 140 p.

Pantoja, A.J. (1959) Estudio geologico de reconocimiento de la region de Huetamo, Estado de Michoacan. *Consejo de Recursos Naturales no Renovables – Boletin*, v. 50, 1-33.

Patchett, P.J., and Ruiz, J. (1987) Nd isotopic ages of crust formation and metamorphism in the Precambrian of eastern and southern Mexico. *Contributions to Mineralogy and Petrology*, v. 96, 523-528.

Patchett, P.J., and Ruiz, J. (1989) Nd isotopes and the origin of Grenville-age rocks in Texas: Implications for Proterozoic evolution of the United States mid-continent region. *Journal of Geology*, v. 97, 685-695.

Pearce, J.A. (1983) Role of the sub-continental lithosphere in magma genesis at active continental margins. *In* Hawkesworth, C.J., and Norry, N.J., eds., *Continental*

basalts and mantle xenoliths. Nantwich, Shiva Publishing Ltd., United Kingdom (GBR).

Pearson, M.F., Clark, K.F., and Porter, E.W. (1988) Mineralogy, fluid characteristics, and silver distribution at Real de Angeles, Zacatecas, Mexico. *Economic Geology*, v. 83, no. 8:1737-1759.

PETDB Database (2002) Geochemical database of the Ocean Floor. www.petdb.org.

Pindell, J.L. (1994) Evolution of the Gulf of Mexico and the Caribbean. *In* Trevor, A.J., ed., *Caribbean Geology: An Introduction*. University of the West Indies Publishers' Association, Kingston, Jamaica (JAM), 13-39.

Poole, F.G., Perry, W.J., Madrid R.J., and Amaya-Martinez, R. (2005) Tectonic synthesis of the Ouachita-Marathon-Sonora orogenic margin of southern Laurentia: Stratigraphic and structural implications for timing of deformational events and plate tectonic model. *In* Anderson, T.H., et al., eds., The Mojave-Sonora Megashear Hypothesis: Development, Assessment, and Alternatives. *Geological Society of America Special Paper* 393, 543-596.

Puig, A. (1988) Geologic and metallogenic significance of the isotopic composition of lead in galenas of the Chilean Andes.*Economic Geology*, v. 83, 843-858.

Ramirez-Espinosa, J., Campa, M.F., Talavera, O., and Guerrero, M. (1991) Caracterizacion de los arcos insulares de la Sierra Madre del Sur y sus implicaciones tectonicas. Characterization of the island arcs from the Sierra Madre del Sur and their tectonic implications. *Meeting on the Geological Evolution of Mexico and the First Mexican Congress on Mineralogy – Memoirs*, 163-166.

Ranson, W.A., Fernandez, L.A., Simmons, W.B.J., and de la Vega, E.S. (1982) Petrology of the metamorphic rocks of Zacatecas, Mexico. *Boletin de la Sociedad Geologica Mexicana*, v. 43, 37-59.

Restrepo-Pace, P., Ruiz, J., Gehrels, G.E., and Cosca, M. (1997) Geochronology and Nd isotopic data of Grenville-age rocks in the Colombian Andes: new constraints for late Proterozoic-early Paleozoic paleocontinental reconstructions of the Americas. *Earth and Planetary Science Letters*, v. 150, 427-441.

Rhys, D.A., Enns, S.G., and Ross, K.V. (2000) Geological setting of deformed VMS-type mineralization in the Azulaquez-Tlanilpa area, northern Guerrero State, Mexico. *Geological Association of Canada, Mineral Deposits Division Special Publication*, v. 2, 113-133.

Richard, P., Shimizu, N., and Allegre, C.J. (1976) (super 143) Nd/ (super 146) Nd, a natural tracer: an application to oceanic basalts. *Earth and Planetary Science Letters*, v. 31, 269-278.

Robb, L. (2005) *Introduction to ore-forming processes.* Blackwell Publishing, Malden, MA, United States (USA), 373 p.

Ruiz, J., and Coney, P.J. (1985) Correlation between lead isotopes in Mexican ore deposits and tectono-stratigraphic terranes. *Geological Society of America Abstracts with Programs*, v. 17, no. 7, 704.

Ruiz, J., Patchett, P.J., and Arculus, R.J. (1988a) Nd/Sr isotope composition of lower crustal xenoliths: evidence for the origin of mid-Tertiary felsic volcanics in Mexico. *Contributions to Mineralogy and Petrology*, v. 99, 36-43.

Ruiz, J., Patchett, P.J., and Ortega-Gutierrez, F. (1988b) Proterozoic and Phanerozoic basement terranes of Mexico from Nd isotopic studies. *Geological Society of America Bulletin*, v. 100, 274-281.

Ruiz, J., Tosdal, R.M., Restrepo, P.A., and Murillo-Muneton, G. (1999) Pb isotope evidence for Colombia-southern Mexico connections in the Proterozoic. *In* Ramos, V.A. and Keppie, J.D., eds., Laurentia-Gondwana Connections before Pangea. *Geological Society of America Special Paper* 336, 183-197.

Sanford, R.F. (1992) Lead isotopic compositions and paleohydrology of caldera-related epithermal veins, Lake City, Colorado. *Geological Society of America Bulletin*, v. 104, 1236-1245.

Sangster, D.F., Savard, M.M., and Kontak, D.J. (1998) Sub-basin-specific Pb and Sr sources in Zn-Pb deposits of the Lower Windsor Group, Nova Scotia, Canada. *Economic Geology*, v. 93, 911-919.

Schaaf, P., Kohler, H., Muller-Sohnius, D., and Von Drach, V. (1990) Rb-Sr, Sm-Nd and K-Ar data on granitoids from the Pacific coast of Mexico between 21 degrees and 17 degrees N. Seventh international conference on Geochronology, cosmochronology and isotope geology: abstracts volume. *Geological Society of Australia Abstracts*, v. 27, 89.

Schaaf, P., Kohler, H., Muller-Sohnius, D., Von Drach, V., and Negendank, J.F.W. (1991) Sr-Nd and K-Ar data on age and genesis of West-Mexico Cordilleran batholiths. Sixth meeting of the European Union of Geosciences. *Terra Abstracts*, v. 3, 38.

Schaaf, P., Moran-Zenteno, D., Hernandez-Bernal, M.S., Solis-Pichardo, G., Tolson, G., and Kohler, H. (1995) Paleogene continental margin truncation in southwestern Mexico: Geochronological evidence. *Tectonics*, v. 14, 1339-1350.

Sedlock, R.L., Ortega-Gutierrez, F., and Speed, R.C. (1993) Tectonostratigrahic Terranes of Mexico. *In* Sedlock, R.L., Ortega-Gutierrez, F., and Speed, R.C., eds., Tectonostratigrahic Terranes and Tectonic Evolution of Mexico. *Geological Society of America Special paper* 278, 2-74.

Sillitoe, R.H., and Hart, S.R. (1984) Lead-isotopic signature of porphyry copper deposits in oceanic and continental settings, Colombian Andes. *Geochimica et Cosmochimica Acta*, v. 48, 2135-2142.

Simmons, S.F. (1995) Magmatic contributions to low-sulfidation epithermal deposits. *In* Thompson, J.F.H., ed., Magmas, fluids, and ore deposits. *Mineralogical Association of Canada Short Course Series*, v. 23, 455-477.

Simmons, S.F., Gemmell, J.B., and Sawkins, F.J. (1988) The Santo Nino silver-lead-zinc vein, Fresnillo District, Zacatecas, Mexico: Part II. Physical and chemical nature of ore-forming solutions. *Economic Geology*, v. 83, 1619-1641.

Smith, D.R., Barnes, C.G., Shannon, W., Roback, R.C., and James, E. (1997) Petrogenesis of Mid-Proterozoic granitic magmas; examples from central and West Texas. *Precambrian Research*, v. 85, 53-79.

Solis-Pichardo, G., Schaaf, P., Hernandez, T., Salazar, J., and Villanueva, D. (2008) Mantle-type granites from Jilotlan, Jalisco, Mexico: Geochemical and isotopic evidence. *EOS Transactions, American Geophysical Union*, v. 89, no. 53, Suppl., Abstract V31B-2136.

Stacey, J.S., and Kramers, J.D. (1975) Approximation of terrestrial lead isotope evolution by a two-stage model. *Earth and Planetary Science Letters*, v. 26, 207-221.

Stacey, J. S., Zartman, R.E., and NKomo, I.T. (1968) A lead isotope study of galenas and selected feldspars from mining districts in Utah. *Economic Geology*, v. 63, 796-814.

Staude, J.M.G., and Barton, M.D. (2001) Jurassic to Holocene tectonics, magmatism, and metallogeny of northwestern Mexico. *Geological Society of America Bulletin*, v. 113, 1357-1374.

Stephan, J. F., Mercier de Lepinay, B., Calais, E., Tardy, M., Beck, C., Carfantan, J.C., Olivet, J.L., Vila, J.M., Bouysse, P., Mauffret, A., Bourgois, J., Thery, J.M., Tournon, J., Blanchet, R., and Dercourt, J. (1990) Paleogeodynamic maps of the Caribbean: 14 steps from Lias to present. *Bulletin de la Societe Geologique de France*, v. 6, 915-919.

Stewart, J.H. (1988) Latest Proterozoic and Paleozoic southern margin of North America and the accretion of Mexico. *Geology*, v. 16, 186-189.

Sturm, M.E., Klein, E.M., Graham, D.W., and Karsten, J. (1999) Age constraints on crustal recycling to the mantle beneath the southern Chile Ridge: He-Pb-Sr-Nd isotope systematics. *Journal of Geophysical Research*, v. 104, 5097-5114.

Sundblad, K., Cumming, G.L., and Krstic, D. (1991) Lead isotope evidence for the formation of epithermal gold quartz veins in the Chortis Block, Nicaragua. *Economic Geology*, v. 86, 944-959.

Talavera, M.O. (1993) *Les Formations Orogeniques Mesozoiques du Guerrero (Mexique meridional). Contribution a la Connaissance de l'Evolution Geodinamique des Cordilleres Mexicaines* [Ph.D. Dissertation]. Grenoble, Universite Joseph Fourier, 462 p.

Talavera, M.O. (2000) Melanges in southern Mexico: geochemistry and metamorphism of Las Ollas Complex (Guerrero Terrane). *Canadian Journal of Earth Sciences*, v. 37, 1309-1320.

Talavera, M.O., Ramirez, J., and Guerrero, M. (1993) Geochemical evolution of the Guerrero Terrane : example of a Late Mesozoic multi-arc system. *In* Ortega-Gutierrez, F., Centeno-Garcia, E., Moran-Zenteno, D.J., and Gomez-Caballero, D.J., eds., *Proceedings of the First Circum-Pacific and Circum-Atlantic Terrane Conference, Guanajuato, Mexico,* 150-152.

Talavera, M.O., Ramirez, J., and Guerrero M. (1995) Petrology and geochemistry of the Teloloapan subterrane: a Lower Cretaceous evolved intra-oceanic island arc. *Geofisica Internacional*, v. 34, 3-22.

Tardy, M., Lapierre, H., Freydier, C., Coulon, C., Gill, J.B., Mercier de Lepinay, B., Beck, C., Martinez, R.J., Talavera, M.O., Ortiz, H.E., Stein, G., Bourdier, J.L., and Yta, M. (1994) The Guerrero suspect terrane (western Mexico) and coeval arc terranes (the Greater Antilles and the Western Cordillera of Colombia): a late Mesozoic intra-oceanic arc accreted to cratonal America during the Cretaceous. *Tectonophysics*, v. 230, 49-73.

Tilton, G.R., and Barreiro, B.A. (1980) Origin of lead in Andean calcalkaline lavas, southern Peru. *Science*, v. 210, 1245-1247.

Tilton, G.R., Pollak, R.J., Clark, A.H., Robertson, R.C. (1981) Isotopic composition of Pb in Central Andean ore deposits. *Geological Society of America Memoir*, v. 154, 791-816.

Todt, W., Cliff, R.A., Hanser, A., and Hofmann, A.W. (1996) Evaluation of a (super 202) Pb- (super 205) Pb double spike for high-precision lead isotope analysis. *In* Basu, R., and Hart, S.R., eds., Earth processes: reading the isotopic code. *American Geophysical Union Monograph*, v. 95, 429-437.

Tosdal, R.M., Wooden, J.L., and Bouse, R.M. (1999) Pb isotopes, ore deposits, and metallogenic terranes. Application of radiogenic isotopes to ore deposit research and exploration. *Reviews in Economic Geology*, v. 12, 1-28.

Urrutia-Fucugauchi, J., and Uribe-Cifuentes, R. (1999) Lower-crustal xenoliths from the Valle de Santiago maar field, Michoacan-Guanajuato volcanic field, central Mexico. *International Geology Review*, v. 41, 1067-1081.

Valencia-Moreno, M., Ruiz, J., Barton, M.D., Patchett, P.J., Zurcher, L., Hodkinson, D.G., Roldan-Quintana, J. (2001) A chemical and isotopic study of the Laramide granitic belt of northwestern Mexico: Identification of the southern edge of the North American Precambrian basement. *Geological Society of America Bulletin*, v. 113, 1409-1422.

Valencia-Moreno, M., Ruiz, J., and Patchett, P.J. (2003) Location of the southwestern edge of Proterozoic North America based on Sr and Nd isotopic data from Laramide granitic rocks of Sonora, NW Mexico. *Geological Society of America 99th Cordilleran Section Annual Meeting Abstracts with Programs*, v. 35, no. 4, 68.

Valencia-Moreno, M. Ochoa-Landin, L., Noguez-Alcantara, Ruiz, J., and Perez-Segura, E. (2007) Geological and metallogenetic characteristics of the porphyry copper deposits of Mexico and their situation in the world context. *In* Alaniz-Alvarez, S.A., and Nieto-Samaniego, A.F., eds., Geology of Mexico: Celebrating the centenary of the Geological Society of Mexico. *Geological Society of America Special Paper* 422, 433-458.

Verma, S.P. (2000) Geochemistry of the subducting Cocos Plate and the origin of subduction-unrelated mafic volcanism at the volcanic front of the central Mexican volcanic belt. *In* Delgado-Granados, H., et al., eds., Cenozoic tectonics and volcanism of Mexico. *Geological Society of America Special Paper* 334, 195-222.

Wadge, G., and Burke, K. (1983) Neogene Caribbean plate rotation and associated Central American tectonic evolution. *Tectonics*, v. 2, 633-643.

Walker, N.W. (1988) U-Pb zircon evidence for 1305-1231 Ma crust in the Llano Uplift, central Texas. *Geological Society of America Abstracts with Programs*, v. 20, A205.

Weston, R.J. (2002) *Volcanic reconstruction of the El Largo and Naranjo VMS deposits, Campo Morado district, Guerrero terrane, Mexico* [M.S. Thesis]. Sudbury, Laurentian University, 135 p.

White, W.M., and Hofmann, A.W. (1982) Sr and Nd isotope geochemistry of oceanic basalts and mantle evolution. *Nature*, v. 296, 821-825.

White, W.M., and Dupre, B. (1986) Sediment subduction and magma genesis in the Lesser Antilles: Isotopic and trace element constraints. *Journal of Geophysical Research*, v. 91, 5927-5941.

White, W.M., Hofmann, A.W., and Puchelt, H. (1987) Isotope geochemistry of Pacific mid-ocean ridge basalt. *Journal of Geophysical Research*, v. 92, 4881-4893.

Wood, S.A., Crerar, D.A., and Borcsik, M.P. (1987) Solubility of the assemblage pyrite-pyrrhotite-magnetite-sphalerite-galena-gold-stibnite-bismuthinite-argentite molybdenite in H (sub 2) O-NaCl-CO (sub 2) solutions from 200 degrees to 350 degrees C degrees. *Economic Geology*, v. 82, 1864-1887.

Woodhead, J.D., and Fraser, D.G. (1985) Pb, Sr and (super 10) Be isotopic studies of volcanic rocks from the northern Mariana Islands: Implications for magma genesis and crustal recycling in the western Pacific. *Geochimica et Cosmochimica Acta*, v. 49, 1925-1930.

Yanez, P., Ruiz, J., Patchett, P.J., Ortega-Gutierrez, F., and Gehrels, G.E. (1991) Isotopic studies of the Acatlan Complex, southern Mexico: Implications for Paleozoic North American tectonics. *Geological Society of America Bulletin*, v. 103, 817-828.

Yta, M. (1992) *Etude geodynamique et metallogenique d'un secteur de la "Faja de Plata" (Mexique : La zone de Zacatecas - Francisco I. Madero – Saucito* [Ph.D. Dissertation]. Orleans, Universite d'Orleans, 266 p.

Zartman, R.E., and Doe, B.R. (1981) Plumbotectonics - the model. *Tectonophysics*, v. 75, 135-162.

APPENDICES

Appendix 1

CHARACTERISTICS OF IMPORTANT METALLIC ORE DEPOSITS OF THE GUERRERO TERRANE

A1.1 Characteristics of important VMS deposits

Deposit (d) / District (D)	Metallic mineralogy[1]	Metal contents	Host rock	Age (Ma) / Method	Refs.[2]
Francisco Madero (d) (Zacatecas)	py, cpy, sph, gn, po	31 ppm Ag; 17 ppm Sn 1.7 % Pb	metamorphosed calcareous black shales	151.3 - 147.9 U-Pb (zircon)	1,2
Guanajuato (D) (Guanajuato)	py, cpy, sph	3 ppm Ag; 0.2 ppm Au; 16 ppm Sn 0.2 % Zn	intermediate and felsic flows and volcaniclastic rocks	146.1 ± 1.1 U-Pb (zircon)	1,2
Tizapa (d) (Teloloapan)	py, cpy, sph, gn, st, apy	324 ppm Ag; 1.9 ppm Au 1.9 % Pb; 7.8 % Zn; 0.7 % Cu	sericite schist	191 common Pb (sulfides)	1,3, 8
Tlanilpa-Azulaquez (D) (Teloloapan)	py, cpy, sph, gn, fre, bn, tt	600 ppm Ag; 2 ppm Au 5 % Pb; 14 % Zn; 0.8 % Cu	carbonaceous mudstone and felsic tuff	139.7 - 137.7 U-Pb (zircon)	1,2
Rey de Plata (d) (Teloloapan)	py, cpy, sph, gn, tt, te, bn	275 ppm Ag; 0.8 ppm Au; 13 ppm Sn 1.7 % Pb; 7.8 % Zn; 0.3 % Cu	black shales, sericite schists, rhyolitic and andesitic volcanics	Albian-Aptian	1,2
Campo Morado (D) (Teloloapan)	py, cpy, sph, gn, tt, apy, el	112 ppm Ag; 1.2 ppm Au; 37 ppm Sn 1.1 % Pb; 3.1 % Zn; 0.7 % Cu	upper contact of felsic volcanic and clastic sedimentary rocks	146.2 - 142.3 U-Pb (zircon)	1,2
Copper King (d) (Las Ollas Complex)	py, cpy, sph, gn, bn, po	7 ppm Ag; 0.2 ppm Au; 2 ppm Sn 0.1 % Zn; 1.3 % Cu	metamorphosed andesitic to basaltic tuffs with interlayered black slates	? early or middle Mesozoic	1
Arroyo Seco (d) (Zihuatanejo)	py, cpy, sph, gn, tt, te	180 ppm Ag 2.8 % Pb; 0.5 % Zn	carbonaceous shales and sandstones (entirely sedimentary host)	Albian - Cenomanian fossil record of host	1,2,4
La Minita (d) (Zihuatanejo)	py, cpy, sph, gn, tt, mt	58 ppm Ag 0.3 % Pb; 4.5 % Zn; 0.2 % Cu	felsic tuff; tuffaceous shales and sandstones	Aptian-Albian	1, 7
Cuale (D) (Zihuatanejo)	py, cpy, sph, gn, tt, fre	165 ppm Ag; 1.1 ppm Au; 2 ppm Sn 1.1 % Pb; 4.7 % Zn; 0.3 % Cu	rhyolitic flows and tuffs, interlayered with volcaniclastic units	157.2 - 154 U-Pb (zircon)	1,2,5,6
El Bramador (D) (Zihuatanejo)	py, cpy, sph, gn, tt	212 ppm Ag; 1.2 ppm Au; 9 ppm Sn 3.1 % Pb; 12 % Zn; 0.6 % Cu	contact between rhyolitic tuffs and overlying carbonaceous shales	157.2 - 154 inferred from Cuale	1,2,6

[1]Metallic mineralogy: apy-arsenopyrite; bn-bornite; cpy-chalcopyrite; el-electrum; fre-freibergite; gn-galena; mt-magnetite; po-pyrrhotite; py-pyrite; sph-sphalerite; st-stannite; te-tennantite; tt-tetrahedrite.

[2]Sources of data: 1-Miranda-Gasca, 1995; 2-Mortensen et al., 2008; 3-Lewis and Rhys, 2000; 4-Centeno-Garcia et al., 2003a; 5-Bissig et al., 2008; 6-Hall and Gomez-Torres, 2000c; 7-De La Campa J., 1991; 8-Elias-Herrera et al., 2000.

A1.2 Characteristics of important porphyry copper deposits

Deposit / District	Metal	Deposit type	Metallic mineralogy[1]	Metal contents	Host rock	Age (Ma) / Method	Refs[2]
La Sorpresa	Cu	breccia	py, cpy	1.2 % Cu	quartz-monzonite	54 / K-Ar	1, 6, 7
Tepalcuatita	Cu-Au	stockwork and veins, breccia	py, cpy, Au	0.32 % Cu	granodiorite, quartz-diorite	N/A	1, 6
La Verde	Cu	breccia, vein	cpy, py, sch	0.7 % Cu	granodiorite	33.4 ± 0.7 / K-Ar	1, 2, 3, 4, 6
San Isidro	Cu	breccia, stockwork, and veins	py, cpy, gn, sph	0.4 % Cu	granodiorite	32.5 ± 0.7 / K-Ar	1, 2, 3, 4, 6
Inguaran	Cu-W	breccia, stockwork, and veins	py, cpy, mo	1-1.4 % Cu	quartz-monzonite	35.6 ± 0.8 / K-AR	2, 4, 6
Tiamaro	Cu	stockwork and veins, breccia	py, cpy, bn, cc	0.1 % Cu	granodiorite, quartz-diorite	Oligocene-Miocene	1, 4, 6, 7
Las Salinas	Cu	dissemination, veins	py, cpy, oxides	1-1.6 % Cu	quartz-monzonite	62.8 ± 1.4 /K-Ar	2, 3, 5, 6

[1]Metallic mineralogy: bn-bornite; cc-chalcocite; cpy-chalcopyrite; gn-galena; mo-molybdenite; py-pyrite; sch-scheelite; sph-sphalerite.

[2]Sources of data: 1-Solano-Rico, 1995; 2-Barton et al., 1995; 3-Damon et al., 1983; 4-CRM, 1995; 5-CRM, 1999; 6-Valencia-Moreno et al., 2007; 7-Miranda-Gasca, 2000.

A1.3 Characteristics of important Zn-Pb-Cu-Ag (Au) and Ag-Au deposits

Deposit (d) / District (D)	Deposit type	Metallic mineralogy[1]	Metal contents	Host rock	Age (Ma) / Method	Refs[2]
Fresnillo (D)	1. mantos, chimneys 2. diss. sulfide 3. veins	1. py, po, sph, cpy, gn, mt, apy, Ag minerals 2. py, po, sph, cpy, gn, mt, apy, Ag minerals 3. pr, aca, pr, tt, gn, sph, cpy	190 ppm Ag; 0.3 ppm Au (oxides) 274 ppm Ag; 0.63 ppm Au (sulfides) 3 % Pb; 4 % Zn; 0.32 % Cu (sulfides)	* Tertiary volcanic rocks (29-31 Ma) * Cretaceous sedimentary and mafic volcanic rocks	32 – 28 / K-Ar	1, 2
Zacatecas	veins	aca, freibergite, el, Ag, Au py, sph, gn, cpy	120 ppm Ag; 1.5 ppm Au 3 % Pb; 5.1 % Zn; 0.16 % Cu	* Cretaceous siltstones and shales * Triassic pelitic rocks		2
Real de Guadalupe	veins	arg, hessite, Au tt, py, cpy, sph, gn	250 ppm Ag; 0.5 ppm Au 0.5 % Pb; 1 % Zn; 0.5 % Cu	* shales interbedded with sandstone * Tertiary dacitic porphyry	37 – 40 / K-Ar	1, 2
Guanajuato (D)	veins	aca, el, py, pyr, polybasite, miargyrite, naumannite, cpy, gn, sph, po	34,850 t Ag (production until 1990) 175 t Au (production until 1990)	* ultramafic to felsic plutons * submarine volcanic rocks * continental redbed	27.4 - 30.7 / K-Ar	1, 2
El Oro - Tlalpujahua	veins	arg, pr, pyr, stephanite, Au, Ag, py, sph, cpy, cov, bn	~ 12 ppm Au	* Cretaceous andesites, slates, and sandstones	27 / K-Ar	1, 2
Sultepec (d)	veins	pyr, pr, arg, el, pearceite, Ag, tt, tennantite, py, sph, gn, apy	165 ppm Au; 0.92 ppm Ag 0.91 % Pb; 0.93 % Zn; 0.07 % Cu	* Cretaceous schists and limestones		2
Zacualpan (D)	veins	pr, pyr, el, polybasite, chlorargyrite, Ag, Au, cpy, gn, sph, tt	more than 0.6 t Ag (production)	* Cretaceous black shales * Tertiary rhyolites and basalts		2
Temascaltepec (d)	veins	pr, arg, pyr, sph, gn, py, cpy, stibnite	~ 3 mil. ounces Ag (production)		33.3 - 32.9 / Ar-Ar	1, 2

[1]Metallic mineralogy: aca-acanthite; apy-arsenopyrite; arg-argentite; bn-bornite; cov-covellite; cpy-chalcopyrite; el-electrum; gn-galena; mt-magnetite; po-pyrrhotite; pr-proustite; py-pyrite; pyr-pyrargyrite; sph-sphalerite; tt-tetrahedrite.

[2]Sources of data: 1-Camprubi et al., 2003, and references therein; 2- Miranda-Gasca, 2000, and references therein.

Appendix 2

LOCATION AND DESCRIPTION OF ANALYZED SAMPLES

Sample	Latitude (N)	Longitude (W)	Area	Material	Description
Metamorphic rocks					
96MR060	19°50.369'	105°18.687'	between Tomatlan and Chamela	meta-basalt	strongly jointed meta-basalt
96MR101	18°19.361'	102°17.111'	south of Arteaga	schist	Tr high-grade rock, between schist and gneiss
96MR102	18°19.361'	102°17.111'	south of Arteaga	schist	Tr high-grade rock, between schist and gneiss
96MR103	18°19.361'	102°17.111'	south of Arteaga, ~ 100 m from previous	schist	Tr high-grade rock, between schist and gneiss
96MR105	18°18.879'	102°17.142'	south of Arteaga, further toward the coast	schist	Tr coarse-grained schist, probably meta-basalt
96MR107	18°18.406'	102°16.995'	south of Arteaga, toward Playa Azul	schist	low-grade granoblastic schist
96MR111	19°02.062'	100°02.454'	near Tejupilco	phyllite	J black phyllite
96MR129	18°23.174'	100°14.722'	near Arcelia	phyllite	phyllite (meta-siltstone)
96MR131	18°23.754'	100°05.098'	between Arcelia and Iguala	phyllite	phyllite (meta-sandstone)
96MR133	18°22.547'	099°40.596'	near Iguala	slate	slate
Sedimentary rocks					
96MR055	19º40.000'	104º04.000'	near Zanzontle	siltstone	calcareous siltstone
96MR057	19°40.000'	104°43.000'	near San Miguel, in the Purificacion area	mudstone	mudstone
96MR067	19°03.570'	103°39.124'	south of Colima	siltstone	calcareous red siltstone
96MR068	19°03.570'	103°39.124'	south of Colima	siltstone	calcareous white/green siltstone
96MR069	19º03.570'	103º39.124'	south of Colima	siltstone	red calcareous siltstone
96MR114	18°28.594'	100°43.091'	between Altamirano and Huetamo	marl	K marl
96MR116	18°34.133'	100°50.085'	between Altamirano and Huetamo	sandstone	K sandstone
96MR117	18°34.133'	100°50.085'	between Altamirano and Huetamo	siltstone	K siltstone
96MR118	18°35.221'	100°56.717'	between Altamirano and Huetamo	siltstone	K red siltstone
96MR119	18°35.221'	100°56.717'	between Altamirano and Huetamo	sandstone	K coarse-grained, red sandstone
96MR121	18°32.412'	100°58.402'	between Altamirano and Huetamo	sandstone	K coarse-grained, red sandstone
96MR127	18°40.511'	100°51.471'	near Huetamo	mudstone	K mudstone
96MR128	18°40.332'	100°51.481'	near Huetamo	siltstone	K siltstone

Igneous rocks					
96MR071	19°05.098'	102°02.880'	La Verde - mine area; West Hill (~566 m)	granodiorite	possibly potassically altered granodiorite
96MR076	19°05.190'	102°02.748'	La Verde - mine area; East Hill	diorite	intensely altered and silicified diorite
96MR078	19°04.904'	102°03.203'	La Verde - near the mine	granodiorite	much fresher granodiorite
96MR079	19°05.223'	102°02.044'	La Verde - mine area; East Hill	granodiorite	altered, silicified granodiorite
96MR083	19°05.038'	102°01.800'	La Verde - mine area	granodiorite	fresh looking granodiorite
96MR088	19°09.460'	101°58.322'	La Verde - big quarry	granite	fresh granite
96MR095	18°53.566'	101°38.600'	Inguaran	granodiorite	massive granodiorite
96MR096	18°54.003'	101°34.282'	El Malacate mine; altitude ~ 1300 m	granodiorite	fresh granodiorite
96MR099	18°53.502'	101°37.013'	La Esmeralda	granodiorite	slightly altered / weathered granodiorite
96MR157	20º47.900'	099º26.904'	Zimapan mine	monzonite	monzonite
96MR166	20º47.900'	099º26.904'	Zimapan mine	endoskarn	endoskarn (level 360)
96MR167	20º47.900'	099º26.904'	Zimapan mine	monzonite	Carrizal intrusive (level 360) / monzonite
96MR173	20º47.900'	099º26.904'	Zimapan mine	monzonite	monzonite
96MR177	20º50.612'	099º30.169'	La Negra mine	diorite	diorite (level 2200)
Ores					
96MR079	19°05.223'	102°02.044'	La Verde area	pyrite	pyrite from altered, silicified granodiorite
96MR082	19°05.077'	102°01.991'	La Verde mine; altitide ~ 606 m	pyrite	pyrite from fresh looking granodiorite
96MR084	19°05.038'	102°01.800'	La Verde mine	bornite	bornite-bearing ore with potassic alteration
96MR095g	18°54.003'	101°34.282'	El Malacate	galena	galena
96MR098B	18°53.695'	101°37.147'	La Esmeralda mine; altitude ~ 1255 m	pyrite	breccia ore; pyrite
96MR098G	18°53.695'	101°37.147'	La Esmeralda mine; altitude ~ 1255 m	pyrite	pyrite from altered granodiorite
96MR152	20º47.900'	099º26.904'	Zimapan mining district	pyrite	pyrite
96MR153	20º47.900'	099º26.904'	Zimapan mining district	pyrite	pyrite
96MR154	20º47.900'	099º26.904'	Zimapan mining district	pyrite	pyrite
96MR159	20º47.900'	099º26.904'	Zimapan mining district; Carrizal intrusive	sphalerite	sphalerite (San Carlos orebody; level 460)
96MR164	20º47.900'	099º26.904'	Zimapan mining district	sphalerite	sphalerite (San Carlos orebody; level 410)
96MR165g	20º47.900'	099º26.904'	Zimapan mining district	galena	galena (Juan Pablo orebody; level 360)
96MR169	20º47.900'	099º26.904'	Zimapan mining district; Carrizal intrusive	chalcopyrite	chalcopyrite (level 360)
96MR170g	20º47.900'	099º26.904'	Zimapan mining district; Carrizal intrusive	galena	galena (Santa Fe 1 orebody; level 360)

96MR170	20º47.900'	099º26.904'	Zimapan mining district; Carrizal intrusive	pyrite	pyrite (Santa Fe 1 orebody; level 360)
96MR171g	20º47.900'	099º26.904'	Zimapan mining district; Carrizal intrusive	galena	galena (Santa Fe 2 orebody; level 360)
96MR182	20º50.612'	099º30.169'	La Negra mining unit	pyrite	pyrite (Buenaventura 1; level 2215)
96MR183	20º50.612'	099º30.169'	La Negra mining unit	sphalerite	sphalerite (Buenaventura1; level 2215)
96MR183g	20º50.612'	099º30.169'	La Negra mining unit	galena	galena (Buenaventura1; level 2215)
96MR184	20º50.612'	099º30.169'	La Negra mining unit	sphalerite	sphalerite (Manto La Cruz; sublevel 2185)

Appendix 3

ANALYTICAL METHODS

A3.1 Sample preparation for Pb isotope measurements

A3.1.1 Whole rock and low-lead sulfide samples

Most samples analuzed were relatively fresh in order to minimize the effects of weathering and alteration. The rocks were cut into approximately 1 cm-thick slabs using a water-cooled saw. Both sides of the slabs were polished to remove the saw marks using silicon carbide abrasive sheets. The polished slabs were cleaned in an ultrasonic bath with deionized water three times and dried. The clean slabs were wrapped in several layers of aluminum foil and plastic bags and broken into small chips (less than 1 cm across) with a hammer. The chips showing signs of alteration were discarded and around 15 g of unaltered chips were collected. Whole rock powders were prepared using an alumina-lined shatter box that was cleaned between samples by grinding three batches of acid-cleaned quartz sand, and rinsing with deionized water after each batch. A few chips of each sample were powdered in the clean, dry shatter box and discarded to self-contaminate the shatter box before the remaining chips were powdered for use.actual powdering step. Powders were transferred to clean, HNO_3-leached polyethylene jars. The sulfide minerals (pyrite, chalcopyrite, sphalerite, and bornite) were hand picked from crushed samples.

Whole rock samples and sulfide minerals were chemically processed in the class 100 clean laboratory at Florida International University. The relatively low concentrations of Pb in most geologic samples and the great hazards posed by environmental contamination

require chemical separation of Pb to be done in rigorous standards of cleanliness (Kamenov, 2000).

Teflon beakers used for dissolution and collection of final samples were soaked in cold aqua regia for at least 48 hours and boiled for about one hour in 1:1 HCl and 1:1 HNO_3. After the boiling process, they were rinsed in successively purer water, from deionized, Corning still, quartz still, and two-bottle (2B) teflon distilled water. Deionized water purified by a resin filter system was used to feed a commercial boiling still (CORNING Mega-Pure ^{TM} System); Corning water was used in turn to feed a quartz glass sub-boiling still; further purification of the quartz water using a Teflon 2B sub-boiling still generated the 2B water. Blank levels for water distilled at FIU are uniformly better than 1.2 ρg/g for Pb and Sr, 0.1 ρg/g for Rb, and 0.01 ρg/g for Nd (measured by isotope dilution mass spectrometry, IDMS) (Panneerselvam, 2001). Blanks for 0.5N HBr and 0.5N HNO_3 prepared from Seastar and Optima reagents are not significantly different from the water blank (Panneerselvam, 2001). The resin (Dowex AG1-8X, 200-400 mesh) used in Pb separation was mixed with 6.2N HCl and cleaned with 0.5N HNO_3 and 2B water. Ten-ml syringe bodies with filters attached at the narrow end were used as columns. These columns were stored in 1:1 HCl bath between uses; before use, they were leached in 1:1 HNO_3 and rinsed successively with deionized, Corning, quartz, and 2B water.

Approximately 500 mg of whole rock powder were dissolved in ~ 3 ml of a 3:2 HF-HBr mixture in 15-ml Teflon beakers and allowed to sit overnight. About 200 mg of mineral separates were dissolved in ~ 2 ml of 0.5N HNO_3 and 2 ml of Optima or Seastar grade HBr. Two ml of Optima or Seastar HBr were then added to the dissolved samples

and evaporated in laminar flow boxes under air filtered at 0.3 μm. The dried samples were re-dissolved in 0.5N HBr and dried down three times. Four to 5 ml of 0.5N HBr were added to the samples, ultrasonicated for around 5 minutes, and transferred to clean, HNO_3-leached, centrifuge tubes. To maximize the recovery of samples from the Teflon beakers, this operation was repeated two more times, with the addition of only 2 ml of 0.5N HBr each time. The samples from the centrifuge tubes were diluted with additional 0.5N HBr to finally obtain 10 ml solution and centrifuged twice for about 15 minutes each time. The centrifuging process separated the Pb-bearing HBr solution from suspended particles, which were mainly represented by organic carbon in sedimentary samples.

Lead was separated and purified using cation exchange columns and an HBr medium (Manhes et al., 1978). Each column was cleaned with 10 ml of 0.2N HNO_3 and conditioned successively with 0.3 ml of 2B water and 0.3 ml of 0.5N HBr before loading the samples. The samples, contained in around 10 ml of 0.5N HBr, were loaded on the columns and allowed to drain through. Lead was adsorbed on the clean resin while other elements passed through. Before collecting the samples in 1 ml of 0.5N HNO_3, the columns were rinsed twice with 1 ml of 0.5N HBr. After adding a drop of 0.1N H_3PO_4, the samples were dried down to a tiny drop at 100°C. For further purification of the samples, these tiny drops were re-dissolved in 0.5N HBr and loaded for the second time on the columns that were cleaned and conditioned the same way as the first time. After allowing the solution to drain thoroughly for the second time, the columns were rinsed two times with 0.5N HBr. 1 ml of 0.5N HNO_3 was used to collect the purified samples.

After adding one drop of 0.1N H_3PO_4, the samples were dried down to a tiny drop at 150°C.

A3.1.2 Galena samples

About 1 mg of clean, hand-picked galena was dissolved in 5 ml of 2N trace metal grade HNO_3 in a plastic beaker and dried on a hot plate at 60°C. More acid was added and dried in case the sample did not dissolve entirely the first time. Ten ml of 2N HNO_3 was added to the sample and warmed. Two clean platinum electrodes were rinsed with 1:4 trace metal grade (Pb < 0.1 ppb) HCl and then deionized water using plastic tongs. These electrodes were connected through wires to a 6V lantern battery terminals and immersed in HNO_3 containing the dissolved Pb until a visible bead of Pb oxide precipitated on the anode. Both electrodes were removed and immersed in a new beaker containing 10 ml of 2N HNO_3 until most of the oxide fell off. The HNO_3 solution from the old beaker was discarded carefully and the platinum electrodes were returned to the cleaning bath 1 consisting of 1:1 reagent grade HCl. The new beaker was placed on a hot plate at relatively low temperature until the Pb oxide dissolved. One ml of solution containing about 100,000 ng Pb was pipetted into a small centrifuge tube, closed carefully, and stored. The rest of the solution and the beaker were disposed of. After the electrodes had soaked in the cleaning bath for at least 2 hours, they were removed with plastic tongs, rinsed carefully with 1N HNO_3, and moved to the cleaning bath 2 consisting of 1:1 reagent grade HNO_3.

A3.2 Leaching experiments

Leaching experiments were carried out using Parr Acid Digestion Bombs with metal bodies and removable Teflon liners. A 23 ml general purpose acid digestion bomb

(number 4749) with a maximum recommended temperature of 250°C was used. The Teflon cups were cleaned lust like other Teflon beakers used in the dissolution of whole rock powder. A Blue M (STABIL-THERM®, Model OV-12A) brand bench type gravity convection oven was used to perform these experiments. Ultrapure 2B distilled HCl was used in the experiments, which were conducted for 8 hours at 120ºC.

500 mg of whole rock powder was placed in the Teflon cups and 4 ml of 0.5N HCl were added to the powder. The cups were placed in the bombs that were tightly closed and placed in the oven. The temperature was stabilized at 120°C before placing the acid digestion bombs in the oven.

After the experiments, the bombs were allowed to cool completely for about 2 hours and then carefully opened. There was no obvious loss of solution in any of the conducted experiments. As much leachate as possible was carefully separated from each sample with an adjustable pipette in order to prevent entering of residue in solution; the leachates were placed into 1:1 HNO_3-leached centrifuge tubes and capped. The residue from each sample was rinsed out of the Teflon liner with 0.5N HNO_3 and poured carefully into clean 15 ml screw-top Teflon beakers. The leachates were centrifuged for about 5 minutes and the clear ones were transferred to clean 5 ml snap-cap Teflon beakers.

A3.3 Lead isotope ratio measurements using the VG-354 mass spectrometer

Lead isotope ratios were determined by thermal ionization mass spectrometry on a VG-354 multicollector mass spectrometer, equipped with five Faraday cups. Lead was loaded on outgassed rhenium (Re) single filaments with silica gel and phosphoric acid. The data were gathered by static multicollection and, in most cases, represented averages of 150 ratio measurements each.

The average standard errors on the analyzed samples were 0.0090 % for $^{204}Pb/^{208}Pb$, 0.0024 % for $^{206}Pb/^{208}Pb$, and 0.0040 % for $^{207}Pb/^{204}Pb$ (Appendix 4.1). The data were corrected for instrumental fractionation by comparison with replicate analyses of the National Bureau of Standards common Pb standard SRM-981. Measured average values of 43 analyses of this standard (Appendix 4.2) are as follows: $^{204}Pb/^{208}Pb=0.027341$; $^{206}Pb/^{208}Pb=0.462381$ and $^{207}Pb/^{208}Pb=0.422345$. Normalization of these values against the average values published for that standard by Todt et al. (1996) and Hamelin et al. (1985) ($^{206}Pb/^{204}Pb=16.939$; $^{207}Pb/^{204}Pb=15.484$; $^{208}Pb/^{204}Pb=36.712$) yielded correction factors of 0.996280 (or 0.093 percent/amu) on $^{204}Pb/^{208}Pb$, 0.997883 (or 0.105 percent/amu) on $^{206}Pb/^{208}Pb$, and 0.998636 (or 0.136 percent/amu) on $^{207}Pb/^{208}Pb$ (Appendix 4.2). The average standard errors on the analyzed Pb standard were 0.0066 % for $^{204}Pb/^{208}Pb$, 0.0014 % for $^{206}Pb/^{208}Pb$, and 0.0027 % for $^{207}Pb/^{208}Pb$ (Appendix 4.2). Duplicate analyses of standards determined at different labs demonstrate the overall reproducibility to be better than ±0.05 percent/amu. The error for value can be determined using the following formula: Δmass x overall reproducibility x value. Thus, for $^{206}Pb/^{204}Pb$ the correction for fractionation is 0.02, for $^{207}Pb/^{204}Pb$ it is 0.023, and for $^{208}Pb/^{204}Pb$ it equals 0.077. The analytical errors are thus smaller than the symbols indicate.

A3.4 Chemical procedure for Sr and Nd separation

A3.4.1 Sample preparation

Around 90 mg of sample powder was weighed in a clean beaker and 5-7 ml HF:$HClO_4$ (4:1) dissolution mix was added to it. The solution was covered and left overnight on the hot plate at 125ºC. The next day the beaker was opened and the

temperature was slowly increased to around 220ºC to allow complete evaporation of the perchloric acid. Approximately 3 ml 6.2N HCl was added while carefully washing down the beaker sides, and let evaporate to dryness at 120ºC. This 6.2N HCl step was repreated twice to ensure removal of all perchloric acid. 0.2 ml 2.5N HCl was added to the cooled dry sample and let sit for around one hour. The solution was then poured into a clean centrifuge tube and centrifuged for around 2 minutes.

A3.4.2 First column chemistry for Sr and REE separation

The Sr separation chemistry followed the procedure described by Hart and Brooks (1977). The first column consists of a 0.5 cm diameter x 19 cm height (in 2.5N HCl) Dowex AG50W-X8 (200-400 mesh) cation exchange resin. These columns are cleaned with 36 ml of 6N HCl (three loads of 12ml) and backwashed with 2.5N HCl. The sample is loaded in 0.25 ml 2.5N HCl and washed with three aliquots of 2.5N HCl totaling 1 ml. 18 ml 2.5N HCl are loaded in the column and discarded. After this step, 5.5 ml 2.5N HCl are added and the Sr fraction is collected. 3.5 ml 6.0N HCl are loaded in the column and discarded. The REE fraction is eluted in 4.5 ml 6.0N HCl. After this stage, the column is cleaned three times with 12 ml 6N HCl and then backwashed with 2.5N HCl.

A3.4.3 Drydown after first column chemistry

The collected Sr samples are dried down at 125ºC until the HCl has evaporated. One drop of $HClO_4$ is added to them and dried at 175ºC. The temperature is then increased incrementally to 220ºC and the samples are cooked for around one hour. The addition and drying down of $HClO_4$ step is repeated two more times. Two drops of concentrated HNO_3 are added and cooked at 150º and this procedure is done two more times. At this stage, the Sr is ready to be loaded on the W filament.

The collected Nd samples are dried down at 125ºC until the HCl has evaporated. 0.25 ml of 0.25N HCl is added at room temperature to dissolve the REE fraction.

A3.4.4 Second column chemistry for Nd separation

The Nd separation chemistry follows the technique described by Richard et al. (1976). The second column, 0.5 cm diameter x 10 cm height, is HDEHP attached to Teflon powder and capped with 0.5 cm of Dowex AG1-X8 (200-400 mesh) anion resin to prevent Teflon flotation. 0.25 ml of REE sample in 0.25N HCl is loaded onto the anion resin and three aliquots (0.25 ml each time) of 0.25N HCl wash are followed. 5.25 ml of 0.25N HCl are loaded and the Ce fraction is discarded. After this step, the Nd fraction is eluted in 2.5 ml of 0.25N HCl. Following this procedure, the column is cleaned by adding four loads of 10 ml 6N HCl and conditioned with two loads of 5ml 0.25N HCl.

A3.4.5 Drydown after second column chemistry

The collected Nd samples are dried down at 125ºC and one drop of $HClO_4$ is added to them. The mixture is cooked at 175ºC and the temperature is incrementally increased to 250ºC over a period of one hour. The addition and drying down of the $HClO_4$ step is repreated two more times. After cooling, 2 drops of concentrated HNO_3 are added to the sample and the mixture is dried at 175ºC. The procedure of adding the HNO_3 and drying it down is done two more times.

A3.5 Strontium isotope ratio measurements using the FINNIGAN MAT 262 mass spectrometer

Strontium isotope ratios were determined by thermal ionization mass spectrometry on a Finnigan MAT 262 RPQ mass spectrometer, equipped with seven Faraday cups. Strontium was loaded on outgassed tungsten (W) single filaments. The sample was

dissolved in 1-2 µl of 0.25N HNO_3. Around 1 µl of TAPH solution (10 g H_2O + 0.5 g $TaCl_5$ + 3 g 0.1N H_3PO_4 + 0.5 g concentrated HF) was added to half of the dissolved sample, and loaded in small aliquots on the filament at 1 Amp. After drydown, the current was increased incrementally to 3-3.2 Amp.

The data were acquired by static multicollection and represented averages of between 77 and 167 isotope ratio measurements each (when the 2se on the average ratios reached 0.000007, the data acquisition was halted). Filament temperature ranged roughly between 1400ºC and 1500ºC and the beam intensity of ^{88}Sr varied between around 3.5 and 8 V. The $^{87}Sr/^{86}Sr$ ratios are corrected for mass fractionation using $^{86}Sr/^{88}Sr = 0.1194$. During the time period of my data acquisition, the $^{87}Sr/^{86}Sr$ for the E&A standard was measured at 0.708002 (n = 5) which agrees with the long term (years) average of the E&A standard. Reported values are corrected to an assumed "true" value of 0.708000 for the E&A standard, giving a correction factor of -0.000002 (Appendix 4.3). In most cases, the 2se on the analyzed samples and on the E&A standard was ±7 (Appendix 4.3).

A3.6 Neodymium isotope ratio measurements using the FINNIGAN NEPTUNE MC-ICP-MS

The Nd isotopic compositions were determined using a multi-collector inductively coupled plasma mass spectrometer: Thermo Finnigan NEPTUNE. One ml high purity 2 % HNO_3 was added to the dry samples and 300 µl of each sample solution was placed in clean beakers. This sample was diluted with between 650 µl and 1100 µl 2 % HNO_3 was added to the sample solution, the purpose being to obtain a beam intensity of ^{144}Nd between 10 – 15 V. The sample is introduced into the plasma by an APEX introduction system (Elemental Scientific). The sample solution uptake rate by the nebulizer is 63

µl/min. The fine aerosol from the nebulizer is injected into the center region of the plasma and desolvated and ionized.

The data represented averages of 60 isotope ratio measurements each and the 2se on the $^{143}Nd/^{144}Nd$ composition was ±0.000003 or ±0.000004 (Appendix 4.4). $^{143}Nd/^{144}Nd$ value for the La Jolla standard over the course of data collection was 0.511838 (n = 27) which agrees with the long term average measured for this standard. $^{143}Nd/^{144}Nd$ were normalized for instrumental mass fractionation using $^{146}Nd/^{144}Nd = 0.7219$. Nd isotope ratios are reported to the "true" value for the LaJolla standard of 0.511850, resulting in a correction factor of +0.000012 (Appendix 4.4). Overall, the 2se on the standard varied between ±4 and ±9 (Appendix 4.4) and the beam intensity of ^{144}Nd ranged between 3.7 and 6.2 V.

Appendix 4

DETAILED LEAD, STRONTIUM, AND NEODYMIUM ISOTOPE MEASUREMENT DATA

A4.1 Detailed Pb isotope measurement data of the analyzed rocks and minerals

Sample	$^{204}Pb/^{208}Pb$ (M)	% error	$^{204}Pb/^{208}Pb$ (C)	$^{206}Pb/^{208}Pb$ (M)	% error	$^{206}Pb/^{208}Pb$ (C)	$^{207}Pb/^{208}Pb$ (M)	% error	$^{207}Pb/^{208}Pb$ (C)
Correction factors			0.996280			0.997883			0.998636
Metamorphic rocks									
96MR060	0.025929	0.0116	0.025833	0.484132	0.0047	0.483107	0.404814	0.0044	0.404262
96MR101	0.025799	0.0071	0.025703	0.485734	0.0026	0.484706	0.402578	0.0031	0.402029
96MR102	0.025779	0.0095	0.025683	0.488526	0.0035	0.487492	0.401785	0.0021	0.401237
96MR103	0.025687	0.0112	0.025591	0.486152	0.0033	0.485123	0.401422	0.0037	0.400874
96MR105	0.025604	0.0059	0.025509	0.485661	0.0011	0.484633	0.400375	0.0013	0.399829
96MR107	0.025595	0.0080	0.025500	0.484555	0.0012	0.483529	0.400724	0.0021	0.400177
96MR111	0.025940	0.0069	0.025844	0.488854	0.0017	0.487819	0.405003	0.0027	0.404451
96MR129	0.025672	0.0068	0.025577	0.493556	0.0012	0.492511	0.400711	0.0026	0.400164
96MR131	0.025865	0.0080	0.025769	0.491502	0.0028	0.490461	0.403760	0.0022	0.403209
96MR133	0.025883	0.0076	0.025787	0.491809	0.0015	0.490768	0.403942	0.0023	0.403391
Igneous rocks									
96MR071	0.025800	0.0092	0.025704	0.488577	0.0031	0.487543	0.401410	0.0028	0.400862
96MR076 (135)*	0.025929	0.0140	0.025833	0.491584	0.0039	0.490543	0.402636	0.0033	0.402087
96MR078	0.025888	0.0116	0.025792	0.487050	0.0015	0.486019	0.402841	0.0026	0.402292
96MR079	0.025748	0.0057	0.025652	0.489265	0.0009	0.488229	0.401450	0.0012	0.400902
96MR083	0.026021	0.0121	0.025924	0.485946	0.0063	0.484917	0.405316	0.0017	0.404763
96MR088	0.025820	0.0061	0.025724	0.486765	0.0009	0.485735	0.403239	0.0017	0.402689
96MR095	0.025900	0.0067	0.025804	0.487149	0.0011	0.486118	0.403622	0.0014	0.403071
96MR096	0.025961	0.0126	0.025864	0.486368	0.0017	0.485338	0.404554	0.0036	0.404002
96MR099	0.026089	0.0127	0.025992	0.489044	0.0064	0.488009	0.404446	0.0038	0.403894

96MR157	0.025699	0.0077	0.025603	0.486772	0.0009	0.485742	0.403250	0.0020	0.402700
96MR166	0.025837	0.0055	0.025741	0.485928	0.0009	0.484899	0.403726	0.0066	0.403175
96MR167	0.025779	0.0090	0.025683	0.487597	0.0016	0.486565	0.402990	0.0028	0.402440
96MR173	0.025956	0.0069	0.025859	0.487300	0.0018	0.486268	0.404556	0.0023	0.404004
96MR177	0.025842	0.0117	0.025746	0.488141	0.0014	0.487108	0.403418	0.0038	0.402868
Sedimentary rocks									
96MR055	0.026039	0.0102	0.025942	0.495259	0.0024	0.494211	0.406358	0.0023	0.405804
96MR057	0.025808	0.0093	0.025712	0.500828	0.0025	0.499768	0.402542	0.0023	0.401993
96MR067	0.025873	0.0103	0.025777	0.490818	0.0021	0.489779	0.402686	0.0035	0.402137
96MR068	0.026064	0.0086	0.025967	0.488241	0.0013	0.487207	0.405126	0.0024	0.404573
96MR069	0.025837	0.0064	0.025741	0.491490	0.0008	0.490450	0.402661	0.0024	0.402112
96MR114	0.025997	0.0075	0.025900	0.493104	0.0013	0.492060	0.405307	0.0018	0.404754
96MR116	0.026012	0.0102	0.025915	0.484321	0.0020	0.483296	0.405891	0.0037	0.405337
96MR117 (135)*	0.026152	0.0083	0.026055	0.486432	0.0011	0.485402	0.406045	0.0025	0.405491
96MR118	0.026029	0.0092	0.025932	0.488450	0.0015	0.487416	0.405926	0.0025	0.405372
96MR119	0.026136	0.0058	0.026039	0.487860	0.0012	0.486827	0.406839	0.0015	0.406284
96MR121	0.026083	0.0135	0.025986	0.487086	0.0016	0.486055	0.405457	0.0053	0.404904
96MR127	0.026054	0.0127	0.025957	0.488166	0.0093	0.487133	0.406108	0.0033	0.405554
96MR128	0.026160	0.0071	0.026063	0.486585	0.0033	0.485555	0.406674	0.0045	0.406119
Ore samples									
96MR079	0.026025	0.0091	0.025928	0.486490	0.0012	0.485460	0.404631	0.0022	0.404079
96MR082	0.026058	0.0047	0.025961	0.506197	0.0010	0.505125	0.406467	0.0010	0.405913
96MR084	0.026123	0.0041	0.026026	0.487136	0.0008	0.486105	0.405750	0.0014	0.405197
96MR095g	0.026057	0.0073	0.025960	0.486447	0.0030	0.485417	0.405454	0.0046	0.404901
96MR098B	0.026029	0.0056	0.025932	0.485938	0.0011	0.484909	0.405289	0.0014	0.404736
96MR098G (90)*	0.026002	0.0076	0.025905	0.485994	0.0023	0.484965	0.405140	0.0028	0.404587
96MR152	0.025959	0.0068	0.025862	0.486632	0.0007	0.485602	0.404486	0.0018	0.403934
96MR153	0.025824	0.0095	0.025728	0.485395	0.0028	0.484367	0.404066	0.0037	0.403515
96MR154	0.025903	0.0049	0.025807	0.486371	0.0009	0.485341	0.404394	0.0009	0.403842

96MR159 (105)*	0.025717	0.0064	0.025621	0.484441	0.0026	0.483415	0.403770	0.0220	0.403219
96MR164 (120)*	0.025473	0.0119	0.025378	0.482564	0.0051	0.481542	0.402634	0.0041	0.402085
96MR165g	0.025877	0.0246	0.025781	0.485919	0.0036	0.484890	0.404431	0.0245	0.403879
96MR169	0.026035	0.0062	0.025938	0.488020	0.0031	0.486987	0.404997	0.0032	0.404445
96MR170g	0.025946	0.0117	0.025849	0.486939	0.0027	0.485908	0.404470	0.0106	0.403918
96MR170 (135)*	0.025901	0.0131	0.025805	0.486652	0.0012	0.485622	0.404349	0.0063	0.403797
96MR171g (120)*	0.025810	0.0125	0.025714	0.485773	0.0019	0.484745	0.404102	0.0073	0.403551
96MR182	0.025503	0.0109	0.025408	0.483096	0.0050	0.482073	0.402992	0.0034	0.402442
96MR183	0.025652	0.0095	0.025557	0.484574	0.0043	0.483548	0.403458	0.0042	0.402908
96MR183g	0.025924	0.0080	0.025828	0.487305	0.0020	0.486273	0.404047	0.0144	0.403496
96MR184	0.025834	0.0066	0.025738	0.486568	0.0024	0.485538	0.404104	0.0036	0.403553
Average		0.0090			0.0024			0.0040	
Leachates / Residues									
Correction factors			0.995759			0.997554			0.998508
96MR060L	0.025997	0.0038	0.025887	0.484684	0.0006	0.483498	0.404974	0.0007	0.404370
96MR060R	0.025982	0.0072	0.025872	0.484801	0.0018	0.483615	0.404876	0.0011	0.404272
96MR069R	0.025812	N/A	0.025703	0.490643	N/A	0.489443	0.402554	N/A	0.401953
96MR069L (75)*	0.025806	0.0288	0.025697	0.492741	0.0048	0.491536	0.401527	0.0038	0.400928
96MR105L (90)*	0.025711	0.0304	0.025602	0.485241	0.0028	0.484054	0.401557	0.0023	0.400958
96MR105R (135)*	0.025568	0.0079	0.025460	0.485326	0.0021	0.484139	0.400441	0.0018	0.399844
96MR114R	0.025977	0.0042	0.025867	0.492808	0.0021	0.491603	0.405087	0.0012	0.404483
96MR117L	0.026106	0.008	0.025995	0.485145	0.0016	0.483958	0.40615	0.0015	0.405544
96MR117R	0.026153	0.0107	0.026042	0.488480	0.0013	0.487285	0.405875	0.0008	0.405269
96MR127R	0.026051	0.0079	0.025941	0.488263	0.0049	0.487069	0.405788	0.0013	0.405183
96MR129L	0.025777	0.0064	0.025668	0.486071	0.0036	0.484882	0.402601	0.0009	0.402000
96MR129R	0.025120	0.0045	0.025013	0.509787	0.0008	0.508540	0.394267	0.0006	0.393679
96MR133R	0.025897	0.0047	0.025787	0.491535	0.0009	0.490333	0.404123	0.001	0.403520

* - number of measured ratios, if different from 150; M – measured values; C – corrected values; L – HCl leachates; R – HCl residues; N/A – unable to determine due to technical difficulties

A4.2 Detailed Pb isotope measurement data of the Pb standard

Lead standard	$^{204}Pb/^{208}Pb$ (M)	% error	$^{206}Pb/^{208}Pb$ (M)	% error	$^{207}Pb/^{208}Pb$ (M)	% error	$^{206}Pb/^{204}Pb$ (M)	$^{207}Pb/^{204}Pb$ (M)	$^{208}Pb/^{204}Pb$ (M)
A. Lead standard values used for correction of the whole-rock and mineral experiments (performed between August 2006 and July 2009)									
SRM-981	0.027351	0.0035	0.462503	0.0009	0.422387	0.0007	16.909	15.443	36.561
SRM-981	0.027342	0.0037	0.462471	0.0011	0.422368	0.0008	16.914	15.447	36.573
SRM-981	0.027356	0.0049	0.462506	0.0010	0.422398	0.0010	16.906	15.440	36.555
SRM-981	0.027369	0.0037	0.462571	0.0007	0.422465	0.0008	16.901	15.435	36.537
SRM-981	0.027370	0.0050	0.462985	0.0016	0.422532	0.0010	16.915	15.437	36.536
SRM-981	0.027345	0.0049	0.462776	0.0008	0.422423	0.0006	16.923	15.447	36.569
SRM-981	0.027278	0.0061	0.461757	0.0019	0.422148	0.0028	16.927	15.475	36.659
SRM-981	0.027324	0.0090	0.462395	0.0011	0.422336	0.0068	16.922	15.456	36.597
SRM-981	0.027359	0.0063	0.462603	0.0009	0.422408	0.0029	16.908	15.439	36.551
SRM-981	0.027379	0.0076	0.463015	0.0009	0.422502	0.0032	16.911	15.431	36.524
SRM-981	0.027365	0.0056	0.462860	0.0010	0.422440	0.0015	16.914	15.437	36.543
SRM-981	0.027342	0.0069	0.462518	0.0011	0.422348	0.0020	16.916	15.446	36.573
SRM-981	0.027346	0.0055	0.462572	0.0011	0.422344	0.0013	16.915	15.444	36.568
SRM-981	0.027329	0.0094	0.461805	0.0030	0.422401	0.0029	16.897	15.456	36.591
SRM-981	0.027339	0.0092	0.462526	0.0013	0.422246	0.0067	16.918	15.444	36.577
SRM-981	0.027356	0.0060	0.462535	0.0010	0.422335	0.0013	16.907	15.438	36.555
SRM-981	0.027327	0.0090	0.462099	0.0035	0.422346	0.0060	16.909	15.455	36.593
SRM-981	0.027324	0.0064	0.462239	0.0015	0.422230	0.0026	16.916	15.452	36.597
SRM-981	0.027351	0.0084	0.462625	0.0016	0.422290	0.0045	16.914	15.439	36.561
SRM-981	0.027376	0.0073	0.462663	0.0021	0.422492	0.0025	16.900	15.432	36.528
SRM-981	0.027384	0.0063	0.462828	0.0011	0.422553	0.0015	16.901	15.430	36.517
SRM-981	0.027313	0.0072	0.461885	0.0021	0.422247	0.0025	16.910	15.459	36.612
SRM-981	0.027335	0.0053	0.462097	0.0009	0.422318	0.0014	16.904	15.449	36.583
SRM-981	0.027314	0.0098	0.461868	0.0012	0.422302	0.0020	16.909	15.461	36.611
SRM-981	0.027363	0.0058	0.462413	0.0009	0.422430	0.0013	16.899	15.438	36.545

SRM-981	0.027370	0.0078	0.462606	0.0014	0.422431	0.0038	16.901	15.434	36.536
SRM-981	0.027266	0.0065	0.461787	0.0013	0.422136	0.0019	16.936	15.482	36.675
SRM-981	0.027257	0.0072	0.461712	0.0022	0.422246	0.0029	16.939	15.491	36.687
SRM-981	0.027355	0.0074	0.462244	0.0009	0.422389	0.0019	16.897	15.441	36.556
SRM-981	0.027367	0.0078	0.462484	0.0010	0.422415	0.0036	16.899	15.435	36.540
SRM-981	0.027352	0.0071	0.462436	0.0012	0.422372	0.0017	16.906	15.442	36.560
SRM-981	0.027343	0.0088	0.462472	0.0033	0.422263	0.0063	16.913	15.443	36.572
SRM-981	0.027405	0.0063	0.463031	0.0016	0.422720	0.0027	16.895	15.424	36.489
SRM-981	0.027365	0.0044	0.462303	0.0008	0.422381	0.0009	16.893	15.435	36.543
SRM-981	0.027278	0.0074	0.462109	0.0014	0.422198	0.0021	16.940	15.477	36.659
SRM-981	0.027324	0.0073	0.462066	0.0012	0.422094	0.0059	16.910	15.447	36.597
SRM-981	0.027303	0.0083	0.462045	0.0015	0.421980	0.0066	16.922	15.455	36.626
SRM-981	0.027360	0.0034	0.462438	0.0009	0.422365	0.0009	16.901	15.437	36.549
SRM-981	0.027331	0.0044	0.462268	0.0008	0.422284	0.0023	16.913	15.450	36.588
SRM-981	0.027255	0.0096	0.461467	0.0030	0.421987	0.0030	16.931	15.482	36.690
SRM-981	0.027390	0.0038	0.462973	0.0013	0.422679	0.0022	16.902	15.431	36.509
SRM-981	0.027333	0.0054	0.462372	0.0011	0.422240	0.0037	16.916	15.447	36.585
SRM-981	0.027359	0.0067	0.462452	0.0009	0.422362	0.0015	16.903	15.437	36.551
Average (n = 43)	0.027341	0.0066	0.462381	0.0014	0.422345	0.0027	16.911	15.447	36.575
Hamelin et al., 1985 Todt et al., 1996	0.027239		0.461402		0.421769		16.939	15.484	36.712
Correction factors	0.996280		0.997883		0.998636				
(percent/amu)	0.092991		0.105858		0.136359				
B. Lead standard values used for correction of the leaching experiments (performed in September 2009)									
SRM-981	0.027376	0.0063	0.462660	0.0010	0.422482	0.0010	16.900	15.432	36.528
SRM-981	0.027355	0.0044	0.462543	0.0008	0.422409	0.0006	16.908	15.441	36.556
SRM-981	0.027345	0.0069	0.462484	0.0017	0.422331	0.0013	16.912	15.444	36.569

SRM-981	0.027366	0.0058	0.462780	0.0013	0.422466	0.0009	16.910	15.437	36.541
SRM-981	0.027326	0.0065	0.462183	0.0011	0.422266	0.0007	16.913	15.452	36.595
SRM-981	0.027362	0.0053	0.462549	0.0014	0.422441	0.0008	16.904	15.438	36.547
Average (n = 6)	0.027355		0.462533		0.422399		16.908	15.441	36.556
Todt et al., 1996 Hamelin et al., 1985	0.027239		0.461402		0.421769		16.939	15.484	36.712
Correction factors	0.995759		0.997554		0.998508				

A4.3 Detailed Sr isotope measurement data of the analyzed rocks and Sr standard

Sample	$^{87}Sr/^{86}Sr$ (M)	1sd	1sd (%)	2se (M)	2se (M) (%)	n	$^{87}Sr/^{86}Sr$ (C)
Correction factor	-0.000002						
Metamorphic rocks							
96MR101	0.708380	0.000033	0.0047	0.000007	0.0010	93	0.708378
96MR105	0.726496	0.000044	0.0061	0.000007	0.0010	151	0.726494
96MR111	0.707759	0.000039	0.0055	0.000007	0.0010	131	0.707757
96MR129	0.722948	0.000046	0.0063	0.000007	0.0010	167	0.722946
Igneous rocks							
96MR088	0.708786	0.000043	0.0061	0.000007	0.0010	163	0.708784
96MR095	0.704862	0.000031	0.0044	0.000007	0.0009	87	0.704860
96MR096	0.704911	0.000033	0.0047	0.000007	0.0010	97	0.704909
96MR099	0.705757	0.000030	0.0042	0.000007	0.0010	77	0.705755
Sedimentary rocks							
96MR067	0.708850	0.000041	0.0058	0.000007	0.0010	140	0.708848
96MR069	0.709364	0.000039	0.0055	0.000007	0.0010	127	0.709362
96MR117	0.705303	0.000038	0.0054	0.000007	0.0009	133	0.705301
96MR127	0.707577	0.000057	0.0081	0.000010	0.0015	125	0.707575
E&A standard							
	0.707996	0.000034	0.0048	0.000007	0.0010	95	
	0.708007	0.000036	0.0051	0.000007	0.0010	110	
	0.708000	0.000030	0.0043	0.000007	0.0009	83	
	0.708007	0.000041	0.0058	0.000008	0.0012	94	
	0.708000	0.000058	0.0082	0.000008	0.0012	192	
Average (n=5)	0.708002						
Correction factor (values normalized to $^{87}Sr/^{86}Sr$ = 0.708000) : -0.000002							

A4.4 Detailed Nd isotope measurement data of the analyzed rocks and Nd standard

Sample	$^{143}Nd/^{144}Nd$ (M)	1se (abs)	2se (abs)	$^{143}Nd/^{144}Nd$ (C)
Correction factor	0.000012			
Metamorphic rocks				
96MR101	0.512554	0.000001	0.000003	0.512567
96MR105	0.512121	0.000001	0.000003	0.512133
96MR111	0.512577	0.000002	0.000004	0.512589
96MR129	0.512665	0.000001	0.000003	0.512677
Igneous rocks				
96MR088	0.512627	0.000001	0.000003	0.512640
96MR095	0.512760	0.000002	0.000004	0.512772
96MR096	0.512753	0.000002	0.000004	0.512765
96MR099	0.512758	0.000001	0.000003	0.512771
Sedimentary rocks				
96MR067	0.512740	0.000002	0.000004	0.512753
96MR069	0.512741	0.000001	0.000003	0.512753
96MR117	0.512798	0.000002	0.000003	0.512810
96MR127	0.512553	0.000002	0.000003	0.512565
La Jolla Standard				
	0.511810	0.000003	0.000007	
	0.511829	0.000003	0.000006	
	0.511825	0.000004	0.000007	
	0.511839	0.000004	0.000007	
	0.511834	0.000004	0.000008	
	0.511840	0.000003	0.000006	
	0.511832	0.000003	0.000006	
	0.511841	0.000003	0.000006	
	0.511846	0.000018	0.000035	
	0.511836	0.000003	0.000006	
	0.511844	0.000002	0.000005	
	0.511840	0.000003	0.000006	
	0.511851	0.000007	0.000014	
	0.511848	0.000004	0.000009	
	0.511843	0.000003	0.000006	
	0.511835	0.000003	0.000005	
	0.511842	0.000003	0.000005	
	0.511849	0.000003	0.000006	
	0.511857	0.000008	0.000017	
	0.511846	0.000003	0.000006	
	0.511831	0.000004	0.000007	
	0.511830	0.000002	0.000004	

	0.511831	0.000003	0.000006	
	0.511833	0.000002	0.000004	
	0.511836	0.000003	0.000005	
	0.511839	0.000002	0.000004	
	0.511832	0.000002	0.000004	
Average (n=27)	0.511838			

Correction factor (values normalized to $^{143}Nd/^{144}Nd = 0.511850$ for La Jolla standard): 0.000012.
Each value represents the average of 60 ratios.

VITA
ADRIANA POTRA

January 29, 1977	Born, Sfântu Gheorghe, Romania
1999	B.S., Geology Babeş-Bolyai University Cluj-Napoca, Romania
2001	M.S., Geology Babeş-Bolyai University Cluj-Napoca, Romania
2005	Doctoral Candidate in Geology Florida International University Miami, Florida

PUBLICATIONS AND PRESENTATIONS

Potra, A., Macfarlane, W.A., Salters, V.J.M., and Sachi-Kocher, A. (2010). *Isotopic Studies of the Guerrero Composite Terrane, West-Central Mexico: Implications for Provenance of Crustal Rocks and Ore Metals*. Eos, Transactions, American Geophysical Union, Supplement, Abstract V23B-2419, Dec. 2010.

Potra, A., and Macfarlane, W.A. (2010). *Lead Isotope Variations and Tectonic Terranes in Southern Mexico*. Geochimica et Cosmochimica Acta, vol. 74, Issue 11, Supplement 1, pp. A826, June 2010.

Potra, A., and Macfarlane, W.A. (2009). *Ore Metal Sources in Tertiary Mineral Deposits of the Guerrero and Sierra Madre Terranes, Mexico, as Inferred from Lead Isotope Studies*. Geological Society of America Abstracts with Programs, vol. 41, no. 7, pp. 438, Oct. 2009.

Potra, A., and Macfarlane, W. A. (2008). *Lead Isotope Constraints on the Sources of Ore Metals in Deposits from the Guerrero Terrane, West-Central Mexico*. Geological Society of America Abstracts with Programs, vol. 40, no. 6, pp. 135-136, Oct. 2008.

Potra, A., and Macfarlane, W. A. (2007). *Lead Isotope Constraints on the Sources of Ore Metals in SW Mexican Deposits*. Eos, Transactions, American Geophysical Union, vol. 88, no. 52, Supplement, Abstract V41D-0818, Dec. 2007.